TRANSLATION FROM RUSSIAN TO ENGLISH THE BOOK "BLAST EFFECTS CAUSED BY EXPLOSIONS" AUTHORED BY B. GELFAND AND M. SILNIKOV

Final Technical Report
by

Gelfand Boris
(April 2004)

United States Army

EUROPEAN RESEARCH OFFICE OF THE U.S. ARMY

London, England

CONTRACT NUMBER N62558-04-M-0004

Professor Boris Gelfand

Report Documentation Page

Form Approved
OMB No. 0704-0188

1. REPORT DATE	2. REPORT TYPE	3. DATES COVERED
00 APR 2004	**N/A**	**-**

4. TITLE AND SUBTITLE	5a. CONTRACT NUMBER
Translation from Russian to English the Book "Blast Effects Caused by Explosions" Authored by B. Gelfand and M. Silnikov, Final Technical Report	5b. GRANT NUMBER **N62558-04-M-0004**
	5c. PROGRAM ELEMENT NUMBER
6. AUTHOR(S)	5d. PROJECT NUMBER
	5e. TASK NUMBER
	5f. WORK UNIT NUMBER
7. PERFORMING ORGANIZATION NAME(S) AND ADDRESS(ES) **European Research Office of the U.S. Army, London, England**	8. PERFORMING ORGANIZATION REPORT NUMBER
9. SPONSORING/MONITORING AGENCY NAME(S) AND ADDRESS(ES)	10. SPONSOR/MONITOR'S ACRONYM(S)
	11. SPONSOR/MONITOR'S REPORT NUMBER(S)

12. DISTRIBUTION/AVAILABILITY STATEMENT
Approved for public release, distribution unlimited

13. SUPPLEMENTARY NOTES
The original document contains color images.

14. ABSTRACT

15. SUBJECT TERMS

16. SECURITY CLASSIFICATION OF:			17. LIMITATION OF ABSTRACT	18. NUMBER OF PAGES	19a. NAME OF RESPONSIBLE PERSON
a. REPORT **unclassified**	b. ABSTRACT **unclassified**	c. THIS PAGE **unclassified**	**UU**	**249**	

Abstract

This report contains the translation from Russian to English of the book "Blast effects caused by explosions" authored by B. Gelfand and M. Silnikov.

Key words:
Blast waves, Explosions, Safety, Explosion protection

CONTENT

INTRODUCTION

The expected development of criminal situation and the analysis of terrorist activity over the recent years give rise to the necessity of in-depth study of modern methods of application, search, classification, and neutralization of explosive devices (ED). Particular attention must be paid to the prevention of the non-authorized operation and the reduction of destructive consequences of ED [1... 16].

The reason of ED becoming widespread is the availability of the information about the technology of ED manufacturing and application, as well as the data on initial materials and accessories (blocks) for their manufacture in home-craft conditions. For example, originally published in 1971 (and repeatedly republished) in USA the book "The Anarchist Cooking Book" contains the comprehensive technological data and instructions for manufacturing of the simple ED in a kitchen! Criminalistic analysis showed, that significant part of high explosives (HE) and ED used by the terrorists and criminals were really produced at home conditions, and necessary ingredients were freely b ought in the popular shops of chemicals.

The following facts can serve as the evidence of wide use of mine-explosive devices in terroristic acts. According to the report of the Ministry of Justice more than 3000 cases of illegal application of ED were registered in 1995 in USA. In Great Britain after covenant with the Irish republican army (IRA) on the discontinuance of fire in Ulster the amount of terroristic acts with the use of ED was not reduced, but even has increased approximately by 15 percents.

The number of criminal explosions in Russia sharply increases after the disintegration of USSR.

The statistical data show, that ED with small and average energy of explosion (up to 1 kg of TNT equivalent) are mainly used in Western Europe and Russia; in USA - more powerful ED (from 3 up to 5 kg of TNT equivalent). In recent years the terrorists more often use the explosive devices with large weight of HE.

The most known terroristic act of this category is the undermining of office buildings in Oklahoma city (USA, 1997), in which ED containing more than 400 kgs of TNT equivalent charge was used. The number of victims can illustrate the scale of this crime: 168 men were died and more than 500 were heavy injured.

The tendency of increasing the ED power, used by terrorists in Russia, is distinctly traced since 1995. Suffice it to say about the undermining of apartment houses of the families of Russian frontier guards in Caspyisk, explosion of railway station in Pyatigorsk, terroristic act in the house belonged to the mayor of Makhachkala, where 17 men were died and 26 men were heavy wounded. 30 buildings were destroyed and damaged. ED power exceeded 100 kg of TNT equivalent (1998). In September 1999 explosions in Buinaksk, Moscow, and Volgodonsk took place one behind another. The explosion of the apartment house in the Gurianov Street in Moscow of September 9, 1999 resulted in the death of 23 men; about 250 were injured, including 73 heavy wounded.

The explosive device at the center of Moscow was left near the stall with the cosmetic goods in pedestrian subway under Pushkin Square (2000). The saleswoman has noticed the suspicious plastic bag, left near her workplace, and has addressed to a safety service of a mall. The personnel responsible for the safety started to discuss what to undertake. Meanwhile, about 5 minutes has passed, and explosion took place. 13 men were died, 118 wounded. The power of the explosive device was about 500... 600 g of TNT equivalent.

After analysis of the situation, the experts came to a conclusion: the tragedy could be avoided, if the mall safety service had ready for use one of the known anti-explosion protection devices. The conclusion is applicable to a set of terrorist explosions occurred not only in Russia, but also in other countries.

The efforts of law machinery should be directed not only on investigation of previous crimes, but first of all also on their prevention.

Major element in accident prevention is the development of mobilization measures in case of terrorist explosion threat carried out by law machinery in cooperation with safety

services of firms and organizations. In Great Britain, for example, "Rules of maintenance of health and the safety at work" demand the obligatory planning the mobilization measures. They include the use of explosions covers, the application of anti-fragment film in window glasses, elaboration of the plans of personnel evacuation, and other measures.

At ED terroristic threat the counter-measure should estimate the degree of danger by the analysis of risk and vulnerability. The experts carrying out the analysis should have the experience in such fields as HE chemisrty, structural strength of building, organization of safety systems. It is necessary to develop a system of measures for reduction of vulnerability of buildings and personnel. However, it is necessary to take into consideration, that the measures, which limit the freedom of action too much, will not be maintained by the personnel and consequently will not ensure the safety.

The interest to searching the methods of destructive explosion suppression is not weakening for a long time. The need for the decision of this problem exists in army, in law machinery activity, and also at realization of industrial blasting operations.

The intensive development of technological processes involving the energy of explosion essentially expands the area of application of explosive substances in industry. Thus, considerably increased is the specific volume of technological blasting operations, which should be carried out not only at specially equipped testing areas and explosive chambers, but also at urban conditions, the workshop rooms etc. The HE charges weight restrictions developed for conducting of blasting operations in open-cast mines and testing areas, are generally inapplicable, as they do not satisfy to existing ecological safety regulations of the energy sources application at urban conditions, on water areas of the seas having economic importance, and in other similar situations.

In the process of development of accident protection devices and safety regulations for the technological operations, which use the explosion energy, the allowable effect of the shock wave on the object should be determined by criterion of acceptable risk but for the criterion of absolute safety. This can be done by comparison, for example, with the risk from the effect of the similar natural factors or other kinds energy sources, used on practice.

The most hazardous factor of condensed HE detonation is the shock (blast) wave. The analysis of experimental data of the shock wave loads onto the objects testifies about the probabilistic character of their damage at dynamic loadings. The probability of damage depends both on the individual characteristics of the object, and also on uncontrollable factors of dynamic impacts in particular conditions.

In the book, the modern concepts for the determination of the parameters of the blast waves from explosion of HE charges in air and water are presented. The given information allows constructing the diagrams of a damage of bio-objects and typical structural elements in relation to the parameters of the blast loadings. The examples of the damage diagrams in coordinates "pressure – impulse" are shown. Some technical solutions directed on the suppression of the blast loadings from HE explosions are considered both for the destruction of criminal explosive objects, and for industrial use of explosive technologies. In particular, we present the analysis of efficiency of attenuating of the blast loadings (pressure and impulse characteristics) with the help of the perforated screens and by placing of the explosive sources in elastic envelopes containing gaseous substances.

The book is constructed on the basis of the original and detailed analysis of results of the research works executed at practical application of proposed methods of blast loadings suppression by the scientists and the experts of Paton's Institute of Electrical Welding, Semenov's Institute of Chemical Physics, Lavrent'ev's Institute of Hydrodynamics, NPO Special Materials, and also on the basis of a number of the foreign publications and original publications of the authors.

The choice of simple and effective ways of blast protection created by explosive substances remains an urgent task for fundamental and applied researches. The authors analyze the ways of reduction of the blast loadings by placing the sources (HE charges) in various explosion protection envelopes or immersing in various explosion absorption media. The chosen ways of suppression of the blast waves have found the direct technical solution in a series of devices for operative and reliable protection of the equipment and personnel at preservation and/or liquidations of explosive objects and devices.

References

1. Silnikov M.V., Kozlov A.V., Orlov A.V., Petrov A.V., Titov A.M. The explosion protection device «Fountain» // Proc. of the 1st All-Russia scientific - practical conference «Urgent problems of protection and safety ». St.Petersburgh, 1998, p. 125. (*in Russian*)
2. Kozlov A.V., Titov A.M., Petrov A.V. «Fountain» will extinguish explosion // Protection and safety, № 1 (4), 1998. p. 22. (*in Russian*)
3. Mikhailin A.I., Orlov A.V., Sadyrin A.I., Silnikov M.V.. Principles of weakening of the dangerous factors of explosion // Proc. of Scientific conference of the Volga regional center RARAN «Modern methods of design and improvement of rocket-artillery arms », 1999 - Sarov: VNIIEF - 2000. - p. 517. (*in Russian*)
4. Orlov A.V. Daunting the fire // Protection and safety . — № 4, 1998.-p. 14. (*in Russian*)
5. Orlov A.V. The bomb in «Fountain» and under a blanket // Protection and safety — № 4,1999. — p. 46. (*in Russian*)
6. Mikhailin A.I., Orlov A.V., Sadyrin A.I., Silnikov M.V. The method of fire prevention at the detonation of the explosive device // Proc. of the 5th inter-university scientific - practical conference « New information technologies in practice of law-enforcement institutions ». — St.Petersbugh. — 1999. (*in Russian*)
7. Tjurin M.V., Mikhailin A.I., Orlov A.V. Historical aspects of the research of the mechanism of dangerous effects of shock waves // Proc. of the 2nd All-Russia scientific - practical conference «Urgent problems of protection and safety ». St.Petersburgh. - 1999. - v. 2. - p. 157. (*in Russian*)
8. Silnikov M.V., Serdtsev N.I., Nelezin P.V. On the prospects of methods of explosion localization for the increase of safety of mine clearing in districts and urban areas // Works Second interregional is scientific - practical conferences « Development new special technique for law-enforcement ». — SPb University MVD Russian Federation, St.-Petersburg. - 2000. - p. 261. (*in Russian*)

9. Silnikov M.V. Engineering methods of protection of banks and office buildings. The manual. — NPO Special Materials, St.-Petersburg Inst. of mechanical engineering (VTUZ-LMZ), 1997. (*in Russian*)
10. Silnikov M.V. Engineering protection of nuclear objects // Protection and safety. — 1998, № 2. (*in Russian*)
11. Silnikov M.V., Nelezin P.V., Kalugin V.S. The analysis of application of explosion localizators in MVD // Works Second interregional is scientific - practical conferences « Development new special technique for law-enforcement ». - SPb University МВД Russian Federation, St.-Petersburg. - 2000.-p. 257. (*in Russian*)
12. Silnikov M.V., Serdtsev N.I., Nelezin P.V. On the prospects of methods of explosion localization for the increase of safety of mine clearing in districts and urban areas // Works Second interregional is scientific - practical conferences « Development new special technique for law-enforcement ». — SPb University MVD Russian Federation, St.-Petersburg. - 2000. - p. 261. (*in Russian*)
13. Silnikov M.V., Mikhailin A.I., Orlov A.V., Kozlov A.V. The analysis of design features and efficiency of application of protection methods from terroristic explosion. // Proc. of the 2nd All-Russia scientific - practical conference «Urgent problems of protection and safety ». St.Petersburgh. - 1999- v. 2.-p. 129. (*in Russian*)
14. Gelfand B.E., Silnikov M.V., Mikhailin A.I., Orlov A.V. The attenuation of air-blast waves from the HE explosion in a liquid volume bounded by an elastic envelope // Fizika gorenija i vzryva — 2001. — T. 37. — № 5. — p. 128. (*in Russian*)
15. Silnikov M.V., Mikhailin A.I., Orlov A.V.. The counteraction to terroristic acts involving explosive devices // Proc. of the 2nd All-Russia scientific - practical conference «Urgent problems of protection and safety ». St.Petersburgh. - 1999. - v. 2.-p. 199. (*in Russian*)

16. Gelfand B.E., Silnikov M.V. A choice of the optimal scheme of suppression of air shock waves from HE explosion // Doklady RAN. - 2002. - v. 383, № 1. - p. 37 - 39. (*in Russian*)

CHAPTER 1. EXPLOSION AND EXPLOSIVE PHENOMENA

1.1. Basic concepts

The energy of the substance (or the energy of any process) determines the ability to perform a mechanical work or to release the known amount of heat. The energy of natural processes changes over the wide range represented in Table 1.1.

Table 1.1 Energy of some processes

Process	Energy, J
Photon (wavelength 650 nm)	10^{-19}
Vibration of mosquito wings	10^{-5}
Apple falling from the height of 1 m	1
X-ray radiation (lethal doze)	10^{4}
Atmospheric electricity discharge	10^{8}
Start of the space shuttle	10^{12}
Nuclear bomb explosion	10^{18}
Earthquake	10^{20}
Star explosion	10^{44}

The concept of explosion is closely related to the concept of energy. As a rule, explosion is brought into correlation with noise/sound and thermal effects, as well as damages. Generally explosion can be considered as the sudden physical or chemical change of the state accompanied by thermal and kinetic energy release. The explosion in the atmosphere represents the energy release in rather limited volume during a short time

interval resulting in occurrence of an explosive (blast) wave with finite amplitude [1.1... 1.14]. The pressure wave attenuates with distance from the source of explosion.

Different types of explosions are known:

- Explosion of the boiling devices [1.1];
- Nuclear explosion [1.2,1.3];
- Explosions in the internal combustion engines;
- Electrical discharges [1.3];
- Self-accelerating chemical reactions [1.1,1.3];
- Dust explosions in mines and elevators [1.17].

Some explosions have a natural origin: the volcanoes, the lightning. Others are intentional ones and therefore controllable: explosions of pyrotechnic substances, industrial HE detonation. It is also possible to consider the explosions at industrial man-caused accidents [1.1,1.3] as an individual class of explosions.

Depending on the source of energy it is possible to distinguish physical and chemical explosions. At physical explosions there is no heat release, and the source of explosion is the energy of compressed gas, dust or two-phase gas-liquid system. The example of physical explosion is the bursting of a vessel containing compressed gas [1.6].

The chemical explosions are accompanied by the thermal energy release due to the chemical reactions. Formally, one can consider here such phenomena as nuclear explosions, HE detonations, gas and dust explosions. The most dangerous consequences of explosion is the generation of the dynamic impulse in the form of the blast wave resulting in the destruction of equipment, buildings and the damage of alive organisms. The thermal radiation of explosion products can promote fires [1.1,1.17]. The thermal impulse may cause the damages of surfaces, thermal deformations, break of carrying elements, roof fall.

Table 1.2 Pressure in the products of explosion

Substance	Explosion pressure, kPa

Milk-sugar	380
Sulfur	540
Hydrogen	710
Methane	740
Aluminum	1250
PETN	$34 \cdot 10^6$

It is useful to remind the magnitudes of pressure in the explosion products for various substances, including condensed HE (for example, PETN [1.17]) - see Table 1.2.

1.2. Energy distribution at explosion

The parameters of explosion depend on the energy distribution in the field of explosion and its redistribution as the blast wave propagates away from the source. Initially the energy is stored in the source of explosion in the form of potential energy. At the instant of explosion this energy transforms into the kinetic energy and the thermal energy of the system, which includes now all substance inside propagating shock wave. System is non-steady owing to the increase of the mass of the substance involved in the movement. Another reason of unsteadiness is the proceeding redistribution of energy both in the explosion products and in the gas subjected to shock compression [1.1].

For the analysis of energy distribution we shall accept the following idealization: 1) explosions have the strictly spherical form in originally homogeneous unconfined gas environment; 2) sources of explosion consist both of energy containing material, and of inert confining material, and during the explosion process these substances do not mix up with each other or with an environment atmosphere; 3) shock wave is the only factor resulting in energy dissipation. In such idealized system the potential energy of a source transforms into thermal and kinetics energies of various parts of the system, as well as into the energy of radiation.

Blast wave energy

The energy of the blast wave, which here is understood as a driven part of gas, contains the thermal energy

$$E_p = \int_V \rho C_V (\theta - \theta_0) dV$$

and the kinetic energy

$$E_k = \frac{1}{2} \int_V \rho u^2 dV$$

Where:

ρ is the density;

C_V is the specific heat capacity of a gas at constant volume;

θ is the temperature;

θ_0 is the reference temperature in fresh mixture;

u is the mass speed of a gas;

V is the gas volume. This volume does not include the volume occupied by the explosion products or by the fragments of confinement.

At late stage of the process development, when the kinetics energy of the source and confining material approaches zero, and the amplitude of the blast wave is small (so the energy of dissipation can be neglected) the total wave energy $E_m = E_p + E_k$ remains constant with time. The constancy of the wave energy at the stage of weak explosion is the characteristic feature for explosive processes [1.15].

Residual energy in the atmosphere (« waste energy »)

As the explosions are accompanied by the shock waves, and the atmosphere is subjected to non-isentropic compression, then after returning of the central part of a system to initial pressure, there will be a residual temperature rise. The residual energy (« the waste energy ») [1.2] becomes of a constant value at the stage of weak explosion [1.16].

Kinetic and thermal energies of the fragments

Initially the material of confining envelope will move with acceleration and to be heated due to heat transfer, friction etc. Then the speed of the fragments will decrease (in a limit - down to zero), but the thermal energy partially will be kept.

Kinetic energy of the source material

In any explosion the material of the source or combustion products will be involved in a movement. Kinetic energy of the source material finally will decrease down to zero, when the movement in the near field of explosion will be stopped.

Thermal (potential) energy of the source

The source originally contains all the energy of the explosion in the form of potential energy. During the explosion the portion of the energy of the source is transferred to the other parts of the system, and another portion remains in the source as thermal (potential) energy of the explosion products. This thermal energy dissipates by mixing. The mixing process is rather slow, and it is possible to accept with good accuracy, that the thermal energy of the source is the constant value at late time.

Radiation

The rate of energy radiation quickly decreases, so the losses by radiation reach constant value at quite early stage of explosion.

Distribution of energy in the blast wave

The redistribution of the energy in the blast wave with time is schematically shown in the fig. 1.1 according [1.3]. Note, that at the late stage of process, when the explosion is weak (far field wave), the total energy consists of thermal and kinetic energies of the wave, residual thermal energy, and thermal energy of fragments and products of explosion. Besides, some part of the energy has been lost as a result of radiation, however the losses by radiation are essential only for nuclear explosions [1.2].

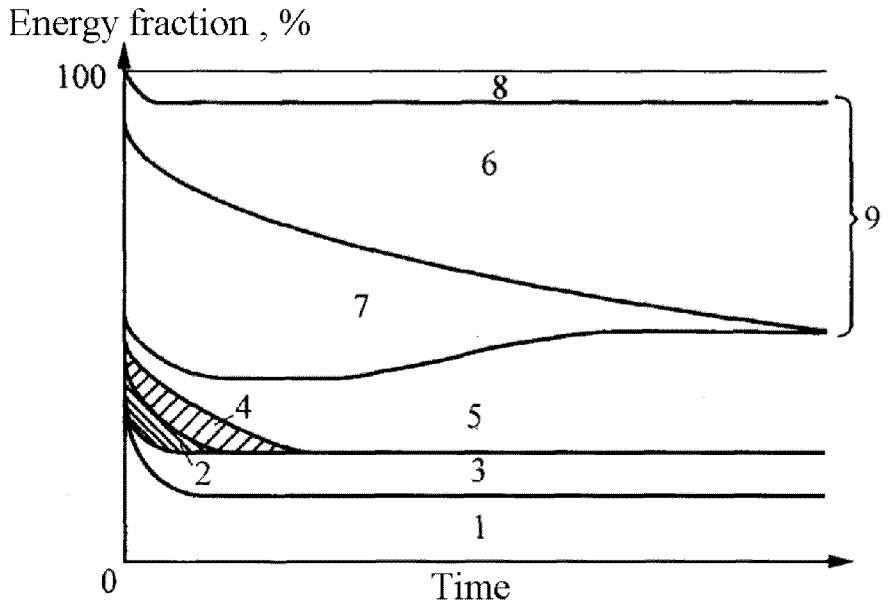

Fig. 1.1. Typical scheme of energy distribution in the blast wave with time: 1 and 2 - thermal and kinetics energies of a source; 3 and 4 - thermal and kinetics energies of fragments; 5 - residual energy; 6 and 7 - thermal and kinetics energies of the wave itself; 8 - energy of radiation; 9 - energy of a wave in a zone of weak explosion

Only portion of the released energy transforms into blast energy in the far field of explosion. The amount of this part must depend on the character of the explosion [1.2,1.4,1.5]. For accidental explosions, when the source volume is rather large, and energy release is, as a rule, rather slow, it is possible to expect the dependence of explosion efficiency on the character of heat release [1.3].

1.3. Propagation of explosion

The blast waves are capable to propagate in all types of medium: air, water, ground and solids. The propagation of the air blast waves depends on the blast wave source type and the geometrical restrictions, i.e. from the presence of obstacles and friction losses [1.10].

For the blast wave propagation in gaseous or condensed medium it is possible to distinguish three characteristic zones (fig. 1.2):

Zone of the initial (not burnout) mixture — *U*;

Zone of reaction — *R*;

Zone of combustion products — *Pr*.

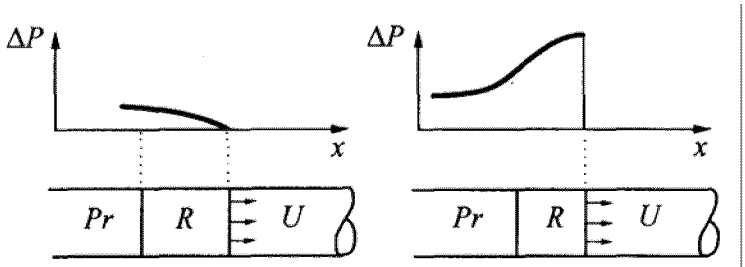

Fig. 1.2. The schemes of pressure distribution for detonation and for deflagration: U — zone of initial products; R — zone of reaction; Pr — zone of combustion products; ΔP— overpressure.

Two basic modes of explosive transformation are known: deflagration and detonation [1.10].

For deflagration mode the movement of the reaction zone on «fresh» (not burned) mixture is controlled by diffusion and heat conduction processes. The density, the pressure and the temperature vary continuously from zone *U* up to zone *Pr*.

For detonation mode the movement of the reaction zone is controlled by the shock compression of «fresh» mixture behind the leading shock wave. The density, the pressure and the temperature in fresh mixture have a discontinuity at the shock front.

In deflagration process, the pressure waves generated in the combustion zone propagate ahead of the front. In detonation process, the «fresh» mixture does not receive any information because of the supersonic speed of the shock front. The speed of the detonation wave is strongly connected to the speed of the combustion zone. The specific features of deflagration and detonation are listed in Table 1.3.

Table 1.3 Properties of detonation and deflagration

Property	Deflagration	Detonation
Pressure	Moderate up to 10^2... 10^5 kPa	High up to 10^4 MPa
Speed	Subsonic < 100 m/s	Supersonic > 1000 m/s
Reaction zone – shock front	Diverge	interrelated
Movement of explosion products	From the combustion wave front	Behind the shock wave front

The formal description of explosive process as isobaric one does not exclude possible effect on the environment. According to the Table 1.3 the speed of deflagration can change in a wide range: from several mm/s up to tens and several hundred meters per second.

For the completeness of the description it is necessary to note, that in long channels at the presence of obstacles the speed of deflagration can exceed the speed of the sound in «fresh» mixture. Such processes were called as quasi-detonations [1.10].

The propagation of the explosion in elongated vessels, pipes, and galleries frequently is accompanied by pressure fluctuations with clearly distinguished phases of compression and rarefaction. Such a behavior is explained by the interaction of the combustion zone with the waves reflected from the end-wall of the channel.

Non-uniformity of combustion speed along the cross-section of the tube and gas flow turbulence increase the combustion velocity. The acceleration of the combustion leads to the generation of the pressure waves according to the scheme given in the fig. 1.3. The compression waves ahead of the combustion zone overtake each other and form the blast wave with sharp pressure discontinuity. Under certain conditions such wave is capable to generate detonation [1.10].

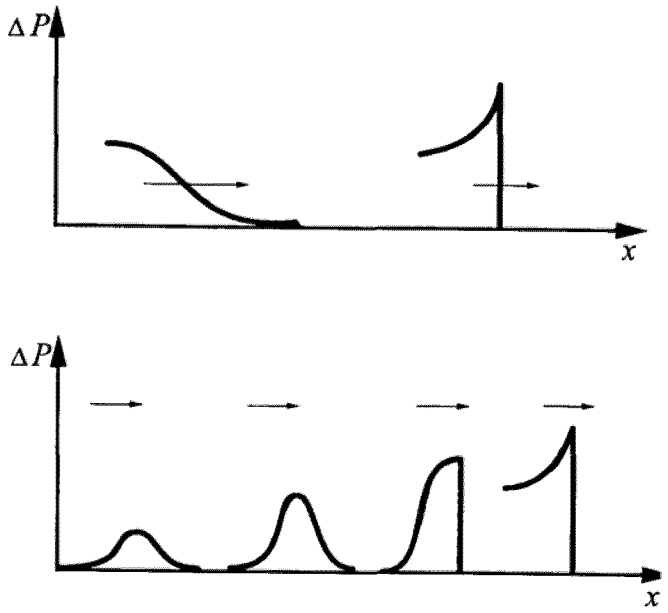

Fig. 1.3. The schemes of shock wave formation: ΔP is the overpressure; x is the distance

The transition of deflagration to detonation is characterized by the jump of the speed, which is caused by "explosion into explosion" effect in space between combustion zone and the leading shock wave. The effect of "explosion into explosion" is also characterized by the retonation wave propagating against the flow [1.8,1.9].

Along with the smooth transition of accelerated flame into detonation wave, the initiation of detonation by a strong shock wave is possible, as it is realized at use of percussion caps in case of industrial HE.

The classical Chapmen Jouguet model, developed more than 100 years ago, predicts the speed, the temperature, and the pressure of detonation products. The model of Zeldovich-von Neumann-Doring (ZND) describes the structure of the detonation wave. The detonation was observed in materials at various conditions:

- The gas detonation was observed and described in 1881 by Berthelot, Vieille, Mallard and le Chatelier. They obtained the speeds of detonation up to 3500 m/s [1.10];

- The detonation in dust suspensions is rare phenomenon in comparison with gaseous detonation. The measure of dust to be exploded frequently described by an explosion index $K_{st} = (dP/dt)_{max}.V^{1/3}$. Here: $(dP/dt)_{max}$ is the highest rate of pressure rise during explosion in the vessel of volume V. Indexes K_{st} are used for the subdivision of dust systems according to explosion classes. A coal dust gets into the lowest, first explosion class, and the detonation in such system was detected only in tubes with the diameter more than 0,6 m [1.17];

- Black gunpowder or rocket propellants usually burn down in deflagration mode.

The explosive transformation of condensed HE is realized in detonation mode [1.1]. In Table 1.4 the properties of some HE are indicated.

Table 1.4 Properties of some condensed HE

Explosive substances	TNT equivalent	Density, 10^{-3} kg/m^3	Detonation speed km/s
Protective explosives	0,40	1,15	2,5
ANFO	0,75	0,80	3,0
Water gels	0,85	1,20	4,5
Emulsions	0,69	1,15	5,1
Gelatins	0,90	1,45	6,0
Nitroglycerine	1,48	1,59	7,6
PETN	1,28	1,77	8,3
RDX	1,18	1,65	8,7

As an example we specify, that the detonation of 1 kg HE with specific heat of explosion of 5000 kJ/kg and packed in the tube of length 1 м results in power of $30 \cdot 10^6$ kW. It is equivalent to the power of 30 electrical power stations with 1000 MW each.

1.4 Exothermal reactions, thermal explosions and auto-accelerating processes in the condensed media

The energy during combustion is released by means of the chemical reactions. Burning represents the self-sustaining exothermal process. The most important phenomena at combustion are the physical processes of heat and mass transfer. Heat of combustion, diffusion of chemical products and gas movement are determined by the transformation of chemical energy into thermal energy by exothermal reactions [1.10].

The explosions are frequently accompanied by the release of gaseous products. However it is possible to specify fast and power-intensive explosive processes without the formation of gaseous products [1.1]. For example the gasless explosion of thermit structures:

$Fe_2O_3 + 2Al \rightarrow Al_2O_3 + 2Fe.$

This reaction releases about 4000 kJ/kg of heat, but is not accompanied by serious mechanical effects.

Some exothermal reactions exhibit significant pre-warming-up, capable to convert into an open fire [1.3]. As an example we specify the reaction

$2FeS_2 + 7O_2 + 16\ H_2O \rightarrow 2H_2SO_4 + 2FeSO_4 \cdot 7H_2O + 1321$ kJ.

With this reaction there is an accumulation of heat, and the self-ignition is possible if no cooling exists in a system.

Other chemical substances are capable to decomposition in the absence of the oxidizer at increased temperature. The process can occur with the release (exo -) or the absorption (endo -) of heat. The thermal explosion is rather probable under conditions of

exothermal decomposition and insufficient heat losses. The pressure starts to increase if the disintegration of substance occurs with gas production in closed volume. There is a real danger of vessel burst followed by the selfignition of disintegration products, if those are combustible substances [1 .3].

When solid combustible materials are burning, the heat conduction process dominates, and diffusion is negligible in comparison with gases. Therefore, the processes of heat transfer are basic at burning of solid combustible structures.

The thermal explosions or auto-accelerating reactions are possible in vessels, reactors or power-intensive substances depots. In all cases the thermal explosions are connected to the accumulation of heat and the acceleration of chemical reaction. Dynamics of thermal explosion depends on the sizes and geometrical form of reacting substance, the temperature. If there is a gas release during thermal explosion, then the pressure growth is marked and the external explosive effects in the form of blast waves are possible. The reasons of auto acceleration of chemical reactions are various, and most principal of them are [1.1]:

- Auto-catalytic processes with the formation of intermediate substances accelerating the basic reaction;
- Sudden exothermal disintegration of half-products;
- Rapid transition of explosive process into the mass of the not reacted «fresh» products.

The uncontrollable course of chemical reactions at nitration, polymerization is not similar to the typical gaseous or dust explosion by a number of reasons. More often the auto-accelerating chemical processes occur in the substance with the high initial density at the large stored energy. The same processes differ by significant final pressures because of large gas generation in the confined space. The two-phase medium (gas bubbles - condensed phase) is formed during explosion. Emission of half-products from space, where there was a thermal explosion, into surrounding atmosphere quite often becomes the reason of the secondary fires and explosions. Here pertinently to note two dangerous scripts.

The first script is realized, when the container (vessel, capacity) bursts under the influence of pressure from the heated combustible vapor or half-products of disintegration and the contents of the container, quickly evaporating, is thrown out into the atmosphere. Such phenomenon is accompanied by moderate blast effect [1.6]. More essential is the occurrence of the fireball making a powerful thermal impulse on the environment at explosion location.

Besides, under the influence of thrust from two-phase jets, the parts of the reaction vessel are rejected to significant distances and make additional destructions. In the literature this type of explosion was called BLEVE (boiling liquid evaporation with the subsequent vapor explosion). Finally question on a demolition effect due to BLEVE is not solved yet [1.3].

The second script of explosive process develops, when the large mass of explosive material is thrown out from the confinement and is not ignited immediately. The fuel is mixed up with the air and forms a cloud of the mixture within explosion concentration limits. Three ways of development of a dangerous situation are possible:

- The cloud does not find a source of ignition and safely dissipates in the atmosphere;
- The cloud finds a source of ignition, but burns down in a safe, slow mode of burning without essential blast effects [1.3];
- After ignition the cloud burns down in fast (up to a detonation) mode of combustion with essential demolition effects.

Last variant of explosion is called UVCE (unconfined vapor cloud explosion) [1.1].

1.5. Gas and dust explosions

Typical examples of chemical explosions are gas and dust explosions. The necessary condition of their realization is the simultaneous presence of the ignition source and explosive atmosphere. Such atmosphere is formed when the air is mixing with the combustible gas or the combustible dust in the certain proportions. The upper and lower

concentration limits outside which the explosive transformation is impossible [1.17] are known.

The state of a gaseous mixture is supported quite long period of time due to the diffusion process. The dust accumulates due to the gravitational forces. The combustible gas mixture is formed easier, than the dust one. Necessary conditions for dust explosion are following:

- The dust must be combustible, i.e. could burn in air or in oxygen;
- The distribution of particles of a dust by size should provide the propagation of the flame;
- The dust does not agglomerate at the emission in an atmosphere;
- The concentration of a dust should be within explosion limits;
- The concentration of gaseous oxidizer should be sufficient to support combustion;
- The presence of the powerful ignition source.

It is quite clear, that in real conditions the simultaneous performance of the listed conditions in all points of dusty space is not plausible. One of the reasons of formation and development of dust explosion is the occurrence of pressure waves at local energy release. These waves pass the dust layers causing the additional formation of the combustible mixture, either because of friction at the boundary of the dust layer - air or due to the vibration under the action of pressure waves. According to the described sequence of events the initial explosive process is called the primary explosion, and the subsequent stages – the secondary explosion [1.17].

1.6. Characteristics of gas or dust explosion

The typical pattern of pressure history at gas or dust explosion is shown in the fig. 1.4 [1.17].

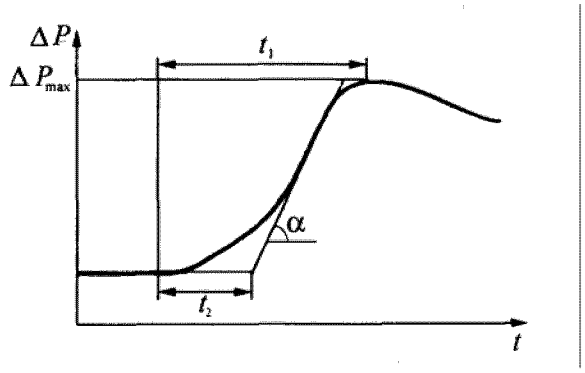

Fig. 1.4. The basic parameters of a pressure wave at explosion: ΔP_{max} — maximal explosion pressure increase; $tg\alpha=(dP/dt)_{max}$ — maximal rate of pressure increase; t_1 — time of pressure increase; t_2 — delay time

Explosion can be characterized by the parameters:

- Maximal pressure of explosion P_{max}
- Maximal rate of pressure rise $(dP/dt)_{max}$

The listed parameters are determined experimentally by standard equipment at central ignition of the dust in a wide range of concentration. Sometimes in addition the time of pressure rise at burning t_1, and the time of explosion delay t_2 are measured.

The value P_{max} at explosion in a spherical or cubic vessel does not depend on the size of a vessel. The rate of pressure rise $(dP/dt)_{max}$ decreases with the increase of the vessel size according to the formula $(dP/dt)_{max} V^{0.33} = K_{st}$.

Parameter K_{st} is the characteristic value of the dust for each substance. According to the value K_{st}, combustible dusts are referred to the various explosion classes, as it is shown in Table 1.5.

Table 1.5 Explosion classes of the combustible dusts [1.17]

Designations of classes	K_{st} , MPa м c^{-1}
St0	0
Stl	1... 20

St2	20... 30
St3	> 30

It is necessary to remember that K_{st} depends on the conditions of explosion and use only the values measured by standard technique. Other factors (some of them are listed in tab. 1.6 [1.17]) may influence the value of explosion index.

For example, the dependence $P_{\max}$ and $(dP/dt)_{max}$ on initial pressure for coal dust explosion in air is shown in fig. 1.5.

Table 1.6 Factors, influencing the rate of pressure rise at explosion [1.17]

The factor of influence	dP/dt_{max} corresponds to
The size of particles	Fine particles
Concentration	Stoichiometric
Source of ignition	Powerful source
Type of a source	Central
Reference temperature	Increased
Initial pressure	Increased
Turbulence	Increased
Gases	Additives of combustible gases and vapors

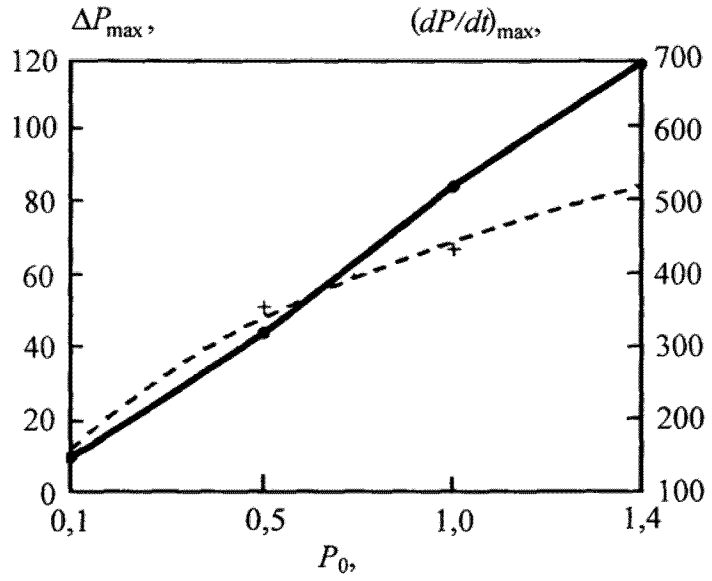

Fig. 1.5. Effect of initial pressure P_0 on the explosion parameters: — Dependence of P_{max} on P_0; — — Dependence of $(dP/dt)_{max}$ on P_0

The practice shows, that any measures aimed to increase the dust particles size, dust accumulation, decrease of the turbulence, elimination of potential sources of ignition really reduce the danger of explosion [1.17].

1.7. «Ideal» explosions

Some characteristics of explosions in air can essentially depend on the parameters of the source, which forms the blast wave. By definition, the process is considered as an explosion, if the energy is released rather quickly and inside the quite small volume [1.1]. The energy of explosion E, density of energy release E/V and the rate of energy release, i.e. power are the basic parameters of the source, which determine amplitude, duration and other characteristics of the blast wave. Is established, that the main properties of blast waves can be determined on the basis of unilateral parameter - total energy - without taking into account the density of energy release and the source power. The point sources, nuclear bombs, laser sparks and condensed explosive substances (HE) are the basic four sources of «ideal» explosions. The nuclear bombs and laser sparks are mentioned here for completeness of the review and will not be discussed further.

The explosions generated by condensed HE are useful for investigating the accidental explosions, because the majority of experimental data on ideal explosive waves are obtained using detonation of condensed HE. These HE generate practically ideal explosive waves, because the density of HE is large in comparison with the density of air and, subsequently, the energy release per unit volume is significant. For the military purposes, the most important characteristic of HE efficiency is the energy content per unit mass (or specific heat of explosion), therefore usually in tables both this characteristic, and the density of HE are listed.

The point explosion source is the model, which is convenient for the mathematical description of the real explosion process and, hence, has theoretical importance. Point explosion is considered as the explosive process, at which the blast wave is formed as a result of instant release of finite amount of energy at some point of the homogeneous atmosphere. Numerous studies of point explosions were performed for the cases of both the atmosphere «of real air», and the atmosphere «of ideal gas», where the ratio of specific heats at constant pressure and constant volume is $\gamma = 1{,}4$.

The blast waves are attenuating with distance from the source of explosion, therefore it is accepted to specify three basic zones. In the zone, nearest to a source, so-called zone of strong explosion, the pressure in the wave is so high, that the external pressure can be neglected. The flow is self-similar and is described by known analytical dependences [1.7, 1.8,1.9]. The intermediate zone represents significant practical interest because overpressure and impulse are rather high to produce significant destructions. However the description of the process in this zone has no analytical solution and should be done with the help of numerical methods [1.4, 1.6, 1.11]. The far field of explosion (or zone of weak explosion) is following the intermediate zone. The analytical solution in far field is admitted from the viewpoint that if at some distance the time history of overpressure is known, then it is easy to construct the appropriate dependence for the larger distances [1.15].

There are theoretical indications that in the zone of weak explosion the self-sustained N-wave can be observed, in which the process in a positive phase of overpressure does not depend on the flow in internal area [1.12].

1.8. Basic features of nonideal explosions

The majority of sources of nonideal explosions has essentially smaller (than the ideal sources) density of energy release, final time energy release, and also requires some environment for realization of explosion. The explosions of chemical reactors, as a rule, are preceded by uncontrolled development of reaction in reactor, until the threshold pressure will be exceeded. The explosions of gases and dust in the open-ended volumes usually result into fires only. The damages of vessels under pressure with non reacting gases can serve as the sources of strong explosions, but such explosions will take place only at strength (before damage) construction.

The researches specify the presence of two factors resulting in nonideal blast waves from the spherical source. These are the final volume of the source and the final time of energy release in it.

By calculating the external work at slow adiabatic expansion of sphere to the initial pressure level, we shall obtain the formula for effective energy of exploding sphere at relative density of energy $q=(T_e/T_0)$-1 [1.13,1.14]:

$$\frac{E_s}{Q}=\frac{1}{q}\left[(1+q)-(1+q)^{1/\gamma}\right]$$

Where Q is the total heat released by the source. The value E_s describes the maximal work, which can be made by any spherical explosion. In a limit at $q\to\infty$ for fixed Q (point source) $E_s/Q\to 1$, whereas at $q\to 0$ and for fixed Q :

$$E_s/Q\to(\gamma\text{-}1)/\gamma$$

The essential factor for nonideal explosion is the time of energy release in a source t_c. Comparing this value to the time of sound propagation from the center to border of the source, we shall obtain dimensionless time of energy release

$$\tau = t_c c_0 / r_0$$

Here c_0 is the sound speed in the source before energy release, r_0 is the radius of the source.

It is necessary to indicate the other characteristics of nonideal explosions. At rather slow energy release (for example, at burning speeds smaller 45 m/s, or at dimensionless time of heat release $\tau > 0{,}5$) the formation of shock waves is not observed, though the positive impulse of pressure in quasi-acoustic compression wave is kept. Other specific feature of blast waves from the sources with small density of energy release is that the amplitude of pressure of a negative phase becomes comparable to the amplitude of the positive phase [1.15]. For this reason the blast waves from the specified sources essentially differ from the blast waves of ideal sources. In the blast wave from ideal source there is a negative phase, but its amplitude, as a rule, is small in comparison with amplitude of a positive phase, and the damage caused by the negative pulse, is insignificant.

Refernces to chapter 1

1.1. Baker W.E., Cox P.A., Westine P.S., et.al. Explosion hazards and evaluation, Elsevier, Amsterdam-N.Y.-Oxford, 1983,798 p.

1.2. Bethe HA, Fuchs K., Hirschfelder H.O., Magee J.L., Peierls R.E., and von Neumann J. Blast Wave, LASL 2000, Los Alamos Scientific Laboratory (August 1947) (distributed March 27,1958).

1.3. Strehlow R.A. and Baker W.E. The Characterization and Evaluation of Accidental Explosions. Progress in Energy and Combustion Science, 1976, 2, 1, pp. 27 - 60 (Also NASA CR134779), 1976.

1.4. Thornhill C. K. Explosions in Air ARDE Memo (B) 57/60, Armament Research and Development Establishment, England, 1960.

1.5. Lehto D.L. and Larson R.A. Long Range Propagation of Spherical Shock Waves from Explosions in Air. NOLTR 69 — 88, Naval Ordnance Laboratory, White Oak, Maryland, 1969.

1.6. Baker W.E., Kulesz J.J., Ricker R.E., Westine P.S., Parr V.B., Vargas L.M. and Moseley P.K. Workbook for Estimating the Effects of Accidental Explosions in Propellant Handling Systems. NASA Contractor Report 3023, Contract NAS3-20497, NASA Lewis Research Center, 1978.

1.7. Sakurai A. Blast Wave Theory. In: Basic Developments in Fluid Mechanics, 1. Morris Holt, Editor, Academic Press, New York, pp. 309-375,1965.

1.8. Bach G.G. and Lee J.H.S. An Analytic Solution for Blast Waves. AIAA Journal, 8, pp. 271 - 275,1970.

1.9. Oppenheim A.K., Kuhl A.L., Lundstrom E.A. and Kamel M.M. A Parametric Study of Self-Similar Blast Waves. J. Fluid Mech., 52, Part 4pp. 657 - 682,1972.

1.10. Zeldovitch Ya.B., and Kompaneetz A.C. The theory of detonation. Fizmatgiz, M., 1956 *(in Russian)*.

1.11. VonNeumann J. and Goldstine H. Blast Wave Calculation. Communication on Pure and Applied Mathematics, 8, pp. 327 — 353 (Reprinted in John von Neumann Collected Works, A.H. Taub, Editor, Volume VI, Pergamon Press, New York, pp. 386 — 412), 1955.

1.12. Whitman G. Linear and nonlinear waves. D.Wiley Interscience Public., New York — London — Sydney - Toronto, 1974,636p.

1.13. Brinkley S.R. Determination of Explosion Yields. AIChE Loss Prevention, 3, pp. 79 - 82,1969.

1.14. Baker W.E. Explosions in Air, University of Texas Press, Austin, Texas, 1973,266 p.

1.15. Rayleigh L. The Theory of Sound, Volume II, Dover Publications, 1945, pp. 109 - 114.

1.16. Zeldovitch Ya.B. Theory of shock waves and introduction in gasdynamics. - M.: USSR Ac.Sci Publ., 1946,186p. *(in Russian)* .

1.17. Ekchoff R. Dust explosions in the process industries Buterworth-Heineman, Oxford, 1991,591 p.

CHAPTER 2. THE BASIC PARAMETERS OF BLAST WAVES FROM CONDENSED HE DETONATION IN AIR

2.1. Initial status

The application of condensed HE in practical tasks has resulted in the necessity of numerous measurements of the parameters of the blast waves generated by detonation products expanding into environment. Such an environment can be a solid body, liquid or multiphase medium. Below we consider basically the cases of HE charges detonation in a gas - usually in an air.

What causes the necessity of new revision of a question about the parameters of the blast waves generated by the detonation of condensed HE in air? The existence of classical measurements of blast waves parameters in air [2.1], unfortunately, does not allow considering the case been resolved completely and finally. Moreover, the use of these data frequently results in mistakes connected to the restrictions, at which the measurements were carried out.

It is interesting to note, that in the above mentioned reference [2.1] majorities of possible restrictions are considered and the appropriate precautions are given. However, these precautions were not analyzed subsequently, and, as a result, the most of the given expressions were used without any reservations.

The dependence of blast waves parameters on the power and geometrical characteristics are experimentally determined. Form the other side, these dependencies, been applied as reference analytical expressions, often did not take into account the errors of measurements and areas of applicability, that was emphasized in the appropriate primary sources.

There were no reliable measurements of parameters of air shock waves after publishing the works [2.1,2.2,2.3] in the domestic literature. At the same time, the detailed materials on the measurements of fields of explosive parameters under various conditions

of HE charges detonation in air in view of the presence of limiting surfaces were published continuously in the world literature.

Additional collection of actual measurements of air shock waves parameters is now gathered in [2.4... 2.25,2.39... 2.41]. On the basis of these measurements it is possible to add the results given in the mentioned above sources, and correct them in particular cases. Moreover, it is possible to consider additional formulas for calculating the parameters of the normal and oblique reflected waves at limiting surfaces. The generalization of well-known and new data allows more correctly to estimate the scale of errors arising from the use the so-called TNT equivalents for explosions of fuel-air mixtures, dust explosions etc., but for the condensed HE only.

In the literature the various types of condensed HE detonations are analyzed:

1. Free-air (or simply air) explosion — detonation of HE charge in a gas (more often in air) in absence of reflecting surfaces (fig. 2.1, a).
2. Surface (ground) explosion — detonation of HE charge in a gas (air) in case, when the HE charge is placed on a limiting surface (ground) (fig. 2.1, b).
3. Above-ground explosion — detonation of HE charge in air at certain distance from a limiting surface (ground) (fig. 2.1, c).
4. Underground explosion — detonation of HE charge inside the ground.
5. Underwater explosion — detonation of HE charge, inside the liquid.

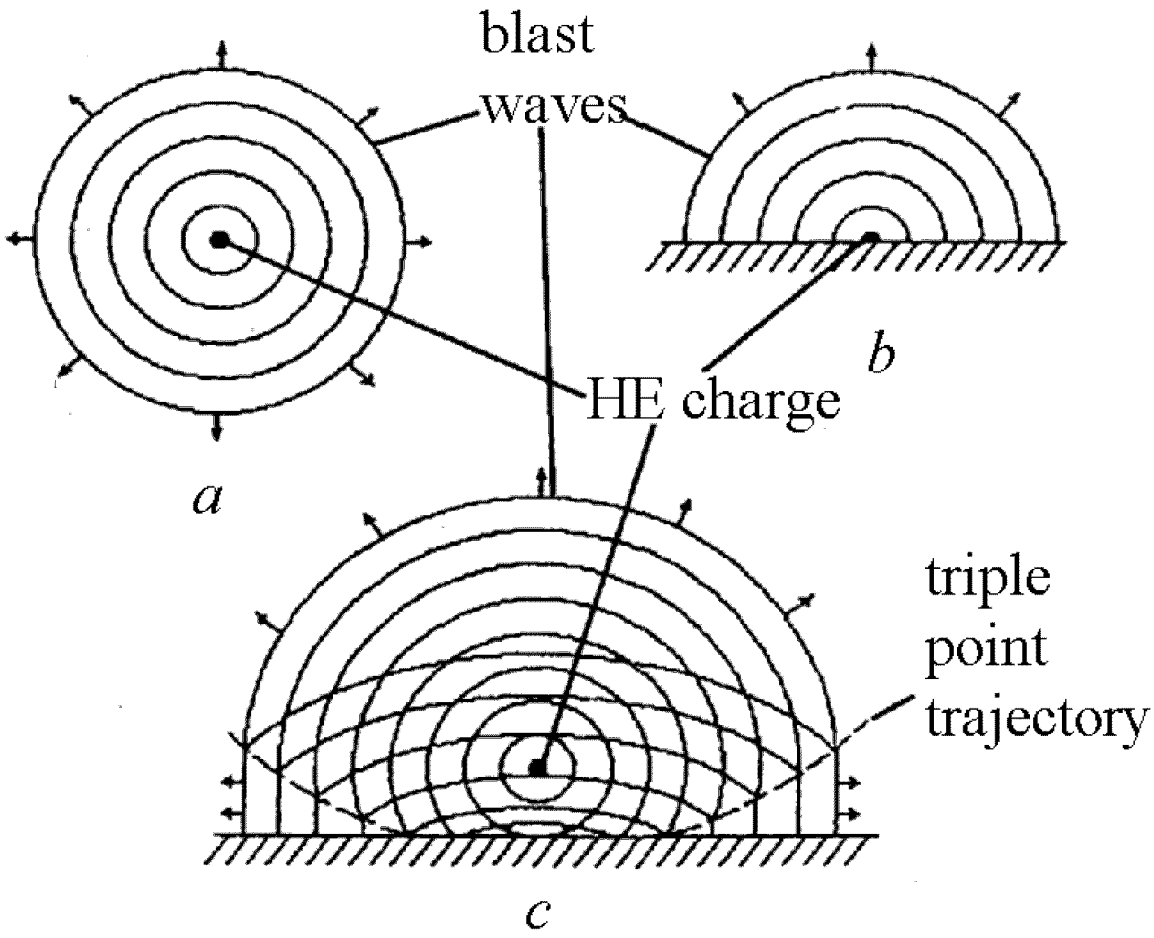

Fig. 2.1. The scheme of HE charge detonation: a — Air explosion; b — Ground explosion; c — Above - ground explosion

The wave overpressure is usually measured with satisfactory accuracy ±10%. This fact must be taken into account when performing the analysis of the experimental dependences. Note, that other parameters of the waves are measured with greater error that must be also taken into account when they are used as the standards.

2.2. Parameters of shock waves for free-air explosion

The air explosion of HE is characterized by the minimal distortions of the process of explosion products expansion into the environment and, hence, is least complicated by various waves refractions and reflections at any obstacles nearby the charge (such, as the solid walls or the surface of a ground or liquid).

In order to minimize the distortion of expansion process, the air explosions, as a rule, are carried out with the small or moderate (by weight) HE charges. In [2.1] most of the measurements were performed for ground explosion. The sufficient number of correct measurements of air explosion parameters is presented in [2.4... 2.9] at shock waves (SW) front overpressures $\Delta P = P_1 - P_0$ from 5.5 up to 0.003 MPa. Here P_1 and P_0 are the pressures behind and ahead of the front accordingly. In the field of small overpressures $\Delta P < 0.003$ MPa the data were obtained on the basis of the analysis [2.7] and some measurements in [2.8,2.9]. A lot of information on the parameters of air explosion may be gathered from [2.4,2.5].

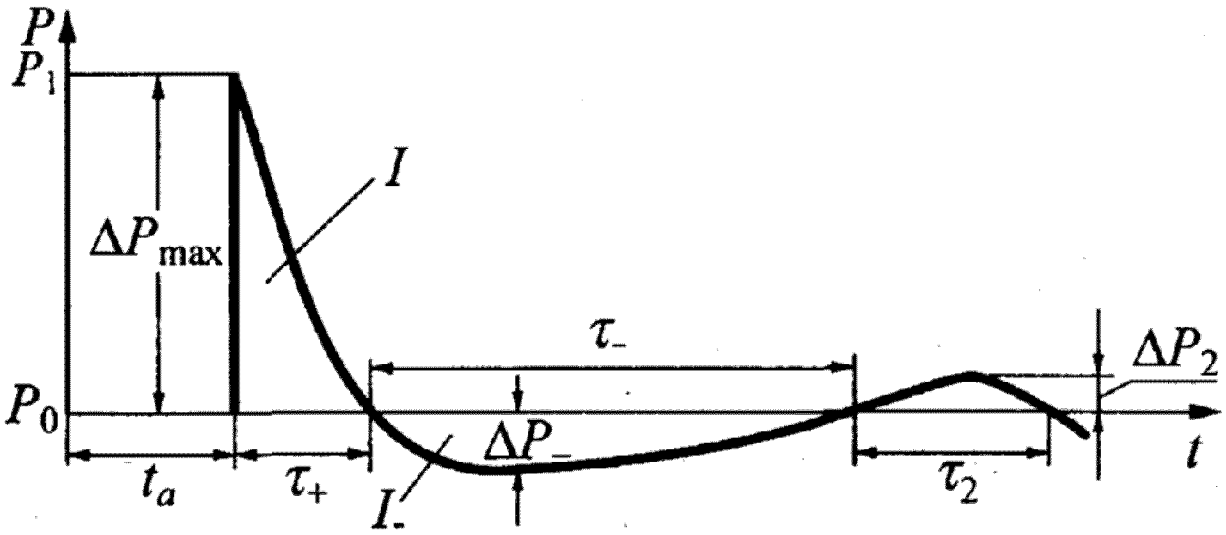

Fig. 2.2. The scheme of measured parameters of the blast wave: t_a is the time of arrival; τ_+ is the duration of a positive phase; τ_- is the duration of rarefaction wave; ΔP_{max} is the amplitude of pressure wave; ΔP_- is the amplitude of rarefaction wave; I is the impulse of a compression phase; I_- is the impulse of a rarefaction phase; ΔP_2 and τ_2 - secondary pressure rise and its duration

The diagram of the pressure structure in the blast wave is given in the fig. 2.2 in order to obtain clear understanding of the parameters discussed further. The starting time is counted from the moment of the blast wave emerges from the center. The value t_a means the time of arrival of the wave to the position of measurement at the distance R from the center of explosion of the spherical charge of radius R_0. The impulse of the phase of compression is calculated using formula:

$$I = \int_{t_a}^{t_a+\tau_+} \Delta P dt$$

The impulse of the compression phase is the most important characteristic of an air wave together with value of overpressure ΔP.

To characterize some consequences of explosion the magnitudes of amplitude of rarefaction waveΔP_- and impulse of a negative phase of pressure

$$I = \int_{t_a+\tau_+}^{t_a+\tau_++\tau_-} \Delta P dt$$

can be indicated.

The durations of compression wave τ_+ and rarefaction waveτ_- are important for the analysis of the resonant response of a target under the action of air shock wave. The parameters of the secondary pressure increase ΔP_2 and τ_2 are usually ignored, though for estimations it is possible to assume with high accuracy that $\Delta P_0 = \Delta P_-$.

2.3. Shock waves overpressures at air explosion

Various formulas for determination of overpressure at the shock front are presented in published works. Let's outline some of them. Brode [2.10] on the basis of data processing of the numerical calculations proposed two expressions for calculation of the overpressures:

$$\Delta P = 0{,}657 R_*^{-3} + 0{,}098 \qquad \text{for } \Delta P > 0{,}1 \text{ MPa}$$

$$\Delta P = 0{,}096 R_*^{-1} + 0{,}143 R_*^{-2} + 0{,}574 R_*^{-3} - 0{,}002 \qquad \text{for } \Delta P = < 0{,}1 \text{ MPa}$$

Here ΔP , MPa; $R_* = R / G^{0{,}33}$, m/kg$^{0{,}33}$; R, m, - distance; G, kg, - weight of HE charge.

In [2.11] three expressions for calculation are given for different intensities of the wave (TNT explosion):

$\Delta P = 1{,}38R_*^{-1} + 0{,}543R_*^{-2} - 0{,}035R_*^{-3}$ For range 0,05 < R* < 0,3, m/kg^{0,33};

$\Delta P = 0{,}607R_*^{-1} + 0{,}032R_*^{-2} + 0{,}209R_*^{-3}$ For range 0,3 < R* < 1,0, m/kg^{0,33},

$\Delta P = 0{,}065R_*^{-1} + 0{,}397R_*^{-2} + 0{,}322R_*^{-3}$ For range 1,0 < R* < 10, m/kg^{0,33}.

In [2.1,2.3] for TNT-RDX mixture (50 % TNT and 50 % RDX) the following expression is written:

for air explosion, in the range 1> R* > 0,1, m/kg^{0,33}

$$\Delta P = 0{,}085R_*^{-1} + 0{,}3R_*^{-2} + 0{,}82R_*^{-3},$$

or for ground explosion

$$\Delta P = 0{,}106R_*^{-1} + 0{,}45R_*^{-2} + 1{,}6R_*^{-3},$$

(2.5)

The above expression is more convenient, than three formulas from [2.11]. The coefficients in (2.1... 2.5) depend on the type of HE and must be corrected to take into account the heat of explosive transformation for particular HE. For example, the formula from [2.3] for TNT air explosion takes a form

$$\Delta P = 0{,}081R_*^{-1} + 0{,}28R_*^{-2} + 0{,}707R_*^{-3},$$

(2.6)

or for ground explosion

$$\Delta P = 0{,}101R_*^{-1} + 0{,}42R_*^{-2} + 1{,}41R_*^{-3},$$

(2.7)

Generalization of the experimental data made in [2.5] in [2.12] for TNT air explosion yields

$$\Delta P = 1{,}7 \cdot 10^{+3} \exp\left(-7{,}5 R_*^{0{,}28}\right) + 0{,}0156,$$

and for ground TNT explosion

$$\Delta P = 1{,}7 \cdot 10^{+3} \exp\left(-7{,}14 R_*^{0{,}28}\right) + 0{,}0156$$

At $0{,}1 < R^* < 8$ m/kg$^{0{,}33}$.

In a far field of explosion, namely at $R^* > 8$ m/kg$^{0{,}33}$ for TNT air explosion

$$\Delta P = 8 \cdot 10^{+3} \exp\left(-10{,}7 R_*^{0{,}1}\right),$$

For ground TNT explosion

$$\Delta P = 8 \cdot 10^{+3} \exp\left(-10{,}46 R_*^{0{,}1}\right).$$

All presented dependences are written with the help of Sadovsky – Hopkinson variable $R. = R/G^{0,33}$. Other Sadovsky – Hopkinson variables are $\tau^* = t / E^{0,33}$, $I_* = I / E^{0,33}$, where E is the energy of explosion.

Sadovsky – Hopkinson variables are not dimensionless. Therefore all expressions for the blast waves parameters in Sadovsky – Hopkinson variables are valid only at that pressure of an environment and speed of a sound, at which the measurements are made. The dependences of the blast waves parameters on geometrical and power values are not universal, since the effects of initial pressure and sound speeds in the gas are not taken into account. Sachs variables are more universal for the description of blast waves parameters:

$$\overline{P} = \Delta P / P_0 \qquad \overline{R} = R_* P_0^{0,33} / E^{0,33},$$

$$\overline{t} = t c_0 P_0^{0,33} / E^{0,33} \qquad \overline{I} = I c_0 \left(E P_0^2\right)^{-0,33}.$$

Here P_0, c_0 - pressure and sound speed in an environment. Sachs variables are dimensionless, and one can construct the dependences of the appropriate functions $P = f(R)$; $t = f(R)$; $I = f(R)$ suitable for any initial conditions. Quite often the researches use the ratio of the distance from the center of explosion R to a radius of the charge R_0. It is possible to show, that there are rather simple relation between three arguments:

$$\overline{R} = R_* \left(P_0 / E_{sp} \right)^{0,33},$$

$$R = \overline{R} / R_0 \left[P_0 \left(\frac{4}{3} \pi \rho_0 E_{sp} \right)^{-1} \right]^{0,33}.$$

Here E_{sp} is the specific heat of explosion, ρ_0 is the density of HE. It is possible to use the following formulas in calculations for different geometrical sizes:

$$R / R_0 = K_1 \overline{R}, \quad R_* = K_2 \overline{R}, \quad R / R_0 = \left(K_1 / K_2 \right) R_*.$$

The values of the coefficients for some HE are given in table 2.1. K_{TNT} is the TNT energetic equivalent of HE other, than TNT.

Table 2.1 Geometrical factors for the calculation of the blast fields and the TNT equivalents

HE type	ρ, kg/m^3	$E_{\text{уд}}$, J/kg	P_0 = 0.1 MPa		P_0 = 1MPa		K_{TNT}
			κ_1	κ_2	κ_1	κ_2	
TNT/RDX 50/50	1660	$5{,}107 \cdot 10^6$	67,37	3,66	31,5	1,72	1,13
TNT	1590	$4{,}517 \cdot 10^6$	64,29	3,51	30,2	1,65	1,00
RDX	1650	$5{,}356 \cdot 10^6$	68,76	3,71	32,3	1,74	1,18
TNT/RDX 40/60	1690	$5{,}182 \cdot 10^6$	68,50	3,68	31,12	1,73	1,15
Nitromethane	1000	$4{,}517 \cdot 10^6$	55,2	3,51	25,6	1,65	1,00
PETN	1770	$5{,}800 \cdot 10^6$	74,2	3,81	34,4	1,74	1,28
Nitroglycerine	1590	$6{,}7 \cdot 10^6$	77,1	4,1	35,7	1,88	1,48
HMX	1900	$5{,}68 \cdot 10^6$	75,3	3,79	34,9	1,78	1,26
Nitrogyanidine	1620	$3{,}02 \cdot 10^6$	58,8	3,11	27,3	1,44	0,67
Tetryl	1730	$4{,}517 \cdot 10^6$	67,7	3,51	31,4	1,65	1,00

HE type	ρ, kg/m^3	$E_{уд}$, J/kg	P_0 = 0.1 MPa		P_0 = 1MPa		K_{TNT}
			κ_1	κ_2	κ_1	κ_2	
Ammonium Nitrate	–	$3{,}8 \cdot 10^6$	–	3,35	–	1,56	0,84

What is the difficulty of application of some of the given dependences for ΔP estimations?

It was specified in [2.1], that when calculating the argument R^* one must use not complete weight of the charge G, but only the weight of its so-called «active» part G_a. The value G_a decreases with the decrease of G. There are also specified the values of $\alpha = G/Ga$ for TNT. At G = 1 kg we have α = 30 %, accordingly at G = 8 kg, α = 65 % and at G = 50 kg, α = 80 %. In the case of amatol there is additionally dependence on the distance from the center of explosion (or from the wave overpressure). The corresponding data are listed in tab. 2.2.

Table 2.2 Relative weight of an active part of a charge (amatol), %

Weight of a charge, kg	Pressure in the wave, MPa				
	0,2	0,4	0,6	1,0	2,0
25	70	66	64	60	60
100	77	73	74	73	73
500	84	86	86	83	83

As can be seen from above presented information, only at G> 50 kg it is possible to apply the formula from [2.1] to estimate ΔP without any exceptions. Even larger limit G > 200 kg is indicated in [2.1].

Let's analyze the type of curves $\Delta P/P_0 = f(R_*)$, shown in the fig. 2.3 for various expressions, taking into account the above remarks. The line 1 is plotted using the

Sadovsky formula, line 2 – Baker – Held dependence from [2,4], line 3 using expression (2.2) from [2.11], line 4 - Brode formula [2.10], and line 5 - are the data from [2.6]. As it is seen at $\Delta P/P_0 > 40$ the formulas of Sadovsky and Brode are not suitable for estimations and deviate from the data of experiment. It was already pointed out in [2.3]. One must take into attention rather wide disorder of the ΔP measurements, which was also underlined in the review [2.4]. As an illustration, some more dependences are given in the fig. 2.4. Line 1 is obtained in [2.7], line 2 - in [2.8], line 3 - in [2.9].

The analysis of the presented data shows, that the accuracy of the formulas from [2.1, 2.11] in the field of their applicability in definition of pressure does not exceed 15 %. A smaller accuracy of ΔP measurements (up to 30 %) was pointed out in [2.10].

The specified accuracy is satisfactory at the direct estimation of overpressure by the value of explosion energy in view of the remarks from [2.1]. However one can obtain significant error (up to 100%) in the backward expert estimations of the released energy by overpressure (as in cases of TNT equivalent use).

The error is especially great in the practically important far field, at $R^* > 1$ m/kg$^{1/3}$, where $E \sim (\Delta PR)^3$.

Finishing the consideration of expressions for overpressure in a wave from air explosion, we shall present the data for the amplitudes of rarefaction waves [2.6]. In table 2.3 the amplitude of rarefaction wave in comparison with the amplitude of the shock wave are shown for various R^*.

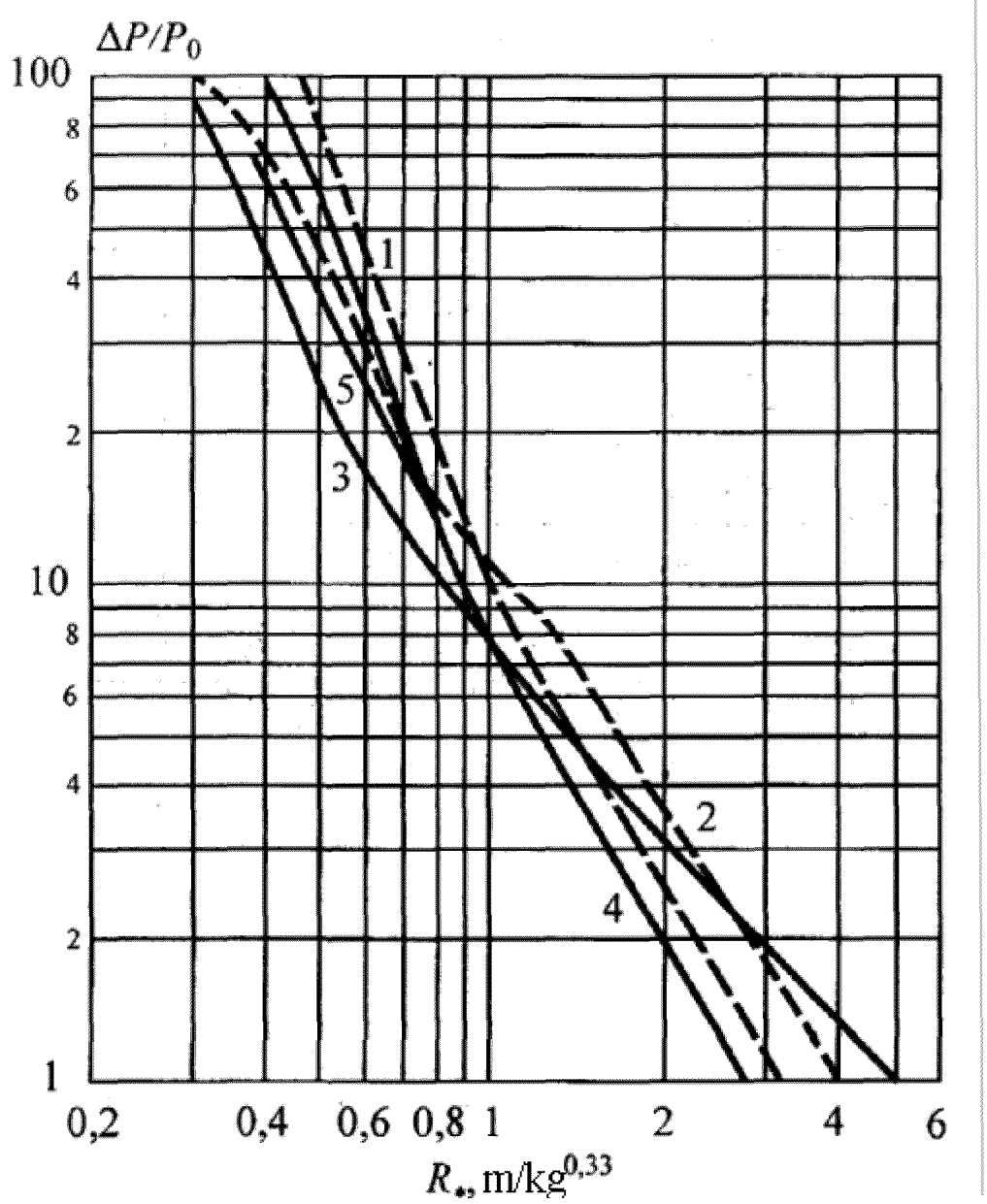

Fig. 2.3. Dependence of the shock wave intensity on the distance: 1 - by [2.1]; 2-by [2.4, 2.12]; 3 - by [2.11]; 4-by [2.10]; 5-by [2.6]

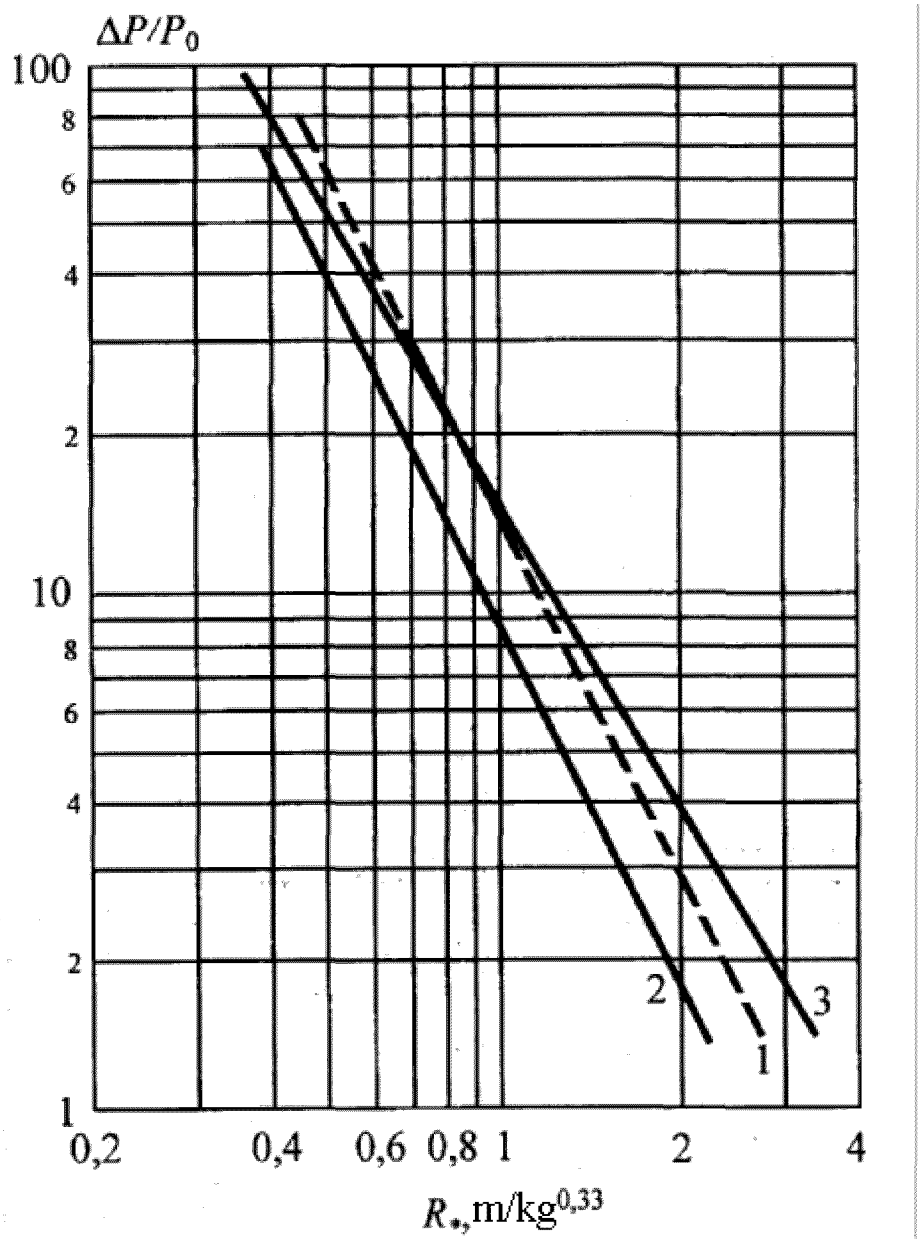

Fig. 2.4. Dependence of the shock wave intensity on the distance: 1 - by [2.7], 2-by [2.8], 3-by [2.9]

Table 2.3 Parameters of rarefaction wave for air explosion

R^*, m/kg^{0,33}	$\Delta P_-/P_0$	$\Delta P/P_0$
1	0,70	10
1,2	0,50	8,2
1,6	0,30	3,9
2	0,20	2,1
2,4	0,14	0,72
4	0,1	0,21
8	0,05	0,149

It is possible to derive the approximated formulas for the calculation of the rarefaction wave amplitude $\Delta P_-/P_0 = 0{,}48\ R_*^{-1}$ at $R_* > 1{,}2$ m/kg$^{1/3}$. For $R_* < 1$ m/kg$^{1/3}$ $\Delta P_-/P_0 \sim$ const and $\Delta P_- \sim 0{,}1$ MPa at $P_0 = 0{,}1$ MPa.

The important addition to the listed data on intensity of shock waves is the data from [2.17] for HE charges with various densities. It was shown in [2.17], that the energy similarity in the form [2.1] takes place only at $R^* > 0{,}8$ m/kg$^{1/3}$, when the front pressure does not depend on HE properties. In the near zone $0{,}053 < R^* < 0{,}8$ m/kg$^{1/3}$ the energy similarity is not valid, and the geometrical similarity of explosions is kept only at identical parameters of a detonation. For the description of parameters of shock waves in a near zone it is required to adopt additional parameters describing the rate of heat release, such as the pressure or detonation speed as offered in [2.17].

Note, that the measurements in the specified reference can be used for determination of the overpressures in the near zone of explosion at $4 < \Delta P/P_0 < 200$.

2.4. Shock waves intensity for ground and above-ground explosions.

The rule of doubling of explosion energy in any of the above presented formulas is often used to transfer the consideration from the air explosion case to the ground explosion case. The experiments show, that this rule is not universal and has a bad accuracy at the

distances $R < 25R_0$ from the center of explosion. Let's compare the energies for ground and air explosion by the impulse of compression phase and by overpressure using the data from [2.5, 2.6].

In the fig 2.5 the dependence of TNT equivalent of ground explosion in relation to air explosion (by impulse) as a function of dimensionless overpressure in a wave is given. It is seen, that even at $\Delta P/P_0 > 2$ $K_I > 2$. At $\Delta P/P_0 = 10$ according to the data [2.5] - (line 1) $K_I \approx 3{,}8$, and according to the data [2.6] - (line 2) $K_I \approx 3$. The reason of deviation from equality $K_I = 2$ is, that at $\Delta P/P_0 \approx 10$ and $R/R_0 < 20$ the behavior of the wave is influenced by the expansion of reaction products which, apparently, is unequal for ground and air explosions in the near zone.

In the fig 2.6 the dependence of TNT equivalent by pressure for ground explosion in relation to air explosion [2.6] is presented. It is seen, that K_P is within the limits of 1,6 … 1,8. Even more complex is the dependence of TNT equivalent by pressure and impulse for the above-ground explosion in comparison to air explosion. In the fig 2.7 the dependence of TNT equivalents for the above-ground explosion from overpressure in a wave is given. The lines 1, 2 correspond to TNT equivalent by pressure for $\lambda_н = H/G^{0,33} =$ 2 and 0,44 m/kg^{0,33} (H- is the height of explosion), line 3 and 4 — TNT equivalent by impulse for heights 0,4 and 3 m/kg^{0,33} . The line 5 indicates the change of TNT equivalent by impulse between the above-ground and ground explosions at $\lambda_н$ =0,6 м/кг^{0,33}. For the above-ground explosion at $0{,}1 < \Delta P < 1$ MPa and $P_0 = 0{,}1$ MPa its efficiency is higher, than in the case of ground explosion.

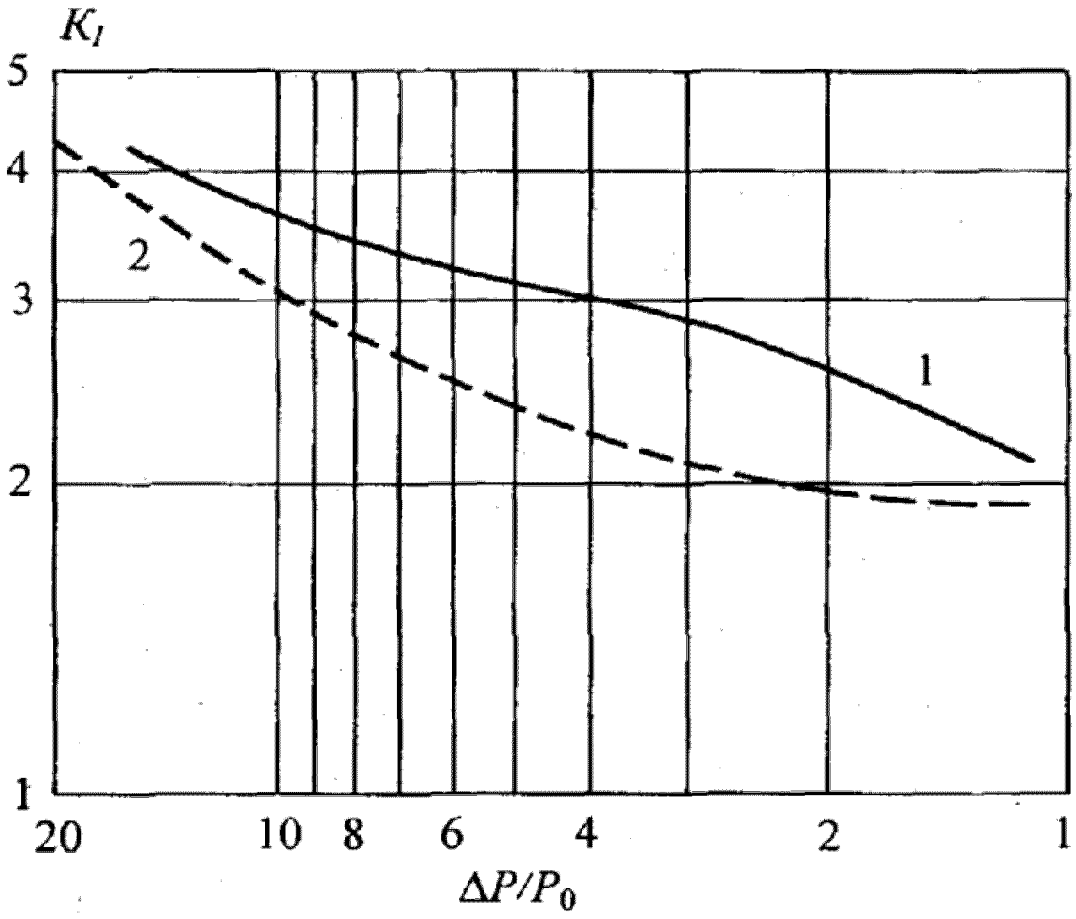

Fig. 2.5. Dependence of TNT equivalent by impulse for ground explosion in relation to air explosion on the intensity of the wave: 1 - by [2.5], 2-by [2.6]

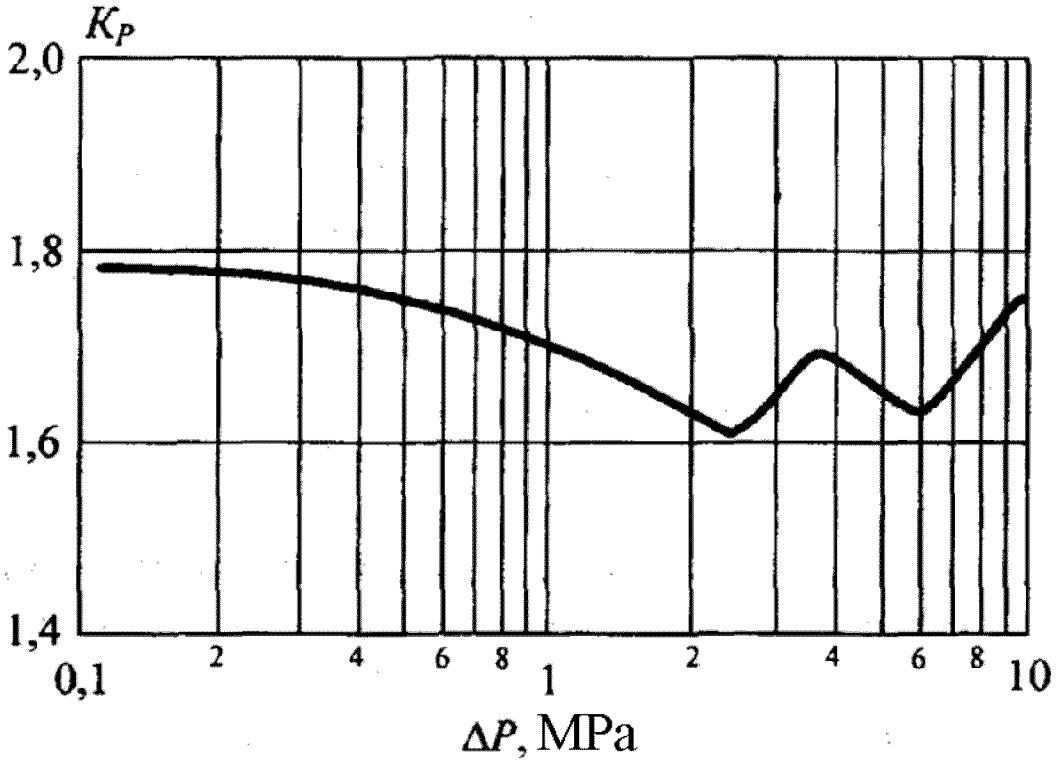

Fig. 2.6. Dependence of TNT equivalent by pressure for ground explosion in relation to air explosion on the overpressure at the wave front [2.6]

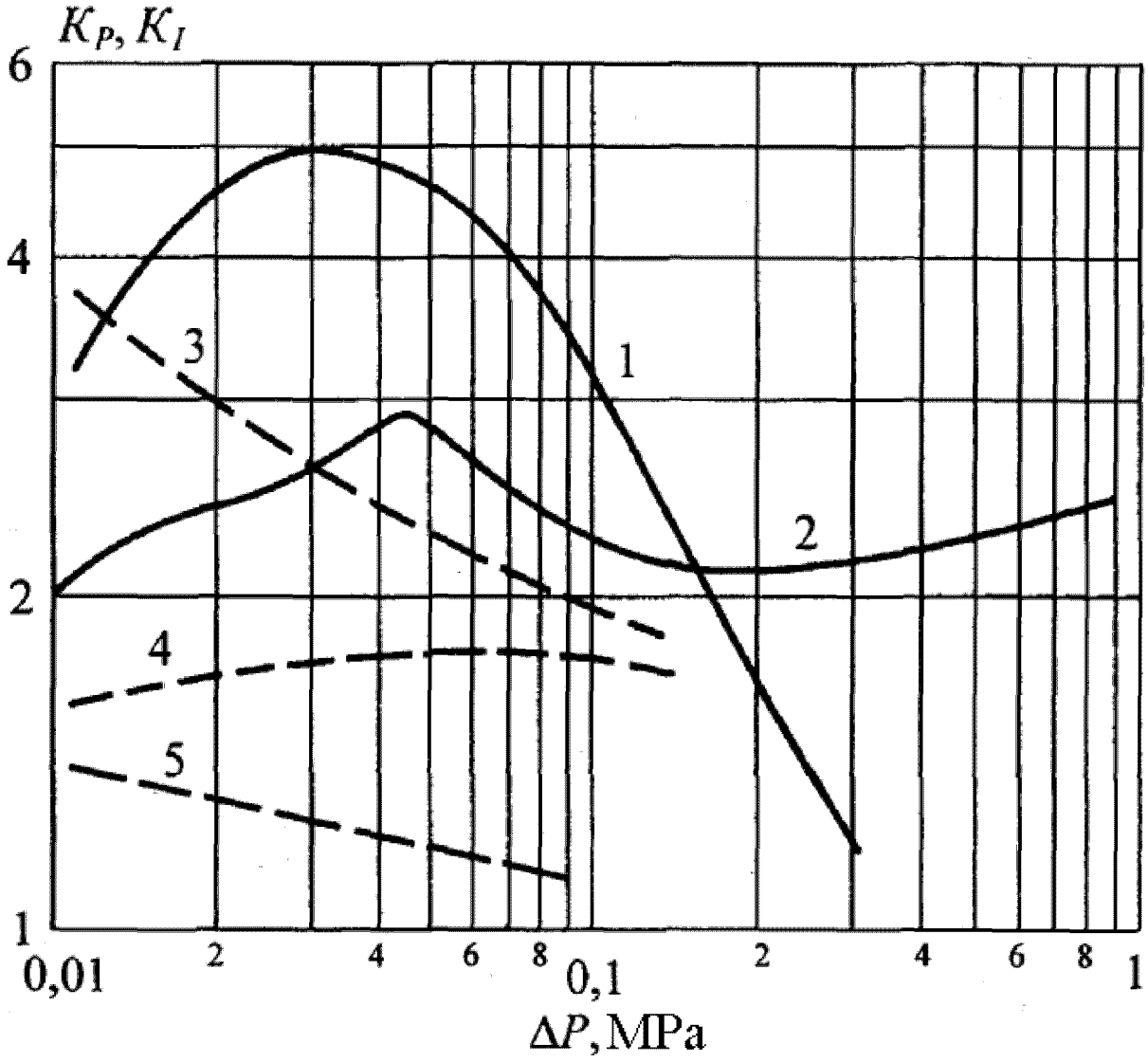

Fig. 2.7. Dependence of TNT equivalents by pressure (1, 2) and by impulse (3, 4, 5) for the above-ground explosion on the overpressure at the wave front ($\lambda_н$ = 2 (1); 0,44 (2); 0,4 (3); 3 (4); 0,6 m/kg^{0,33} (5))

In [2.16] the generalized dependence of TNT equivalent of any explosion on the height of the charge position above the surface of the earth is reported. In the fig. 2.8 these dependences are reproduced. Specific feature of the given dependence is the fact, that already at insignificant height of the charge $H/G^{0,33} > 1,25$ m/kg$^{0.33}$ explosion cannot be considered as ideally ground. It is possible also to claim, that the ideal case of air explosion is realized at $H/G^{0,33} > 8$ m/kg$^{0.33}$, i.e. the presence of limiting surfaces results in appreciable distortions to the given measurements.

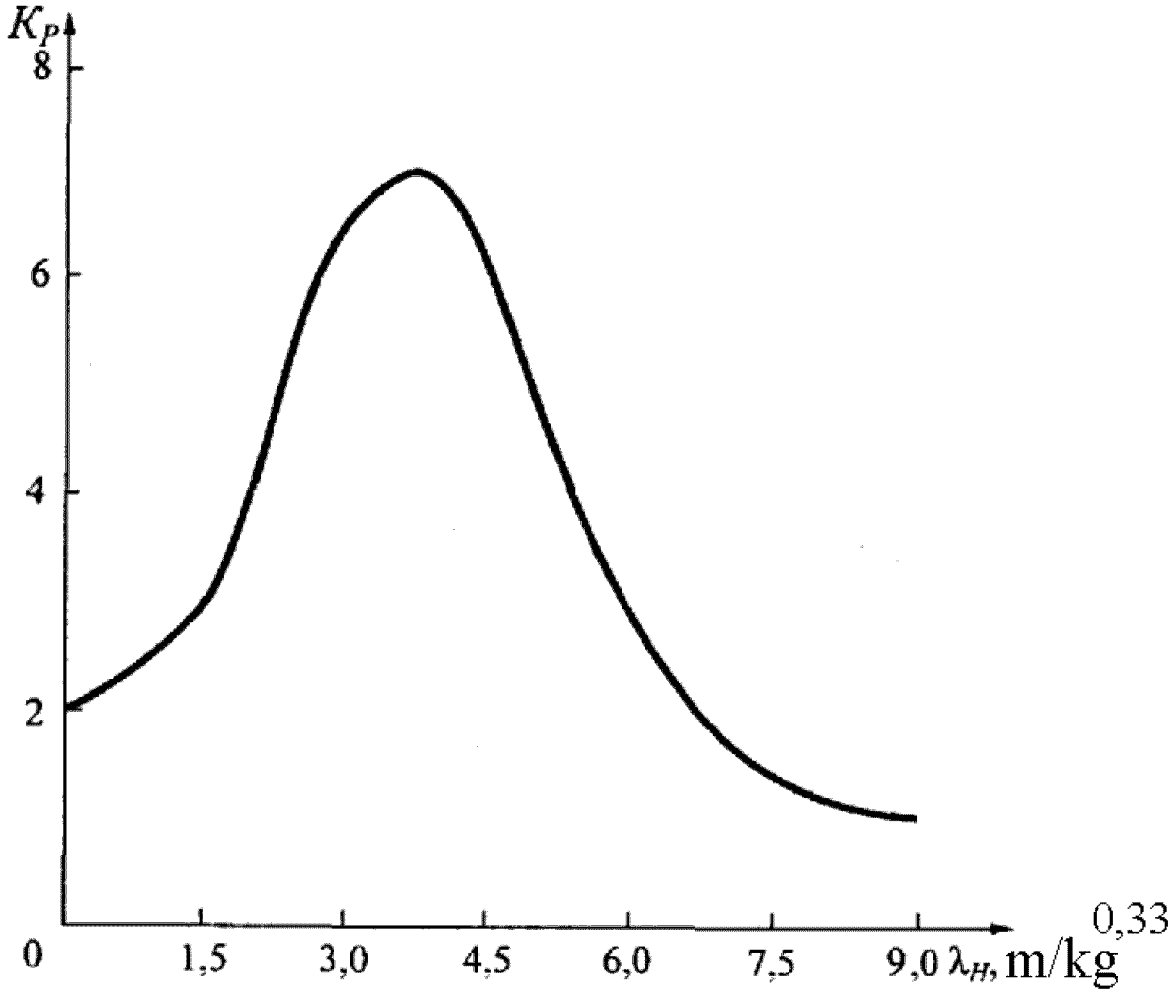

Fig. 2.8. Dependence of TNT equivalent by pressure on $\lambda_H = H/G^{0.33}$ for the above-ground explosion (by data [2.16])

When performing the estimations of pressure fields the researchers frequently do not make distinctions between strong nuclear explosion and HE detonation. The existing data on pressure fields demonstrate the inconsistency of such approach. In the fig. 2.9 the dependence of TNT equivalent of strong nuclear explosion relative to HE detonation is shown. Depending on the intensity of the shock wave at $\Delta P/P_0 < 20$ the TNT equivalent of strong nuclear explosion is reduced to 0,45... 0,60 [2.14, 2.15]. In [2.6] this circumstance is connected to the greater loss of energy by radiation at strong explosion. When explosion takes place nearby the limiting surface, the pressure in a wave normally reflected from a rigid wall worth to be measured. Using the data [2.5,2.6] for a rough estimation of pressure

in the reflected wave it is possible to offer an expression $P_r/P_0 \sim (70\ R_0/R)^3$ at $8 < R/R_0 < 60$. Here R is the distance to the reflecting surface.

For the above-ground explosion the pressure P_r, strictly speaking, is realized precisely under the center of the raised charge. At some distance from a vertical connecting the center of the charge to a ground, the pressure will vary. Therefore, for the above-ground explosion it is necessary to distinguish the zones of regular and irregular reflection. In the zone of regular reflection the gauges on a ground will record the pressure behind the oblique reflected shock wave. In the zone of irregular reflection the gauges will record the parameters of the wave corresponding to Mach stem. This wave is close by intensity to the wave from the air explosion with the corrected value of energy. In the zone of regular reflection and in the space above a reflecting surface, the gauges at first will record the parameters of the passing wave, and after that – the parameters of reflected wave. The data [2.5, 2.6] allow specifying the division of zones of regular and irregular reflection at the above-ground explosion. The trajectory of the triple point is shown in the fig.2.10 in Sadovsky – Hopkinson variables by height and radial distance.

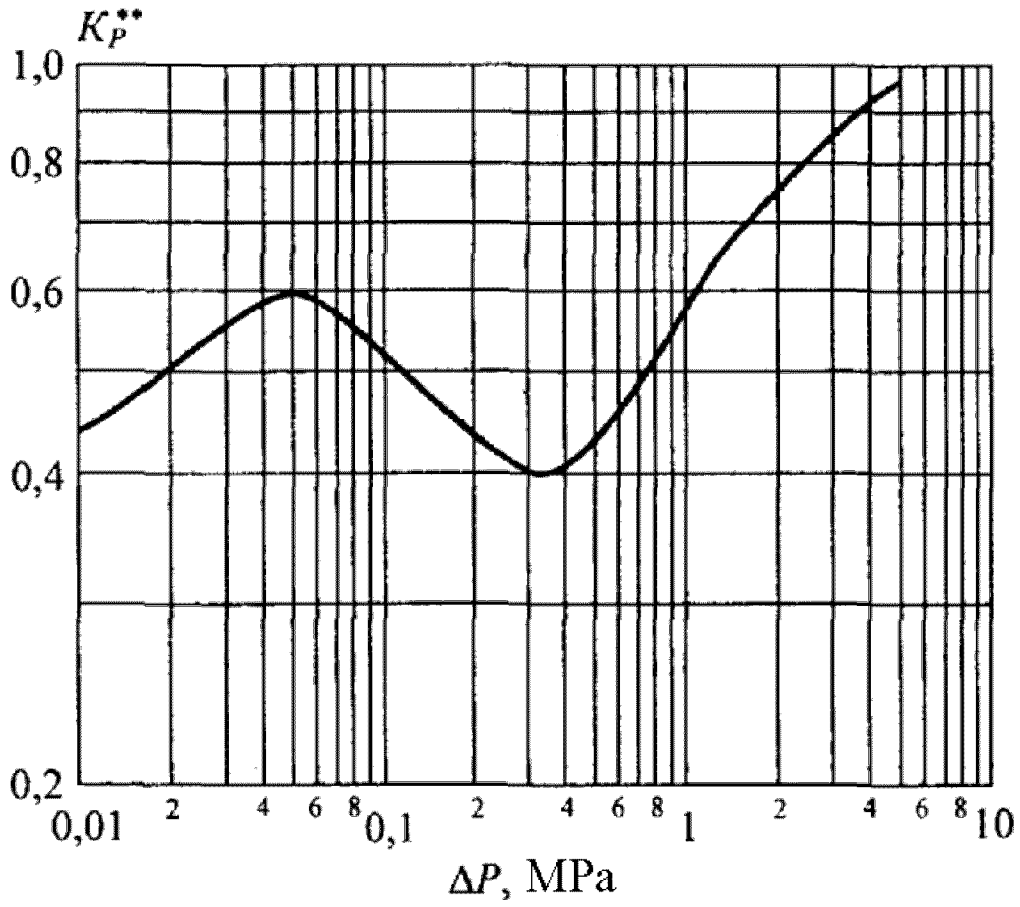

Fig. 2.9. Dependence of TNT equivalent of nuclear explosion (by pressure) on the overpressure

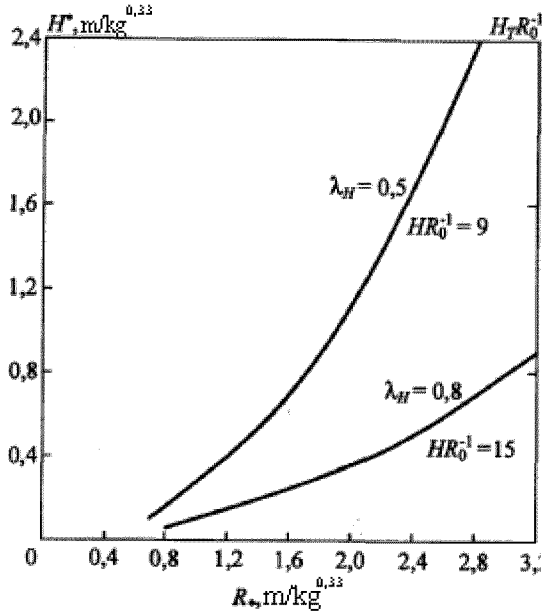

Fig. 2.10. A trajectory of the triple point for the above-ground explosions at a various heights of charge position

In the fig.2.10 $H^* = h/G^{0,33}$ is the height of a triple point, and H_T/R_0 is the same height relatively to the radius of the charge. The trajectories are given for two magnitudes of parameter $\lambda_н = 0,5$ and 0,8 m/kg$^{0.33}$, i.e. at the heights of explosion $H/R_0 = 9$ and 15.

2.5. Velocity of blast waves

Using the pressure measurements one can determine the blast wave velocity. According to the data [2.5] at $1.5 < R/R_0 < 70$ the velocity of the shock wave can be estimated as $M \approx (70\ R/R_0)^{0,84}$. Here $M = D/c_0$ is the Mach number, D is the speed of the wave, c_0 is the sound speed in unperturbed medium. There are also slightly different data in the literature. Thus, according [2.2] for the detonation of charges TNT/RDX 50/50 $M = 27,9\ (R_0/R)^{0,6}$ at $1 < R/R_0 < 10$, for the explosion of charges PETN $M= 27(R_0/R)^{0.65}$ at $1 < R/R_0 < 10$. In the fig. 2.11 the corresponding dependences are compared. The line 1 is obtained for the speed of the wave [2.5], the line 3 for RDX [2.2], line 2 corresponds to the speed of the gas at the front of wave W/c_0 [2.5].

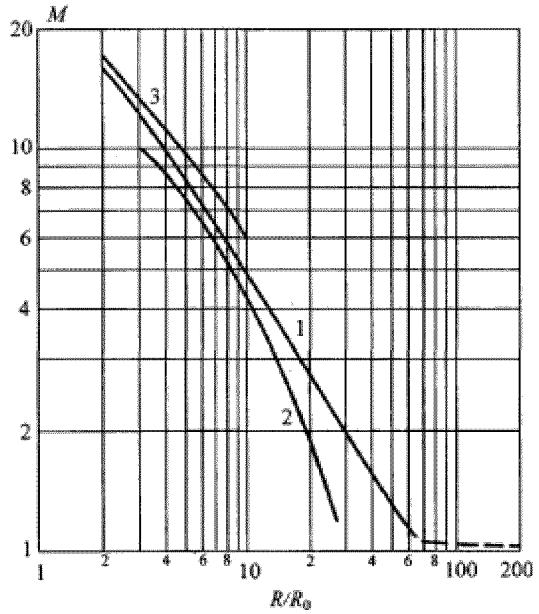

Fig. 2.11. Dependence of the shock wave Mach number on distance: 1-by [2.5], 2-by [2.5]; 3-by [2.2]

The magnitude of the dynamic head behind the wave is related to the speed and the intensity of a wave. The ratio of dynamic head to initial pressure $Q = q/P_0$ can be estimated

using the approximate expression from [2.5]: $Q = (35R_0/R)^{3,6}$ at $7 < R/R_0 < 70$. The dependence of Q on the R/R_0 for TNT is given in the fig. 2.12.

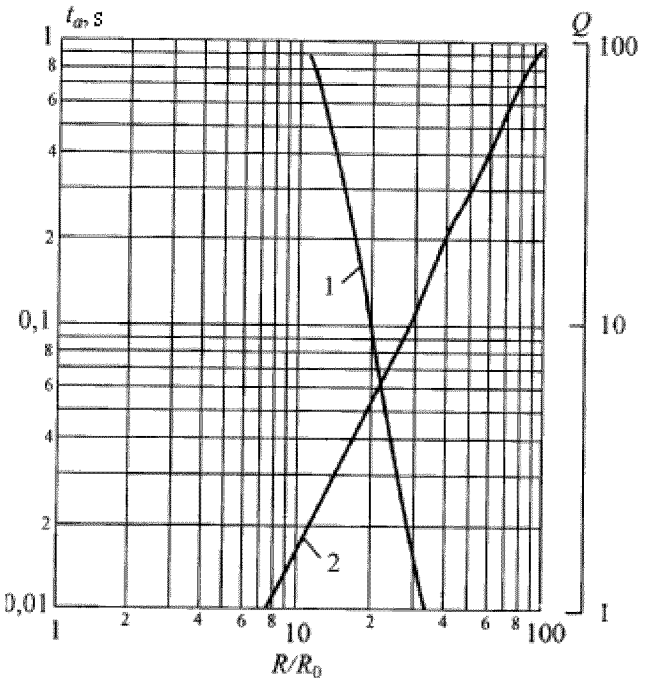

Fig. 2.12. Dependence of the dynamic head and the time of wave arrival on distance: 1 — Q by [2.5], 2 — t_a by [2.5]

2.6. Impulse characteristics of blast waves

Let's analyze the relations for another important parameter of the air shock wave – the impulse of the compression phase.

In case of impulses it is necessary to distinguish zones, where the movement of expanding products of explosion influences the pressure fall behind the wave front. According to the data [2.3] the width of a layer between the products of explosion and front of a wave δ and the radius of the pressure wave R_s will be:

$$(\delta R_s^{-1})(R_S / R_0) \sim 0{,}045\ ((R_S / R_0)^{1.4} - 1)$$

Or at $R_0/R_S << 1$ $\quad \delta R_s^{-1} = 0{,}045\ (R_0/R_S)^{0.4}$.

Even at the distance from the center of explosion $R_0/R_S << 35$, i.e. at $R^* < 1{,}8$ m/kg$^{0.33}$ and $\Delta P/P_0 > 2{,}6$ $\delta R_S^{-1} \sim 0{,}25$. The products of explosion occupy an essential part of volume involved into the movement behind the shock wave. Frequently, the calculations of the impulse of compression phase use the expression from [2.3] for air explosion of TNT/RDX 50/50 charge

$$I_* = 20R_*^{-1}, \quad I_* = G^{-0,33} I, \quad R_* = RG^{-0,33}.$$

And for detonation of TNT charge

$$I_* = 18{,}4R_*^{-1}$$

In these expressions I is measured in kgf s/m^2, and G in kg. However, authors [2.1] present the similar formulas and make the caution about the low accuracy of the factor of proportionality. The further experiments have confirmed the insufficient accuracy of the given formulas. The results of measurements of impulses from different references are given in the fig.2.13 in coordinates I^* and R^* or $\Delta P/P_0$. The line 1 is plotted by expression $I^* = 20/R_*$, line 2 - by measurements of Adushkin and Korotkov [2.2], and line 3 - by the data [2.5, 2.6]. The experimental points (solid circles) correspond to the measurements of the pressure impulse in the rarefaction phase by the data [2.6]. As it is seen from the fig.2.13 the empirical formula $I^* = 20/R^*$ for TNT/RDX 50/50 has the best accuracy. Therefore the formula $I^* = 20/R^*$ is suitable only for the estimations of the impulse in rarefaction phase with accuracy ~ (20 … 30) %.

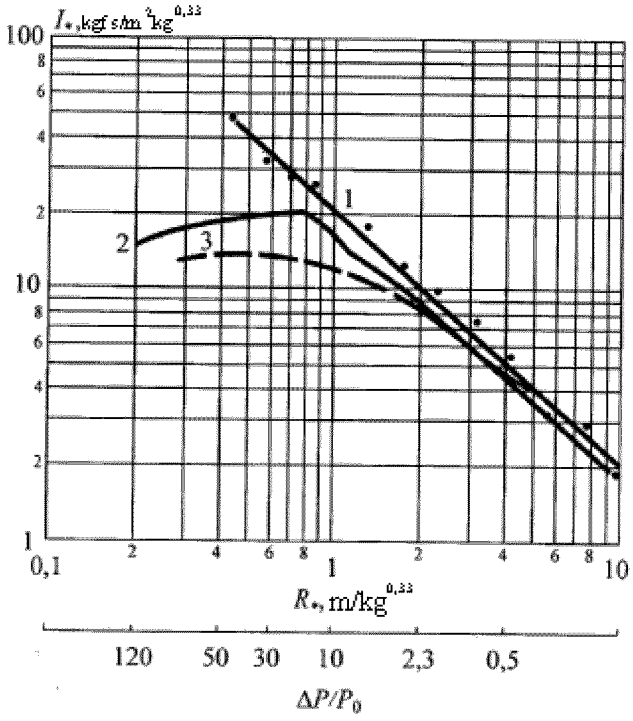

Fig. 2.13. Dependence of the impulse of pressure wave on distance and intensity of a wave: 1 - by [2.3]; 2 — by [2.2]; 3 — by [2.5, 2.6]; • — by [2.6] for rarefaction phase

In the far field of explosion at $\Delta P/P_0 < 2.3$ the impulses of compression I and rarefaction I_- waves are close to each other, that for the first time was marked in [2.1]. At $\Delta P/P_0 > 1$ the value of pressure impulse in the wave should be estimated by the corrected expressions. So at $10 > \Delta P/P_0 > 1$ the factor of proportionality in the formula I* = A/R *, A < A_1, where A_1 from [2.1, 2.3]. For TNT/RDX 50/50 $I_* = (15 \pm 2)/R_*$ is closer to experimental data, and for TNT $I_* = (13{,}8 \pm 2)/R_*$. Applying the energetic modeling for ground explosion relative to air explosion, the impulse of compression in a wave at ground explosion will be $I_* = (20 \pm 3)/R_*$..

In the near zone $\Delta P/P_0 > 10$ the values of the measured impulse quickly reach a maximum and does not grow by approaching to the center of explosion. The influence of explosion products expansion in this zone is reduced, so a simple rule of power modeling - «doubling of energy of explosion» is not valid anymore. On a descending branch of dependence $I = I(R, E)$, i.e. at $\Delta P/P_0 < 10$ the dimensionless impulses can be calculated in Sachs form by the formula

$$\bar{I} \approx 1{,}8 R_0 / R$$

Or dimensional impulse by the formula

$$I = 1{,}8 \left(P_0\right)^{0{,}66} \left(E^{0{,}33}\right) R_0 / c_0 R .$$

In a number of works the change of the pressure impulse in a wave at normal reflection of a wave from a rigid wall was studied. Korotkov and Tsykulin [2.13] have shown for the first time, that the increase of the pressure impulse in reflected wave corresponds to the change of pressure. In table 2.4 the ratios of impulses in reflected and incident waves [2.13], and overpressures in the waves are listed.

Later, the measurements [2.13] were confirmed in [2.5]. It is possible to offer an expression $I_r/I \sim \Delta P_r/\Delta P$ [2.5, 2.13] for the calculations of pressure impulse in the normally reflected wave. Here I_r, ΔP_r are the impulse and the amplitude of the reflected wave. The validity of equality $I_r/I \approx \Delta P_r/\Delta P$ means that the durations of phases of compression for incident τ and reflected wave τ_r are close and with good accuracy it is possible to take $\tau = \tau_r$. Because of the increase of the impulse at reflection it is possible to introduce the concept of TNT equivalent by impulse relative to the air explosion. In the fig.2.7 the lines 3, 4 indicate TNT equivalent of the above-ground explosion for reference heights $\lambda_H = 0{,}4$ and 3 m/kg^{0,33}. The line 5 shows the change of TNT equivalent by impulse between the above-ground and ground explosion at $\lambda_H = 0{,}6$ m/kg^{0,33}. It is clear, that at such reference height the explosion is almost equivalent by impulse to ground one.

Table 2.4 Parameters of the reflected and incident waves at normal reflection at the wall

I_r/I	$\Delta P_r/\Delta P$	ΔP, MPa
3,9	5,1	0,75
3,4	4,2	0,36
3,2	3,4	0,22
3,0	3,1	0,15

2,7	2,7	0,096
2,65	2,5	0,065

The generalization of dependences for intensity of a shock wave and impulse of compression phase allows specifying universal link of the basic parameters of the blast wave and the energy of explosion. On the basis of the analysis of numerous measurements it is possible to find the following relation

$$\bar{I} = \dot{\omega}\left(\Delta P / P_0\right)^n$$

Here $\bar{I}$ - dimensionless impulse in Sachs variables, $\dot{\omega}$ - factor of proportionality. For the data in [2.5] $\dot{\omega}$ = 0,04.

In dimensional form

$$I = \left(\dot{\omega}\frac{P_0^{0,26}}{c_0}\right)\Delta P^{0,44} E^{0,44}.$$

For a constant parameters of an environment, for example c_0 = 340 m/s and P_0 = 0,1 MPa

$$I = 2{,}3 \cdot 10^{-3}\,\Delta P^{0,44} E^{0,33}.$$

Here I - Pa s , ΔP - Pa, E - J.

In Sadovsky – Hopkinson variables $I_* = IE^{-0,33} \cong B\Delta P^{0,44}$.

Dependence of the dimensionless impulse on the overpressure is shown in fig. 2.14

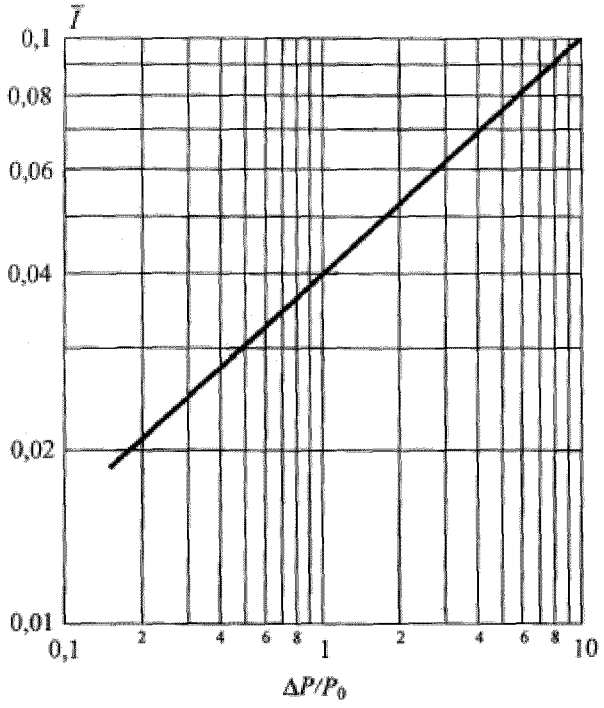

Fig. 2.14 Dependence of the dimensionless impulse on the overpressure

The proposed formula $\bar{I} = 0{,}04\ (\Delta P/P_0)^{0{,}44}$ describes a branch of a curve at $\Delta P/P_0 < 10$.

Dependence of a type

$I = k_1^* \Delta P^n E^{0{,}33}$, where $0{,}4 < n < 0{,}6$

is suitable for other types of explosive transformation. So in [2.14] for strong explosion the validity of expression $I = k_2^* \Delta P^{0{,}55} E^{0{,}33}$ was shown at $\Delta P < 400$ MPa. For the gaseous detonation it is possible to specify the dependence

$I = k_3^* \Delta P^{0{,}588} E^{0{,}33}$.

Let's analyze time characteristics of the blast wave. To calculate the duration of a phase of compression the expression $\tau^* = 1{,}2R_*^{0.5}$ was offered in [2.1]. Here τ - ms, $\tau_* = \tau / G^{0{,}33}$, G - kg HE.

In [2.12] another expression for $\tau^* - 0.06\exp\left(1.4R_*^{0.5}\right)$ was given at $0{,}1 < R^* < 1{,}3$ m/kg$^{1/3}$ and $\tau^* = 13{,}8 - 14R_*^{0{,}18}$ at $R^* > 1{,}3$ m/kg$^{1/3}$.

In the fig. 2.15 the dependences [2.1] is given by a line 1, and [2.12] – by line 3. The line 2 - is plotted by the results of measurements [2.3]. The greatest divergence of τ^* values in a zone $R^* < 1$ m/kg$^{1/3}$ where, apparently, the data [2.3] and dependence from [2.12] are closer to the experimental data, than formula from [2.1], that was also specified by the measurements of τ^* in [2.5]. At $R^* > 2$ m/kg$^{1/3}$, i.e. at $\Delta P < 0{,}2$ MPa all formulas lead to the close values of τ^*.

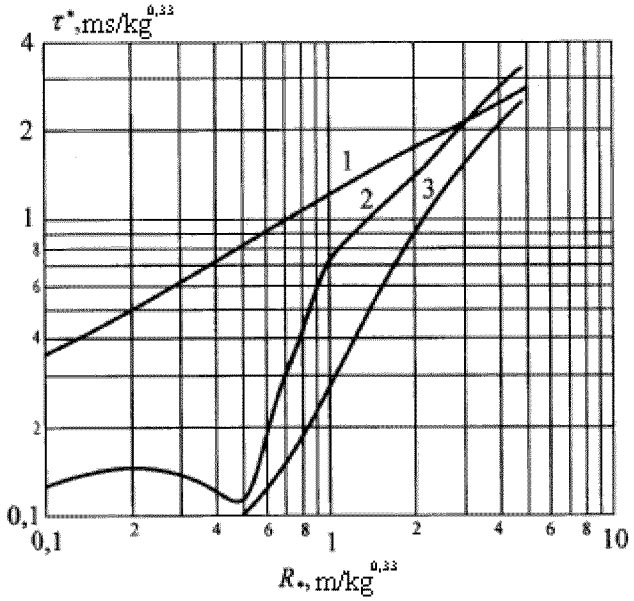

Fig.2.15 Dependence of the duration of the compression phase on the distance: 1 - by [2.1], 2 - by [2.3], 3 - by [2.12]

Using the approximate equality of pressure impulses in compression and rarefaction phases at $\Delta P/P_0 < 10$ it is possible to specify the ratio of durations of these phases. The

dependence of the ratio of durations of phases of rarefaction (τ_-) and compression (τ_+) on distance in the Sadovsky – Hopkinson form is presented in the fig.2.16. At R* < 2 m/kg$^{1/3}$, i.e. at $\Delta P > 2{,}3\ P_0$ the ratio (τ_-/τ_+) is in a range 8 … 14. In connection with elongation of the rarefaction wave in time and its small amplitude, the effect of the rarefaction wave on a target is small in comparison with the pressure wave [2.1].

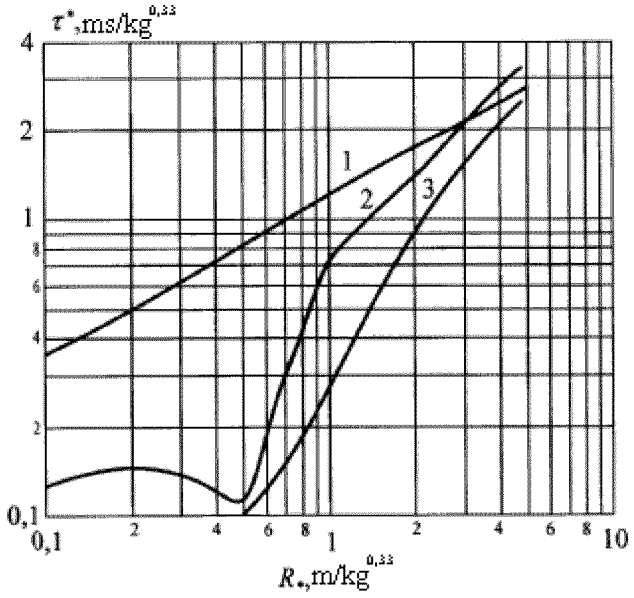

Fig. 2.16 Ratio of durations of rarefaction and compression phases in the blast wave

Another parameter of explosive process is the time of arrival of a shock wave from explosion to the given location. As a first approximation for estimations it is possible to use an expression

$$\tilde{t}_a = 10^{-2}\left(R/8R_0\right)^{1,74}.$$

Here $\tilde{t}_a = t_a c_0 \left(P_0/E\right)^{0,33}$ - time of arrival of a wave for distance R in Sachs variables. In dimensional form

$$t_a = 10^{-2}\left(\frac{E}{c_0^3 P_0}\right)^{0,33}\left(\frac{R}{8R_0}\right)^{1,74}$$

Dimensions t_a - s; E – J; P_0 - Pa.

The formula has satisfactory accuracy at $R/R_0 > 8$ and is plotted in the fig.2.12

2.7. Wave perturbations in the homogeneous atmosphere at the far distances from the center of explosion

Due to the attenuation of the air shock wave at far distances from the source of perturbation, the speed of propagation smoothly reduces to the sound speed in an atmosphere. At quasi-acoustic and acoustic stages the pressure wave depends on the condition of the atmosphere and, first of all on the gradient of the temperature field and the speed of a wind. It is considered, that at the distance, where the wave overpressure reaches the magnitude $\Delta P \sim 2{,}5$ kPa, i.e. at $R/R_0 > 500$ it is possible to expect appreciable distortions of the wave front due to the effect of meteorological conditions. According to the correlation for acoustic pulses $\Delta P \sim \rho_0 c_0 u$ (where $\rho_0 = 1{,}29$ kg/m^3, $c_0 = 340$ m/s are the density of air and the sound speed accordingly) the overpressure $\Delta P < 2{,}5$ kPa corresponds to the speed of air movement behind the wave 6 m/s.

Such speed of air movement is comparable to the speed of atmospheric movements, which explains the appreciable influence of an atmosphere on wave process. Depending on the condition of an atmosphere the movement of the wave front can deviate either into direction out or to the ground surface. For the specified reason the overpressure at the far distance from the center of explosion in a non-uniform atmosphere can change essentially. The expression for calculation of overpressure at the far distance from the center of explosion is given in [2.16] on the basis of the experimental data At ground explosion in a homogeneous atmosphere the overpressure versus the distance R will be [2.16]:

$$\Delta P = 668\left(2G\right)^{0,37} R^{-1,1}\left(P/P_0\right)^{0,33}.$$

Here ΔP - in kPa; G - weight of TNT charge, t; P_0 - atmospheric pressure at the sea level - 102 kPa; P - atmospheric pressure at the position of explosion, kPa, R - distance in km.

The factor of doubling of the charge weight is considered only at ground explosion. According to the data measurement [2.16] the real air explosions without influence of a surface are realized only at heights $H/G^{0,33} > 6$ m/kg$^{1/3}$.

Sometimes, it is useful to apply the other scale of measurements at the analysis of the magnitudes of quasi-acoustic perturbations, created by HE detonation. The detonation of HE charge at far distance is considered as a pulse of low-frequency sound signal. The overpressure ΔP in Pa corresponds to the intensity of the sound signal in dB by relation $A = 20 \log (\Delta p) + 94$. For convenience of recalculation the diagram is presented in the fig 2.17.

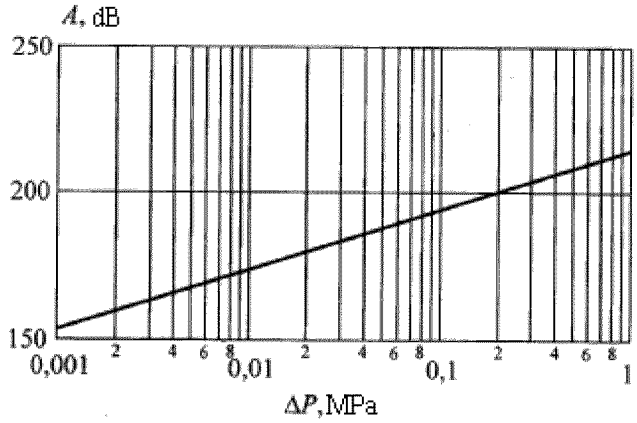

Fig.2.17 The diagram of recalculation of intensity of a sound signal by the overpressure.

It is possible to specify the dependences for the amplitude and duration of a shock wave at the acoustic stage given in [2.24]. Thus, at explosion of HE charge on a soft ground the amplitude of the air wave will be

$$\Delta P = 4,4\left(G^{1/3}/R\right)^{1,4}$$

At $1000 > R/G^{1/3} > 10$ m/kg$^{1/3}$; R - m, G - kg, ΔP - bar.

At explosion of charges on a rocky ground

$$\Delta P = 5,3\left(G^{1/3}/R\right)^{1,5}$$

in the same range of lengths and weights of the charge.

The duration of compression phase in ms is:

$$\tau_{+} = 3,15G^{1/3}\lg\left(R/G^{1/3}\right).$$

2.8. Wave perturbations in a non-uniform atmosphere

The gradients of wind speed and the temperatures, which are characteristic features for an atmosphere, affect the propagation of quasi-acoustic pressure impulses. The reducing of air temperature with height, characteristic for daytime, promotes a deviation of wave front from the earth surface and attenuates the perturbations in comparison with predicted values of ΔP. In an inverse atmosphere, where temperature of air grows with height, the wave front turns to the surface of earth and the level of perturbations can be larger than predicted values of ΔP.

The increase of the wind speed with height results in a deviation of the wave front from the ground during the propagation of the wave against a wind and the turn of the wave to ground during the propagation of a wave alongside with a wind. Thus the level of perturbations in the direction against a wind is less than predicted ΔP, and vice versa: they are higher in the opposite direction of wind propagation. The marked fluctuations of waves parameters are so essential, that frequently are taken into account at blasting operations, especially with the large HE weights [2.24].

It is well known, that atmospheric pressure and temperature change with from a sea level. Let's consider the dependence of the basic parameters of demolition action on atmospheric conditions. Let the amplitude of the blast wave from explosion under the normal conditions (P_0 = 10^5 Pa and T_0 = 288) is ΔP_0, impulse I_0, time of arrival to the reference point t_0, duration of phases of compression and rarefaction τ_{+0} and τ_{-0}. After

rearranging dimensionless parameters of similarity at temperature T_n/T_0 and pressure P_n/P_0 we obtain:

$$\Delta P_n / \Delta P_0 = \left(P_n / P_0\right),$$

$$I_n / I_0 = \left(P_n / P_0\right)^{2/3} \left(288 / T_n\right)^{0,5},$$

$$\tau_{+n} / \tau_{+0} = \tau_{-n} / \tau_{-0} = t_{an} / t_{a0} = \left(P_0 / P_n\right)^{0,33} \left(288 / T_n\right)^{0,5}.$$

All parameters with an index n correspond to explosion at P_n and T_n. As seen, the decrease of initial pressure leads to the decreasing of overpressure and impulse, transferred by the wave.

2.9. Cup formation at explosion

Underground, ground and above-ground the explosions of HE charge result in emission of the ground and the formation of a cup (crater). The sizes of a crater depend on the large number of the factors. The most essential ones are the energy of explosion and charge location relatively the surface of the ground. $H = 0$ - ground explosion, $H < 0$ - underground explosion and $H > 0$ - above-ground explosion. The type of the ground is essential, above or inside which the explosion takes place. The parameters of relative efficiency of ground emission for a number of HE are collected in table 2.5.

Table 2.5 Relative efficiency of HE detonation on emission

HE Type	Weight factor of equivalence
TNT	1
Amatol	0,94
Dynamite	0,68
Pentolite	1,23
Ammonium nitrate	1,00
Nitromethane	1,1

RDX	1,34

The form of a charge and HE type in comparison with depth of the charge location and type of the ground are unimportant. The sizes of a crater can vary in ten times in case of transition from one type of ground to another. The generalization of the information has resulted in the empirical formula [2.16]

$$V_a / V_0 = G \exp\left[-5{,}2H\left(V_0 G\right)^{-0{,}33}\right],$$

Where V_a - volume of a crater, m^3;

V_0 - characteristic parameter of a ground type, m^3/t;

G - Weight of HE charge (TNT), t;

H - Height (depth) of a charge location above (under) the ground, m.

It is possible to calculate characteristic radius R_a and depths of a crater D_a, using simple relations

$$R_a = 1{,}2V_a^{0,33},$$

$$D_a = 0{,}5V_a^{0,33}.$$

The typical values of the parameter V_0 are listed in table 2.6.

Table 2.6 Characteristic parameters of crater formation efficiency for different soils

Soil	V_0, m^3/t
Damp clay	283
Damp fine sand	170
Damp large sand	113
Damp shelf silt	113

Dry clay	42
Sand dry	14
Sandstone, tufa	42
Granite, basalt	20

The accuracy is ± 30%.

After explosion the most part of the material, which has been thrown out from a crater, is concentrated at the distance $R < (3 \ldots 5)\ R_a$ from the center of explosion. The ground explosion of HE charge is accompanied by displacement of ground [2.20, 2.21]. The maximal speed of displacement for non-buried charge can be found by the formula from [2.16]

$$D_{\max} = 2700\left(R / G^{0,33}\right)^{-1,4},$$

Where D_{max} in sm/s, R - in meters, G - weight of an equivalent TNT charge in tons. For buried charge $D_{max} \sim 10^4\left(R / G^{0,33}\right)^{-1,4}$. The peak value of ground acceleration in cm/s^2 is about $a_{\max} \sim 10^5\left(R / G^{0,33}\right)^{-1,4}$.

It worth to note, that the formation of a crater at the ground and above-ground explosion is a characteristic feature of condensed HE detonation [2.42]. The critical value $\Delta P^* \sim 2{,}0$ MPa of the wave front overpressure required for the emission of the ground is given in [2.9]. At explosion of fuel - air mixtures (FAE) such level of pressure cannot be achieved anywhere, including inside area of the detonating cloud. For the specified reason the FAE above the surface of the ground is not accompanied by the cup formation, and the messages, known in the popular literature, do not correspond to the truth.

2.10. Sizes of a cloud of explosion products

The thermal energy released in HE explosion, results in emission of hot products of explosion (EP) into surrounding atmosphere. These products involve into the movement a part of the fragmented material of the soil. The EP cloud and dusty substance rises in an

atmosphere and drifts with a wind, leaving a dusty trace on the earth ground. According to [2.16], in 120 s after explosion the top border of a cloud will reach the height $H = 506G^{0,25}$ m, here G is the weight of an equivalent TNT charge in tons. Finally, at the moment of cloud hanging, the top border will be at height $H_t = 670\ G^{0,2}$, and the bottom border of EP cloud will be at height $H_b = 335G^{0,25}$. Thus the diameter of a cloud is $D_m = 335G^{0,25}$, and the volume $V_m = 3\cdot 10^7\ G^{0,75}\ m^3 = 3\cdot 10^{-2}\ G^{0,75}\ km^3$.

2.11. Afterburning of detonation products

In spite of long – time investigation of the dangerous factors accompanying the free-air explosion of condensed explosive substances, a number of questions left which require additional consideration. One of this poorly known parameters of explosion effect concerns the amplitude - temporary characteristics of the thermal impulse due to the chemical interaction of expanding (after the detonation of initial charge) products of explosion with an environment (for example, with air).

Conditionally it is possible to distinguish internal and external changes of temperature at HE detonation. The internal changes of temperature in the charge volume are caused by detonation complex passing through it and occur for a short-term interval of time with duration $\Delta t < 10^{-5}$ s. To study these temperature changes the special methods of optical pyrometry [2.36] are offered. In HE detonation studies these methods are directed only to the obtaining the information about the nature of radiation from the detonation complex, temperature of detonation products, and the change of the diagram pressure — time in the charge itself [2.36].

The external changes of temperature are caused by the expansion of EP and their mixing with air. The afterburning of products of incomplete transformation is separated from the act of the detonation by an interval of time $\Theta >> \Delta t$ and occurs in an environment much later than its shock compression by the blast air wave responsible for a demolition defeat. In the literature there is no information on the amplitude - temporary parameters of external temperature fields or molecular or mixed HE of various structure.

In recent time the complex investigation of the damage factors from the explosion of systems with time-delayed energy release due expanding EP afterburning becomes of growing interest. In this case (against to the standard schemes HE detonation study) the technique of registration of governing parameters, such, as EP temperature and intensity of radiation in the given ranges of wavelengths at all stages of explosion - from initial (with a time scale ten micro seconds) up to late, of ten milliseconds after the start of explosive process is necessary.

The temperature and intensity of EP radiation for various stages expansion of detonation products for TNT and RDX based HE were registered in [2.36] for the first time with the help of original double-wavelength photoreception devices.

As expected, the explosion of molecular HE is accompanied in general case by two temperature impulses (T-impulses):,

The 1-st T-impulse has the duration up to 10^{-4} s and is caused actually by the HE detonation itself; the danger of a defeat due to radiation from the first T-impulse can not be taken into account in view of its small duration;

The 2-nd T-impulse has duration up to 10^{-1} s and is caused by process of HE burning in surrounding air; the danger of radiation from the second T-impulse should be taken into account at the complex estimation of consequences of HE explosion because of baric-thermal nature of blast loading.

The relation of amplitude - temporary parameters of the 2-nd T-impulse from the chemical structure of explosive substance is established for the first time in [2.36]. The explosion of molecular HE of RDX type (oxygen balance OB = - 21,6) differs insignificantly by secondary increase of temperature by amplitude. The consequences of explosion basically are connected with baric loading. The explosion of molecular HE of a TNT type (oxygen balance OB = - 74) is characterized by essential secondary increase of temperature. The estimation of consequences of such HE explosion should be complex and must take into account the thermobaric effect on the target.

The explosives under study were TNT, RDX, mixture 50% TNT + 50% RDX (TG 50/50) and mixture 95%RDX + 5% paraffin (RDX(p.)). Table 2.7 presents some properties of these high explosives: ρ – initial density, D and p – detonation velocity and pressure, T_p – temperature of detonation products and C – content of carbon (soot) in detonation products (calculated by [2.36]). The composition was calculated for the expansion level in 2-3 times. All the charges of mass 100 g were cylindrically shaped with diameter 40 mm prepared by cold press technique. Initiation of detonation was performed by means of blasting cap and intermediate 8 g RDX charge (diameter 20 mm).

Table 2.7 Properties of high explosives

HE	ρ, g/sm^3	D, km/s	p, GPa	T_p, K	C, mol/kg
TNT	1,60	6,94	20,3	3140	16,51
RDX	1,71	8,39	31,4	3740	2,81
TG 50/50	1,67	7,60	25,4	3460	9,30
RDX(p.)	1,67	8,34	26,7	3300	6,97

Figure 2.18 presents relative displacement of the charge and photodetectors (PD) in the explosion chamber. The distance between horizontally hanging charge and the floor was 0.94 m. One of the photodetectors was positioned along the axis of the charge, while another PD was focused on the sidewall of the charge. The main element of the photodetector is Si-Ge photodiode of sandwich structure containing the thin semi-transparent silicon layer that covers germanium substrate.

The essential feature of Si-Ge photodiode is a very small intersection between the Si and Ge spectral responses. The advantage of the PD is the possibility of measuring radiation simultaneously in two portions of spectrum, namely $0,4 \leq \lambda \leq 1,1$ μm (Si-

channel) и $1{,}0 \leq \lambda \leq 1{,}8$ μm (Ge-channel). The photodetectors are equipped by specially designed preamplifiers. The preamplifier features low-noise high-speed operational amplifiers AD823. Since the absolute values of the expected radiation fluxes can change in an extremely wide range (up to five orders of magnitude variation), special attention was given to the possibility of changing the proper measuring range. The preamplifier is designed to operate at six sensitivity values. The faster time response achieves 1 μs. PC-based analog-digital converter T512 was used to register the outputs of the PD units. The photodetectors were equipped by objectives thus providing view angle 0.04 rad.

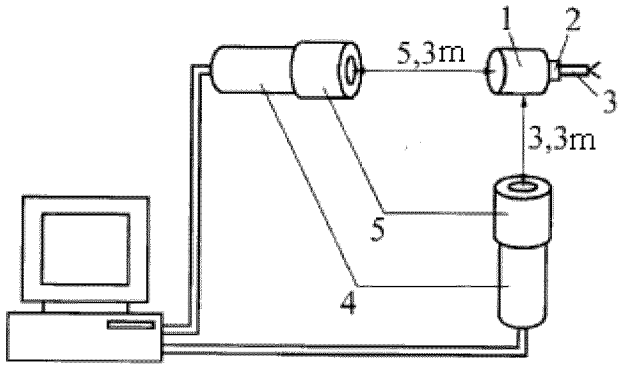

Fig.2.18 Experimental arrangement. 1 – *charge;* 2 – *intermediate charge;* 3 – *blasting cap;* 4 – *photodetectors;* 5 – *objectives.*

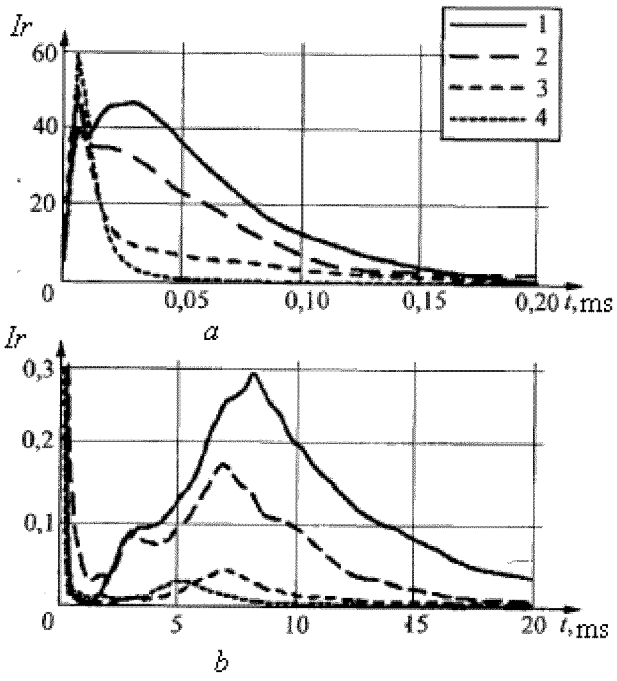

Fig.2.19 Outputs of Si channel (arbitrary units) of the PD placed perpendicular to the charge axis (sidewall view). a – initial stage of explosions; b – full-time registrations.

Each photodetector unit (Si-Ge photodiode + preamplifier) was calibrated by the use of standard light source in accordance with commonly used procedure.

Specific features of emission related to the HE explosions can be elucidated by the consideration of outputs of Si-channel of the photodetector placed across the axis of a charge (see fig.2.19). As seen all the emission traces exhibit regular trends, namely, the presence of two amplitude-time stages. The duration of initial stage (fig.2.19*a*) is about 200 μs after the initiation of a charge. During this stage the intensity of emission (radiation flux) changes significantly, i.e. sharply increasing up to some maximum value and afterwards smoothly decreasing. The second (later) stage (fig.2.19*b*) also can be characterized by the appearance of a maximum (at t = 5 – 8 ms). However, the value of this maximum seems to be one-two orders of magnitude lower than that at the initial stage of explosion.

The intensity and dynamics of variation of the measured radiation flax depend heavily on the composition of a given HE as well as on the orientation of the photodetector. The most pronounced differences are observed between the cases of TNT and RDX explosions. The parameters of emission related to the burst of TG 50/50 and RDX(p.) exhibit intermediate behaviors.

These peculiarities reflect both qualitative and quantitative variations of explosion emissivity properties in the set RDX $\rightarrow$ RDX(p.) $\rightarrow$ TG 50/50 $\rightarrow$ TNT. As seen from the table 2.7 this sequence is characterized by the monotonic increase of carbon content in detonation products. On the strength of these data one can interpret the observed photodetector's outputs in the following way. Initial sharply increasing emission seems to be associated with the air heated by shock wave. However, since short time interval (of order 10 – 20 μs) after initiation the optical thickness of the shock falls and expanded detonation products starts to be responsible for the luminosity. In this connection it should be noted that the intensity of radiation of carbon (soot) particles is substantially higher than that of gaseous components of detonation products. From this point of view at the initial stage of explosion (Fig.2.19*a*) the radiation flux in the case of RDX burst reflects the attenuation of shock wave and expansion of gaseous components of detonation products. Considerable increase of soot content, as in the case of TNT explosion, results in the fact that the contribution of soot particles into radiation intensity becomes dominant at least at 40 – 50 μs after initiation of the charge. Among other things the presence of carbon as a fuel is a likely reason for after-burning phenomena at the later stage of explosion. These phenomena result in increase of the observed radiation intensity at the later stage of explosions (Fig.2.19*b*).

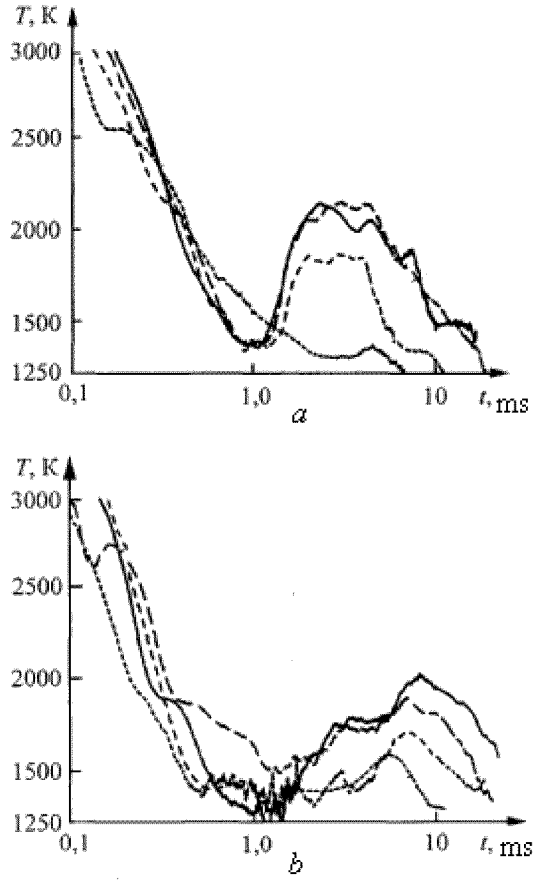

Fig.2.20 Temperature-time histories in the course of longitudinal (a) and lateral (b) expansion of HE detonation products.

The dynamics of after-burning processes can be clearly illustrated by the temperature-time histories calculated by the model of black body radiation. As it is seen from fig.2.20 at the first 800 – 900 μs temperature of detonation products falls down to values about T = 1200 – 1500 K. Further one can easily observe relatively smooth temperature rise to be associated with the burning phenomenon. The intensity of the after-burning process (i.e. heating rate and maximum temperature value) depends significantly from the soot content. Maximum temperature levels are achieved in the case of TNT and TG 50/50 explosions, while in the case of RDX burst the after-burning effects seem to be negligibly small. An important thing is that the after-burning process is spatially non-uniformed. The longitudinal expansion (fig.2.20*a*) results in more intensive combustion (i.e. combustion starts earlier and temperature seems to be higher) than that lateral expansion (fig.2.20*b*). This difference can be explained in the frame of the model, in which

the rate of the reaction of oxidizing of detonation products is controlled by the rate of turbulent mixing of EP with surrounding air. In the scheme of relative displacement of the charge and detonator the initial velocity of expanding products in longitudinal direction is 2-2.5 times higher than in lateral direction.

Note, that the up to date known spectrum of different HE by nature and composition make possible to investigate the processes of afterburning in mixtures with another than soot reactive components. An example is the work [2.37], where specific features of oxidizing of the secondary products of HMX with Mg and Polytetrafluorethylen additives were studied on the basis of qualitative pattern of emission.

Performed tests show that the photodetector based on the double-wavelength Si-Ge photodiode presents a universal mobile tool for registration of emission and temperature measurements in expanding clouds of HE detonation products. Due to the simple design, it is especially suitable for multi-channel registration in both outdoors and laboratory conditions. The use of the PD system makes possible to compare the characteristics of emission in different kinds of explosives. Application of the double-wavelength photodetectors to the burst of TNT- and RDX-based explosives enables to reveal peculiarities of after-burning phenomena associated with turbulent mixing of detonation products with surrounding air.

2.12. Shock waves from non-spherical charges

The HE charges are the spheres or hemispheres only in specially prepared experiments. More often the form of the charge is the cylinder of length L and diameter D, i.e. cylinder with ratio $L/D > 1$. Generally, the form of the shock wave generated by explosion of cylindrical HE charge is not spherical at rather far distance from the source of explosion. The nonspherical shape of a wave means the inconstancy of overpressure at the shock front. The nonspherical shape of a wave and the inconstancy of pressure in different directions is kept till the overpressure $\Delta P \sim 0{,}014$ MPa. For the less intensive waves the nonspherical wave shape and inconstancy of overpressure in different directions are not so essential and can be disregarded. For the long cylindrical charges with $L/D > 1$ it is

possible to use the following expression for calculating the orientation diagram of a pressure field

$$y = [2{,}0467 - 0{,}1146\,x + (0{,}1285 - 0{,}0342\,x)\cos(\theta) + (0{,}0621 - 0{,}3280\,x)\cos(2\theta) + (-0{,}0029 + 0{,}0304\,x)\cos(3\theta) + (-0{,}1532 - 0{,}998\,x)\cos(4\theta)] + [-2{,}1617 + 0{,}1422\,x + 0{,}2079 + 0{,}1161\,x)\cos(\theta) + (-0{,}4178 + 0{,}3686\,x)\cos(2\theta) + (-0{,}1372 + 0{,}0648\,x)\cos(3e) + (-0{,}3484 + 0{,}1191\,x)\cos(4\theta)]\,\lambda + [0{,}4366 + 0{,}0418\,x) + (0{,}0138 + 0{,}0938\,x)\cos(\theta) + (0{,}1178 + 0{,}1451\,x)\cos(2\theta) + (0{,}2556 - 0{,}043\,x)\cos(3\theta) + (0{,}3121 + 0{,}161\,x)\cos(4\theta)]\,\lambda^2.$$

For the short cylindrical charges at L/D < 1 the following expression for calculating the orientation diagram of a pressure field is offered

$$y = [2{,}0467 - 0{,}1753\,x + (0{,}1285 + 0{,}072\,x)\cos(\theta) + (0{,}0621 - 0{,}2503\,x)\cos(2\theta) + (-0{,}0029 + 0{,}0079\,x)\cos(3\theta) - 0{,}1534\cos(4\theta)] + [-2{,}1616 + 0{,}0464\,x + (-0{,}2079 - 0{,}2174\,x)\cos(\theta) + (-0{,}4178 + 0{,}3426\,x)\cos(2\theta) + (0{,}1372 - 0{,}1171\,x)\cos(3\theta) + (-0{,}3484 - 0{,}3449\,x)\cos(4\theta)]\,\lambda + [0{,}4366 + 0{,}0059\,x + (0{,}0138 - 0{,}0006\,x)\cos(\theta) + (0{,}1178 - 0{,}2695\,x)\cos(2\theta) + (0{,}2556 + 0{,}2072\,x)\cos(3\theta) + (0{,}3123 - 0{,}2160\,x)\cos(4\theta)]\,\lambda^2.$$

In these formulas

$x - \ln(L/D)$;

$\lambda - \ln(0{,}0348\,R/G^{0{,}33})$;

$P_3 = 8 \cdot 10^{-2}\,e^y$, bar;

θ – azimuth (horizontal) angle.

Calculation configuration is shown in the fig 2.21.

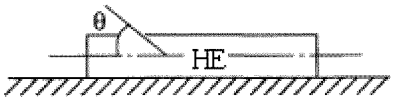

Fig. 2.21. The elongated cylindrical charge

In case of ground explosion it is necessary to double the weight of a charge to calculate λ.

For understanding the opportunities of modeling of various types of charges explosions of the nonspherical form and arbitrary oriented relatively reflecting surface (as a rule, the surfaces of ground) the data on the measurements which have been carried out in [2.19] are rather useful. For the cylindrical HE charge with the length to diameter ratios from 1:1 up to 5:1, fixed on a cylindrical surface on ground, in directions on an azimuth 0^0, $22{,}5^0$, 45^0, $67{,}5^0$, 90^0, $112{,}5^0$, 135^0, $157{,}5^0$, 180^0 the overpressures were determined. The azimuth 180^0 corresponds to a direction of the blast wave propagation, and the azimuth 0^0 is the opposite direction. The azimuth 90^0 corresponds the perpendicular direction relative the blast wave.

Along with the basic charge position, when the cylinder lies on the ground, the additional measurements were carried out for the inclined charge in 45^0 and 60^0 relative to ground. Explosion of the cylinder vertically standing on the ground also is considered. The results of measurements demonstrated, that the distinctions in ΔP are kept for arbitrary - oriented charges only at $\Delta P > 0{,}1$ MPa, i.e. at distances $R/G^{1/3} < 5$ m/kg$^{1/3}$. Otherwise, the distinction of ΔP falls within the limits of the accuracy of measurements. It permits to not consider the azimuth direction of wave propagation and to not take into account the orientation of the charge axis relative the earth surface at $R/G^{1/3} > 5$ m/kg$^{1/3}$.

2.13. Parameters of shock waves at underwater explosion

The reference homogeneous systems for two-phase fluids depending on a mass (volumetric) content of the condensed phase are either gas, or degassed liquid. Therefore, it is worth to list the dependences of the basic parameters for underwater explosion. On the

basis of generalization of the information from [2.25 … 2.33] the amplitude of the blast wave P, duration of the phase of compression τ_+ and the impulse of the phase of compression I at explosion of G kg of HE under water at the distance R m from the center of explosion will be

$$P_2 = K_{11}\left(G^{1/3}R^{-1}\right)^{\alpha},$$

$$\tau_+ = K_{12}\left(G^{1/3}R^{-1}\right)^{\beta},$$

$$I = K_{13}\left(G^{1/3}R^{-1}\right)^{\gamma}.$$

The empirical factors K_{11}, K_{12}, K_{13}, α,β, and γ are summarized in table 2.8.

Table 2.8 The basic parameters for calculation of the blast wave at underwater explosion

Reference	Bjorn [2.30, 2.33]	Cole [2.26]		Poche [2.31]	Bebb [2.32]	Arons [2.29]
HE	Tetryl	TNT	Tetryl	RDX	TNT	TNT
$R/G^{1/3}$, m/kg$^{1/3}$	4 … 60	0,45 … 11	0,48 … 1,7	3,2 … 210	0,16 … 5,3	0,46 … 795
K_{11}, Pa	$506 \cdot 10^5$	$523 \cdot 10^5$	$509 \cdot 10^5$	$560 \cdot 10^5$	$411 \cdot 10^5$	$522 \cdot 10^5$
α	1,1	1,13	1,15	1,12	1,1	1,13
K_{12}, ms	87	96,5	87,5	–	–	92,5
β	0,23	0,18	0,23	–	–	0,23

K_{13}, Pa s	5,9	5,75	6,27	–	–	–
γ	0,87	0,89	0,98	–	–	–

For completeness we shall specify, that the measurements in [2.27, 2.28, 2.30, 2.31] were made for small charges, measurements in [2.26] - for the large charges, measurements in [2.29, 2.32] are executed at the far distances from the location of explosion.

2.14. Estimation of the explosion parameters

The preformed analysis together with the data [2.34,2.35], shows, that there is a significant scatter of experimental data for all blast wave parameters and for all types of HE explosion in gaseous atmosphere (air). The known formulas for calculating the overpressure have the accuracy not more than 10 % even for an ideal case of air explosion. Therefore the accuracy of calibrating measuring systems with the help of HE will never exceed of accuracy of measurements of blast waves parameters. In the near zone of explosion at $\Delta P/P_0 > 2{,}3$ and $R/R_0 < 35$ expressions for the impulse of a wave in the form [2.1] can not be recommended for use. In connection with the marked discrepancy of measurements of the pressure and the impulse the backward recalculation of the energy of explosion by overpressure and impulse leads to the errors in 1,5... 2 times.

Therefore, the use of the parameters of the blast waves generated by HE charges for power estimations of other types of explosions should be applied taking into account the possible errors and is suitable only for qualitative estimations. At the ground explosion the uncontrollable and significant loss of energy on crater formation can be observed, in this connection the energy equivalent of the ground explosion in relation to air one frequently falls below theoretically expected value [2.34]. The measurements of the ground explosion parameters potentially comprise an uncontrollable error because of the energy losses.

For this reason the data on the blast waves parameters are less suitable for calibrating of the measuring equipment, than the data on the air explosion. It is necessary

to prefer here the measurements of blast waves parameters for the above-ground explosion, because already at a specific reference heights $\lambda_н = 0{,}44$ m/kg$^{0{,}33}$ the energy losses due to cup formation are small, so they could be neglected. Use of the data on blast parameters performed in the frame of equivalent estimations leads to even larger mistakes, than the use of the data on explosion of condensed HE. It is predetermined by a wide scatter of the measured parameters of strong explosions, by their small accuracy, and by their small number [2.15].

In most publications only the measurements of blast parameters from detonation of HE charges in air is reported.. Actually, the dependence on surrounding air density and speed of a sound really exists, and the increase of speed of a sound in gas environment (at constant initial pressure), should be accompanied by the reduction of overpressure. In general, the expected wave attenuation is caused by the tendency to decrease the acoustic resistance by the growth of speed of a sound, under uniform pressure.

The magnitude of acoustic resistance $\rho c_0 = \Omega$ depends on pressure by formula $\Omega = \gamma P_0/c_0$ Thus, having warmed up the gas, addition of lightweight gases (hydrogen, helium etc.) promotes the decrease of acoustic resistance of gaseous atmosphere. As a result the smaller pressure perturbations will penetrate into surrounding atmosphere than in the case of heavyweight gases. The further change of wave parameters will depend on speed of wave propagation and the time of arrival of a wave the fixed point. It is necessary to mention as practically important feature the expected distinction of pressure waves parameters in a hot and cold season. Really, the acoustic resistance of gas (air) depends on temperature as $\Omega = P_0(\gamma/RT)^{0,5}$. Thus, as a result of the blast wave reflection from the boundary of a cold gas, the wave with larger amplitude penetrates into the cold gas. Nowadays on the basis of available measurements there is no opportunity to establish a degree of correction, which is must be implemented into the known expressions at the realization of expert estimations. Most likely, the expected scatter of blast waves parameters depending on the weather condition does not exceed 20 % error.

Below we list a set of the formulas for estimations of HE explosion parameters:

1. Air explosion:

$$\Delta P\ [\text{MPa}] = 1.7 \cdot 10^3 \exp\left\{-7.5 R_*^{0.28}\right\} + 0.0156 \quad \text{for } 0{,}1\ \text{m/kg}^{0{,}33} < R_* = R/G^{0{,}33} < 8\ \text{m/kg}^{0{,}33};$$

$$\Delta P\ [\text{MPa}] = 8 \cdot 10^3 \exp\left\{-10.7 R_*^{0.1}\right\} \quad \text{for } R_* > 8\ \text{m/kg}^{0{,}33};$$

2. Ground explosion:

$$\Delta P\ [\text{MPa}] = 1.7 \cdot 10^3 \exp\left\{-7.14 R_*^{0.28}\right\} + 0.0156 \quad \text{for } 0{,}1\ \text{m/kg}^{0{,}33} < R_* \ 8\ \text{m/kg}^{0{,}33};$$

$$\Delta P\ [\text{MPa}] = 8 \cdot 10^3 \exp\left\{-10.46 R_*^{0.1}\right\} \quad \text{for } R_* > 8\ \text{m/kg}^{0{,}33};$$

3. Duration of the compression phase:

$$\tau_+ / G^{0.33}\ [\text{ms/kg}^{0{,}33}] = \tau_*^+ = 0.06 \exp\left\{1.4 R_*^{1.4}\right\} \quad \text{for } 0{,}1\ \text{m/kg}^{0{,}33} < R_* < 1{,}3\ \text{m/kg}^{0{,}33};$$

$$\tau_+ / G^{0.33} = \tau_*^+ = 13.8 - R_*^{0.18} \quad \text{for } R_* > 1{,}3\ \text{m/kg}^{0{,}33};$$

At transition from TNT to another HE it is necessary to take $G_{\text{HE}} = K_{\text{TNT}} G$ instead of G, where the values K_{TNT} are given in table 2.1.

References to chapter 2

2.1. Sadovsky M.A. Mechanical action of air shock waves by the data of experimental study. «Fizika vzryva». M., USSR Ac. Sci., 1952, p.20 - 111. (*in Russian*)

2.2. Adushkin V.V. On the formation of a shock wave and the expansion of HE products at explosion in air // PMTF, 1963, № 5, p. 107-114. (*in Russian*)

2.3. Adushkin V.V., Korotkov A.I. Parameters of a shock wave near to HE charge at explosion in air // PMTF, 1961, № 5, p.119-123. (*in Russian*)

2.4. Strehlow R.A., Baker W.E. The characterization andevaluation of accidental explosions. Prog. Energy Comb. Sci. 1976, v.2, № l, c.27-60.

2.5. Baker W.E. Explosions in air. Univ. Texas, 1973, p.266.

2.6. Lewis W.J. Condensed phase explosions and their blastcharacteristics // Paper at Euromech 139,1981, 7p.

2.7. Tornhill C.K. Explosion in air. ARDE Mem 57/60,1960.

2.8. Kinney L.F. Explosive shocks in air. McMillan. N.Y. 1962.

2.9. Brasil W.C., Simpson B.W. Damage from chemicalexplosions // Paper at Loss Prev. Symp., preprint 21 -A, St. Louis, 1968,15p.

2.10. Clancey V.J. The propagation of shock waves // Paper at Euromech 139,1981.

2.11. Henrich J. The dynamics of explosions. Elsevier, Amsterdam, 1979.

2.12. Held M., Jager E.H., Stolzl B. TNT-blast equivalence forbursting or pressurezed gas conventionalvessels // Paper at 6thSMIRTconf. Paris, 1961.

2.13. Korotkov A.I., Tsikulin M.A. A ratio of impulses in the reflected and incident wave // «Fizika vzryva» .M., USSR Ac. Sci., 1956, p. 56 - 60. (*in Russian*)

2.14. Brode H.L. Review of nuclear weapons effects // Ann. Review of Nuclear Sci. 1968, v. 8, p. 53-202.

2.15. Brode H. L. The real thing: blast waves from atmospheric nuclear explosions. Proceed. 12th Intern. Symp. On shock tube. Jerusalem, 1980, p.31-47.

2.16. Gold K.F., Tempo K. High-explosive field tests. DNA-6187F, 1983.

2.17. Khristoforov B.D. Parameters of the wave front in air at explosion of charges of lead azide and PETN of different density. ZhPMTF, 1961, № 6, p. 175-181. (*in Russian*)

2.18. Lannoy A. Analyze des explosions air-hydrocarbures. Bull. EOF, 1984, v. 4,390 p.

2.19. Guerke G., Scheklinski-Giueck G. Blast parameters from cylindrical charges detonated on the Surface of the Ground // 20thExpl. Saf. Seminar, 1983, DTIC, v.l, p.87.

2.20. Coulter G., Kingery C. Effects of low loading density onblast propagation from earth covered magazines // ibid., p. 11.

2.21. Reed J.W. Blast properties for coyote canyon explosions // ibid, p. 169.

2.22. Held M. Blast waves in free air // Propell., Explos., Pyrotechn., 1983, v.8, № 1, p. 1 - 7.

2.23. Austing J.A., lulls A.J., Napadensky N.S., Heberlein D.The output of detonating binary and ternary pyrotechnic formulations // Pros. 9-th Int. Symp. Pyrotechn., IIT Res. Inst., 1984, p.29.

2.24. Tzeitlin Ya. N., Smolii N.I. On the effect of weak shock-air waves at explosions on excavations. Vzryvnoe delo № 82/39,1980, p. 232 - 247. (*in Russian*)

2.25. Held M. Similarities of Shockwave damage in air and in water // Propell. Explos. Pyrotechnics, 1990, v.15, № 2, pp. 149 - 156.

2.26. Cole R.H. Underwater Explosions, Princ. Univ. Press. 1948,242 p.

2.27. Khristoforov B.D. Underwater explosion in an air cavity // ZhPMTF, 1962, № 6, p. 128-132. (*in Russian*)

2.28. Khristoforov B.D. On the similarity of shock waves at explosion of spherical charges in water and air // ZhPMTF, 1963, № 2, p. 142-146. (*in Russian*)

2.29. Arons A.B. Underwater explosion Shockwaves parametersat large distances from charge // J. Acoust. Soc. Amer., 1954, v.26, N7, p. 1225.

2.30. Bjorn L. On underwater explosions and transmission ofshock waves through foam plates immersed in water, Rep LFM-R-68-1-196.

2.31. Poche C.B. Underwater shock wave pressures from small detonate // J. Acoust. Soc. Amer., 1972, v.51, № 12, p. 1733.

2.32. BebbA, H. Underwater explosion measurements from small charges at short ranges // Phil. Trans. Roy. Soc., London, Ser. A, 1952, p. 1.

2.33. Bjorn L. Underwater explosion research based on model experimental // Problems of nonlinear acoustics, Novosibirsk, 1987, pt. II, pp. 163-177.

2.34. Dvoinishnikov A.E., Dorofeev S.B., Gelfand B.E. Анализ of the data by the parameters of the air shock wave from CHE // Preprint IAE, 1993, IAE5005-13. (*in Russian*)

2.35. Kirmey G.F., Graham KJ. Explosive shocks in air. SpringerVerlag, N.Y.Inc., 1985,269 p.

2.36. Gelfand B.E., Gogulja M.F., Medvedev S.P., Polenov A.N., Khomik S.V. Diagnostics of afterburning of detonation products of the condensed explosive substances // Doklady RAN, 2001, v. 379, № 3, p. 348-352. (*in Russian*)

2.37. Gudzilo S., Trczinski W., Maranda A. Detonation behaviorin HMS-based explosives containing magnesium and polytetrafluorethylen // Proc. Of 27-th Intern. Annual Confer, ofICT, Karlsruhe, FRG, 1993, p. 71.1-71.14.

2.38. Kedrinsky V.K. Hydrodynamics of explosion. Experiment and models. Novosibirsk, SB RAN Publ., 2000,434 p. (*in Russian*)

2.39. Silnikov M.V , Petrov A.V., Orlov A.V., The pressure at the a shock wave front at explosion of 0,075 — 1,2 kg TNT charge // Proc. of the 2nd interregional scientific - practical conference «Development new special technique for MVD ». — ST.Peterspurgh, University MVD Russian Federation, St.-Petersburg. - 2000. - p. 226. (*in Russian*)

2.40. Silnikov M.V., Mikhailin A.I., Orlov A.V., Khimichev V.A., Nozdrachev A.V. Parameters of the shock wave at explosion of 0,075 — 1,2 kg TNT charge // Proc. of the 4th All-Russia scientific - practical conference «Urgent problems of protection and safety ». St.Petersburgh. - 2000. - v. 2. - p. 572 (*in Russian*)

2.41. Silnikov M.V , Petrov A.V., Sergeev V.E. The experimental measurement of the impulse of air shock wave at explosion of <1 kg TNT charge// Proc. of the 2nd interregional scientific - practical conference «Development new special technique for MVD ». — ST.Peterspurgh, University MVD Russian Federation, St.-Petersburg. - 2000. - p. 230. (*in Russian*)

2.42. Ambrosini R.D., Luccioni P.M., Danes! R.F., Riera J.D., Rocha M.M. Size of craters' produced by explosive charges on or above the ground surface shock waves, 2002, V. 12, N1, p. 69 - 78.

CHAPTER 3 CRITERIA OF BLAST WAVES DAMAGE

3.1 Interaction of the blast waves with targets

When a blast wave meets to a target a partial reflection takes place (fig.3.1). The lateral and top surfaces of the target are subjected by the pressure behind the passing wave ΔP. Windward side of the target will be exposed by at least doubled pressure load due to the stop of the flow. Nearby the lateral and top surfaces of the target there will be a flow with significant pressure gradients due to the rarefaction waves. Because of these waves the pressure at the windward side will decrease down to the stagnation pressure of a gaseous flow. After attaining the backside the wave bends the target and generate the turbulent zones. After the blast wave moves away, the target is subjected only by the wind load due to the friction forces arising from the streaming flow around the body.

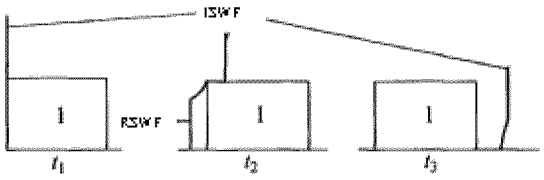

Fig.3.1 Scheme of blast wave interaction with a target. 1- target, ISWF – incident shock wave front, RSWF – reflected shock wave front.

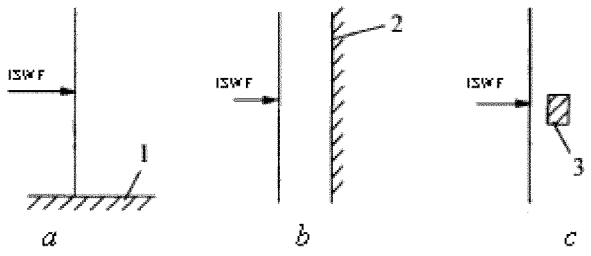

Fig.3.2 Three cases of passing wave interaction with obstacle: a) wave propagation alongside the surface, b) normal reflection, c) streaming flow around the small body

It is possible to distinguish three limiting cases of targets blast loading (fig. 3.2)

1. Wave does not "feel" the target. So, the target is subjected to the effect of the pressure behind the incident wave.
2. Wave reflects at the target. So, the target is subjected to the effect of the pressure behind the reflected wave.
3. Size of a target is small in comparison with the size of a blast wave. This provides almost instantaneous release of the target from loading. The target is subjected only by wind loading, which is determined by gas flow breaking.

The magnitude of wind loading Q depend on the gas density ρ, the gas velocity u, and the shape of a target:

$$Q=C_d 0.5\rho u^2$$

The friction parameter C_d is found by experimental methods [3.4…3.7].

3.2 Dynamics response of the target to the blast loading.

The simplest scheme of blast loading of the target of mass m is presented in the fig.3.3. The magnitude of the active load P is determined by the above described schemes. The response force R defines the resistance of the target to the displacement:

$$P=R+md^2x/dt^2,$$

where $q= d^2x/dt^2$ is the acceleration of the target.

At the static loading and at low acceleration $P=R$.

At minor acceleration $P\neq R$

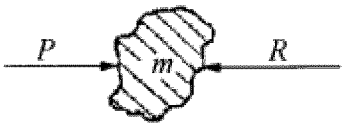

Fig.3.3 The scheme of the forces acting to a target

The response force R depends on the displacement x and the possible variants are shown in the fig.3.4. The variant in the fig.3.4*a* corresponds to the ideal elastic case: the resistance is directly proportional to the displacement. The ideal plastic case is represented in fig.3.4*b*: the resistance does not depend on the displacement. Usually, in practice, the mixed variant takes place (see fig.3.4*c, d*): elastic case at small shift and plastic one at large displacement.

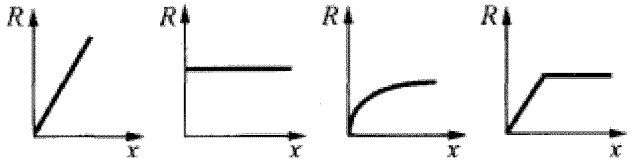

Fig.3.4 The main types of target response to the force. a) – ideal elastic, b) – ideal plastic, c, d) – mixed.

The notion of the dynamic loading factor DLF is often used to calculate the target response to the blast loading. Using the DLF the static loading can be found, which generate the same effect as the dynamic loading under study. Usually the question of destroying loads is discussed [3.1, 3.2].

Let the system behavior is described by equation:

$Mq+Kx=P(t)$,where $q=d^2x/dt^2$ and K – is elasticity coefficient.

The profile of the loading is plotted in fig.3.5.

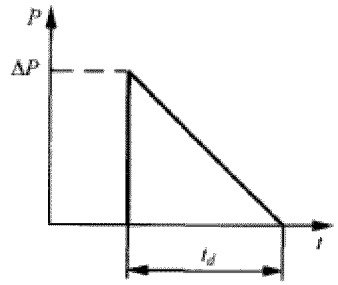

Fig.3.5 Scheme of the short-time loading of the target.

The value of DLF depends on the parameter t_d/T (fig.3.6). The period of natural oscillations of the target is $T=2\pi(m/K)^{0,5}$.

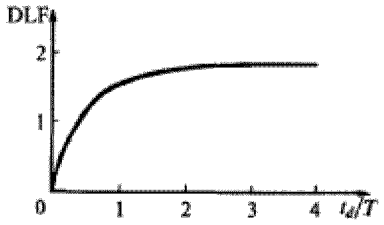

Fig.3.6 Dependence of dynamic loading factor on the relative loading duration.

Two limiting cases can be marked:

- for low t_d/T <<1 the DLF parameter is proportional to the loading duration, the so-called impulse loading;
- for high t_d/T > 1 the DLF parameter →2, the so-called step loading.

The cases of impulse and stepped loading are illustrated in fig.3.7.

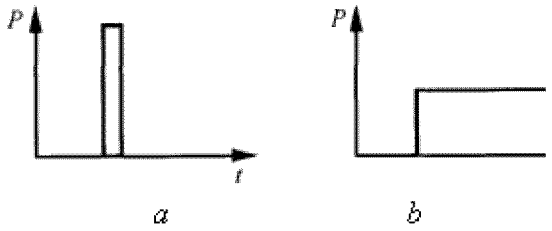

Fig.3.7 Two types of loading: a – impulse, b – step

The target response at the impulse loading is determined as $\int Pdt$ and weakly depends on the function $P=P(t)$. In case of step loading the time of the action is not of importance and can be considered as infinite value. Of importance is the time of the loading growth t_s –see fig 3.8.

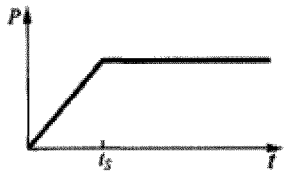

Fig.3.8 Scheme of loading with preliminary compression phase.

The dependence of the dynamic loading factor DLF on the parameter t_s/T is shown in the fig.3.9. For $t_s \to 0$ the DLF $\to 2$, as in the case of ideal stepped loading. In the case of long –time loading growth DLF $\to 1$, and one can say about residual type of influence at DLF=1. More detailed illustration of the loading type on DLF is presented in the fig.3.10.

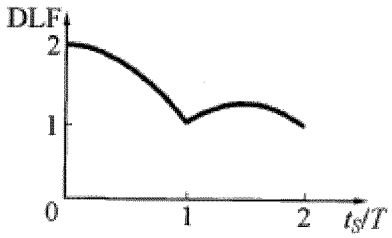

Fig.3.9 Dependence of dynamic loading factor on relative duration of preliminary compression phase

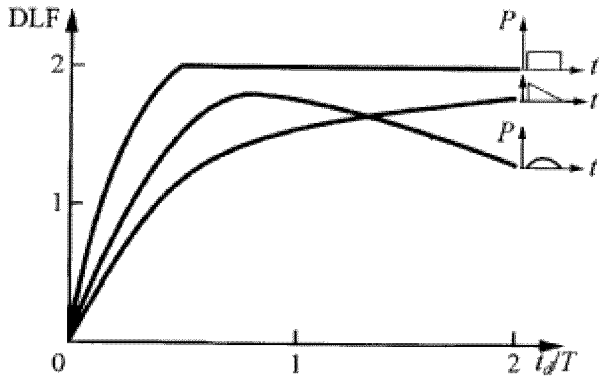

Fig.3.10 Dependence of dynamic loading factor on relative duration of loading for different types of loading [3.6]

Blast and shock waves generated by explosion processes produce the impulse and stepped loads. The compression waves with long phase of pressure rise are closer to the static load.

The method of diagrams overpressure ΔP- impulse I is often used to estimate the effect of dynamic target response on its vulnerability [3.4, 3.19, 3.32]. The idea of such diagrams construction is based on the dependence of vulnerability on the duration of loading. The space below or above the line of defeat corresponds to the dangerous or not dangerous combination of pressure and impulse for the particular target (fig.3.11)

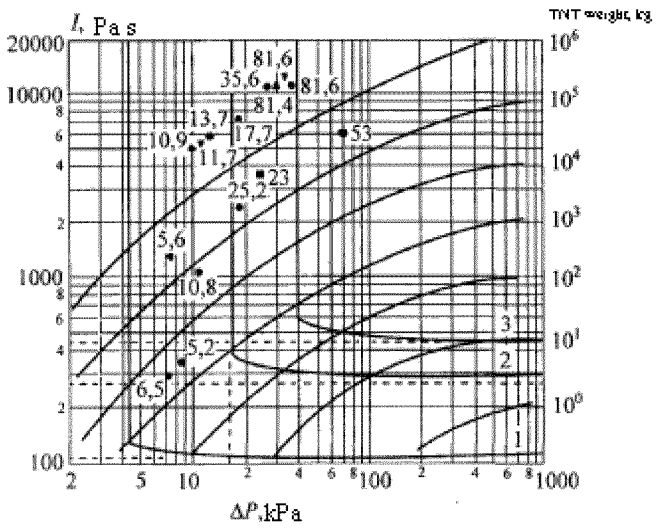

Fig.3.11 The pressure – Impulse diagram for building damage. 1- threshold of the minor structural damage, 2 – threshold of the significant structural damage, 3 – the boundary of the full (total) damage. [3.6] • *- group 1,* ▲ *- group 2,* ▼ *- group 3,* ■ *- group 4.*

The points of the group 1 are the two-story wood buildings.

The points of the group 2 are the two-story stone buildings.

The points of the group 3 are the one-story wood buildings.

The points of the group 4 are the one-story brick buildings.

The numbers near the points denote the relative costs (in %) of the damage. Thin lines correspond to the relation between the impulse and the amplitude of a blast wave for indicated TNT weight.

3.3 Critical levels of overpressure.

One of the most significant and prevail factor (at any explosion accident) of damage is the impulse of pressure (velocity) generated of the pressure wave of a shock wave. Blast waves are created in surrounding atmosphere by the fast energy release as a result of explosion of a mass of energy carrier of any type, high pressure vessels burst, the

failure of the vessels containing overheated liquid, etc. The only parameter – overpressure ΔP is used at the moment almost in all guides, technical references and expert handbooks for assessing the damage. No attention is paid to the shape of the wave and the durations of compression and rarefaction phases. No attention is paid also to the impulse of pressure carried by the wave

$$I = \int_0^t \Delta P dt$$

Here $\Delta P = P_{11} - P_0 = \Delta P_i$, P_{11} and P_0 are the pressures behind the wave and in the initial medium. Traditional approach means the correlation between expected damage to the blast wave amplitude. Thus, the particular level of damage (often subjectively) is attributed to the characteristic value of ΔP_i^*. The values ΔP_i^* are presented in table 3.1 by phenomenological observations [3.1, 3.2, 3.3]. Note satisfactory agreement between domestic and foreign data.

Table 3.1 Critical overpressures

ΔP_i^*	*[3.1]*	*[3.2]*	*[3.3]*
0,20 Pa		*Limit of sound pressure for industrial personnel*	
0,20...0,22kPa	*Rare damages of large windows*	*1 window broken per 10 people*	*0,6... 1kPa*
1,4 к Pa	*(137dB) ringing in the ears*	-	-
2kPa		*ringing in the ears (160 dB) 1 window broken per 1 man*	*1…2kPa*
1,4kPa		*Dangerous for light aerotechnics*	
3,5 kPa		*Injuries by window fragments*	
7kPa	*Small glass windows are broken*	*Light damage of roof and walls*	

10kPa	*Typical pressure for glass window failure*		*3 … 6 kPa*
20 kPa	*5% probability of severe damage*	*Rooting out of small trees*	
22 kPa	*More than 10% windows are broken*		
22kPa	*Damage of ceiling boards*		*20... 40kPa*
28kPa	*Lower limit of structural damage*		*20... 40kPa*
40...70kPa	*All large windows are broken, rare damage of window frame*	*Rooting out of trees, death of flying birds*	*30... 50kPa*
20…35kPa		*Contusion of uncovered animals*	
50kPa	*Light damage of buildings*		
45... 85 kPa	*Window frames are broken, partial damage of buildings*	*Big and small animals lung laceration*	*40...60kPa*
70...140kPa	*Asbestos covers are broken, bending and blown off of aluminum covers. Failure of wood panels.*		
55kPa		*Lower lethal limit*	
100 kPa	*Damage of steel frames*		*50... 60 кПа*
140kPa	*Partial demolition of walls*		
140... ...210kPa	*Demolition of slag-concrete walls*		

160 kPa	*Lower limit of severe damage*		*60... 50 kPa*
175 kPa	*Demolition of brick walls*		
210 кПа	*Light damage of equipment*		*70…60kPa*
210... ...280 kPa	*Demolition of steel panels*		
210... ...280kPa	*Vessels bursting*		*50... 100kPa*
350... ...490 kPa	*Complete demolition of buildings, turning over of rail cars, crushing of walls*		*100... 200 kPa*
630 kPa	*Deformation of loaded rail cars*		

The discrepancy of quantitative characteristics for the same level of damage is approximately 2 times, which is not acceptable for expert assessment of the real accident.

In fact, the discrepancy in explosion energy estimations can reach 5-10 times. This can prejudice the determination of the energetic potential of the accident. The difference in ΔP_i^* values is conditioned by the subjective nature of the damage evaluation. Below, as an example, we consider the critical values of ΔP_i^* corresponding to the damage of window glasses, which are basically used in expert evaluations.

The existing data on the critical overpressures able to destroy the window glasses are contradictory and therefore must be used very carefully. The critical value of overpressure depends on the width of the glass, window area, type of glass fixing, character of blast loading (duration, front steepness, amplitude modulation), and many others no controllable of badly controllable parameters. Thus, the indication of any exact value of the critical damage level of ΔP_i^* without the fixing of the discrepancy $\delta(\Delta P_i^*)$ is incorrect. American Bureau of Standards proposes the modern method on the consequences of single HE detonation in air. According to the standard S-2-54 (1976) [3.2] for every level of the overpressure the number of window glasses per 1000 habitants is indicated. For the urban areas the reference data are following:

Overpressure ΔP, MPa	Number of broken windows per 1000 people
0.0010	200
0.0015	400
0.0020	600

The plot of the probability P of window failure on the overpressure in the wave ΔP is presented in fig. 3.12. The additional ordinate axis indicates the number of window glasses per 1000 habitants. One can expect the failure of at least 1 window per 1000 people at the pressure perturbations much less than usually reported in typical handbooks. For example, most of the domestic documents declare, that there is no window demolition at $\Delta P \leq 0.001$MPa. According to USA standard at $\Delta P = 0.001$MPa 1% of all windows (or 200 windows per 1000 people) will be broken. The complete 100% window demolition occurs for the waves with $\Delta P \geq 0.01$MPa.

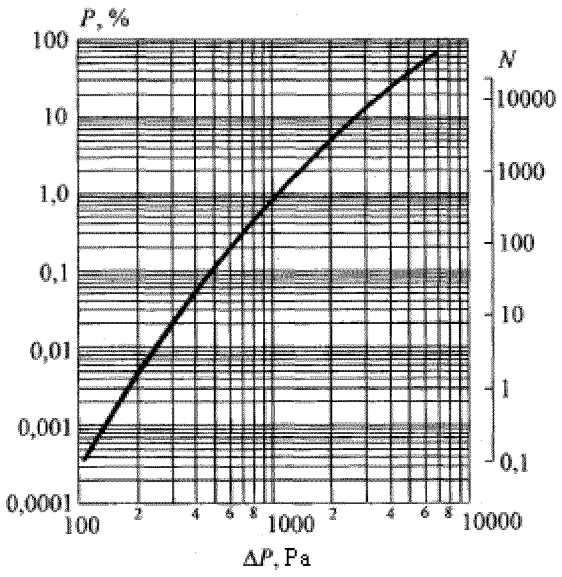

Fig.3.12 Dependence of the probability of window failure on the overpressure in the wave

Presented above discussion demonstrates, that the knowledge of the critical overpressures (shown in the table 3.1 or referred in [3.1, 3.2, 3.3] is necessary, but not enough instrument for expert assessment.

3.4 Method of Pressure-Impulse diagrams

More exact representation about an arbitrary system response to the blast loading can be obtained from the analysis, which takes into consideration the finite time of pressure wave action [3.4…3.7].

The time-space scale of the action is described in such a manner that both the amplitude of the wave and static I_{st} and dynamic I_{din} impulses are taking into account.

$$I_{st} = \int_0^t \Delta P dt$$

$$I_{din} = \int_0^t \rho u^2 dt;$$

Here ρu^2 is the doubled dynamic head, ρ and u are the air density and the velocity accordingly. The pressure amplitude and the static impulse determine the expected mechanical damage of the target, and the dynamic impulse and the amplitude of velocity head set the conditions of the possibility to blow off the object from initial location. The use of the impulse and the amplitude of the pressure wave allows to deeper understanding level of conditions and criteria of damages. The so-called danger number DN can be introduced for the quantitative hazard evaluation. For simple systems the danger number is evaluated as [3.4, 3.12]

$$DN = \left(\Delta P - \Delta P_i^*\right)\left(I - I_i^*\right)$$

As earlier ΔP_i^* is the critical pressure amplitude necessary for demolition. Additionally the notion of the critical pressure impulse I_i^* is introduced. In simplest case there exists hyperbolic dependence of DN in coordinates pressure-impulse.

Let us consider a set of typical examples. Fig 3.13 illustrates the data on the human body damage by air blast waves [3.4, 3.5, 3.8, 3.11]. It is seen, that for all types of damage

the decrease of wave duration (decrease of impulse) leads to a situation when any increase of the amplitude does not give rise to irreversible consequences. Qualitatively the same is the response of some mechanical targets to the blast wave.

The typical pressure-impulse diagram for window breaking is shown in the fig. 3.14 [3.14]. Another example of pressure-impulse diagram is presented in the fig. 3.15.

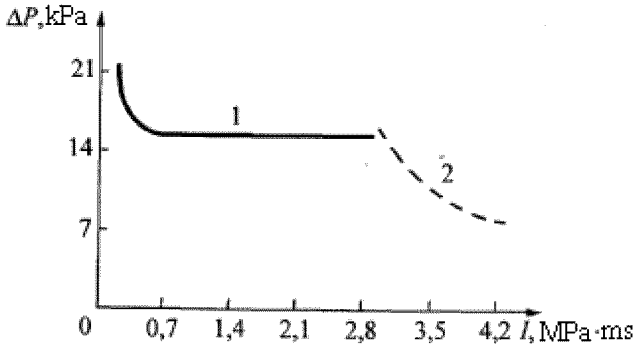

Fig.3.13 Diagram of human body damage by shock waves. 1- eardrums burst, 2- heavy contusion.

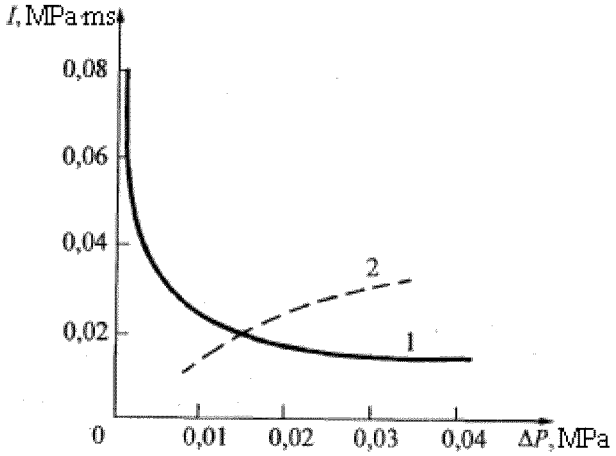

Fig 3.14 Pressure-impulse diagram for window breaking (line 1). Size of the window 45x35 cm, width 3 mm. I-ΔP dependence for 1kg of TNT (line2)

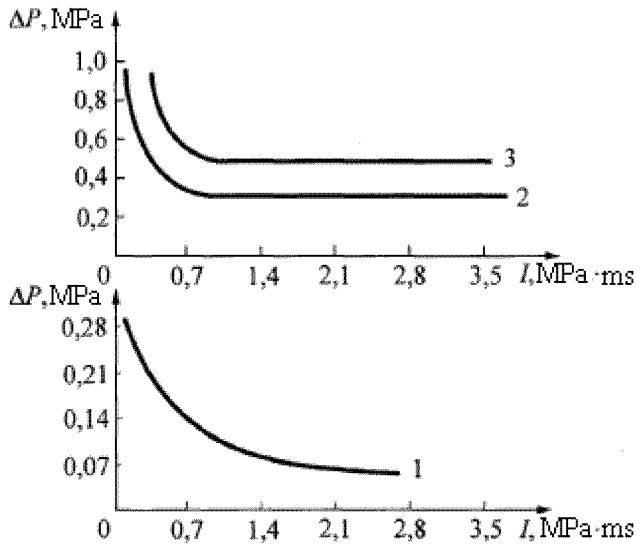

Fig. 3.15 Pressure impulse diagram for some constructions. 1 – turnover of truck, 2 – car cabine deformation, 3 – demolition panel constructions (antenna, panels, arcs)

The problem of attaining the particular damage with the help of pressure – impulse diagrams is solved by the plotting corresponding functional relationship of the main explosion parameters in any of the diagrams in the fig. 3.13, 3.14, 3.15. Mutual position of the damage curve and the curve of wave characteristics determines the possibility and the level of expected effect.

The experience of damage assessment caused by HE explosion nearby typical industrial or civilian objects showed, that the radius of the particular damage zone can be calculated using expression [3.14]:

$$R_{SI} = K_i G^{0,33} \left[1 + \left(\frac{3180}{G} \right)^2 \right]^{-0,17}$$

Here K_i – is the coefficient determining the level of damage i = I, II, III, IV, G – TNT charge weight in kg. The value K_I =3.8 corresponds to the zone of complete demolition. At K_{II} =9.6 the buildings are destroyed, roofs are blow off, the walls are damaged significantly. K_{III} =28 corresponds to the moderate damages. Finally, K_{IV} =55 indicate the zone of light (reparable) damages. The fraction of the broken windows in this

zone is about 10%. Using the R_{SI} dependencies the corresponding pressure – impulse diagrams can be plotted by the following procedure: find the R using the known mass G and recalculate the coordinates at ΔP-I diagram using the known dependencies from [3.4, 3.5].

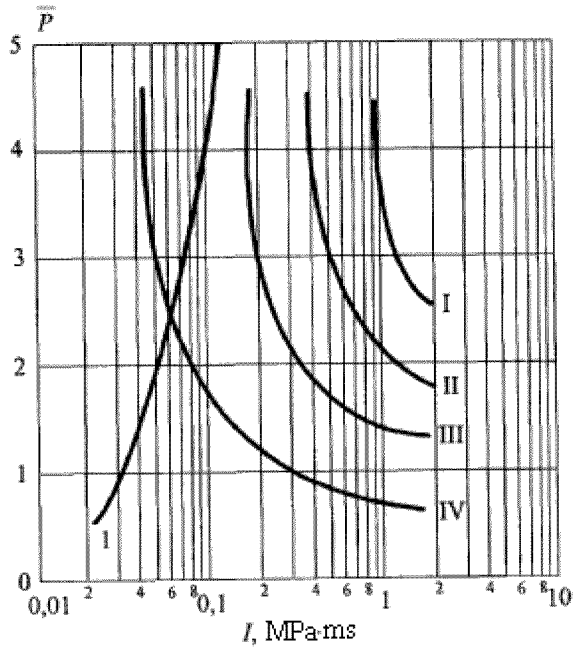

Fig. 3.16 Diagram for different levels of danger I-IV in combination with maximal levels of pressure-impulse for HE (line 1)

Above-mentioned diagram is represented in the fig.3.16. The damage evaluation by overpressure is possible just for $I>>I_i^*$, where I_i^* is the characteristic pressure impulse at the compression phase for the danger level under consideration. Lines I, II, III, IV characterize the response of the industrial and civil constructions to the blast loading. To evaluate the possibility to achieve the marked danger levels the functional relationship of pressure-impulse in the blast wave must be plotted at the same diagram. The use of the magnitude of critical overpressure (as usually done in practice) "silently" assumes that the pressure wave has significant duration, which is incorrect for the explosions of the limited fuels masses. It was shown in [3.4, 3.10] that the method of pressure –impulse diagrams gives the possibility to diminish the magnitudes of the safe distances without decrease of

the level of the safety for the given objects. The expected profit in the safety distances estimation can be represented by the dynamic coefficient of explosion loads [3.2, 3.4]:

$$f = \left[1 + \left(\frac{3180}{G}\right)^2\right]^{-0.17}$$

The dependence of the coefficient f on the weight of the charge (line 1) is presented in the fig.3.17. As seen from the figure, the profit in the safety distances due to the dynamic character of the blast loading can reach 1.2…1.4 times in the range of G under consideration.

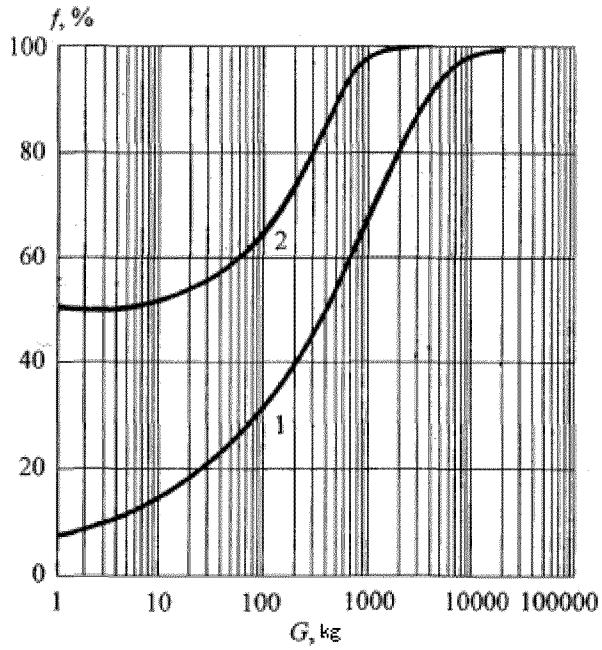

Fig.3.17 The expected profit by the safety distances depending on HE weight.

Recently, on the basis of analogous approach in France, the magnitudes of the safety distances for the small (up to 300-500 kg) HE charges were reconsidered. According to the new rules of HE storage in France the safe distance $R^{**}=f\,R^{*}$, where R^{*} is the safe distance for the wave generated by strong explosion. According to the standards in France:

$$f_1 = 1 - 0.5 \exp\left(-\frac{G}{300}\right)$$

The dependence of f (line 2 in the fig.3.17) on the charge weight additionally takes into account the effects of the fragments from explosion at small distances.

It must be emphasized, that the real subdivision of the pressure-impulse plane into two parts (the internal – demolition zone, and the outer – stability zone) has no sharp boundary. With approaching to the danger threshold the probability of the particular danger increases. Finally the 100% probability of danger for the known pressure and impulse can be attained. This typical specific feature of the diagrams of danger can be represented by introducing the probit – function Pr_i [3.8, 3.13].

The probability of hardly reparable damages of the industrial buildings (line II in the fig.3.16) can be estimated by the equation:

$$\mathrm{Pr}_1 = 5 - 0.26 \ln V_1$$

The factor V_1 is calculated by the overpressure ΔP_5 (in Pa) and the static impulse I_5 (in Pa·s) in the pressure wave.

$$V_1 = \left(\frac{17500}{\Delta P_5}\right)^{8,4} + \left(\frac{290}{I_5}\right)^{9,3}$$

The probability of non – reparable damages of buildings (line I in fig.3.16), which is characterized by their destruction, can be estimated by the equation:

$$\mathrm{Pr}_2 = 5 - 0.22 \ln V_2$$

In this case the factor V_2 is calculated as follows:

$$V_2 = \left(\frac{40000}{\Delta P_5}\right)^{7,4} + \left(\frac{460}{I_5}\right)^{11,3}$$

There also exist the formulas for calculating the probability of bioorganizms (including human body) blast damages. The probability of lungs contusion is estimated by:

$$\mathrm{Pr}_3 = 5 - 5.74 \ln S_3,$$

where

$$S_3 = \frac{4.2}{\overline{P}} + \frac{1.3}{\overline{i}}.$$

In last expression the non-dimensional pressure and impulse are determined by:

$$\overline{P} = 1 + \frac{\Delta P_5}{P_0}; \overline{i} = \frac{I}{P_0^{0,5} m^{0,33}},$$

here m – is the mass of bioobject in kg, pressure in Pa and impulse in Pa·s. The transition zone is shown in the fig.3.18. Some references report about the dependence of probability of human eardrums burst on the overpressure in the air wave: $\mathrm{Pr}_4 = -12.6 + 1.524 \ln \Delta P_5$.

Usually, the pressure wave acts on the live organisms not only by the shock increase of static pressure, but also by the dynamic impulse, which can blow off the human body with high velocity into the direction of wave propagation [3.34…3.36]. The probability of human body blow off is estimated using the value

$\mathrm{Pr}_5 = 5.0 - 2.44 \ln S_5$, where

$$S_5 = \frac{7.38 \cdot 10^5}{\Delta P_5} + \frac{1.3 \cdot 10^9}{\Delta P_5 I_5}.$$

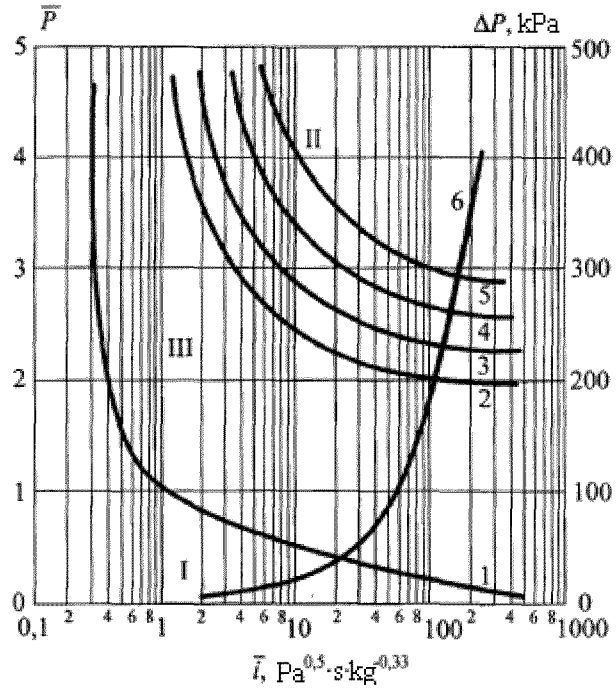

Fig.3.18 Diagram of human damage by blast waves. I – safe zone, II – damage, III – transition zone, 1 - lower threshold, 2 – 1% lethality, 3 – 10% lethality, 4 – 50% lethality, 5 – 90% lethality, 6 – (ΔP-I) for 1 kg TNT.

Additional evaluation of the damage level at the displacement of live organism with finite velocity can be performed with the help of pressure-impulse diagram from [3.6, 3.8] reproduced in the fig. 3.19. Lines 1,2,3,4 in the fig. 3.19 corresponds to the following damage levels:

- safe impact
- critical (impact threshold – lethal case is possible)
- 50% lethality
- 100% lethality

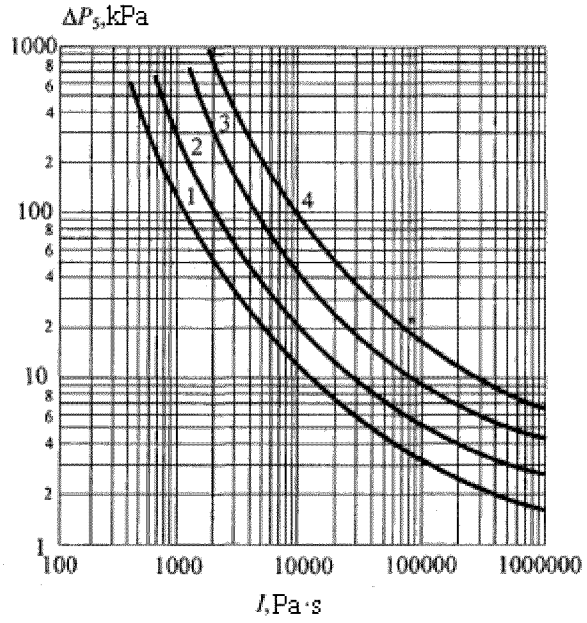

Fig.3.19 Diagram of human damage due to dynamic head.

Analysis of expressions for functions Pr_i (excluding Pr_4) shows their close connection with the impulse characteristics of the pressure wave. Any of the damage levels (typical for Pr_1, Pr_2, Pr_3, Pr_5) can be attained only for the finite value of compression phase impulse, i.e. for $I_5 \neq 0$.

3.5 Secondary effects

In preceding chapters only two direct factors of danger owing to the blast waves were considered: static pressure jump, and sudden air movement by the compression wave. However, of importance are also the secondary effects accompanying the blast loading.

One of the most significant secondary effects is the fragments flight from destroyed structural elements. Above analysis shows, that the window glasses have the lowest threshold of strength. The important practical information on the velocity of window fragments for different window areas and glass widths is contained in the reference [3.9]. The fig. 3.20 represents the data from [3.9].

The dependence of the maximal range (flying distance) of the glass fragments on the blast wave pressure is an important characteristic for hazard evaluation and risk assessment. The plot in bottom part of the fig.3.20 determines the expected range of fragment flight. It is seen, that for the blast overpressure $\Delta P \cong (2\ldots20)$ kPa the fragment flying distance is about 10…30 m, and the velocity of the fragments is about 10…30 m/s. The mass of the fragments of glass does not exceed 100 g in accordance with the data from [3.9]. The probability of light injuries is evaluated by the probit function [3.6,3.8]:

$\mathrm{Pr}_6 = -29.15 + 2.10 \ln S_6$, where

$S_6 = m_0 v^{5.115}$.

Here m_0 is the mass of the fragment in kg, and v is the velocity of the fragment in m/s.

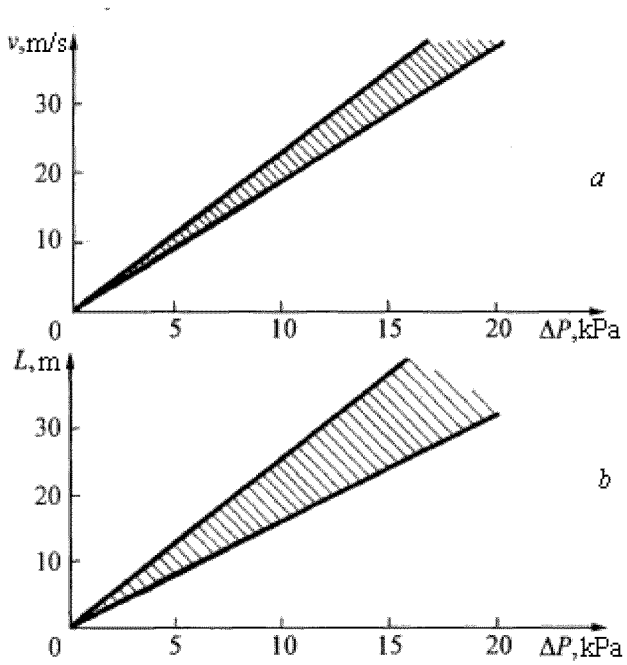

Fig 3.20 The velocity (a) and the maximal distance (b) for the flight of the fragments of glass windows caused by blast wave. The shaded area corresponds to the scatter of data from [3.9].

The function probit Pr_i is related to the probability p of particular level of danger by the table 3.2.

Table 3.2 Probit vs. probability [3.8, 3.13]

P, %	0	1	2	3	4	5	6	7	8	9
0		2.67	2.95	3.12	3.25	3.38	3.45	3.52	3.59	3.66
10	3.72	3.77	3.82	3.86	3.92	3.96	4.01	4.05	4.08	4.12
20	4.16	4.19	4.23	4.26	4.29	4.33	4.36	4.39	4.42	4.45
30	4.48	4.50	4.53	4.56	4.59	4.61	4.64	4.67	4.69	4.72
40	4.75	4.77	4.80	4.82.	4.85	4.87	4.90	4.92	4.95	4.97
50	5.00	5.03	5.05	5.08	5.10	5.13	5.15	5.18	5.20	5.23
60	5.25	5.28	5.31	5.33	5.36	5.39	5.41	5.44	5.47	5.50
70	5.52	5.55	5.58	5.61	5.64	5.67	5.71	5.74	5.77	5.81
80	5.84	5.88	5.92	5.95	5.99	6.04	6.08	6.13	6.18	6.23
90	6.28	6.34	6.41	6.48	6.55	6.64	6.75	6.88	7.05	7.33
99	7.33	7.37	7.41	7.46	7.51	7.58	7.65	7.75	7.88	8.09

3.6 Effect of bio-object position on the damage caused by blast wave.

When the blast wave propagates around the human body, the loading significantly depends on the mutual orientation of the wave front and body position [3.15]:

- The blast wave propagation along the lying body into direction legs – head.
- The facing of the blast wave with the standing body, or its propagation perpendicular lying body.
- The facing of the blast wave with the standing or lying body nearby reflecting surface.

The damage diagrams for the above noted cases are presented in the fig. 3.21*a,b* in coordinates compression phase duration τ_+ - blast wave overpressure ΔP by [3.4, 3.5, 3.15].

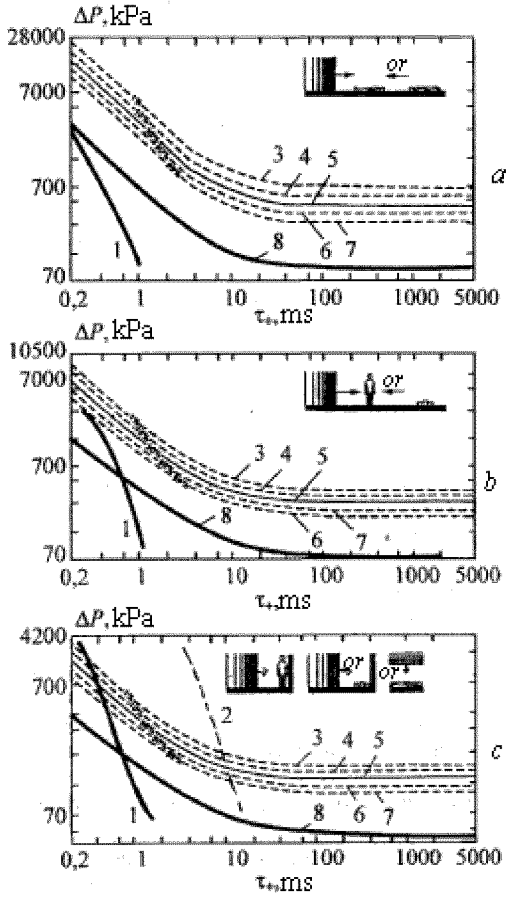

Fig 3.21 Critical levels of blast amplitude and duration for different human body orientations relative to the blast front. a)The blast wave propagation along the lying body into direction legs – head, b) The facing of the blast wave with the standing body, or its propagation perpendicular lying body, c) The facing of the blast wave with the standing or lying body nearby reflecting surface. Line 1 – for 1 kg charge, line 2 – for 1000 kg charge, lines 3…7 – survival levels, line 8 – thorax damage threshold.

The cases where minimal blast pressure and impulse are required for the damage correspond to the positions of human target lying or standing nearby the reflected surface (fig.3.21*c*). However, the consideration of the shape and type of reflecting surface, the incidence angle and the distance of human target from reflecting surface is of great difficulty.

Moreover, in the real conditions, the reflecting surfaces nearby the human target could be absent, which restricts the application the lethality (or survival) curves applications for the case presented in the fig. 3.21*c*. In case of blast wave propagation in free space the maximal effect on human body occurs at perpendicular facing of the incident shock (fig.3.21*b*). This position is rather probable and is considered as the basic one at primary damage assessment at accidental explosions [3.4].

3.7 Blast wave effect for people

Blast damage of human body.

The blast damage of human body is conditioned by the existence of various internal organs with different density and the gas-filled cavities inside the corp. First of all of importance are the lungs. Every lung contains about 300 billion of air cavities – aveols. The thickness of their walls is δ=0.2 μm, that is 370 time narrower than hair width [3.4].

The blast wave, faced to the human body, partially penetrates inside and propagates through viscous multiphase medium. The pressure wave meets the aveols and compress their gaseous filler. This results in their destruction and the burst of neighbor capillary [3.37]. Finally internal blood flow starts which causes lethality. Also dangerous is the gas inflow into blood at rarefaction phase (caisson disease analog).

For the detonation of HE charges up to 20 kg the severe damage threshold takes place at blast wave amplitude ΔP>270 kPa. Such a wave is expected at 250 g HE detonation at the distance of outstretched arm.

In recent years the attention of physicians are attracted to the blast damage of such internal organs as stomach and intestinal tract, resulting in internal blood flow, burst and perforation of walls. The listed injuries are latent and are difficult diagnosed, which causes heavy long-time physiological consequences.

Blast damage of human extremities.

The severe damage of extremities (arms, legs) occurs at the extremely powerful blast load exceeding ΔP>1.5 MPa. The extremities contain small amount of gas, so can be considered as incompressible. The damage takes place as traumatic amputation, therefore requiring larger blast loads than in the case of breathing organs.

At the same time, during the expertise one must take into account the fast attenuation of the blast wave with distance.

Blast damage of human ears

The ear, a sensitive organ system that converts sound waves into nerve impulses, responds to a band of frequencies ranging from 20 Hz to 20,000 Hz. This remarkable organ can respond to energy levels as low as 10^{-12}watt/m^2, which causes the eardrum to deflect less than the diameter of a single hydrogen molecule [3.33]. Not being able to respond faithfully to pulses having periods less than 0.3 ms, it attempts to do so by making a single large excursion. It is this motion, which can cause injury to the ear.

The human ear is divided into the external, middle, and inner ear. The external ear amplifies the overpressure of the sound wave by approximately 20 percent and detects the location of the source of sound. Rupture of the eardrum, or tympanic membrane, which separates the external ear from the middle ear, has captured most of the attention of clinicians although it is not the most severe type of ear injury. The eardrum and ossicles of

the middle ear transfer acoustical energy from the external ear to the inner ear where mechanical energy is finally converted into the electrical energy of the nerve impulse. The middle ear is an impedance matching device as well as an amplification stage. The middle ear contains two dampers: the stapedus muscle and associated ligaments, which limit the vibration of the stapes when subjected to intense signals, and the tensor tympani muscle and its adjoining ligaments, which limit the vibration of the eardrum. The first damper is the most important. These dampers have a reflex time of approximately 0.005 to 0.01 s, which is longer than "fast" rising air blasts. The manner in which the malleus and incus are linked allows far more resistance to inward displacement than to outward displacement. However, if the eardrum ruptures after inward displacement during positive phase of loading of the blast wave, the malleus and incus are less likely to displace as far outward during the negative phase of loading of the blast wave as they would if the eardrum remained intact. In this case, eardrum rupture could be beneficial. The maximum overpressure and its rise time, however, control the characteristics of the negative phase and is, therefore, of prime importance. Rupture of the eardrum, thus, becomes a good measure of serious ear damage [3.4].

3.8 Expert assessment of blast damage.

To perform the fast (urgent) expert estimations of damages from accidental explosions and terroristic acts it is necessary to have the simple and convenient tools based on the validated experimental and theoretical observations [3.15, 3.34…3.37].

One of the useful and simplest instruments is the nomogramm presented in the fig. 3.22. This nomogramm in the simplest form allows determining the consequences of blast loading on unprotected human body at the explosion of up to 22 kg TNT charge in near zone.

The nomogramm can be used in the following manner.

Let we have the explosive object of 4 kg of TNT. The distance to the object is 5 m. According to the nomogramm, the expected blast wave will have the amplitude ΔP=75 kPa. One can expect the eardrums burst with the probability 25% [3.34…3.37].

The same HE charge placed at the distance 1.5m will generate the wave with the amplitude ΔP=1 MPa, that guarantees 15% lethality, complete deafness, and the total burst of eardrums [3.37].

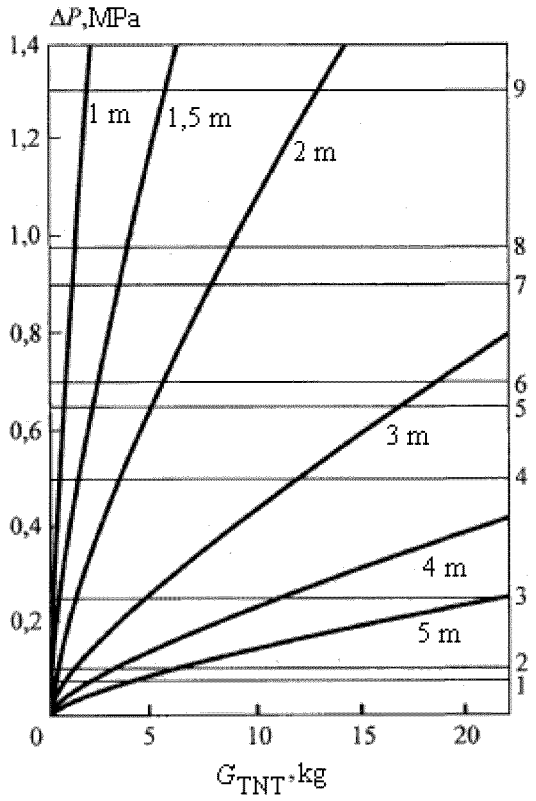

Fig. 3.22 Nomogramm for determining the blast damage of bioobject depending on the distance and HE weight. Horizontal lines: 1 – lower threshold of blast damage for ears, 2 – 50 % damage of ears, 3 - lower threshold of blast damage for lungs, 4 – 50 % damage of lungs, 5 – 1% lethality, 6 – 10% lethality, 7 – 50% lethality, 8 – 90% lethality, 9 – 99% lethality.

3.9 Assessment of shock wave effect on the bio-objects at blasting operations.

The principles of ecological safety [3.16] require the development of the methods for the prediction of the shock waves (SW) effect on the bio-objects at technological

blasting operations. The safety distances for blasting operations are determined by empirical formulas [3.17, 3.18]:

$$r_\sigma = kG^\chi \qquad (3.1)$$

where r_σ is the safety distance in m, G is the energetic characteristic of explosion in kg of TNT equivalent, χ and k are empirical coefficients, characterizing the sensitivity of the object to the blast loading.

The formula (3.1) must be used carefully, because the safety distance has no agreed-upon notion. According to the safety rules [3.17] at χ =1/3 and k = 15 in (3.1) the safety distance for the technical staff at the ground explosions can be obtained. However, these distances are differing from the safety distances accepted in other countries. For example, the requirements of USA Ministry of Defense (DOD 5154.45) of June 23 1980 [3.19] concerning the technical operations with explosives declare, that at the distances, which can be calculated by (3.1) with χ =1/3 and k = 16…20 the expected blast wave effect with high confidence level guarantees the absence of lethal cases, however the injuries connected with walls and windows demolition are possible**.** Ambiguous definitions of the safety criteria give rise to the necessity of serious analysis of the existing norms of safety and the development of the methods for safety distances assessment at blasting operations in different conditions [3.20].

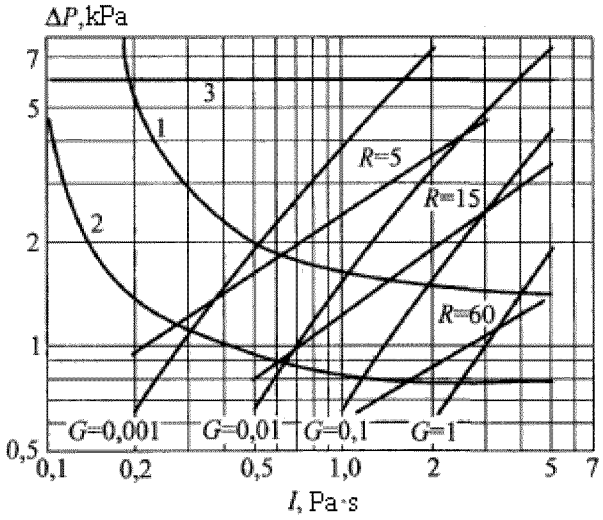

Fig.3.23 Nomogramm [3.16] for determining the SW effect on human body from condensed HE explosion. 1 – 10% of people are temporary deaf , 2- safe distance according norms [3.22], 3 – norms [3.17]. G –HE weight in kg, R distance from the center of explosion in m.

Analogous problems arise in the determining the safety distances for the underwater blasting operations [3.21]. The expected effect of underwater shock waves on the fish is evaluated using the formulas similar to (3.1).

For underwater explosion and for the most sensitive kind of fish [3.18] r_σ is determined from (3.1) at χ =1/2 and k = 45. The dependencies of (3.1) type are valid for the point charges in the narrow range of the explosion energy and represent the particular cases of the bioobject response to the blast loading. To develop the general methods of the damage predicting for bioobjects the data on the blast loading in pressure – impulse coordinates ΔP- I are required. The curve 1 in fig. 3.23 corresponds to the probability of the 10% of people become temporary deaf at normally reflected SW.

The nomogramm of damage of sensitive kinds of fish by blast waves is presented in the fig. 3.24. This nomogramm is taken from [3.16, 3.21] and was obtained on the basis of the experimental data on safe and the lethal distances at the explosion. According to the definition [3.21] r_k denotes the boundary of the zone, inside which the organism is killed,

and r_σ denotes the boundary of the zone, outside which the organism is free of damages. The curve 1 in the fig.3.24 corresponds to the 50% lethality threshold, and the curve 2 characterizes the situation, where the SW effect results into the temporal lost of spatial orientation for the fish and the burst of blood capillary in 50% cases. The comparison between the damage curves for the fish and for the human eardrums judges about the generality of the damage laws for the bioobjects. In each case the damage curves are hyperbolas with two asymptotes corresponding to the critical pressure P_{cr} at quasi-static loading regime and to the critical impulse I_{cr} at impulse loading regime.

The curves 1 and 2 in the fig.3.23 and in the fig 3.24 clearly demonstrate the existence of impulse, transition and quasi-static regions of loading. Also emphasized is the probabilistic character of the bioobject damage, which is conditioned by the individual characteristics of the organism affected by SW.

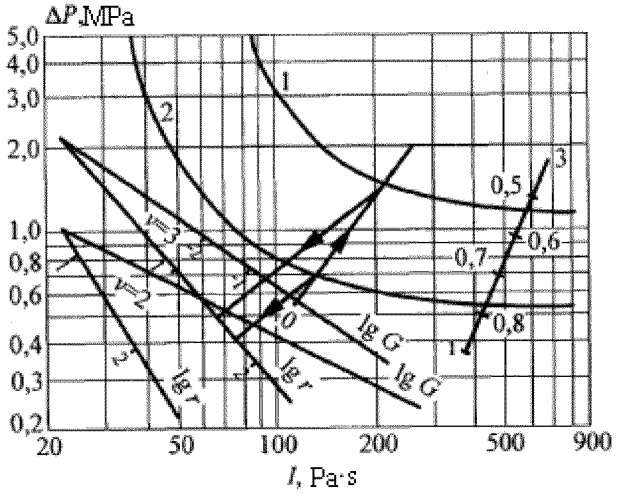

Fig.3.24 Nomogramm of damage of sensitive kinds of fish by blast waves [3.16]. 1 - 50% lethality threshold, 2 - temporal lost of spatial orientation for the fish and the burst of blood capillary in 50% cases, 3 - measured overpressure and impulse after explosion of cylindrical charge (v=2) with linear density 16 g/m in the bubbly medium with volume void fraction β= 2%. For spherical charges (v=3).

The damage diagrams in coordinates ΔP- I are the characteristics of an object and does not depend on the type of condensed HE or another energy sources able to generate

SW. Moreover, the shape of SW (plane, cylindrical, spherical) is unimportant for determination of the damage zone.

Mathematically, the hyperbola equation for the curves in the fig.3.23 and 3.24 can be written as [3.23,3.24]:

$$DN = (\Delta P - P_{cr})(I - I_{cr}) = const \qquad (3.2)$$

where ΔP and I are the overpressure and impulse of dynamic load.

The equation (3.2) determines the third critical parameter DN, which characterizes the object sensitivity to dynamics loading.

Extrapolating the experimental dependences (fig.3.23 and 3.24) into the region of impulse and quasi-static loading, the critical damage parameters were obtained in [3.16] and represented in table 3.3.

Table 3.3 Critical damage parameters of bioobjects at explosion [3.16]

Bioobject	Risk level	Damage %	P_{cr}, Pa	I_{cr}, Pa s	DN, Pa^2 s
Sensitive types of fish	Lethal	50	$9 \cdot 10^5$	65	$7{,}7 \cdot 10^8$
	Lost of spatial orientation for the fish and the burst of blood capillary	50	$4{,}5 \cdot 10^5$	33	$2{,}1 \cdot 10^7$
Human	Temporal deaf	10	$1{,}4 \cdot 10^3$	0,12	$2{,}3 \cdot 10^3$
	Level of accepted influence		800	0,07	75

The analysis of the data obtained in [3.20, 3.25] as well as the ΔP- I diagrams presented in [3.16] gives rise to the conclusion, that the critical parameters of any two lines of bioobject damage in the first approximation will be related as follows:

$$\frac{P_{cr1}}{P_{cr2}} = \frac{I_{cr1}}{I_{cr2}}, \frac{DN_1}{DN_2} = \frac{P_{cr1}}{P_{cr2}} \frac{I_{cr1}}{I_{cr2}} \qquad (3.3)$$

Let us use the ΔP- I diagrams in order to determine the threshold curve of accepted shock-wave influence on the human body at blasting operations in urban areas. According to the requirements [3.17, 3.22] the level of sound wave pressure, measured at frequencies sensible for man ear, should not exceed 125 dB. The experiments with G=0.01…1.00 kg HE charges show, that level of sound pressure is 27 dB lower (in average) than the maximal overpressure at the incident SW front.

Therefore, for the blast loading the accepted level of sound wave pressure 125 dB corresponds to the SW overpressure ΔP =800 Pa. Using the latter value as quasi-static asymptote of blast loading P_{cr} and substituting into equation (3.3), the curve 2 in the fig.3.23 was obtained in [3.16]. This curve defines the region of SW parameters, in which the effect on the human body is under the requirements of technical norms [3.22].

The critical parameters, characterizing the curve 2 (table 3.3), can be used for determination of the safety distances at technological blasting operations in industrial, urban and other conditions.

The prediction of SW effect on the bioobjects with known DN , P_{cr} I_{cr} require the knowledge of the dependencies $\Delta P(R_*)$ and $I(R_*)$.

The dependencies of blast waves parameters and the distances to the HE charge are plotted in fig. 3.23 as a grid r-G. The intersection of the gridlines $\Delta P=f(I)$ with curves 1…3 define the distances corresponding to the different SW damages of human ear organs. Thus, for G=1kg the magnitude of r_σ = 77m by [3.22] and r_σ = 15m by [3.17]. At the distance 47 m one can expect that 10 % of people will be temporary deaf. The comparison of above mentioned data judges the significant underestimation of r_σ in [3.17] and inapplicability of these norms at technological blasting operations in industrial, urban and other conditions.

Fig. 3.24 presents the graphics solution [3.16] of the problem of fish damage regions at underwater explosion. The dependencies $\Delta P=f(I)$ for various G are approximated by the straight lines, which permits to determine the necessary distances using the coordinates r-G for different symmetry. An example of determining r_σ and r_k is demonstrated in the fig 3.24 for the explosion of 1 kg TNT charge. The demolition cords are often used as intermediate detonator at underwater blasting operations. For the cylindrical charge with linear density G=16g/m the distance r_σ will be 49 m, which is close to the r_σ corresponding to 1kg HE charge. The doubling of the specific energy of cylindrical charge will increase the r_σ value up to 86 m. At the same time, the magnitude r_σ =94 m can be attained just for 5 kg HE charge.

The effectiveness of using gas-contained media for explosion effect localization is clearly demonstrated by the curve 3, calculated by the wave parameters at explosion of cylindrical charge with linear density G=16g/m in water containing 2% of the air (bubbly medium). The intersection of lines 3 and 2 corresponds to r_σ =0.75 m. the addition of 2 % vol. of air bubbles permits to decrease the fish damage radius in 50 times.

Specific feature of gas-containing media, used for shock waves damping, is the shift of $\Delta P=f(I)$ curves into direction of quasi-static loading, that can be explained by lower SW impulse suppression in comparison with pressure. Note, that due to probabilistic character of SW damage for bio-object, the notion of safety itself becomes relative one. It is more correctly to say about permission distances but for safety distances.

The permission risk level for particular case must be determined taking into account the economical and social factors, providing the environmental protection and, at the same time, allowing the progressive technologies. Based on above mentioned facts, the conclusion is made in [3.16] that the present requirements [3.17,3.18,3.21] of ecological safety in technologies, using pulse energy sources in offshore water, correspond to the risk level, represented by curve 2 in the fig. 3.24. The use of pulse energy sources in special conditions, when it is required to exclude additional effect of dynamic loading on the fish, the critical pressure (curve 2) must be diminished in 2…3 times, changing all other critical parameters according formula (3.3).

3.10 Estimation of the wave critical parameters for window glasses.

Important part of the requirements for explosions use the predicting of the shock waves effect on the objects located nearby the place of blasting operations [3.38]. The complex character of the object response to the dynamic loading does not allow to connect unilaterally the demolition to the either overpressure or the impulse of the blast wave [3.26…3.28]. As already mentioned above, one of the methods suitable for dynamic loading is the construction of the ΔP-I diagrams. The curve of the object damage (or demolition) under dynamic loading has the hyperbolic dependence (3.2).

The ΔP-I diagrams, corresponding to the window destruction, are taken from [3.28] and presented in the fig.3.25. The curves of damage probability (1, 50, and 100%) for different window glass sizes are plotted on the basis of processing of large number of experimental data [3.14, 3.23, 3.27, 3.38, 3.39]. The curves in diagram demonstrate the existence of two regions, corresponding to the quasi-static and impulse loadings, as well as the probabilistic character of glasses destruction related to the individual properties and ways of fixing of the windows.

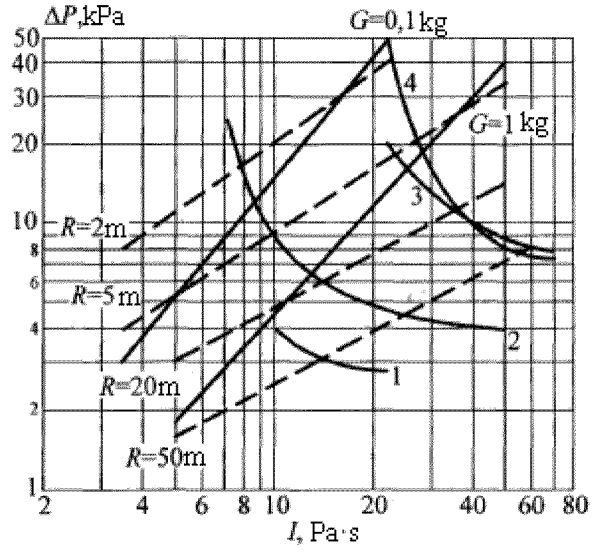

Fig.3.25 Damage diagram for the window demolition and the curves of pressure and impulse change for HE detonations. Destruction: 1-1%; 2-50%;3-100%, [3.23]; 4-50% [3.39] for glass size 450x550x2.1 mm.

The curve 4 corresponds to 50% destruction probability of glass [3.23,3.39] with fixed size. The critical parameters of damage for this curve are following: P_{cr}= 5kPa, I_{cr}= 17.9 Pa s, DN = 5.68 10^4 Pa^2 s. The knowledge of listed critical parameters for the glass of specified size is sufficient to draw the ΔP-I damage diagram.

To predict the damage of glass with arbitrary geometrical sizes it is necessary to find the effect of the width a_1, the length a_2, and the thickness δ on the critical parameters P_{cr} and I_c .

The analysis of presented ΔP-I diagrams for the glass and other objects [3.4] shows that the relationship between the critical parameters in first approach can be written as [3.38]:

$$I_{cr}P_{cr}DN^{-1} = const \qquad (3.4)$$

The equation (3.4) allows constructing the ΔP-I diagram and determining the critical damage parameters for any glass, if the critical parameters for particular glass are known. Moreover, the processing of the diagrams from [3.4] made in [3.38] yields the proportionality law for the critical values of the glass damage:

$$\frac{P_{cr1}}{P_{cr2}} = \frac{I_{cr1}}{I_{cr2}} \qquad (3.5)$$

Using the (3.5) one can determine all set of the critical parameters (including DN by (3.4)) if the change of one particular parameter is known.

The critical blast wave pulse loadings for glass destruction are not realized in practice. Therefore, the existing data on dynamic loads are, in fact, referred to quasi-static loading. The data on critical impulses presented in [3.29] are not actually critical ones in accordance to the definition (3.2).

The critical and permission loads at quasi-static loading are analyzed in [3.38]. Experimental data on the glass destruction at gaseous explosion permit to obtain the

minimal value of P_{cr} for 50% damage for types of glasses corresponding to the State Standard. Thus, for the glass thickness δ=3mm we have $P_{cr\ min}(50\%)$=2.2 kPa, and for δ=4mm the $P_{cr\ min}(50\%)$=4.1 kPa [3.38]. Moreover, the State Standard declares, that the permission pressure should not exceed 850 Pa. According to building rules, the maximal wind pressure on the glass (which corresponds to the quasi-static loading) varies depending on the region from 270 Pa (Moscow region) up to 1 kPa (Arctic Ocean), for Kiev – 350 Pa.

Permission overpressure at special regions was 500 Pa [3.27]. Thus, at blasting operations in urban areas, when the types of window glasses are unknown, on must refer to permission pressures P_{perm} presented in technical documentation. For special regions one can recommend the critical values P_{perm} = 500Pa, or P_{perm} = 850Pa if the glasses are constructed according the State Standard.

If the dependences $\Delta P(R_*)$ and $I(R_*)$ for energy source, which generates the blast wave, are known, then using the relationship between geometrical glass characteristics and critical damage parameters [3.38], one can determine the regions of different damage of windows as well as the safe distances. Due to the complex wave diversion in case of industrial plants the dependencies $\Delta P(R_*)$ and $I(R_*)$ differ from the analogous dependencies obtained analytically for one-dimensional wave propagation. In this case it is more convenient to use directly ΔP-I damage diagrams together with the experimental dependencies $\Delta P(R_*)$ and $I(R_*)$.

The dependencies $\Delta P(R_*)$ and $I(R_*)$ obtained for charge explosion in air or in other media, used for explosion localization (dusty gases, foams, etc.) at any one-dimensional symmetry of space, permit to determine the effect of the blast wave on the window glasses at known parameters P_{cr}, I_{cr}, DN. The curves $\Delta P(R_*)$ and $I(R_*)$ calculated by [3.30] for spherical charge detonation are plotted in the fig. 3.25. The dashed lines correspond to the equal distances from energy source to the object. The intersection of the dashed lines with curves corresponding to the different damage probabilities determines the distances where the indicated damage level is realized.

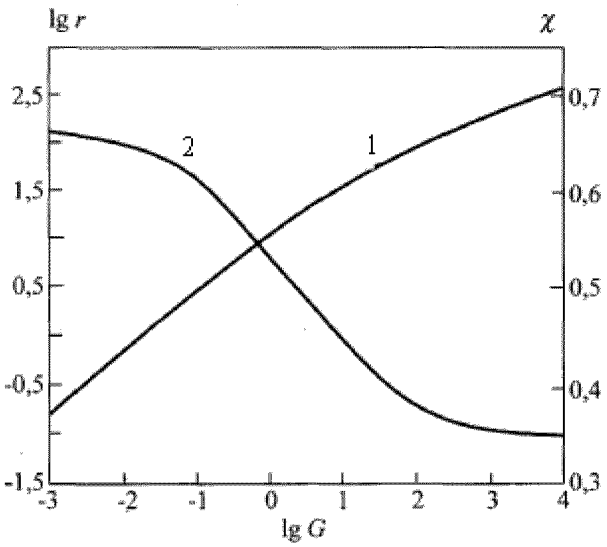

Fig. 3.26 Dependence of the safe distance r_σ (1) and factor χ (2) on the energetic characteristic of explosion for glass (450x350x2.1) at shock wave parameters by [3.14].

For weak shock waves in air (ΔP< 10 kPa) the empirical dependencies from [3.30] are approximated by in [3.38] by relationships:

$$\Delta P=AR^{-\mu},\ I=BG^{0.33}R^{-1},\ R=rG^{-0.33},$$

where μ=1.13, B=200, A=109. Here G is the TNT equivalent in kg, r is the distance to the charge in m, ΔP is the overpressure in kPa, I is the pressure impulse in Pa s. Then the safe distance r_σ can be expressed as a function of the charge weight G, namely:

$$r_\sigma=k(G)\ G^{\chi}.$$

Here $k(G)$ is the weak polynomial function on G.

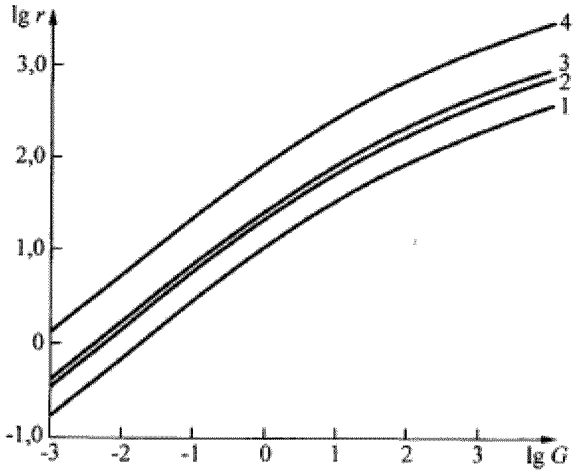

Fig.3.27 Dependence of the standard glass (δ=3mm) destruction on the weight of HE charge: 1 – 50% damage, 2 – 1% damage, 3 – safe distance for passing wave from spherical charge, 4 – safe distance at ground explosion taking into account shock wave reflection.

As example, the dependencies r(50%) and $\chi(G)$ for glass and shock wave source are plotted in the fig. 3.26 [3.14], where good agreement between calculated and measured values is pointed out. Dependence $\chi(G)$ has the limits: χ=2/3 at $G\to 0$ and χ=1/3 at $G\to\infty$. Fig. 3.26 demonstrates, that at χ=0.5 a transition zone is realized for the charges weights 1…10 kg, which are commonly used in metal-working by explosions. It explains the fact that often used empirical formula $r_\sigma = k\, G^{1/2}$ [3.17] predicts the safe distances rather good.

The dependencies $r(G)$ for standard glasses (thickness δ=3mm) and for various damage levels are plotted in the fig. 3.27. The calculation parameters for damage diagrams are listed in the table 3.4.

The choice of critical parameters for reflected semispherical wave was done by taking into account the doubling of shock wave overpressure and wave amplification in the course of ground explosion.

Table 3.4 Critical parameters of damage diagram

Risk level	P_{cr}, Pa	I_{cr}, Pa·s	DN Pa^2·s	R_{cr}, m·kg$^{0.33}$
50%	2200	7,88	$5{,}68\cdot 10^4$	31,7

1%	1100	3,94	$1{,}10 \cdot 10^4$	58,5
r_σ, passing spherical shock wave	850	3,04	$1{,}64 \cdot 10^3$	73,5
r_σ, reflected semi-spherical shock wave	337	1,21	259	151

3.11 Accident prevention at blasting operations

The information presented in chapters 2 and 3 shows that the dangerous consequences of energy release by explosion sources of various types can be parried just by passive and active action on the blast wave with the aim to decrease the overpressure and impulse. This difficult task can be resolved either by direct action on the shock wave or by effective absorption of the explosion products energy.

To develop the regulations of ecological safety at technological blasting operations it is necessary to know:

- the critical parameters of the dynamic loads resulting in damages of the objects to be protected;
- the relationship between the shock waves parameters and energetic and geometrical characteristics of the HE charge in the particular conditions of the blasting operations;
- the correlation dependence between the parameters of shock wave loading at explosion and the existing regulations of practical pulse sources of energy.

The promising way of the solution of the explosion technology safety problem is the development of the explosion localization methods on the basis of gas-contained media (foams, bubble structures, dusty gases etc.).

In accordance with the concept [3.16] the approximate consequence of explosion technology realization can be presented as a scheme in the fig.3.28, suggested by B.I.

Palamarchuk. The decision – making algorithm of accident prevention at blasting operations is shown in the fig. 3.29.

Main operations	Main content
Task	project description Goals, motivation, solutions
Specific features of blasting operations location and safety	planning of neighbor objects vulnerable objects size of damage zones choice of detonation location
Object	object plan disposition of bore-pits disposition of pre-weaken places
Explosion technology	method of destruction type of material type of bore-pits explosion circuit protection
Safety	special methods of protection protection by local measures
Insurance operations	special measures in case of misfire
Scenario of operations	coordination scheme and responsibility complete timing scheme of explosion sequence

Fig. 3.28 Scheme of the explosion technology realization.

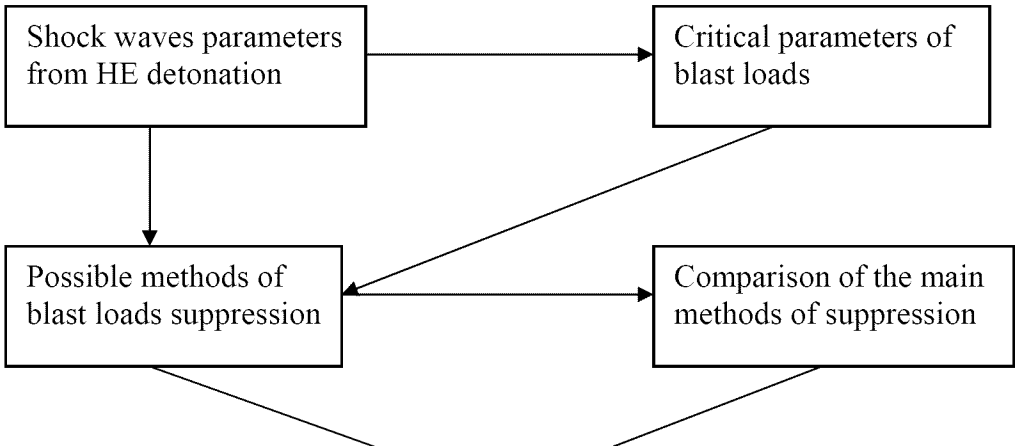

Fig.3.29 Block-scheme of decision – making algorithm

References to chapter 3.

3.1 ClanceyV. J. The eftects of explosions//I. Chem. E. Sympo,Ser.,№71,1982,p.87-108.

3.2 Gould K., Tempo K. High explosive field tests, DMA, 6137F,1981,86p.

3.3 Atamanuk B.G., Shirshev A.G., Akimov N.I. Civil defense, M., 1986,208 p. *(In Russian)*

3.4 Baker W.E., Cox P.A., Westine P.S. et al. et al. Explosion hazards and evaluation. Elsevier, Amsterdam-N.Y.-Oxford: 1983.798 p.

3.5 Strehlow R., Baker W.E. The characterization and evaluation of accidental explosions // Progr. Energy Comb. Sci., 1976, v.2, №1, p. 27-60.

3.6 Methods for the calculation or the physical effects of the escape of dangerous materials, TNO, 1980.

3.7 Held M. Similarities of shock wave damage in air and in water// Propellants, Explosives Pyrotechnics, 1990, v. 15 № 1 - 2p. 149-156.

3.8 Pietersen C.M. Consequences of accidental releases of hazardous materials//I. Loss. Prev. Process. Ind., 1990, v.3, № 1,p. 136-141.

3.9 Harris R.J. et. al. The response of glass windows to explosion pressures, MRS E330, 1977,36 p.

3.10 Geiger W., Synotzik R. A simple model for the explosion of pancake shaped vapor clouds // Prepr. 7-505-514, 3rd, Int. Loss Prev. Symp., 1980.

3.11 Strehlow R.A. Accidental explosions, American Scientist //1980,v.68,№4,p.420-428.

3.12 Sperraza J. Dependence of external blast damage to A25Aircraft on peak pressure impulse, BRC MR575, 1951.

3.13 Finney D., Probit analysis, Cambr. Univ. Press, 1971.

3.14 Giesbrecht H. et al. Analysis or explosion hazards of spontaneous release of inflammable gases // Ger. Chem. Eng. ,1981,v.4,№2-3,p.305-325.

3.15 Richmond D.R., Damon E.G. Biomedical effects of impulse noise. FNNR 209/93, 87p.

3.16 Palamarchuk B.I. Prediction of blast wave effect on bioobjects at blasting operations // Welding, cutting and processing of welded components by explosion. - Kiev: E.O. Paton's Institute of electric welding, 1987, p. 141 - 149. *(In Russian)*

3.17 Safety regulations at blasting operations.-M.; Nedra, 1968,320 p. *(In Russian)*

3.18 Balashkand M.I., Vekilov E.Kh., Lovlja S.A. et al. New sources of exploration seismology safe for ichthyofauna.-M. Nauka, 1980.78p. *(In Russian)*

3.19 Gelfand B.E., PolenovA.N., MedvedevS.P. Possible types of structural response to blast loading. Proc. NIXT-94,1994, p. 93-109.

3.20 Palamarchuk B.I., Malakhov A.T. The effect of medium properties and energy source characteristics on shock waves attenuation // The use of explosion energy for

manufacturing of metal materials with new properties: Proc. VI Int. Symp. Gottwald, Oct. 1985 г. 1985, p. 534 - 544. *(In Russian)*

3.21 Protasov V.R., Bogatyrev P.B., Belikov E.Kh. Methods of preserving of ichthyofauna at different types of underwater blasting operations //M.: Leg. and Pisch prom., 1982,88p. *(In Russian)*

3.22 GOST 12.003-35. Noise, Common safety requirements. Introduced from 01.07.84 till 01.07.89. *(In Russian)*

3.23 Held M. Blast waves in free air// Propellants, Explosives, Pyrotechnics. 1983. № 8, p. 158 - 167.

3.24 Westine P.S., R-W plane Analysis for Vulnerability of Targets to Air Blast//The Shock and Vibration Bulletin. 1972. №42, p. 173-183.

3.25 Palamarchuk B.I., Vakhnenko V.A., Cherkashin A.V. Air shock waves at welding and cutting by explosion and the methods of their localozation //Automat, welding, 1988. № 2, p. 69 — 72. *(In Russian)*

3.26 Raspet R., Butler P.B. Jahani F. The effect of materialproperties on reducing intermediate blast noise //Applied Acoustics.1987. Vol.22, № 3, p. 243 - 259.

3.27 Instruction on the determination of the radius of dangerous zone for window glasses in case of air shock waves.M.: Sojuzvzryvprom, 1979, 20p. *(In Russian)*

3.28 Makhviladze G.M., Roberts J.P., Jakush S.E., Gelfand B.E. Risk analysis of near-surface vapor cloud explosion basing onits fluid dynamics consequences. Proc. lstConf. (Intern.), Computer simulation in risk analysis and hazard mitigation, (Ed. by Rubio J.L., Brebbia C.A., Uso J.L.), Spain, 1998, WIT press, Boston-Southampton, p. 223 - 232.

3.29 Turin A.A., Malyi P.S., Savenko S.K. Air shock waves in excavations. — M.: Nedra, 1983.223 p. *(In Russian)*

3.30 Palamarchuk B.I. On the energetic similarity of shock waves attenuation // The use of explosion energy in welding technique. - Kiev: E.O. Paton's Institute of electric welding, 1985, p. 157 - 167. *(In Russian)*

3.31 Malakhov A. G. Reflection of the shock waves in gas-contained media // Welding, cutting and processing of welded components by explosion. - Kiev: E.O. Paton's Institute of electric welding, 1987, p. 155 - 161. *(In Russian)*

3.32 SOAR on flame acceleration and DDT in nuclear safety.(Breitung W., Eder A., Chan C.K., Dorofeev S.B., Gelfand B.E., Heitsch M., Klein R., MalliakosA., Sheferd J.E., StuderE., ThibaultP.), OECD/NEA/CSNI/R (2000) 7,2000.

3.33 Hirsch F.G. Effects of Overpressure on the Bar - A Review. Annals of the New York Academy of Sciences, 152, Article l, pp. 147(October, 1968), 1968.

3.34 Mikhailin A.I., Silnikov M.V., Turin M.V. Effect of explosion on human body // Proc. of the 2nd interregional scientific - practical conference «Development new special technique for MVD ». — ST.Peterspurgh, University MVD Russian Federation, St.-Petersburg. - 2000. - p. 23. (*in Russian*)

3.35 Silnikov M.V., Turin M.V. The human damage by blast wave // Proc. of the 2nd interregional scientific - practical conference «Development new special technique for MVD ». — ST.Peterspurgh, University MVD Russian Federation, St.-Petersburg. - 2000. - p. 18 (*in Russian*)

3.36 Turin M.V. The damage caused by the shock wave and the development of protection and safety measures // Doctor of medical sciences dissertation, VMA. —St. Petersbugh, 2000,280 p. *(In Russian)*

3.37 Turin M.V. Patomorphological changes in lungs at air blast injury // Proc. of all-russian conf. «Modern gunshot injury». — VMA, St.P, 1998, p. 64-65. *(In Russian)*

3.38 Vakhnenko V.A., Palamarchuk B.I., Cherkashin A.V. Methods of predicting of air shock waves effects on window glasses at technological explosions // Welding,

cutting and processing of welded components by explosion. - Kiev: E.O. Paton's Institute of electric welding, 1987, p. 149-155. *(In Russian)*

3.39 Giesbrecht H., Hemmer G., Hess K. et al. Analysis of Explosion Hazards//Ger. Chem. Eng., 1984, № 4, p. 315 - 325.

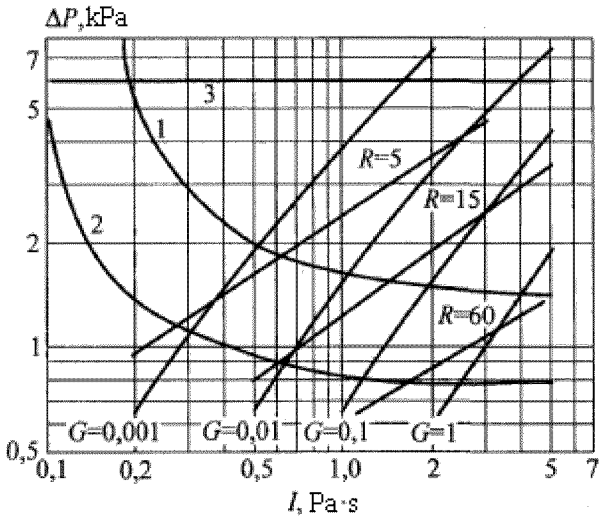

herkashin A.V. Air shock waves at welding and cutting by explosion and the methods of their localozation //Automat, welding, 1988. № 2, p. 69 — 72. *(In Russian)*

3.26 Raspet R., Butler P.B. Jahani F. The effect of materialproperties on reducing intermediate blast noise //Applied Acoustics.1987. Vol.22, № 3, p. 243 - 259.

3.27 Instruction on the determination of the radius of dangerous zone for window glasses in case of air shock waves.M.: Sojuzvzryvprom, 1979, 20p. *(In Russian)*

3.28 Makhviladze G.M., Roberts J.P., Jakush S.E., Gelfand B.E. Risk analysis of near-surface vapor cloud explosion basing onits fluid dynamics consequences. Proc. lstConf. (Intern.), Computer simulation in risk analysis and hazard mitigation, (Ed. by

Rubio J.L., Brebbia C.A., Uso J.L.), Spain, 1998, WIT press, Boston-Southampton, p. 223 - 232.

3.29 Turin A.A., Malyi P.S., Savenko S.K. Air shock waves in excavations. — M.: Nedra, 1983.223 p. *(In Russian)*

3.30 Palamarchuk B.I. On the energetic similarity of shock waves attenuation // The use of explosion energy in welding technique. - Kiev: E.O. Paton's Institute of electric welding, 1985, p. 157 - 167. *(In Russian)*

3.31 Malakhov A. G. Reflection of the shock waves in gas-contained media // Welding, cutting and processing of welded components by explosion. - Kiev: E.O. Paton's Institute of electric welding, 1987, p. 155 - 161. *(In Russian)*

3.32 SOAR on flame acceleration and DDT in nuclear safety.(Breitung W., Eder A., Chan C.K., Dorofeev S.B., Gelfand B.E., Heitsch M., Klein R., MalliakosA., Sheferd J.E., StuderE., ThibaultP.), OECD/NEA/CSNI/R (2000) 7,2000.

3.33 Hirsch F.G. Effects of Overpressure on the Bar - A Review. Annals of the New York Academy of Sciences, 152, Article l, pp. 147(October, 1968), 1968.

3.34 Mikhailin A.I., Silnikov M.V., Turin M.V. Effect of explosion on human body // Proc. of the 2nd interregional scientific - practical conference «Development new special technique for MVD ». — ST.Peterspurgh, University MVD Russian Federation, St.-Petersburg. - 2000. - p. 23. (*in Russian*)

3.35 Silnikov M.V., Turin M.V. The human damage by blast wave // Proc. of the 2nd interregional scientific - practical conference «Development new special technique for MVD ». — ST.Peterspurgh, University MVD Russian Federation, St.-Petersburg. - 2000. - p. 18 (*in Russian*)

3.36 Turin M.V. The damage caused by the shock wave and the development of protection and safety measures // Doctor of medical sciences dissertation, VMA. —St. Petersbugh, 2000,280 p. *(In Russian)*

3.37 Turin M.V. Patomorphological changes in lungs at air blast injury // Proc. of all-russian conf. «Modern gunshot injury». — VMA, St.P, 1998, p. 64-65. *(In Russian)*

3.38 Vakhnenko V.A., Palamarchuk B.I., Cherkashin A.V. Methods of predicting of air shock waves effects on window glasses at technological explosions // Welding, cutting and processing of welded components by explosion. - Kiev: E.O. Paton's Institute of electric welding, 1987, p. 149-155. *(In Russian)*

3.39 Giesbrecht H., Hemmer G., Hess K. et al. Analysis of Explosion Hazards//Ger. Chem. Eng., 1984, № 4, p. 315 - 325.

CHAPTER 4. ELEMENTARY WAYS OF EXPLOSIVE LOADINGS REDUCTION

At early stages of the explosive technologies implementation it seemed, that the simple placement (contact or non-contact) of HE charges in various protecting envelopes will result in lower levels of explosive loadings of an acceptable level [4.1]. However further practical work has revealed hopelessness and significant inconveniences of the given technical decisions. Let's outline some examples.

4.1. Contact placement of charges in a protective envelops

The numerous measurements, made for an estimation of ammunition efficiency, establish the dependence of air shock wave parameters on relative weight of HE charge (G) and weight of closely placed armoured envelope (W). Dependences $\Delta P = f(R, W/G)$, $I = R(W/G)$ were experimentally constructed. It occurred, that the detonation of HE charge is equivalent to explosion of the non-protected charge with weight

$$G_{ef} = \left[0.2 + 0.8/\left(1 + W/G\right)\right] G$$

Thus by [4.2] for $W/G < 1$ the efficiency of demolition action of the armoured charges is higher, than non-armoured charges, because of the absence of dispersion of an external HE layer (see chapter 2). Measurements in [4.1, 4.2] show, that the contact

placement of HE charge in an armoured protective envelope should not be considered at all as the method of shock wave attenuating, except for the obvious case, when the environment does not collapse under the action of explosion.

4.2. Non-contact placement of charges in a protective envelops

More effective, than just above considered, is the way of protection from the shock wave with the help of the continuous screen which is not placed into the contact with HE charge [4.3]. The typical scheme of installation of the non-contact screen and HE charge is shown in the fig. 4.1.

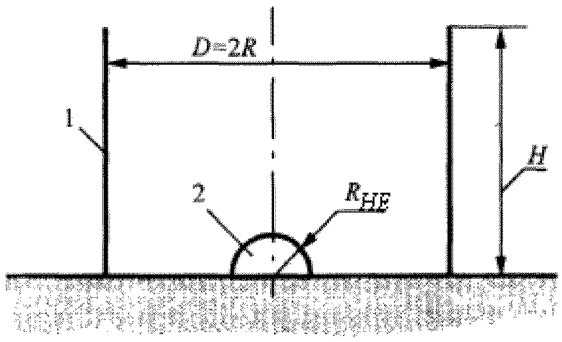

Fig. 4.1. Installation of the non-contact screen

The screen 1 represents an envelope as a lateral surface of the cylinder or prism, inside which the HE charge 2 is placed at its longitudinal axis. The envelope has a height H an internal diameter D. The problem of explosive wave propagation around of the protective envelope with the height H = 100 cm (or 400 cm) and the radius R = 20, 25, 35, 50, 75, 150 and 250 cm was considered in [4.3]. The explosion of spherical TNT charges with the radius R_{HE} = 1 cm (weight 6,83 g) and the radius R_{HE} = 8 cm (weight 3497 g) was studied (fig. 4.2).

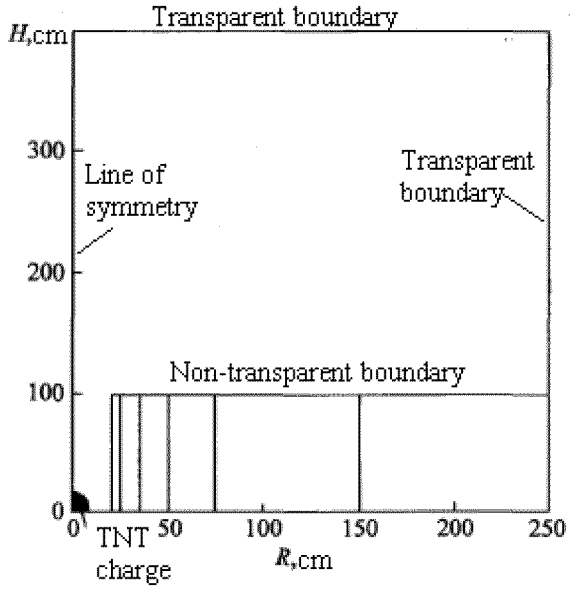

Fig. 4.2. Possible variants of the screens placement

In preliminary calculations the optimum height of the screen by the magnitude of energy carried away by the shock wave was determined. In a fig. 4.3 it is possible to see the reduction of the energy carried away by the shock wave, with the increase of the height of the limiting cylindrical envelope. The time t_0 corresponds to the moment of wave arrival to the open section of an envelope. The obtained results for the screens of 120 and 200 cm height are close to each other, and the optimum height of the envelope for <1 kg TNT charges is 100 cm. The shorter screens actually do not reduce the level of energy of the wave and do not suppress the explosive loading.

The levels of the maximal explosive pressure $P_m = \Delta P + P_0$ and the blast wave amplitude ΔP at initial pressure $P_0 = 10^5$ Pa for various variants are shown in the fig. 4.4 and 4.5. The reference lines 1 in both diagrams correspond to the ground explosion of TNT charges with the radii $R_{HE} = 1$ cm and $R_{HE} = 8$ cm accordingly.

All variety of the variants considered does not confirm the principal difference in expected level of the blast loading suppression. Therefore, the dependence of factor K of

the blast wave amplitude attenuation on the relative distance R/R_{HE} is presented in the fig. 4.6. It is seen, that non-contact protective screen cannot essentially suppress the blast loading. Thus the way of suppression of blast loading by the non-contact screen cannot be recognized effective on the basis of the presented results. The conclusions from [4.3] completely correlate with [4.2], where the other types of non-contact screens are discussed.

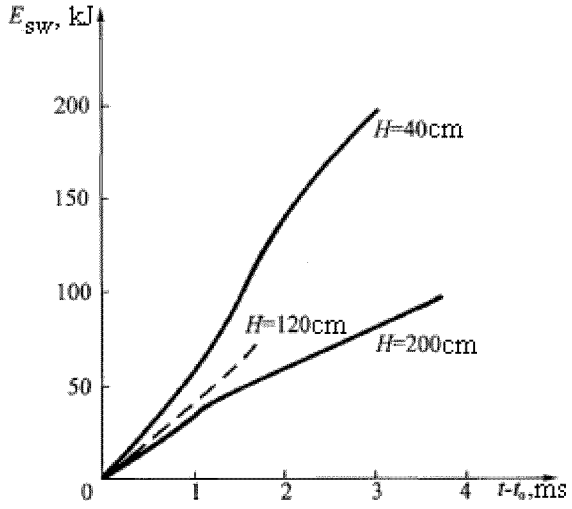

Fig. 4.3. Change of the energy carried away by the shock wave, at increase of the height of limiting cylindrical envelope

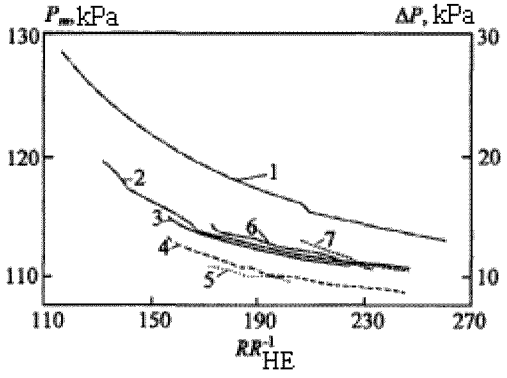

Fig. 4.4. Levels of the maximal blast pressure $\underline{P_m}$ and the amplitude of blast wave ΔP at initial pressure $P_0 = 10^5$ Pa for various radii of envelope (R_{HE} = 1 cm): 1 - R = ∞; 2 - R = 25 cm; 3 - R = 35 cm; 4- R = 75 cm; 5- R = 50 cm; 6 - R = 20 cm; 7 - R = 150 cm

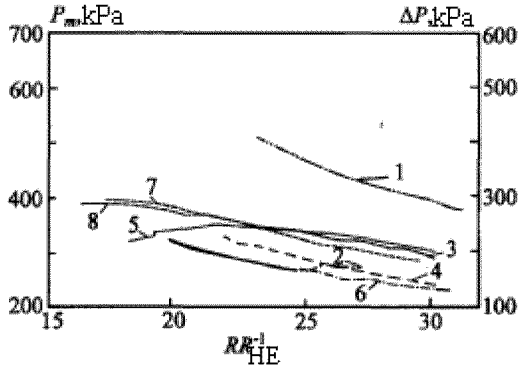

Fig. 4.5. Levels of the maximal blast pressure P_m and the amplitude of blast wave ΔP at initial pressure $P_0 = 10^5$ Pa for various radii of envelope (R_{HE} = 8 cm): 1 - R = ∞; 2 - R = 75 cm; 3 - R = 150 cm; 4- R = 100 cm; 5- R = 35 cm; 6-R = 50 cm; 7-R = 25 cm; 8-R = 20 cm

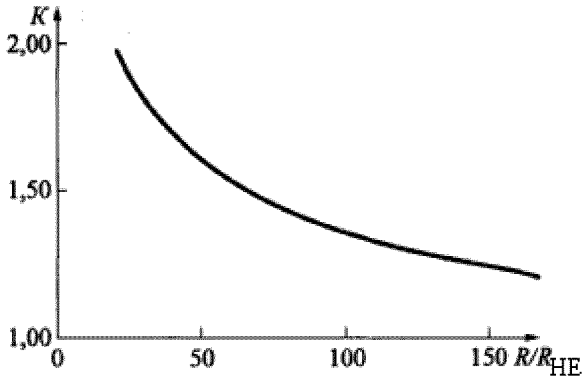

Fig. 4.6. Dependence of the factor of reduction of the explosive wave amplitude K on the relative distance R/R_{HE}

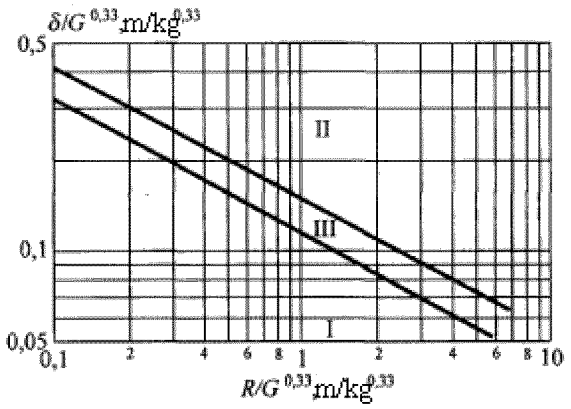

Fig. 4.7. The diagram for a choice of the effective thickness δ of protective envelope ensuring the catching of fragments: I – the fragments penetrate the envelope, II — the fragments do not penetrate the envelope, III The zone of uncertainty [4.4]

The scheme represented in the fig. 4.1, is rather effective for catching the fragments at the known thickness of cylindrical cowling. Using the information given in [4.4], it is possible to construct the diagram (fig. 4.7) for a choice of the effective thickness δ of protective envelope ensuring the catching of the fragments. The diagram is constructed in Sadovsky – Hopkison coordinates. The abscissa is the reference distance $R/G^{0.33}$, and the ordinate is the specific thickness of the concrete envelope $\delta /G^{0.33}$. In the field of parameters I the fragments penetrate the envelope, in zone II — the fragments do not penetrate the envelope, and III is the zone of uncertainty. The diagram is correct if internal space of a protective envelope is filled by air under normal atmospheric conditions.

4.3. Vacuumization of gaseous medium around of a charge

From the dependences of the blast wave overpressure ΔP and impulse of compression phase I follows, that $\Delta P \approx P_0^{0.33}$, and $I \approx P_0^{0.66}$. Thus, the trivial way of reduction of the blast loadings is the decrease of initial pressure P_0 in the gas layer separating HE charge from protected object. However, the vacuumization of cavity around HE charge requires the placing of the charge in special tight containers and actually

excludes the application of the combined ways of protection. Nevertheless in special cases the given way of explosive loadings regulation can be considered as rather effective.

4.4. Shock waves attenuation by perforated plates

One of the effective ways of blast waves amplitude decreasing is the placing of thin perforated plates (PP), grids and other permeable barriers across the gas flow behind the wave. The shock wave propagation with the constant parameters behind the front through PP was studied in [4.5 ...4. 12]. However, in practice it is necessary more often to deal with SW with non-stationary pressure behind the front. The force influence of such waves depends on the overpressure at the front ΔP and the impulse of the compression phase:

$$I = \int_0^{\tau} \Delta P(t) dt$$

Here τ is the duration of compression phase, $\Delta P(t)$ is the pressure – time dependence. It is impossible to make any practical conclusions by the results from [4.5... 4. 12] concerning the change of parameters I and τ at SW propagation of final duration through PP.

In [4.13] the results of experiments on the shock wave attenuation by the perforated screen are given. The shock wave was formed at destruction the gas-filled cylindrical envelope. It was shown, that the duration of SW compression phase does not change at the passage through the screen.

In [4. 1, 4. 15] the attenuation of waves formed in environmental space by the grids and PP after HE detonation was investigated. In [4. 1] the data on measurements of the SW impulse behind a barrier are given.

However at the conditions of the experiments in [4.1,4.15] the two-dimensional effects could essentially influence on the values ΔP an I behind PP, as the barrier were placed in the open space. Thus, for practically important one-dimensional processes in the pipes and the channels the use of results from these two references is wrongful.

In [4. 18] the laws of interaction between the plane SW of final duration formed in a shock tube, with PP, positioned in one of the sections of the tube are found. The parameters of the incident SW ($\Delta P_+, \tau_+$) and passed (transmitted) SW ($\Delta P_-, \tau_-$) were determined by the piezoelectric pressure gauges. The impulses of a compression phase of the incident SW (I_+) and passed SW (I_-) were measured with the help of the electronic integrator of a signal from pressure transducer. Parameters of registration system provided the accuracy of ΔP measurement no more than 10 %, and I — 15%.

The range ΔP = 0,05 …0,25 MPa was investigated. Characteristic values of τ_+ = 0,5... 2 ms. The permeability of partitions, i.e. the ratio of the area of apertures to the total area of PP, in experiments was α = 0,009... 0,25. Thickness of partitions 3... 10 mm. The change of SW parameters at passage through PP can be described by coefficients $\delta = \tau_- / \tau_+$, $\eta = \Delta P_- / \Delta P_+$, and $\xi = I_- / I_+$. With the help of the gauge located directly inside the partition, the parameters of reflected SW ΔP_* and τ_* were determined. In a range under consideration was obtained, that the duration of SW compression phase at passage through PP does not change, i.e. $\tau_- \approx \tau_+ \approx \tau_*$ and $\delta = 1$.

In the fig. 4.8*a* the dependences of SW attenuating factor by pressure η on PP permeability are given. The curve 1 is plotted by the data from [4.5... 4.11] for the plane SW with the constant parameters behind front ΔP = 0,001... 0,2 MPa. The shaded area 2 and points 3 are the data [4.1] and [4.15] accordingly for the spherical blast waves at ΔP_+ = 0,08... 1 MPa. The points 4 are the results of experiments for plane SW of a triangular pressure structure, which at $0{,}009 < \alpha < 0{,}3$ can be described by the empirical relation:

$$\eta = 1.14\alpha^{0.62} \qquad (4.1)$$

In the fig. 4.8*b*, the dependences of factor ξ on PP permeability are shown. Area I corresponds to the data from [4.1], points 2 are the results of the experiments [4.18]. The curve 3 is constructed by (4.1) in coordinates ξ-α. Thus, within the experimental error for the plane waves of triangular pressure structure $\xi = \eta$. In the case of spherical blast waves [4.1] we have another pattern. If the pressure at the front considerably decreases behind the barrier, then the impulse of compression phase is close to initial one, and in the field of

permeability $\alpha > 0{,}04$ even exceeds it. It is probable, that in conditions [4.1] the increase of the impulse is connected to the outside flow around the barrier, as well as the reflected wave. It is shown in [4.12,4.13], that at $\alpha < 0{,}1...\ 0{,}2$ the pressure in the wave reflected from PP only slightly differs from the normal reflection pressure. In the fig. 4.9 the results of $\chi = \Delta P_* / \Delta P_0$ measurements (ΔP_0 is the overpressure at reflection at impenetrable barrier) for the incident SW with a triangular structure of pressure are presented.

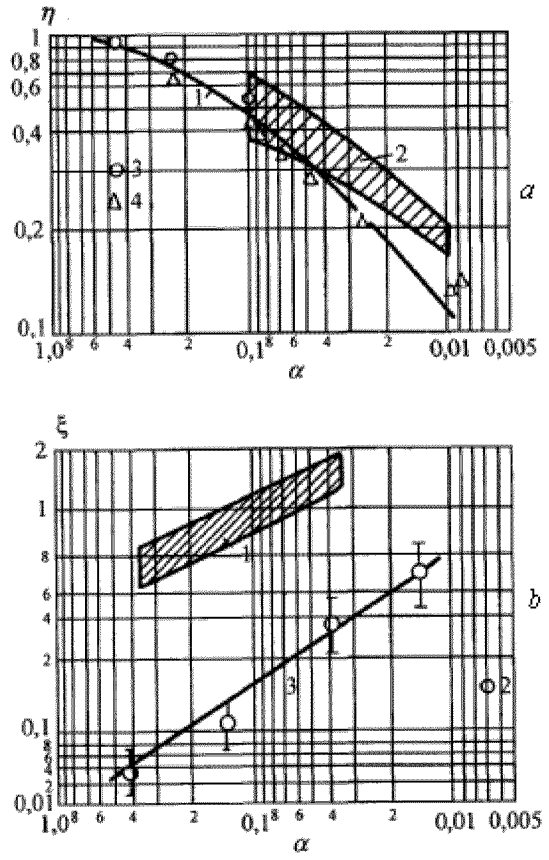

Fig. 4.8. Influence of PP permeability on the parameters of shock waves: a — the factor of SW attenuation by pressure η; b — the factor of SW attenuation by impulse ξ

It is seen, that at $\alpha < 1$, the pressure ΔP_* differs from ΔP_0 less than in 30 %. With the increase of ΔP_+ this distinction decreases. The measurement of ΔP_+ by the pressure gauge located directly in PP, allows to estimate the effective SW influence on the partition.

The detailed study of the process of the formation of the SW reflected from the wall, equipped with an aperture, is presented in [4. 17].

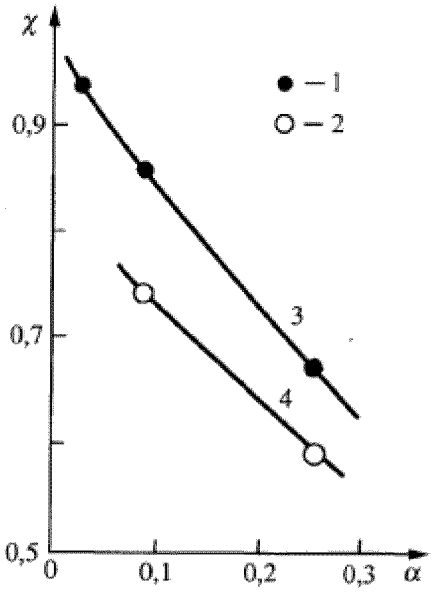

Fig. 4.9. Results of $\chi=\Delta P_*/\Delta P_0$ measurements. Points 1 correspond to $\Delta P_+ =0.2$ MPa, 2 - 0,08 MPa. Curves 3,4 are numerical calculations [4.7] for the plane SW with constant parameters behind the front accordingly at $\Delta P_+ =0.2$ and 0,08 MPa.

For the practical applications it is essential to study an opportunity of using several plates (so-called «package») for SW suppression. Consider a case of two consequently located PP with the permabilities α_1 and α_2. If the distance between the partitions h is large enough in comparison with the distance from the last PP to the place of measurement, then it is possible to consider the plates «as independent» and effective factor of the SW attenuation by amplitude η_{12} will be determined by the values η_1, η_2 for each PP. Then taking into account (4.1) we have:

$$\eta_{12} = \eta_1 \eta_2 \approx 1.3 (\alpha_1 \alpha_2)^{0.62}. \qquad (4.2)$$

In the case, when the measurements are carried out at sufficient distance from the «package», the repeated SW reflections in a gap between partitions will result into the generation of a stronger wave. For the effective permeability of two plates η_{12} in the case of «mutual influence» of PP the semi-empirical formula is offered in [4. 1] at 0,01 < α_1 , α_2 < 0, 13):

$$\alpha_{12} = \alpha_1 \alpha_2 (\alpha_1 + \alpha_2)^{-1} \qquad (4.3)$$

The «package» of two PP with the permeability 0,07 and 0,12 was investigated at h = 25 mm. The partitions were positioned in various combinations. The distance to the place of measurement from the last PP was 13 cm. In the fig. 4.10 the dependences of the attenuating factor η_{12} on the permeability of the second partition are given at the fixed α_1. Here, the curves 1, 2 are calculated by (4.2); 3,4 — experiment; 5, 6 are calculated by (4.1), (4.3); α_1 = 0,07 for 1, 3, 5 and 0,12 for 2, 4, 6. It is seen, that the value η_{12} is higher, than in the case of «independent» partitions, but is not described by the formula (4.3). It is necessary to note, that the duration of the SW compression phase passed through the «package», is increased and, hence, the factor ξ in this case can differ from η.

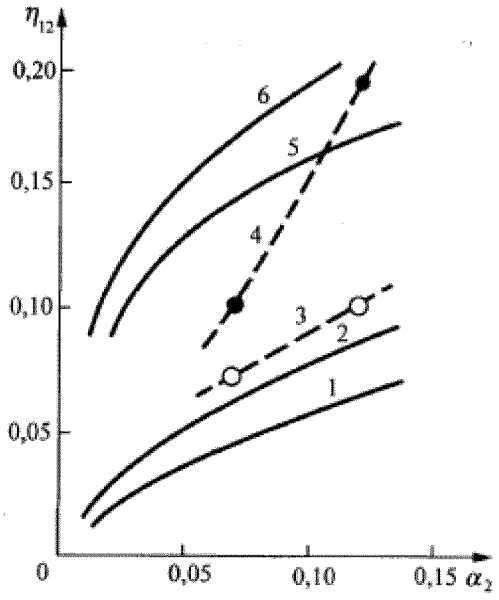

Fig. 4.10. Dependences of the attenuating factor η_{12} on the permeability of the second partition for the fixed α_1.

Alongside with triangular compression waves the problem of interaction of short rarefaction perturbations with PP was investigated. In the experiments with the partitions of α = 0,14; 0,07; 0,012 the measured attenuation factors by pressure were η = 0,54; 0,34; 0,17 accordingly. From the fig. 4.8*a* it follows, that η for the rarefaction waves are 1.5…2 times larger than the corresponding values for the compression waves. The duration of the perturbation at the passage through PP does not change, and, hence, the impulse in the rarefaction wave decreases proportionally to the amplitude, as well as for the plane triangular compression waves.

Thus, the perforated plates are the effective way of attenuating of the non-stationary pressure waves in the tubes and the channels not only by he amplitude, but also by the impulse. By the appropriate selection of α, and using of several partitions it is possible to vary the parameters of the transmitted SW and the reflected wave in a wide range.

4.5. Shock waves attenuation by screens from granular materials

In works [4.14,4.19,4.20,4.24,4.25] the propagation of SW in bulk and porous media is investigated. The obtained fast attenuation of waves allows assuming, that these media can serve as an effective method of SW suppression in channels.

For the determination of attenuating effect generally it is necessary to consider a complete pattern of the wave propagation inside a porous sample. The experiments [4.19] testify that behind the plane SW, penetrating in volume with regularly loaded particles, there is an ordered wave structure, and the forward front has the poorly expressed breaks. The system of the reflected waves, which generates non-uniformity of thermodynamic parameters and speed across the section of the channel, is considerably weakened behind the front at the distances about several diameters of granular particles. The marked features allow assuming, that for the description of dynamics of SW attenuation in considered systems the one-dimensional (hydraulic) approach is applicable.

The interaction of a flow with particles results in losses of the impulse of gas and redistribution of energy because of formation of the secondary jumps and the flow turbulisation. Factor of resistance of particles can be presented as the sum $c_f = c_{fp} + c_{fd}$. The surface friction, as a rule, is small in comparison with the resistance of pressure (shape) (i.e. $c_{fd} << c_{fp}$), and they can be neglected. To calculate c_f in motionless layer of particles with a diameter d in conditions of the steady gaseous flow with density ρ the Ergan equation can be used:

$$c_f \approx c_{fp} = 75/\ Re + 0{,}875, \qquad (4.4)$$

Where $Re = \varepsilon\rho du\ /\ (1 - \varepsilon)/\mu$ at the porosity $0{,}4 < \varepsilon < 0{,}65$. From (4.4) follows, that at $Re \geq 10^4$ the values c_f tend to the constant value of 0,875, i.e. the medium obeys the square-law law of resistance. In the shock waves propagating in porous media of bulk density, such values of Re number are reached at the overpressures larger than 5 kPa (at d ~ 1 mm).

From the analysis of the equations of the perfect gas flowfield in a tube with friction losses follows, that the SW intensity at the exit from the screen with thickness h is defined by the incident SW Mach number and dimensionless parameter $\Theta = 1.75\ (1 - \varepsilon)h/\varepsilon d$, describing the properties of the granular partition [4.22].

The results of the experiments on shock waves attenuation by the screens made from various granular materials (see tab. 4.1) with parameters close to that, used in practice, are given in [4.22].

Table 4.1 Screens, used in experiments [4.22]

Material	Form of particles	Size of the particles d, mm	ε	Thickness of the screen h, mm
Polythene	Round shape	3,9	0,38	10, 25, 60
Steel	Cylindrical	∅10 x 12	0,41	35, 110, 160
Porcelain	Spherical	15,8	0,44	35, 60, 110, 160

Claydite	Round shape	21,9	0,50	60, 160, 250

Calculated and measured ratios of $\Delta P/P_0$ (ΔP is the overpressure in SW transmitted through the screen) versus the Mach number M_0 and the parameters of granular screens are presented in the fig. 4.11. From a fig. 4.11 it follows, that at $\Theta \geq 30$ the amplitude of the passed SW practically does not depend on the initial intensity of waves in a range of M_0 numbers under consideration. Hence, for the shock waves suppression the parameters of screen should satisfy to the condition $\Theta > 30$.

At $h/d \rightarrow 1$ the parameter Θ, and, hence, and amplitude of the wave depend basically on the values M_0 and ε. It is necessary to note, that the ratio for pressure losses used in calculations, is valid under the condition $h/d >> 1$. Nevertheless, similar result was observed in the studies on the shock wave suppression by perforated plates: the SW attenuation is defined only by permeability of the plates and the incident Mach number.

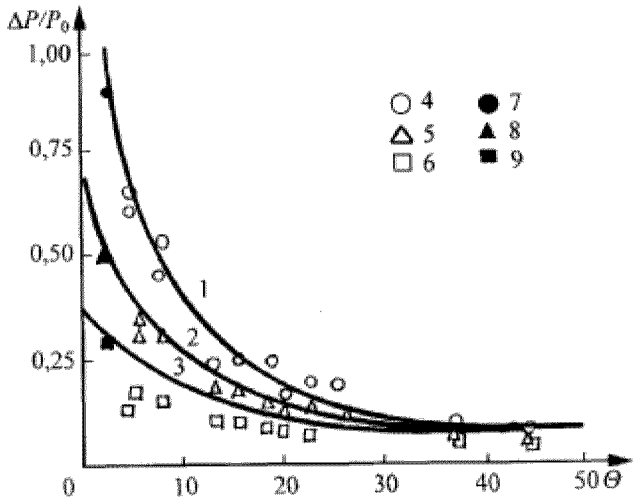

Fig. 4.11. Change of amplitude of the shock wave: 1 — 3 — calculations [4.21], 4 — 6 — experimental data (granular screens), 7 — 9 — experimental data (perforated partitions), M_0 = 1,47 (1, 4, 7), 1,28 (2, 5, 8), 1,15 (3, 6, 9)

Points 7...9 in the fig.4.11 represent the experimental data for the perforated plates with permeability 0,44. Comparison with the experimental results for the screens made from granular material ($\varepsilon = 0{,}38...\ 0{,}50$) shows, that in the limiting case at $h/d \to 1$ the bulk layer is simulated by the perforated partition with permeability equal to ε (if to neglect the possible change of ε at $h/d \to 1$ in comparison with $h/d >> 1$). In this connection, it worth to compare the action of SW on the perforated partition and the granular medium by other parameter, for example by the overpressure ΔP_* in the wave reflected from the bulk medium.

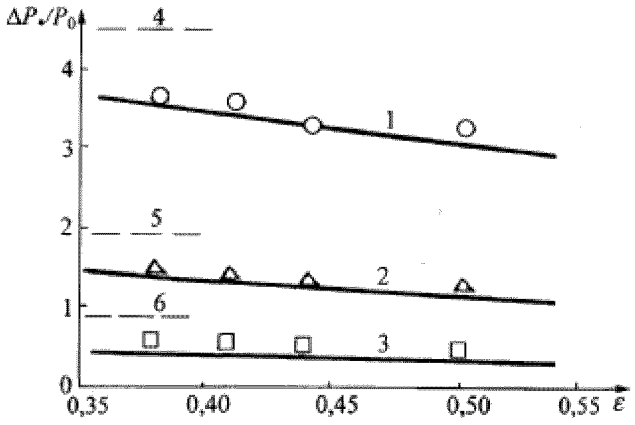

Fig. 4.12. Change of amplitude of the reflected shock wave versus the porosity of a material: 1... 3- experimental data with the perforated partitions, points — experimental data with granular screens; 4... 6 — pressure of reflection from rigid wall, M_0 = 1,47 (1,4), 1,28 (2,5), 1,15 (3,6)

Dependences of $\Delta P_*/\Delta P_0$ on the parameter ε for the screens with minimal length (h/d = 2.2 …3.2) are presented in the fig. 4.12. Also shown are the results for the SW, reflected from the perforated partition, and the ε value corresponds to the permeability of the partition. The satisfactory agreement between the screens and the perforated plates is observed. Slightly higher pressures of reflection for the screens is connected to the absence of the gaps even in the layers h/d = 2... 3. The pressure of reflection from the screen

represents also the practical interest, as it is the value that defines a choice of strength properties of the screen. As well as in the case of the perforated partitions, the value ΔP_* is lower than the pressure of reflection from a rigid impenetrable wall, decreases with the increase of ε and weakly grows with the increase of the screen length. Many of the conclusions are confirmed recently in [4.23].

References to chapter 4

4.1. Baker W.E., Cox P.A., Westine P.S., et al. Explosion hazards and evaluation, Elsevier, Amsterdam-N.Y.-Oxford, 1983,798 p.

4.2. Minutes of 20 th DOD explosion safety seminar, AFOSA 83-0131-012,1983, DOD

4.3. Powers J.M., Krier H. Attenuation of blast waves when detonating explosives inside barriers //J of Haz, Materials, 1983, v. 13,N 1-2, p. 121-133.

4.4. Hader H. Effects or bare and cased explosives charges on reinforced concrete walls. Proc. of Symp. on the interactions of non-nuclear munitions with structures, AD-A132115,1983, v.l, pp. 221 - 227.

4.5. Bowman J.E., Nibblett G.3. F. The passage of a plane shock wave through a wire gauze // Proc. Phys. Soc. Sec. B. 1955, v.68, Pt. 12, No 432, p. 1008-1016.

4.6. Bondarenko A.V., Ibragim M.A. Measurements of shock wave speed, established after the interaction with obstacles as the channels or diafragms // Izv. USSR Ac.Sci, MZhG, 1967, No 3, p.115-119 *(in Russian)*.

4.7. Dain C.G., Hodgson J.P. Generation or weak shock waves in a shock tube // Aeronaut. Quart., 1974, v.25, No 2, p. 101-108.

4.8. Kostochko Yu. P. Interaction of shock waves with perforated surface // Wirks Tomsk Univ, Inst. Appl. Mathematics and mechanics, 1974, v.5, p. 106 — 112 *(in Russian)*.

4.9. Mori Y., Hijikata K., Shimizu T. Attenuation of shock wave by multiorifice. Proc. 10tn Int. Shock Tube Symp. Kyoto. 1973, P.400-407.

4.10. Tong K.O., Knight C.J., Srivastava B.N. Interaction of weak shock waves with screens and honeycombs // AIAA Journal, 1960, v.l6, No 11, p. 1298-1305.

4.11. Shevtsov B.L. Interaction of shock waves with perforated barrier // M., 1952, 20 p. – VINITI 16.03.82, No 1192-82 *(in Russian)*.

4.12. Grin V.T., Kraiko A.N., Miller L.G. On the Riemann problem at perforated partition // ZhPMTF, 1981, No 3, p.95-103 *(in Russian)*.

4.13. Ivanov A. N., Borisovskaja V. L. Study of shock wave attenuation by perforated screen // TsAGI 1977, release. 1834, p.26 – 33 *(in Russian)*.

4.14. Reichenbach H. Uber das verhalten von Kugelschichten und Sandfiltern beim auftreffen einer luftstosswelle. EMI Bericht 5/66,1966,40S.

4.15. Mineev V.N., Klapovsky E.E., Matseevich B.F. et al. Attenuation of air shock wave by perforated barriers // 5th Symp. Explos. Work. Metals, Gottwaldow, 1982, Dum. Techhiky CSVTS Pardubice, 1982, p. 357-361 *(in Russian)*.

4.16. Gelfand B.E., Medvedev S.P., Polenov A.N. et al. Speed measurements of weak perturbations in porous media of bulk density // ZhPMTF, 1986, No 1, p. 141 - 144*(in Russian)*.

4.17. Nikolaev G.N. An experimental research of formation of the shock wave, reflected from a wall with an aperture // Izv. USSR Ac.Sci, MZhG, 1974, No 2, p. 176-181*(in Russian)*.

4.18. Gelfand B.E., Medvedev S.P., Polenov A.N. Interaction of the non-stationary pressure waves with, perforated partitions // Izv. USSR Ac.Sci, MZhG, 1987, No 6, p. 174-176 *(in Russian)*.

4.19. Rogg B., Hermann D., Adomeit G., Shock induced flow in regular arrays of cylinders and packed beds // Int. J. Heat Mass Transfer, 1985, v. 28, No 12, p. 2285 - 2298.

4.20. Zloch N., Shock attenuation in beds of granular solids // Archiv. Mechanics stosowanej, 1976, v. 28, No 5 - 6, p. 817 - 825.

4.21. Strizhevskii I.I., Zakaznov V.F. Industrial Fire Protectors. M., Khimija, 1966 *(in Russian)*.

4.22. Medvedev S.P., Frolov S.M., Gelfand B.E. Shock waves attenuation by screens made from granular materials// IFZh, 1990, v. 58, No 6, p. 924 – 928 *(in Russian)*.

4.23. BritanA., Ben-Dor G., Igra O., Shapiro H. Shockwave attenuation by granular filters // Intern. J. Of Multiphase flow, 2000, v. 27, No 4, p. 617-634.

4.24. Reichenbach H. Messungen des druckverlaufs nach Hindernissen ingangen. EMI Bericht 13/63,1963,28S.

4.25. Reichenbach H. Funkenkinematographischeuntersuchung Der stosswellen dampfung durch mehrfachreflexion an blenden. Proc. Intern. Symp., Stockholm, 1968, p. 362 - 365.

CHAPTER 5. APPLICATION OF POROUS SCREENS AND FILLERS FOR PROTECTION AGAINST BLAST LOADINGS

5.1. Effect of the porous screen on blast loadings

The interaction of plane shock waves with porous compressed materials made from polyurethane foam (PUF) and plastic foam was investigated in [5.1...5.5]. It was shown, that the maximal pressure amplitude at the wall under the PUF layer can considerably exceed the shock wave pressure at normal reflection from the rigid wall in the absence of a porous covering. For the theoretical description of the effects observed in [5.4, 5.5] the method based on representation of two-phase medium (PUF + gas) by the equivalent gas with changed in comparison with pure gas thermo-physical properties is offered. This method allows calculating the maximal loading and understanding the dynamics of the reflected wave. However, within the framework of equivalent gas model some specific features of the phenomenon revealed in [5.1... 5.4] are not described. The reasons of dependence of the pressure peak on the height (thickness) of a layer and the absence of the «shelf» with constant parameters in pressure profile at the wall (at a level of peak pressure) remain unclear. Alternative model of the phenomenon based on consideration of the sample movement at sudden loading is described below.

The essence of nonlinear process of the porous layer response to the blast loading can be presented as follows. At the moment of air shock wave reflection from the border gas - PUF a porous layer at the end plate of the shock tube is instantly loaded by the gas piston with the pressure close to the pressure of normal reflection. If the pressure considerably exceeds the characteristic value of compression stress of the porous material, then, at the initial stage, the force, counteracting to movement, appears negligibly small. During the development of deformation the resistance of a sample grows under the certain law.

Let's present (fig. 5.1) the column of the compressed porous material of the unit cross-section area of mass m and height h by the equivalent mechanical system with one

degree of freedom consisting of a point mass m and a combination of ideally plastic Coulomb element with a zero restoring force (region 1) and elastic elements with elasticity factor k and damping factor a (region 2).

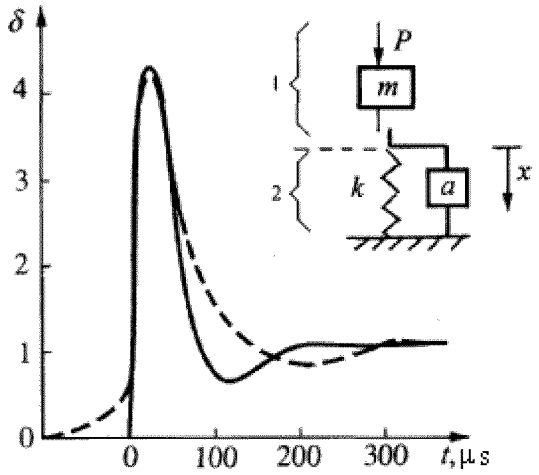

Fig. 5.1. Calculated dependence of the relative loading coefficient δ on time t at h = 50 mm and P = 1.4 MPa. Dashed line corresponds to experiment [5.5]

Let's consider the movement of mass m under the action of the suddenly enclosed constant loading P , corresponding to the overpressure in the reflected shock wave. In the region 1 the body gets the speed

$$v_0=(P\rho^{-1})^{1/2}$$

where ρ is the density of the material (for PUF ρ = 33 kg/m^3). The further motion of the mass is governed by the equation

$$mx'' + ax' + kx = P \qquad (5.1)$$

with the initial conditions

$$x(0) = 0, x'(0) = v_0.$$

(5.2)

At various relationships between a and a_0 (a_0 = 2 $(km)^{1/2}$ is the critical damping coefficient) three types of the solution of the equation (5.1) can be obtained. For the problem under consideration the case $a<a_0$ is the characteristic one. Pressure loading of a rigid support at an arbitrary time $t>0$ is $R=kx$. The relative loading coefficient $\delta = R/\rho$ is found from the solution of the equations (5.1) and (5.2) to be:

$$\delta = \exp(-\alpha t)\left[(\gamma - \alpha)\beta^{-1}\sin\beta t - \cos\beta t\right] + 1$$

(5.3)

where $\alpha = a/2m; \beta = \left(k/m - \alpha^2\right)^{1/2}; \gamma = kv_0/P$

The maximal value of the relative loading coefficient δ_m is attained at the moment of time t_m:

$$t_m = \beta^{-1} arctg\left(\beta\gamma\left[(\gamma - \alpha)\left(\alpha - \beta^2\right)\right]^{-1}\right)$$

(5.4)

Let's estimate the speed v_0, with the assumption, that the mass m is initially located at the center of mass of PUF sample and the compression stress of a sample is much less than applied loading P. If to take into account, that at 40 % deformations the characteristic magnitude of compression stress of PUF is 10^4 Pa, then the last assumption is valid for $P>>10^4$ Pa. Then $v_0 = (0.4\ P\rho^{-1})^{1/2}$, and the speed of the free border of the sample is $2v_0$ and at P = 0.15...0.22 MPa is 85...103 m/s. The speed of the border, measured at the same conditions, is 95 m/s [5.5]. The calculated speed of the border PUF - gas does not depend on the height of the sample, that prove to be true by the measurements in [5.4, 5.5]. The magnitude of k for PUF is determined on the basis of one of the experiments (h = 50 mm, P = 1.4 MPa) and from the condition of equivalence between the values of δ_m in the model and in the experiment. The k value is (4…4.2) 10^9 N/m^3 (assuming a/a_0 = 0.5...0.6). The

dependence of loading $\delta=\delta(t)$ at h = 50 mm and P = 1.4 MPa is indicated by continuous line in the fig. 5.1. The dashed line corresponds to the experimental data [5.5]. The presence of a smooth curved part at the measured profile $\delta(t)$ is connected, probably, to nonzero restoring force in the region 1 (fig. 5.1), and it is possible to explain the deceleration of the pressure decrease by the hysteresis phenomena at PUF loading.

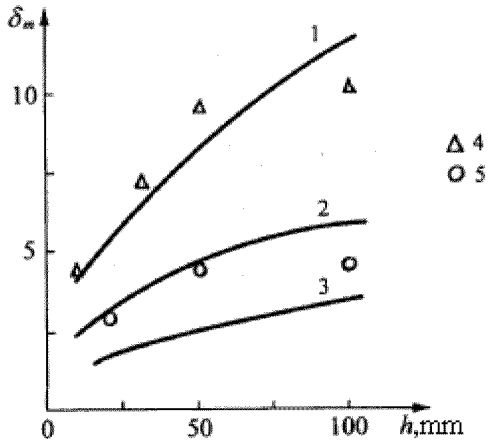

Fig. 5.2. Dependence of the maximal relative loading coefficient δ_m on the height of the PUF sample at different pressures P = 0.32 (1); 1.4 (2) and 5.0 MPa (3). k = 4.2 10^9 N/m^3 and a=0.6 a_0. The points 4 and 5 correspond to the experimental data [5.5] for P = 0.32 and 1.4 MPa.

The dependences of the maximal values of δ_m on the height of the PUF sample at different pressures P = 0.32 (1); 1.4 (2) and 5.0 MPa (3) are presented in the fig. 5.2. The specified dependences were calculated for the same magnitudes of k = 4.2 10^9 N/m^3 and a=0.6 a_0. The points 4 and 5 correspond to the experimental data [5.5] for P = 0.32 and 1.4 MPa. In the pressure range under consideration the maximal relative loading coefficient δ_m can be approximated by the formula:

$$\delta_m \approx\sim 1+0.3\left(khP^{-1}\right)^{1/2}$$

As it is seen, the maximal loading increases with the decreasing of P (i.e. with reduction of the incident shock wave intensity). Note, that in the case of extremely small P, comparable to the PUF compression stress, the value of δ_m expected to be decreasing.

Thus, the character of loading changes at the shock-wave action on the structure with porous compressible covering. In the absence of the covering the structure is loaded quasi-statically. The presence of the covering results in the occurrence of the pulse component, which have to be taken into account in strength calculations. The suggested model correctly describes the phenomenon of amplification of shock-wave loading on a rigid support covered by the porous compressible material, reflects the dependence of the loading on geometrical sizes of the covering and on the pressure at the surface. On the basis of the proposed model the method of determining of shock waves loadings on structures faced by porous compressible materials can be developed. The solution of the inverse problem is possible, when the elastic properties of the covering are determining by known loading.

5.2. Protection against explosive loadings by porous screens

The expansion of technological processes involving explosion demands the further development of the reliable ways of explosion localization (damping, suppression). Widespread method of explosion localization is the use of explosive chambers (EC) [5.6, 5.13]. An issue of the day in technology of material processing by explosion is the increase of maximal weight of HE charge to be detonated safely in the chamber. One of the solutions is the decrease of stress forces in the walls of the chamber by filling the cavity by various damping media and protection screens [5.7]. The reason of the decrease of stress forces, apparently, is that the damping material gives rise to an essential stretching of the pressure impulse in time and, subsequently, to the quasi-static loading of EC, at which the main factor determining the stress in the walls, is the lowered pressure, instead of impulse.

At the same time, as shown experimentally in [5.8], the porous material placed at the rigid wall (as it was done in [5.2...5.4]) can increase the pressure amplitude of the

reflected stationary wave. It causes the necessity of more careful research of the opportunity to use the given materials for loadings suppression and EC protection, that was not considered in [5.13].

In reference [5.8] the screens of various structures containing porous media are considered and the results of research of damping properties of porous media filling the internal volume of the chamber are offered. The screens were placed at the EC wall to decrease the impulse loading. The experiments were performed for the purposes of optimizing the parameters of porous fillers able to damp the loading. The screens made from foam-rubber (density 40 kg/m^3) of different thickness, as well as alternating layers of steel and foam-rubber (stratified screens) were investigated. The loading was carried out by a spherical RDX charge (weight 0.15 kg) located at distance 0.5m from the wall of EC. The screens were mounted at EC wall, and the pressure gauge was set into the wall. The results of experiments are presented in table 5.1.

Table 5.1 Parameters of loadings on walls depending on the barrier structure and thickness [5.8]

Number of experiment	Thickness of the barrier, mm	Maximal, pressure, Pa	Duration of the impulse, μs	Type of the barrier
102	0	5,8	225	
111	30	13	128	foam-rubber
103	50	9,3	100	foam-rubber
112	60	8,5	240	foam-rubber
105	70	7,6	630	foam-rubber
106	100	1,92	1060	foam-rubber
113	150	1,12	1260	foam-rubber
116	65	0,6	5000	stratified screens
117	65	0,28	2160	stratified screens
124	100	0,65	2690	stratified screens

Stratified screens were used in the experiments 116,117 and 124. Structure of the screens and the thickness of layers were following:

- Experiment 116: steel - 2,5 mm + foam-rubber - 30 mm + steel - 2,5 mm + foam-rubber - 30 mm (2 - tier screen).
- Experiment 117: steel - 5 mm + foam-rubber - 60 mm (1 -tier screen).
- Experiment 124: 3 layers, each consisting of a steel plate (thickness 2.3 mm) and foam-rubber layer (thickness 30 mm) (3-tier screen).

As evident from the table, the use of foam-rubber screens with layer thickness < 80 mm, as well as in [5.1,5.4], results in the increase of the SW amplitude at the wall behind the screen. Thereof the SW amplification at reflection could occur, as can be seen from experiments 111 and 105. Screens with layer thickness 100... 150 mm result in the decrease of the pressure amplitude (in comparison with the conditions of EC walls loading by explosion without the screen, experiment 102). Typical pressure records at walls are shown in the fig. 5.3.

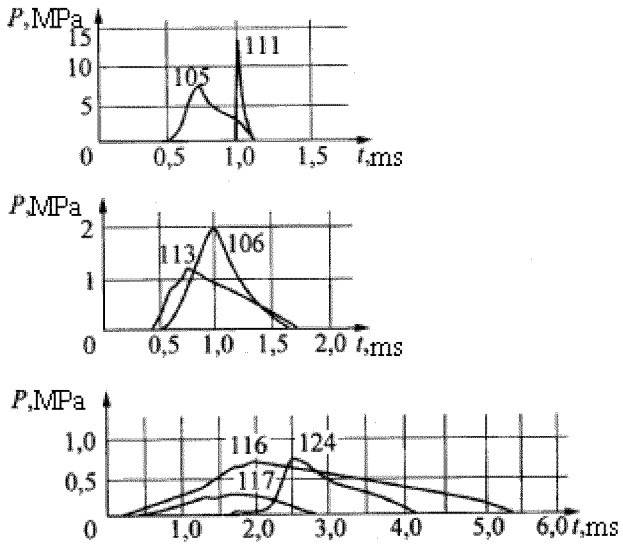

Fig. 5.3. Typical records of pressure at the walls of the explosive chamber [5.7,5.8]

The comparison of the stratified screens of equal thickness and mass (differ only by the amount and the distribution of the layers, the experiments 116 and 117), shows, that two-layer 1 –tier screen is the most effective for the damping. The two-layer screen in view of the stretching of the impulse and the reduction of the pressure is better, than the screen of the larger thickness and mass consisting of three pairs of layers steel – foam-rubber (the experiment 124, 3-tier screen). It is connected with the fact, that the SW splitting in the screen with large number of layers (in acoustic approach leading to the attenuation of the head wave) is suppressed by the nonlinear effects arising at imposing of the reflected waves on the head wave. The impulse, received by the plate due to the interaction with SW, does not depend on structure of the screen and under constant conditions of loading remains constant.

Kinetics energy E_k of the plate is larger for the lower mass M of the plate at the constant acting impulse i. From this point of view it is favorable to have the massive elements of the screen on a surface perceiving the impulse.

It is revealed experimentally, that at the constant parameters of the blast loading on the screen the most effective among the investigated structures are the two-layer screens consisting of the layer of steel (from the side, perceiving the SW impulse) and the porous material. The efficiency of such structure proves to be true by the studies of the blast effect on the animals protected by body armour (flack jacket) (a steel plate + amortization layer from a porous material) [5.12, 5.14]. Of interest is to determine the optimum porous material for the maximal pressure decrease and find the relationship between the degree of damping, amplitude and duration of the blast impulse acting on the screen. For this purpose the RDX charges of the spherical form and weight 0.034 and 0.215 kg were used. Changing the weight of the charge and the distance R to the screen, the amplitude ΔP and blast impulse duration τ was determined in each series of experiments.

Table 5.2 Parameters of the loads at EC walls at the loading by SW generated by the detonation of the charge of weight 0.215 kg through the screen: steel - 2 mm, porous material - 40 mm by [5.8]

Structure of the screen	**Distance to the screen *R* and ($\bar{R}$)**					
	1,4(35)		1(25)		0,4(13)	
	$\Delta P \cdot 10^{-5}$, Pa	τ, ms	$\Delta P \cdot 10^{-5}$, Pa	τ, ms	$\Delta P \cdot 10^{-5}$, Pa	τ, ms
Without screen	4,8	0,8	13,2	0,45	93	0,13
Sand	1,6	4,1	8,3	2,6	64	0,5
Foam-rubber	1,2	4,2	2,1	3,7	11,7	3,6
Pearlite	1,6	3,6	3,0	2,6	35	1,4
Rubber crumb	1,6	4,1	3,3	4,0	12,4	3,9

Table 5.3 Parameters of the loads at EC walls at loading by SW generated by the detonation of the charge of weight 0.034 kg through the screen: steel - 1 mm, porous material - 22 mm by [5.8]

Structure of the screen	**Distance to the screen *R* and ($\bar{R}$)**					
	0,76(35)		0,55(25)		0,27(13)	
	$\Delta P \cdot 10^{-5}$, Pa	τ, ms	$\Delta P \cdot 10^{-5}$, Pa	τ, ms	$\Delta P \cdot 10^{-5}$, Pa	τ, ms
Without screen	4,8	0,43	13,2	0,24	93	0,07
Sand	7,2	1,1	8,8	1,3	110	0,1
Foam-rubber	0,8	1,8	11,5	3	7,6	2,5
Pearlite	1,1	2,8	3,0	3,9	11,5	2,2
Rubber crumb	0,9	3,1	1,7	3	9,6	1,9
Steel shot	6,2	1,8	23	2,2	56	0,5

The results of experiments [5.7, 5.8] with two-layer screens of identical thickness and the structure differed only by the type of a porous material are presented in tables 5.2 and 5.3. The amplitudes and the characteristic duration times of the loadings on EC walls

behind the screens are listed. The characteristics of the blast impulse at the EC wall without the screen are presented for the comparison. The relative distances to the screen $\overline{R} = R / R_0$, where R_0 is the radius of HE charge are given in the tables.

As seen from the tables 5.1, 5.2 and 5.3 the preferable porous materials for damping screens are foam - rubber, rubber crumb and pearlite, which allow essentially reducing the amplitude of the pressure at EC walls with simultaneous increase of the impulse duration in a wide range of governing parameters. The screens containing sand and steel shot, are less effective for the damping. In a number of cases such screens result in the increase of the pressure amplitude at EC walls. It is important to note the dependence of damping properties of screens containing different porous materials, on the duration and the amplitude of the blast pulse. So, for the blast pulse generated by the charge of weight 0.215 kg at the distance 1.4 m ($\overline{R}$ = 35) the degrees of pressure amplitude reduction differed a little for various screens. On the contrary, for $\overline{R}$ = 13 the essential difference in damping properties was observed. The research of the loadings at EC walls filled by porous materials is of interest for the localization of explosion.

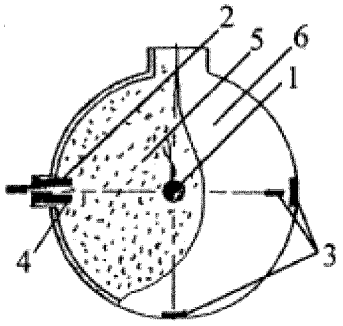

Fig. 5.4. Scheme of determination of blast loadings: 1 - HE charge; 2 and 4 - pressure gauges; 3- deformation gauges; 5 - wood chips; 6 - air [5.8]

The reaction of a thin-walled spherical envelope with a diameter 0.45 m and thickness of walls 0.007 m, loaded by explosion of the concentrated HE charge 1, located in the center of symmetry of the envelope was investigated in the experiments [5.8] (fig. 5.4). The charge was initiated by the detonator. The pressure (gauges 2,4) at the internal

wall of the chamber together with deformations (gauges 3) was measured. The experiments were carried out for the cases, when the envelope was filled by the wood chips 5 with initial density 100 kg/m^3 or air 6 at normal conditions.

In the experiments with sphere filled by air at weight of charges 0,03 and 0,06 kg the peak stresses at walls were accordingly 240 and 370 MPa. The maximal pressure was 17,6 and 15 MPa, and time of loading at the wall was 46 and 50 μs accordingly. When the envelope was filled by the wood chips at explosion of charges of weight 0.03 and 0.06 kg, the parameters of loading and deformation are equal accordingly: pressure — 1,3 MPa, time of action 1800...1230 μs, maximal stress 45 and 150 MPa.

Clearly seen, that for the charge of weight 0.05 kg the filling of EC volume by the wood chips results in decrease of the maximal stress more than in 5 times, and for the charge of weight 0.06 kg of the deformation forces decreased more than in 2 times.

The important result obtained in [5.7... 5.9] is the dependence of the maximal pressure at the wall of the explosive chamber on the degree of compression of porous material in SW. The pressure records at the wall of the explosive chamber filled by wooden chips are presented in the fig. 5.5. Weight of the charge in the experiments is the same.

Introducing the designation $\chi=\rho_0/\rho$, where ρ_0 is the density of the wood chips before explosion; ρ is its density after explosion, it is possible to obtain, that the pressure decreases with increasing compression degree of the chips (or with decreasing χ). So, the curve 1 corresponds to χ= 0,9, the curve 2 — χ = 0,86, and the curve 3 - χ = 0,76.

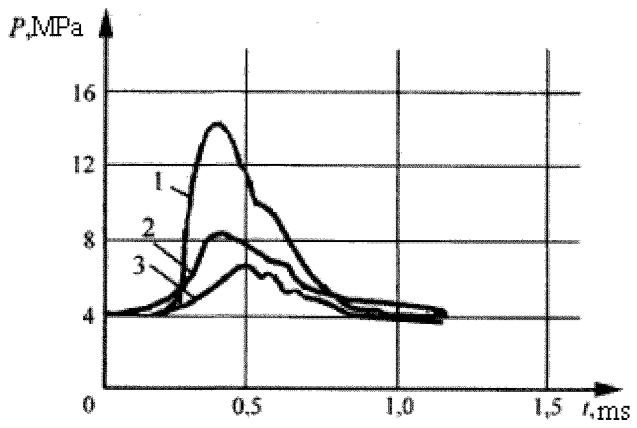

Fig. 5.5. Influence of preliminary compaction of porous media on blast loading [5.8]

Thus as was established in [5.8], the most effective among the investigated types of stratified screens are two-layer ones consisting from a porous and dense (for example, steel) material, located at the side perceiving the impulse.

Among the investigated porous materials in the two-layer screens the most effective are foam-rubber, rubber crumb and pearlite, allowing to reduce the pressure at EC walls with simultaneous increase of loading duration.

The damping effect essentially depends on the amplitude and duration of loading, acting on the screen.

Experimentally shown, that the maximal pressure at the EC wall depends on the degree of compression of porous material.

The filling of EC volume by porous material results in the reduction of the maximal stress in its walls, at least for the investigated relative distances.

5.3. Optimization of protective screens. Problem formulation

The processes of SW propagation and reflection in porous and stratified screens at the loading by the pressure pulse are investigated in [5.9], where the problem of optimization was solves. The stratified screens made from steel plates and polyurethane foam (foam-rubber) were studied.

The optimization of protective screens has the practical importance for designing of the explosion protection equipment with the purpose of reduction of its dimensions, weight and cost.

The behavior of foam rubber is modeled in [5.9] by equilibrium mixture of ideal caloric gas (the first phase) and incompressible particles (the second phase). The governing equations in Lagrangian form in case of one-dimensional flow at plane symmetry are:

$$\frac{1}{v}\frac{\partial v}{\partial t}=\frac{\partial u}{\partial r};\frac{1}{v}\frac{\partial u}{\partial t}=-\frac{\partial P}{\partial r}$$
$$\frac{\partial e}{\partial t}=-P\frac{\partial v}{\partial t};\frac{dr}{dt}=u$$

$$T_1=T_2=T;P_1=P_2=P;u_1=u_2=u;$$
$$m_1+m_2=1;\rho_i=m_i\rho_{ii};e_i=c_iT_i;$$
$$P_1=\rho_{11}R_1T;\rho_{22}=const;\rho_i=\alpha_i\rho;$$
$$e=cT;c=\alpha_1c_1+\alpha_2c_2;\alpha_1+\alpha_2=1$$

where $v=1/\rho$ is the specific volume of the mixture; u is the mass velocity; P is the pressure in the mixture; e is the specific internal energy of the mixture; c_i are the specific heat capacities of the phases; ρ_{ii} are the true densities of the phases; ρ_i are the average densities of the phases; m_i are the volume concentrations of the phases; α_i are the mass concentrations of the phases.

In case of the mixture with a small volume concentration of condensed phase the model take a form:

$$\frac{1}{v}\frac{\partial v}{\partial t}=\frac{\partial u}{\partial r};\frac{1}{v}\frac{\partial u}{\partial t}=-\frac{\partial P}{\partial r};\frac{\partial e}{\partial t}=-P\frac{\partial v}{\partial t};$$
$$P=\rho RT;R=\alpha_1 R_1;e=cT;c=\alpha_1 c_1+\alpha_2 c_2$$

Such a mixture can be considered as ideally caloric gas (*R=const, c=const*) with the specific heats capacity ratio $\gamma=(c+R)c$.

The loading of a flat layer A_1A_2 of rubber-foam with thickness *d* by a triangular pressure pulse *P*(*t*) was considered in [5.9] (fig. 5.6). The border A_2 is an absolute rigid wall. The mathematical formulation of the problem is following: it is required to find functions *u, P, ρ, v, e, T,* ρ_1, ρ_2, ρ_{11}, ρ_{22}, m_1, m_2 in the area z = $\{A_1 \le r \le A_2,\ 0 \le t \le t_D\}$, satisfying to above presented set of the equations, with corresponding initial and boundary conditions.

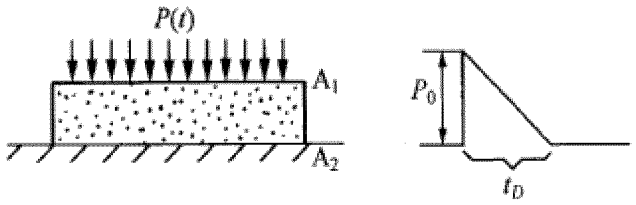

Fig. 5.6. The scheme of the screen loading by the blast wave [5.9]

The initial conditions: at the moment *t* = 0 the layer A_1A_2 is not loaded, therefore

at *t* = 0: *u* = 0, *P*=0, $\rho_{11}=\rho_{11}^{\ 0}$, $\rho_2=\rho_{22}^{\ 0}$, $\rho=\rho_0$, $(A_1 \le r \le A_2)$.

Boundary conditions: at A_1 border, at $t \ge 0$ the dependence *P(t)* is given, at the absolute rigid wall A_2 the condition *u*(*t*) = 0 is given.

P(t) has a form:

$$P(t)=\begin{cases}P_0\left(1-t/t_D\right), & \text{for } 0\le t\le t_D\\ 0, & \text{for } t>t_D\end{cases} \qquad (5.5)$$

Density of the foam-rubber at the initial moment $t = 0$: $\rho_0 = 40$ kg/m^3, true (absolute) density of the condensed phase $\rho_{22}^0 = 1.2 \cdot 10^3$ kg/m^3, density of the gaseous phase (air) $\rho_{11}^0 = 1{,}29$ kg/m^3.

5.4. Shock waves propagation in porous screens

The parameters of the loading pulse are obtained at $P_0 = 5.8$ MPa, $t_D = 200$ μs in expression (5.5).

The calculated and experimental maximal pressures at the absolute rigid wall for different thickness of the sample are presented in the fig.5.7.

The analysis of the calculation results shows, that the model 2, in which the volumetric concentration of a gas phase ($m_1 << 1$) was not taken into account, describes the experimental data unsatisfactorily, because during the interstice reduction the volumetric concentration of the condensed phase can become about unity.

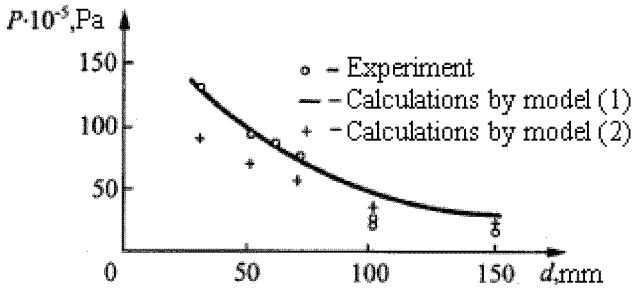

Fig. 5.7. The maximal loading at the wall for screens of different thickness at constant parameters of the blast wave [5.9]

The comparison of the numerical results obtained in [5.9] with the use of the model 1, taking into account the volumetric phase, with experimental data shows their good correspondence, at least up to the thickness of the samples 70... 80 mm. The little bit smaller magnitudes of the experimental data at the thickness of the samples more than 100 mm are explained, apparently, by multi-dimensional character of a physical task, and non-equilibrium of the phases in real conditions as well. Results on the basic model are discussed further in view of the volumetric concentration of the condensed phase.

The calculated and experimental dependences of pressure at the rigid wall on time are given in the fig. 5.8 for the thickness of the sample 60 mm.

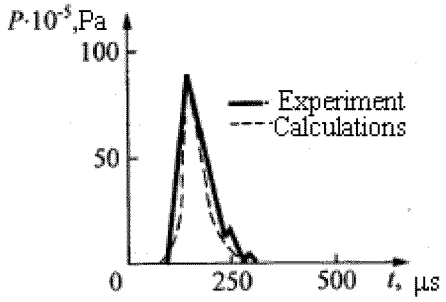

Fig. 5.8. The diagrams of change of pressure at the rigid wall [5.9]

As seen from the numerical and experimental data presented in the fig. 5.7, for the triangular loading pulse with parameters P_0 = 5.8 MPa, t_D = 200 μs there is a critical thickness of a porous layer d^*, below which the amplification (but for the attenuation) of the pressure amplitude in the reflected wave occurs. At the same time, as shown in [5.1], the amplification of stationary SW amplitude, i.e. at $t_D \to \infty$, takes place for all thickness of the layer.

In this connection the dependence of critical thickness of a layer on the parameters of the loading pulse is of interest. In table 5.4 the critical thickness for four-types of loading are presented.

Table 5.4 Critical thickness of protective layers [5.9]

No.	Parameters of the pulse		d^*, mm
	Pressure P_0, MPa	t_D, μs	
1	1,0	130	18
2	6,6	130	87
3	10	130	112
4	6,6	1300	850

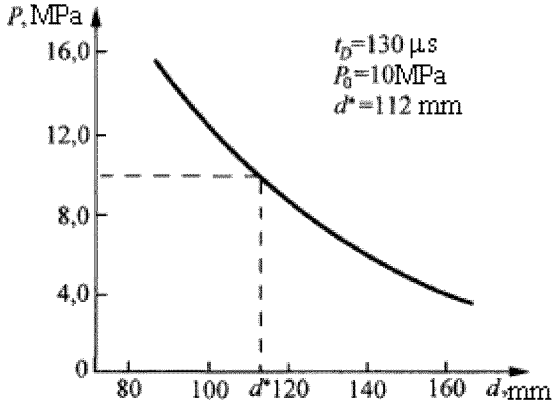

Fig. 5.9. Critical thickness of the porous screen for constant blast loading

It is seen, that the critical thickness of rubber-foam layer depends both on the duration of the pulse, and on its amplitude.

The characteristic dependence (P_0 = 10. MPa, t_D = 130 μs) of the pressure amplitude at the absolute rigid wall on the thickness of the porous layer is shown in the fig. 5.9.

5.5. Efficiency of blast loading suppression by porous screens

The loadings by a triangular pressure pulse of the stratified screen consisting of one, two or three identical tiers were considered in [5.9]. Each tier contains a steel plate and rubber-foam layer (fig. 5.10). The stratified screen is contiguous with the rigid wall. The metal plates were considered incompressible.

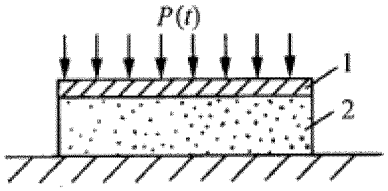

Fig. 5.10. The combined protective screen: a layer of steel (1) and a layer of rubber-foam (2)

At $t \geq 0$ the pressure $P(t)$ is given at the border of the stratified screen from the side perceiving the loading, and $u(t) = 0$ at the absolute rigid wall. At the contact borders of various materials the condition of speed and pressure continuity is given.

The calculated (curve 1) and experimental (curve 2) time dependences of the pressure at the rigid wall behind the stratified screen consisting of one tier are shown in the fig. 5.11*a* by the data from [5.9]. Thickness of the steel plate is 4 mm, rubber-foam layer — 60 mm.

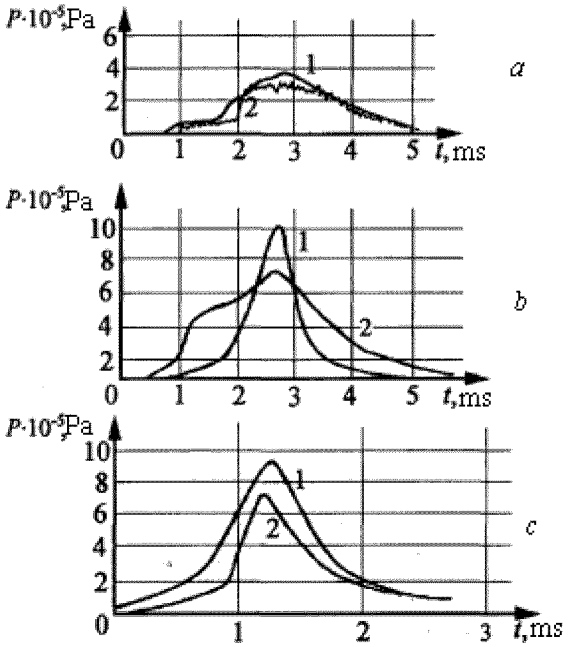

Fig. 5.11. Pressure at the rigid wall behind the stratified screen: a - steel (4 mm) – foam rubber (60 mm); b – 2 tiers: steel (2,5 mm) — rubber-foam (30 mm); c — 3 tiers: steel (2,5 mm) — foam rubber (30 mm). 1 — numerical calculations; 2 — experiment

The time dependences of the pressure at the absolute rigid wall obtained in the numerical calculations (the curve 1) and in the experiments (the curves 2) are compared in the fig 5.11 by [5.9] for the stratified screens, consisting from two tiers, where each tier contains a steel plate by thickness of 2,5 mm and foam rubber layer by thickness of 30 mm. The similar comparison of numerical and experimental dependence of pressure at the rigid wall is given in the fig. 5.11 for triple-tier barrier, where each tier consists of a steel plate by thickness of 2,5 mm and foam rubber layer of 30 mm.

From the comparison of dependences of the pressures for three investigated types of barrier (single, double and triple) it follows, that the most effective for the shock wave loadings damping is the single-tire barrier. This barrier has the least dimensions, weight and is most simple for the practical use. The characteristic dependences $P(t)$ at the rigid wall for three types of single-tire screens are presented in the fig. 5.12. The thickness of the steel plate was 4 mm in all experiments, and the thickness of the foam rubber was 40 mm (the curve 1), and 60 mm (the curve 2) accordingly.

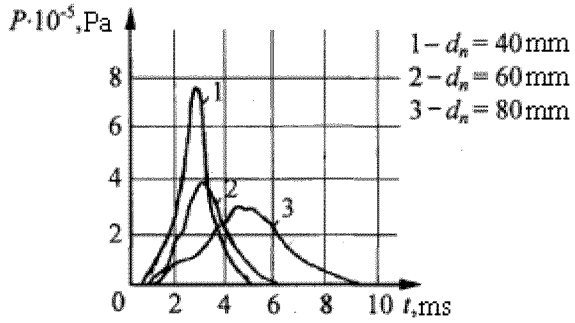

Fig. 5.12. Change of P(t) at the rigid wall for single-tier screens

All types of the investigated screens effectively transform the shockwave impulse of pressure into direction of the reducing of pressure amplitude with the simultaneous increasing of duration.

5.6. Optimization of stratified porous screens

The problem of optimization of stratified screens is considered in [5.9]. The single – tier double-layer screens were investigated as the most effective (system a plate + foam rubber layers).

Dependences of the maximal pressure at the absolute rigid wall on the thickness of foam rubber layer are shown at the fixed thickness of steel plates (fig. 5.13) and on thickness of the steel plate at the fixed thickness of foam rubber layers (fig. 5.14). The calculations were carried out at parameters of pulse loading: P_0 = 5.8 MPa, t_D = 200 μs.

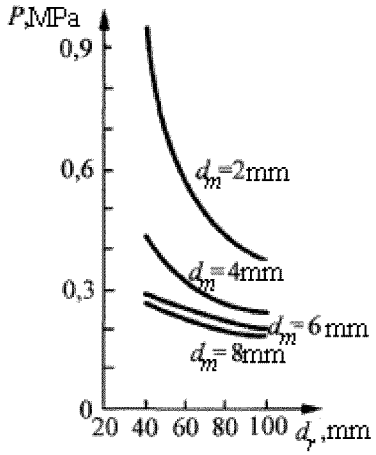

Fig.5.13 Change of the maximal pressure at the rigid wall at various thickness of the foam rubber layer d_r

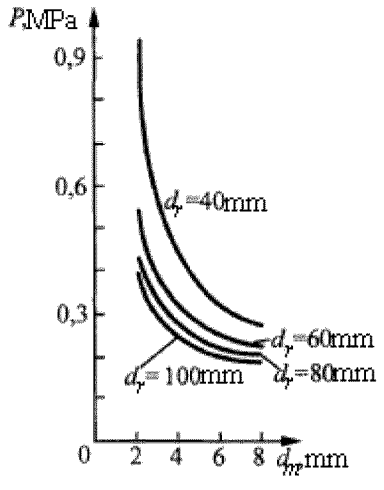

Fig.5.14 Change of the maximal pressure at the rigid wall at various thickness of the metal plate d_m

When there is no restriction on the thickness of the stratified screen, the decrease of the maximal pressure at a rigid wall can be achieved by the simple increase of the thickness of layers. Thus the more thickness of layers, the less maximal pressure at a wall.

Let the permission pressure P at the protected wall is given. As shown in [5.4], the given pressure can be achieved at different thickness of layers, increasing the thickness of that or other layer. The choice of the optimum screen is reduced to selection from all stratified systems by the criteria of minimal weight or cost. This mathematical task in [5.9] is solved as the search of the thickness of layers d_m (metal) and d_r (foam rubber), which minimize the function

$$\rho_m d_m + \rho_r d_r \Rightarrow min$$

restricting the maximal pressure at the wall $P_{max} \leq P^*$. Here ρ_m and ρ_r are the density of steel and foam rubber accordingly.

The analysis of dependences shown in the fig.5.13 and 5.14, has allowed making a conclusion that the value P is the function of the product $d_m d_r$ with sufficient degree of accuracy. This conclusion proves to be true by the data from table 5.5.

From the condition $P_{max}=P^*$ we obtain $P\ (d_m d_r) = P^*$, and therefore $d_m d_r$ =const. Denote $d_m d_r = a$. Then $d_r = a/d_m$ and the required function will take the form:

$$\rho_m d_m + \rho_r a/d_m \Rightarrow min$$

the minimum of the given function was obtained in [5.9] at

$$d_m=(\rho_r a/\rho_m)^{1/2},\ d_r=(\rho_m a/\rho_r)^{1/2}$$

Thus, knowing P^*, we can find a from the diagrams (fig.5.14 and 5.13), and finally — the necessary thickness of layers.

Of interest is the maximal degree of decreasing the pressure at the rigid wall at the given thickness of the single-tier stratified system $d_m + d_r$ =const. Besides, it is important to elucidate the influence of characteristic parameters of triangular loading P_0 and t_D on the damping properties of the screens. The ratio of layers thickness d_m/d_r has to be determined, at which the minimum of pressure at the absolute rigid wall is reached, under condition that thickness of stratified system is constant, i.e. $d_m + d_r$ =const.

Table 5.5 Maximal pressures at the wall for different thickness of layers of steel and foam rubber in the screen

No	P_{max}, 10^5 Pa	Thickness of layers, mm		$d_m d_r$
		d_m	d_r	

1	1,0	7,15 5,70	80 100	572 570
2	1,5	3,50 4,39 5,85	100 80 60	350 351 351
3	2,5	3,45 5,18 2,05	60 40 100	207 207 205
4	3,0	2,10 2,80	80 60	168 168

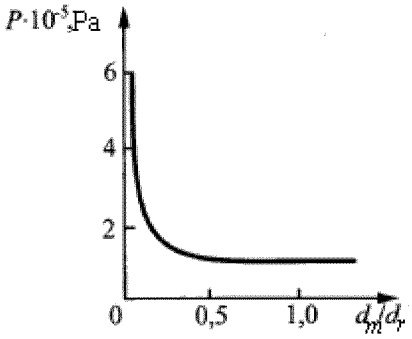

Fig. 5.15. Attenuation of the long-wave pressure pulse: P_0 = 1 MPa, t_D = 1000 μs, $d_m + d_r$ =50 mm.

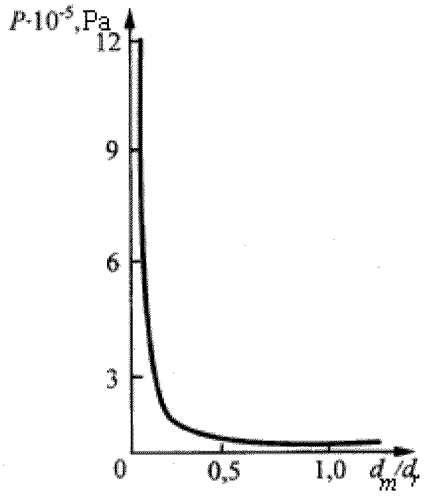

Fig.5.16 Attenuation of the short-wave pressure pulse: P_0 = 10 MPa, t_D = 100 μs, $d_m + d_r$ =50 mm.

Dependences of the maximal pressure at the rigid wall P_{max} on the ratios d_m/d_r are shown below, when $d_m + d_r$ =50 mm, and the loadings were characterized by the parameters: P_0 = 1 MPa, t_D = 1000 μs (fig. 5.15) and : P_0 = 10 MPa, t_D = 100 μs (fig. 5.16). The parameters P_0 and t_D in both cases are chosen from the reasons of preservation of the constant impulse $P_0 t_D$ /2, acting on the screen. It is seen, that the effective decrease P_{max} is observed up to d_m/d_r =0.5, and the minimum is reached at d_m/d_r ranging from 0.3 to 0.9. Further, there is an insignificant growth of loading with the at increase of d_m/d_r .

The position of the minimum of pressure weakly depends on the characteristics of the applied pulse.

The results of similar calculations for the case $d_m + d_r$ = 80 mm and parameters of the loading pulse P_0 = 10 MPa, t_D = 100 μs are presented in the fig.5.17.

The characteristic pressure profiles at the rigid wall for the two-layer screen with the thickness of 80 mm and different ratios of thickness of layers of steel and rubber-foam are shown in the fig. 5.18. Such screen results in strong transformation of the initial pulse.

The amplitude of pressure decreases in 100 times (curves 4), and the duration is increased in 300 times in comparison with parameters of the initial pulse.

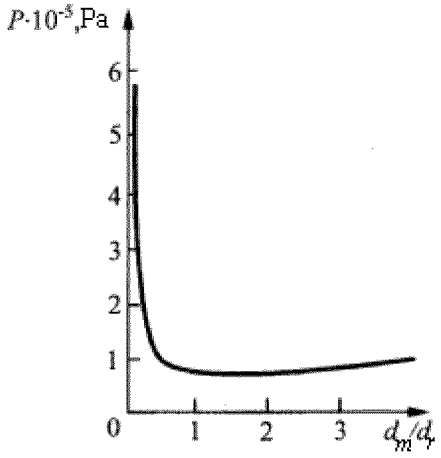

Fig. 5.17. Dependence of the maximal pressure at the rigid wall on the ratio d_m/d_r : pulse P_0 = 10 MPa, t_D = 100 μs; $d_m + d_r$ = 80 mm.

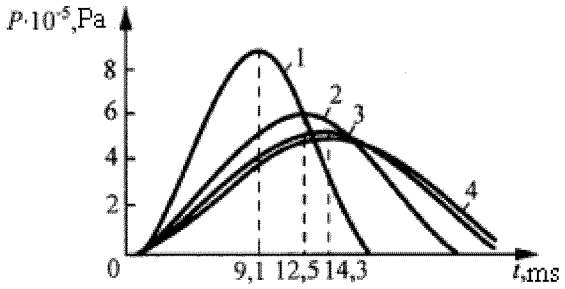

Fig. 5.18. Characteristic pressure profiles at the rigid wall for the two-layer screen with the thickness of 80 mm: 1 — d_m = 10mm, d_r = 70mm; 2- d_m = 20mm, d_r = 60mm; 3- d_m = 30mm, d_r = 50mm; 4- d_m = 40mm, d_r = 40mm by [5.9]

Let's describe the effect of volumetric concentration of the condensed phase (foam rubber) on the maximal pressure at the rigid wall. Consider the two-layer screen consisting of the single tier. The tier contains a steel plate with thickness d_m and foam rubber layer with thickness d_r. The pressure $P(t)$ is given by the dependence (5.5) with the parameters P_0 = 5.8 MPa, t_D = 200 μs. Average density of foam rubber varied from 0.04 up to 0.12 g/cm^3.

The maximal pressures at the rigid wall for stratified screen with the thickness of foam rubber layer 80 mm, and the thickness of a steel plate from 2 to 8 mm are shown in the fig.5.19.

The analysis of the dependences obtained showed, that the increase of volumetric concentration of the condensed phase results in the increase of the maximal pressure at the rigid wall. However this effect is insignificant and shown to be revealed at the small thickness of the steel plate.

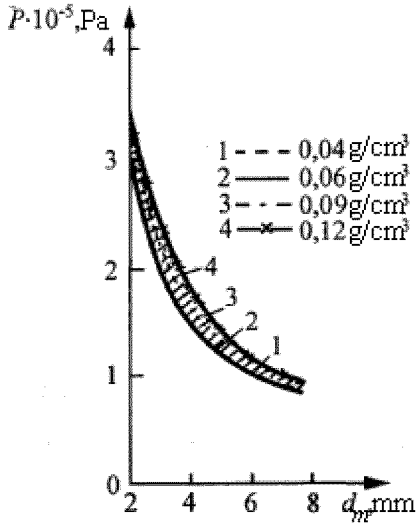

Fig. 5.19. Dependence of the maximal pressure at the rigid wall on the density of a porous layer in the screen, consisting from foam rubber with the thickness 80 mm and the steel plate with the thickness from 2 to 8 mm

The dependences of the maximal pressure at the rigid wall on the thickness of foam rubber layer are presented in the fig.5.20 for different volumetric concentrations of the condensed phase in foam rubber. The effect of volumetric concentration of the condensed phase on the parameters of the shock wave propagation is insignificant for the system under investigation.

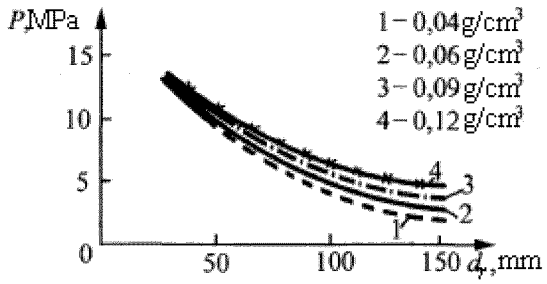

Fig. 5.20. Dependences of the maximal pressure at the rigid wall on the thickness of a foam rubber layer for different volumetric concentrations of the condensed phase in foam rubber.

5.7. Recommendations for the selection of the stratified screen

Thus, the observations and calculations in [5.7... 5.9] show, that:

1. For the loadings with triangular profile, there exists the critical thickness of a porous layer d^*, below which the amplitude in reflected SW from the rigid wall in a porous layer increases in comparison with the amplitude of applied loading P_0. At $d>d^*$ the pressure amplitude at the wall behind the screen will be less, than in initial loading. This paradox is confirmed in [5.11].

The critical thickness d^* depends on the amplitude P_0 and duration t_D of the blast loading.

2. The most effective among the stratified screens is two-layer screen. The denser layer should be located from the side perceiving loading. Moreover, the two-layer screens are easier, have smaller weight and dimensions for the given degree of pressure amplitude attenuation. The degree of the pressure amplitude attenuation is proportional to the layer thickness.

The maximal pressure attenuation is reached at the ratio of thickness of the dense layer to the thickness of porous layer – 0.8 and practically does not depend on the amplitude P_0 and duration t_D of the triangular pulse.

3. The increase of the porous layer density from 40 to 120 kg/m^3 practically has no effect on the damping degree both for two-layer screens, and for porous layers.

5.8. Protection of the human body against explosive loadings by special equipment with use of porous materials

The scientific and technical level of special protective equipment (flack jackets, helmets) permits to decrease the effect of loadings in the area of thorax and stomach in 40... 50 % and in the area of head in 90 % [5.12... 5.15].

The reduction of the damage level for bioobject due to protective clothes is illustrated in the fig. 5.21.

Nomogramm in the fig. 5.21 allows comparing the damage levels the unprotected body (*a*) and the man protected (*b*) by special equipment (miner) [5.15].

The direct studies of the flack jackets influence on the heaviness of the blast trauma at animals (pigs) have shown the protective effect of the «rigid» structures (steel armour plate and damping support from gas-filled, cellular polymeric material) [5.12,5.14]. As a sample, the flack-jacket of the second class of protection "Module 3M» was chosen. The protective elements in this jacket are executed as figured orthopedic plates. As a source of blast wave the HE charges of two types were used: TNT and LDE of complex structure. The experiments were carried out in open field (HE weight 5 kg) and in enclosure (1 kg HE). In each experiment two comparable pairs of animals in flack jackets and without protection were settled down equally spaced from the center of explosion, left side to explosion. 15 comparable pairs of animals were obtained under different experimental conditions (HE type, detonation conditions, distance from explosion). The results of the blast effect were determined as a degree of the heaviness of the blast trauma on the basis of the morphological analysis of animals at macro- and microlevel. Besides, the biochemical studies of the blood were performed. The analysis of the data obtained shows, that the total degree of the heaviness of the blast trauma for the animals in jackets is 25 % lower, than

for the unprotected animals. This parameter practically did not depend on the conditions of experiment and characteristics of HE charge.

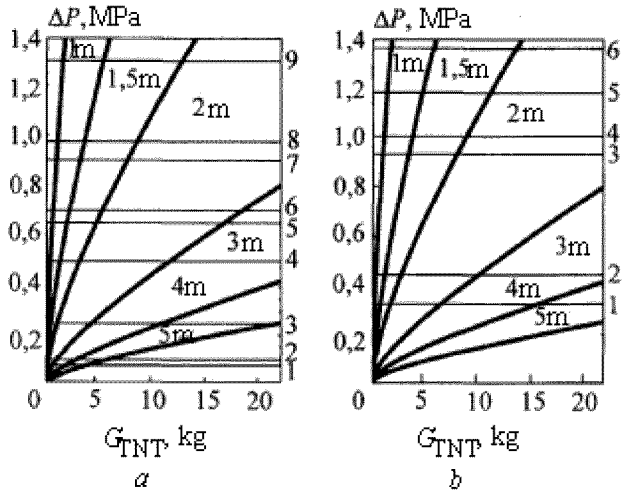

Fig. 5.21. Nomogramm for definition of the damage level of bioobject: unprotected (a) and protected (b) by special equipment, depending on distance and weight of HE charge. Horizontal lines: 1 — lower threshold of eardrums damage; 2 — 50 % of eardrums damage; 3 — lower threshold of lungs damage; 4-50 % of lungs damage; 5-99 % of survival; 6-90 % of survival; 7 — 50 % of survival; 8 — 10 % of survival; 9-1 % of survival

The soft protective clothes are inefficient for counteraction to the blast loading. Moreover, there are direct indications to the amplification of the blast loadings by tight compressed materials that is harmful for the state of gas-filled organs of the human body [5.12,5.14].

The references to chapter 5

5.1. Gelfand B.E., Gubin C.A., Kogarko C.M. et.al. Study of features pressure waves propagation and reflection in porous media// ZhPMTF, 1975, N 6, p.74- 77 *(in Russian)*.

5.2. Gvozdeva L.G., Faresov Yu.M. On the interaction of the shock wave with the wall covered by porous compressed material // ZhTF Letters, 1984, v. 10, rel 19, p. 1153-1156.

5.3. Gvozdeva L.G., Faresov Yu.M., Fokeev V.P. Interaction of shock waves with porous compressed materials // ZhPMTF, 1985, N 3, p. 111 - 115*(in Russian)*.

5.4. Gelfand B.E., Gubanov A.B., Timofeev E.I. Interaction of air shock waves with the porous screen // Izvesija USSR Ac.Sci., MZhG, 1983, N 4, p. 54 - 79*(in Russian)*.

5.5. Gvozdeva L.G., Faresov Yu.M. On the calculation of parameters of stationary shock waves in porous compressed media // ZhTF, 1985, v. 55, rel. 4, p. 773 - 775*(in Russian)*.

5.6. Demchuk A.F. One method of calculation of explosive chambers // ZhPMTF, 1965, N 5, p. 47 - 50*(in Russian)*.

5.7. Afanasenko S.I., Nesterenko V.F., Application of the condensed porous materials for the maximal stress reduction in walls of spherical explosive chambers // VII Int. Symp. on the use of the energy of explosion. CzSSR, Pardubice, October 1988, p. 508 - 512*(in Russian)*.

5.8. Afanasenko S.I., Nesterenko V.F., Application of porous screens and fillers for the increase of the weight of HE charge to be exploded in the chamber // Preprint IGD SB USSR Ac.Sci, 1990 *(in Russian)*.

5.9. Afanasenko S.I., Nesterenko V.F., Cheskidov P.A., Grigor'ev G.S., Ivanovsky B.E., Numerical optimization of protective stratified screens on the basis of metal and porous media // Preprint IGD SB USSR Ac.Sci, 1990 *(in Russian)*.

5.10. Raspet R., Batler P.B., Yahani F. The reduction or blast overpressures from aqueous foam in a rigid confinement // Appl. Acoustics, 1987, v.22, N 1, p. 35 - 45.

5.11. Macris A., Frost D.L., Nernberg J., Lee J.H.S. Attenuation of blast wave with a cellular material. Proc. 20-th Symp. (International) on shock waves (Ed. Sturtevant B., Shepherd J.E., Hornung H.) World Scientific, 1995, v. 2, p. 1375 - 1380.

5.12. Silnikov M.V., Khimichev V.A., The methods of individual armour protection. A series « Special technique for MVD». The manual. St.P. University MVD Russian Federation. — Fund «University», 2000,480 p. *(in Russian)*.

5.13. Destruction of objects of various scales by explosion (ed. by Ivanov, A.G.). RFNC-VNIIEF, Sarov, 2001,482 p. *(in Russian)*.

5.14. Turin M.V., Jarmyshko I.I., The estimation of armour jackets effect on heaviness of a blast trauma by the air shock wave // Works by Third All-Russia scientific - practical conferences « Urgent problems of protection and safety ». — St.Pb. — 2000, — v. 2 -p. 171 *(in Russian)*

5.15. Kleine H., Markis A. Development of blast protection equipment. Proc » Symp. On shock waves, Japan-2000, Tokyo University, 2000, p. 661 - 674.

CHAPTER 6. EFFECTS OF SHOCK WAVES SUPPRESSION BY TWO-PHASE MEDIA

When choosing the methods of influence on the parameters of blast waves, it is pertinently to use as the basic ones the information on the features of the waves propagation after the detonation of the concentrated HE charges. First of all, let's make some assumptions and remarks.

As the energy transmitted from the gas phase into the liquid phase, practically does not cause the pressure increase and, thus, cannot maintain the shock wave propagation, it is necessary to expect essential increase of the effect of the absorption of the shock wave energy by two-phase medium when explosive source is placed into it.

The experiments show, that at the detonation of HE charges placed directly in two-phase medium or at the formation of short perturbations in such medium by other sources, the intensity of wave disturbances is considerably reduced in comparison with the case of the detonation of HE charge placed in continuous medium. Depending on the volumetric contents of bubbles in the liquid the blast waves attenuation can be in 10... 50 times effective in comparison with a pure liquid at volumetric concentration of a gas within the limits of 1 % < α < 50 %. The difference of the considered scheme for the blast waves parameters decreasing from the scheme used earlier is, that the source of a wave is located directly in the two-phase mixture and the products of explosion or compressed gas at expansion contact to the two-phase medium without intermediate layers of continuous medium.

6.1. Relationship of the blast waves parameters and initial conditions of an environment.

The representation of the dependences of the basic parameters of spherical blast waves on the basis of the theory of similarity with the application of dimensionless values

$$\overline{P} = P / P_0; \overline{\tau} = \frac{\tau c}{\left(E / P_0\right)^{0,33}}; \overline{I} = \frac{Ic}{\left(E / P_0^2\right)^{0,33}}; \overline{R} = \frac{R}{\left(E / P_0\right)^{0,33}}$$

permits to establish the influence of initial conditions of the medium (pressure P_0, temperature T_0 and sound speed c_0) at their arbitrary change. Let the parameters of explosion in medium with P_0, T_0, c_0 are known. It is necessary to understand the transformation of the intensity, the duration and the impulse of the wave for explosion in the medium with $P_{11} \neq P_0$, $T_{11} \neq T_0$, or $c_{11} \neq c_0$. The sound speed in the atmosphere is changed due to the fluctuations of the temperature and the humidity of the air. The relationship reflecting these effects (m/s) is known:

$$c_{11} = 340\left(T_0 / 273\right)^{0,5}\left(1 + 0,49\frac{P_v}{P_0}\right)$$

(6.1)

Here T_0, K is the temperature of the air, P_v is the water vapor pressure.

The initial pressure of an environment varies depending on the height above the sea level. Let's consider the basic consequences from the theory of similarity. The adjustment for the SW overpressure will be a multiplier P_{11}/P_0, i.e. $P_{21}/P_1 \approx (P_{11}/P_0)^{0,33}$. At the assumption, that the pressure in the explosion products is much greater than the pressure in the environment, the explosion at higher initial pressure will produce the blast wave with the parameters increased proportionally to the initial pressure. The value of the dynamic head behind the wave also increases in the same proportion.

More complicated is the adjustment multiplier for the pressure impulse in the passing or reflected wave:

$$\frac{I_{11}}{I_0} = \left(\frac{P_{11}}{P_0}\right)^{0,66}\left(\frac{c_0}{c_{11}}\right)$$

It is possible to see, that the impulse increases with pressure, but decreases in inverse proportion to the sound speed in environment.

Let's proceed to the relationships for adjustment multipliers for values describing the time of wave arrival, duration of compression and rarefaction phases. It appears, that in the environment with the initial speed of the sound c_{11}, and the pressure P_{11}, all time intervals change in a proportion:

$$\frac{\tau_{11}}{\tau_0} = \left(\frac{P_0}{P_{11}}\right)^{0,33}\left(\frac{c_0}{c_{11}}\right)$$

Together with the pressure rise, not only the time intervals of the shock-wave process are shortened, but also the spatial scales of system change, where the impulse

moving are essential. It is caused by the change of the characteristic length of explosion R_0, which in spherical case is

$$R_0 = \left(\frac{E}{P_0}\right)^{0,33}$$

Note, that the theory of similarity does not give the information on the dependence of the overpressure at the blast wave front on the relationship of the sound speeds in the explosion products c_4 and in the environment exposed to the shock compression c_0 and on the pressure in explosion products P_4. Actually such relationship exists and in the first approximation can be represented by the basic expression from the theory of shock tubes for the pressure P_2 at the front of the blast wave:

$$\frac{P_4}{P_0} = f\left(\frac{P_2}{P_0}; \frac{c_4}{c_0}; \frac{\gamma_4}{\gamma_0}\right)$$

(6.2)

Here: γ_4 is the specific heats ratio in explosion products; γ_0 is the specific heats ratio in the surroundings.

At $P_4 >> P_0$ the following approximation is valid

$$\left[(\gamma_4 - 1)c_0 c_4^{-1}\left(P_2 P_0^{-1} - 1\right)\right]^2 = 2\gamma_0\left[2\gamma_0 + (\gamma_0 + 1)\left(P_2 P_0^{-1} - 1\right)\right]$$

(6.3)

It is seen, that any event promoting the increase of the sound speed in the explosion products or the reduction of the sound speed in the environment, should be completed by some amplification of the blast explosive wave.

6.2. Change of blast loadings parameters by two-phase medium

On the basis of the above-mentioned information on the blast waves parameters in air together with the hypothesis about an opportunity of the two-phase systems

representation as an equivalent gas with corrected thermo-physical properties, we shall describe some important ways of regulation of the blast waves parameters. We present the expected ways of the blast loadings regulation accompanying the carrying of the explosion source from the continuous to the two-phase medium [6.1,6.3,6.4,6.48... 6.50].

Basing on the concept of equivalent gas, we shall write the known expressions [6.36,6.37] for the speed of the blast wave from the strong spherical explosion as

$$D = \left[\frac{E}{\omega^* (\rho + \sigma)} \right]^{0,2} t^{-0,4}$$

(6.4)

Here ω^* is the energetic parameter [6.38, 6.39], ρ is the gas density, σ is the concentration of particles of continuous medium, t is the time.

For the constant energy of explosion in the same moment of time the speed of the blast wave in two-phase medium D^* and in a gas D are related as:

$$\frac{D^*}{D} = \left[\frac{\omega\rho}{\omega^* \rho_\Sigma} \right]^{0,2} \cong \left[\frac{1+\Gamma}{(1+\gamma)(1+\eta)(1+\gamma\eta\delta)} \right]^{0,2}$$

(6.5)

Here δ is the ratio of the specific heats for the continuous medium and the gas, $\eta=\sigma/\rho$ is the loading parameter (the ratio of the mass of continuous medium to the mass of a gas), $\Gamma=(1+\eta\delta)/(1+\gamma\eta\delta)$. With the velocity of the BW the distance passed by the wave also changes. If the distance passed by the blast wave in a gas is R_{S1} then the distance passed by the blast wave in two -phase mixture R_S^* will be defined as:

$$\frac{R_S^*}{R_{S1}} = \left[\frac{1+\Gamma}{(1+\gamma)(1+\eta)(1+\gamma\eta\delta)} \right]^{0,2}$$

(6.6)

The velocity of the blast wave at the distance R for the strong explosion is

$$D = \left[\frac{E}{\omega^* (\rho + \sigma)} \right]^{0,5} R^{-1,5}$$

(6.7)

At the same distance from the center of explosion the blast wave velocity in two-phase mixture D^* is lower than it's velocity in a gas D:

$$\frac{D^*}{D} = \left[\frac{1+\Gamma}{(1+\gamma)(1+\eta)(1+\gamma\eta\delta)} \right]^{0,5}$$

(6.8)

If the temperature of the particles is constant then

$$D^*/D \approx (1+\eta)^{-0,5}$$

(6.9)

It is seen, that due to the heating of the particles (at $\gamma\delta > 1$) the effective wave attenuation is realized. The inertia of the medium is characterized by the value η and the ability to extract the heat from a gas - by the value $\gamma\delta$. For the large kinematics inertia ($\eta >> 1$) and high ability to the fast heating ($\gamma\eta\delta >> 1$) we have

$$D^*/D \approx (\eta^2 \gamma\delta)^{-0,5}.$$

The reduction of the blast wave speed in water-air foams marked in the experiments (fig.6.1) have appeared closer to the case of isothermal particles, rather than to an equilibrium case. When the wave generated by the strong explosion propagates in two-phase medium, the mass of the substance involved into the movement increases. In the

same moment of time after the explosion the mass of two-phase medium m^* exceeds the mass of the gas m:

$$\frac{m^*}{m} = (1+\eta)^{0,4}\left[\frac{(1+\gamma)(1+\gamma\eta\delta)}{1+\Gamma}\right]^{0,6}$$

(6.10)

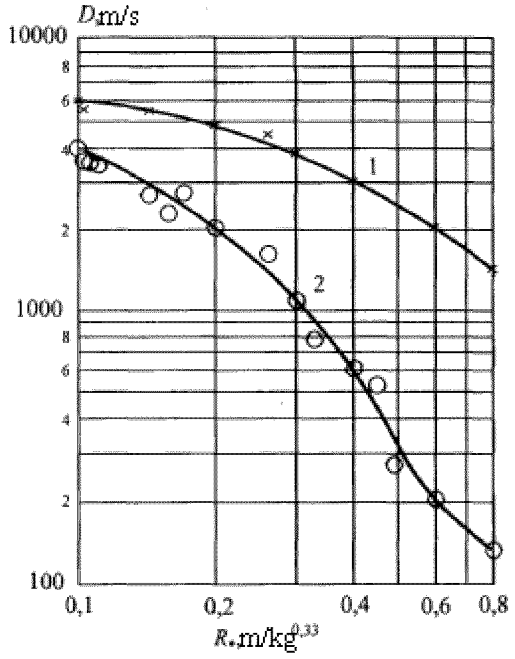

Fig. 6.1 Dependence of the SW speed on the relative (by the weight of the charge) distance for air (1) and foam (2) by [6.48... 6.50]

The difference in the masses and the propagation speeds of the substance at the explosion in two-phase medium and in a gas leads to the change of the explosion pressure at the same distance. For the case of complete equilibrium the explosion pressure in two-phase medium will be P_1*, and in a gas P_1 that gives:

$$P_1^*/P_1 \approx (1+\eta\gamma\delta)^{-1} \quad (6.11)$$

i.e. at $R/R_0 \geq 14$ it is possible to note the decrease of overpressure in a wave, as shown in the fig. 6.2.

The ratio of impulses of pressure in blast waves in foam I^* and in a gas I is

$$\frac{I^*}{I} = \left[\frac{(1+\Gamma)(1+\eta)}{(1+\gamma)(1+\gamma\eta\delta)} \right]^{0,5} \quad (6.12)$$

In two-phase medium with the frozen temperature of the particles, for example at $\delta = 0$, the impulse in the wave exceeds the impulse in the wave propagating in the gas. At strong explosion in two-phase medium there are the zones, where $I^*/I<1$ and $I^*/I > 1$. The first situation is more probable far from the charge, and second one - nearby the charge.

Not only in the strong explosion case the placing of the pressure waves source into two-phase medium will result in the decreasing of demolition action. The same effects will take place in the case of placing the high-pressure vessel in a dusty system.

The filling of the high-pressure vessel by two-phase mixture will result in reduction of the part of the energy transferred to the shock wave at explosion products expansion.

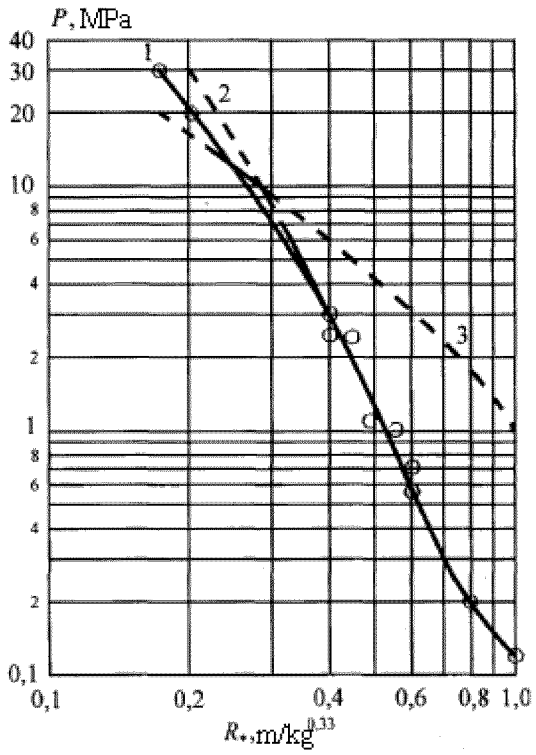

Fig. 6.2. Change of pressure with distance for foam (1, 2) and air (3) by [6.48... 6.50]

The effective suppression of shock waves also can be reached at detonation of HE charges in the tubes filled by the water-air foam or by the liquid with suspended gas bubbles. As shown in [6.1... 6.4,6.50], the physical model for the description of the blast waves attenuation process in the foamy structured medium can be offered.

According to the model [6.1...6.4, 6.50] there is an opportunity of the approached representation of two-phase medium as a gas with an effective parameter of the adiabatic coefficient Γ. Within the framework of such model the change of the shock waves parameters in two-phase medium can be investigated at their propagation into the direction of the acoustic resistance decrease. The cases of transition of the pressure wave from a continuous liquid in gas-liquid medium, from gas-liquid bubbly or foamy structure into the air [6.6, 6.16, 6.17, 6.22, 6.26] are considered. It was shown, that at these transitions the intensity of the shock wave decreases in 4... 6 times at the volumetric contents of the gas in the liquid about 5 %.

The reduction of explosive loadings practically does not depend on the amplitude of the incident wave. For the gas-liquid systems of bubbly structure it was found, that the attenuation of the shock waves, transmitted from a liquid to a gas-liquid medium, is effective at the contents of a gas in a liquid (by volume) $\alpha = 2... 4$ %. The processes of the waves attenuation at crossing interphase boundary into direction of the acoustic resistance decrease can be described on a basis of a simple hydrodynamic model [6.51].

The practical importance of studying the change of the pressure waves parameters at transition through the interphase boundaries is, that it is possible to create a simple calculation model of the interaction of the pressure waves with bubbly screens in a liquid. Such model is constructed for the cases of normal and oblique incidence on a filter. It was shown that bubbly screens become ineffective for the attenuating of extended waves (for which the medium trends to be continuous by compressibility). The efficiency of the screens is reduced with the increase of the initial pressure in the medium. The larger efficiency of the shock waves attenuation was obtained at their oblique incidence on the screen. Direct experiments showed, that the greatest efficiency of the oblique screen is achieved if the screen has a convexity directed towards to the movement of a wave. One more practically important result is marked in the experiments: the bubbly screen placed directly nearby a rigid wall, is not equivalent by efficiency (i.e. does not result in the decrease of the wave amplitude) to the non-contact screen. The efficiency of the screen rises with its removal from a rigid wall.

6.3. Regulation of the blast waves parameters at the charges detonation in various media.

The calculated and experimental data on the intensity of blast waves generated by HE charges in homogeneous and heterogeneous media, allow to specify a range of expected overpressures at the transition from one medium to another [6.72]. The overpressures at the shock waves front from the HE charge (TNT) detonation in dense soil with the minimal number of gaseous inclusions (line 1) [6.76], in the gasless water (line 2) [6.81], and in the air (line 3) [6.39] are indicated in the summary diagram (fig. 6.3). All

lines are plotted for the initial pressure P_0=0,1 MPa. The addition of the gaseous gaps ($\alpha \leq$ 10% vol.) leads to the sharp decrease of the blast waves amplitude.

The shaded area of the overpressures (4) shows, that the level of the pressure can be lowered more than in 10 times when replacing of a dense ground by the porous filler. Transition from a continuous liquid to the system gas bubbles + liquid also results in the decrease of ΔP to a level typical for the pure gas (it is observed at the bubbles volume fraction $\alpha > 1$ %). The greater inclination of the dependences $\Delta P = \Delta P\ (R_*)$ in the gas bubbles + liquid system (also getting in the shaded zone (4)) testifies to the amplification of the dissipation processes.

However, the dependence $\Delta P = \Delta P\ (R_*)$ for a gas (line 3) is not limiting. The smaller overpressures ΔP can be obtained at HE detonation in fine water foam with the concentration of the liquid σ = (5...50) kg/m^3 (area 5). Let's pay attention to a number of specific features. The comparison of the dependence $\Delta P = \Delta P\ (R_*)$ for the air explosion (3) and the explosion in a porous ground (4) shows, that at R_* = 4... 6 m/kg^{0,33} (R/R_0 = 70... 100) the amplitudes of quasi-acoustic pressure perturbations in the air and in the porous ground are almost identical. At R/R_0 = 150... 200 the amplitudes of quasi-acoustic pressure perturbations in the air are higher, than in the porous ground. The final time required for completing the relaxation processes in two-phase medium, means, that in a direct vicinity of HE charge the impulse, as well as the overpressure in two-phase medium is higher, than in a gas.

In the summary diagram the band of experimental values ΔP at the explosion in the foam is complemented by the calculated dependence (dashed line) $\Delta P = \Delta P\ (R_*)$ (taken from [6. 17]) for the water foam with the density σ = 3...6 kg/m^3 in the far zone of the explosion at $R/R_0 > 15$. The inclination of $\Delta P = \Delta P\ (R_*)$ for the explosion in the foam and in the air at $R/R_0 > 150$ is approximately the same, i.e. the achieved level of the reduction of the blast wave amplitude is kept constant and is close to the limiting achievable one. The obtained feature of the blast waves attenuation in the foam and in the air specifies the relationship between the achievable level of attenuation and the ratio of the sizes of HE charge R_0 and the foamy envelope R_f. This relationship can be written as follows

$$\psi^* = 20\lg\frac{\Delta P_1}{\Delta P_2} = 0,366\left(\frac{R_f}{R_0}\right) - 0,19$$

This dependence is valid for the envelopes with the sizes $10 \le R_f/R_0 \le 26$ at any distance from HE charge.

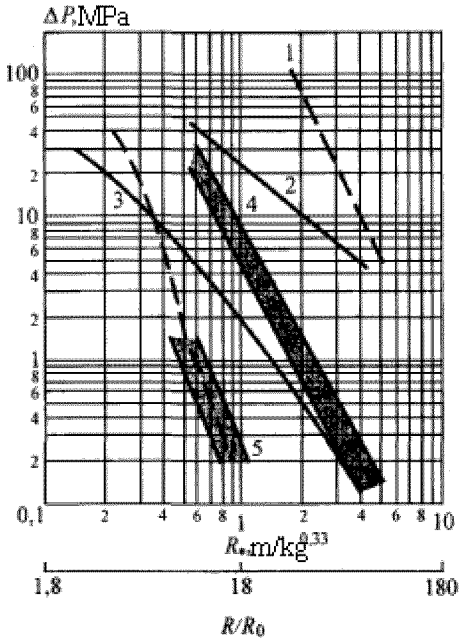

Fig. 6.3. The summary diagram of dependence of blast wave overpressure for various media environments: 1 - dense ground; 2 -gasless water; 3 — air; 4 — porous ground; 5 — water-air foam (water-mechanical foam)

The value of ψ^* in dB does not depend on the distance from the center of explosion in a range $180 \le R/R_0 \le 1800$ or 8... $10 < R_* < 10^3$ m/kg^{0,33}. The intersection of the line 3 with the area 4 for the bulk systems shows, that at the distances from the center of explosion $R/R_0 > 150$ the levels of blast loading can be diminished not only by placing the HE charge in a gas-liquid foamy envelope, but also in a protective envelope made from any granular or porous material. On the basis of generalization of the large amount of the experimental data B.I. Palamarchuk has derived the dependence [6.1]:

$\psi^* = (3z\text{-}4)\pm 2$ for $R/R_0 > 150$ (6.13)

Here $z = (\sigma V/G)^{0,33}$ or $z = (m/G)^{0,33}$;

V — Volume of a protective envelope;

G — Weight of HE charge;

m — mass of a protective envelope.

The given formula is suitable for the estimations of protective properties of envelopes made from the water foam, the snow pillow, protection made from the layers of the sand, the glass fiber, the metal wire. Let's emphasize, that $\psi^* > 0$ at $z > 4/3$, i.e. at $m/G > 2{,}4$. We present some information from [6.1, 6.3, 6.4, 6.16, 6.39... 6.41, 6.48] about the parameters of the blast waves in the foam envelope itself, i.e. in the near zone of explosion. The dependence of the relative impulse of the reflected blat wave on relative distance in the air (1) and in the foam (2) is represented in the fig. 6.4. The impulse of the reflected wave in the foam at $R < 0{,}64$ m/kg^{0,33} is more, and at $R > 0{,}64$ m/kg^{0,33} is less, than in the air.

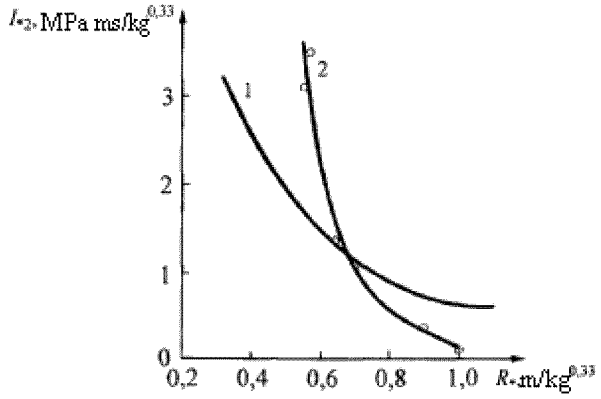

Fig. 6.4. Dependence of the scaled impulse of the reflected wave on relative distance: 1- air; 2 - foams at $\sigma = 5$ kg/m^3

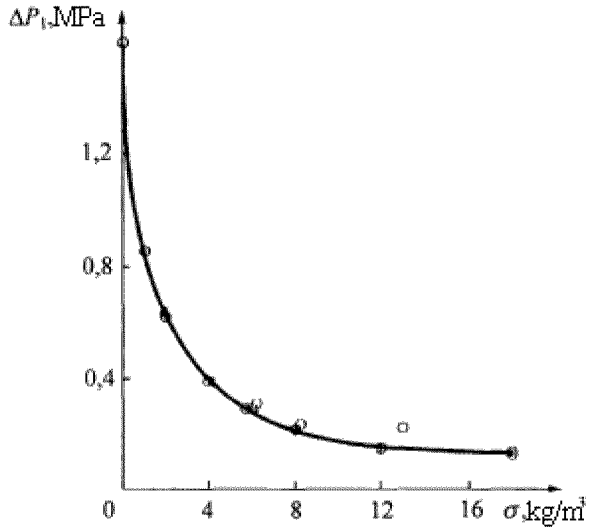

Fig. 6.5. Dependence of the blast wave overpressure on the concentration of the liquid at $R_* = 0,85$ *m/kg*^{0,33}

For determining the influence of mass concentration of the liquid on the blast waves parameters in the foams the experiments with RDX charges [6.40] were carried out. The dependence of the blast wave overpressure on the mass concentration of the liquid is presented in the fig. 6.5 at $R_* = 0,85$ m/kg^{0,33}. As it is seen, the absolute value of the overpressure at the front of the blast wave in the foam is very sensitive to the concentration of the liquid up to $\sigma = 4\ldots5$ kg/m^3. Only slow reduce of the overpressure is marked with the further increase of the foam density.

The relative decrease of the blast wave overpressure in the air and in the foam at the different scaled distances is shown in the fig. 6.6. The relationship between the attenuating factors for the blast wave in foam with the concentration of the liquid inside foamy layer can be approximated by the linear dependence:

$$\frac{\Delta P_{1air}}{\Delta P_{1foam}} = 1 + 0,75\sigma \qquad (6.14)$$

The formula (6.14) is valid at 2 kg/m^3 < σ < 20 kg/m^3, 0,8 m/kg^{0,33} < R_* < 2,5 m/kg^{0,33}. The attenuation by ΔP and I will occur at $R_* \geq 1$ m/kg^{0,33}. It means, that for a charge of mass G = 1 kg a foam layer of radius R = 1 m is required.

All above conclusions are confirmed by the calculations and the experiments in [6.17]. The scheme of HE charge placement represented in the fig. 6.7 was studied: spherical HE charge (TNT) 1 was surrounded by the spherical foamy envelope 2.

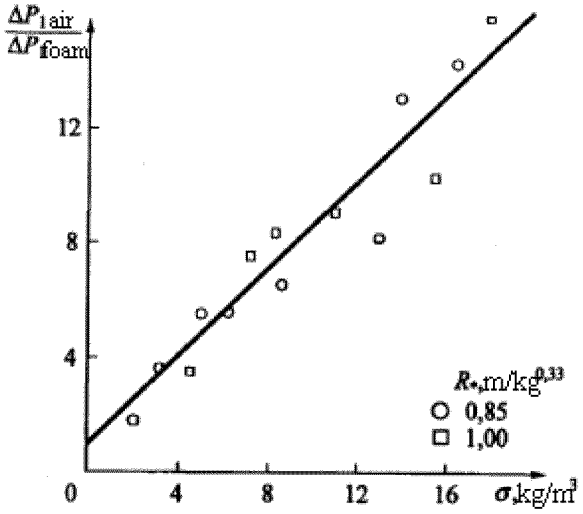

Fig. 6.6. Dependence of the attenuating factor for the blast wave in the foam on the concentration of the liquid at different distances from the center of explosion

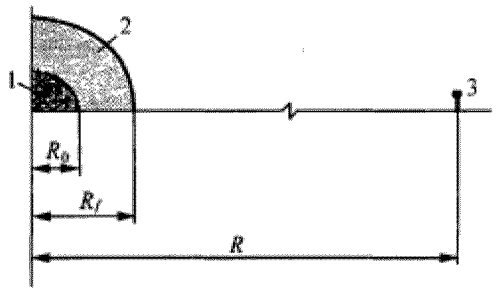

Fig. 6.7. The scheme of a configuration explosive substance — gas-filled envelope: 1 — HE charge; 2 — water foam; 3 — microphone

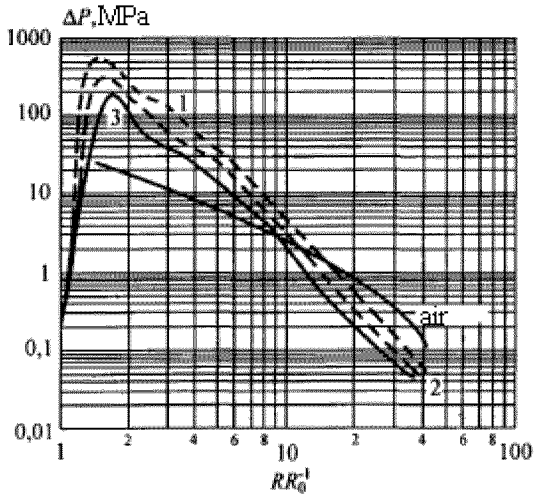

Fig. 6.8. Dependence of overpressure in a blast wave on the distance for air and foams with various multifold: 1 α= 60; 2 α= 200; 3 α= 360

Radius of the charge $R = R_0$, radius of the foamy envelope R_f. Parameters of the shock waves were calculated for $R_f/R_0 = 40$ at the foam multifold α= 60, 200, and 360 (that corresponds to the concentration of water σ = 16,6; 5 and 2,78 kg/m^3 accordingly). The results of calculations are presented in the fig. 6.8. At $R/R_0 < 10$ the shock wave pressure in the foam exceeds the shock wave pressure in the gas. However at $R/R_0 > 10$ the effective decrease of the overpressure is achieved, which increases with σ changing from 2,78 kg/m^3 up to 16,6 kg/m^3.

In the fig. 6.9 the HE charge is separated from the air by a water layer 2. Water is kept in a thin aluminum envelope (3). In [6.55] the calculations of air shock wave amplitude were performed for the detonation of spherical TNT charge of 0,45 kg and the radius R_0 = 4 cm.

The variants are investigated, when the aluminum envelope contacts the surface of HE charge or is separated from it by a water layer with the radii R_w/R_0 equal to 1,5; 2; 3; and 4 accordingly. Thus the ratio of the mass of the water m_w to the mass of the charge G

was m_w/G = 2,1; 5; 16,8; and 40 accordingly. The results of the comparison are presented in the fig. 6.10 in coordinates wave amplitude— relative distance.

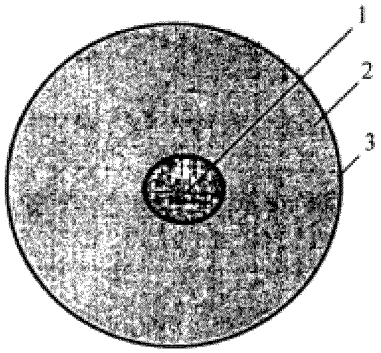

Fig. 6.9. The scheme of a charge placement in the water and in the envelope by [6.55]: 1 — HE charge; 2 — water; 3 — envelope

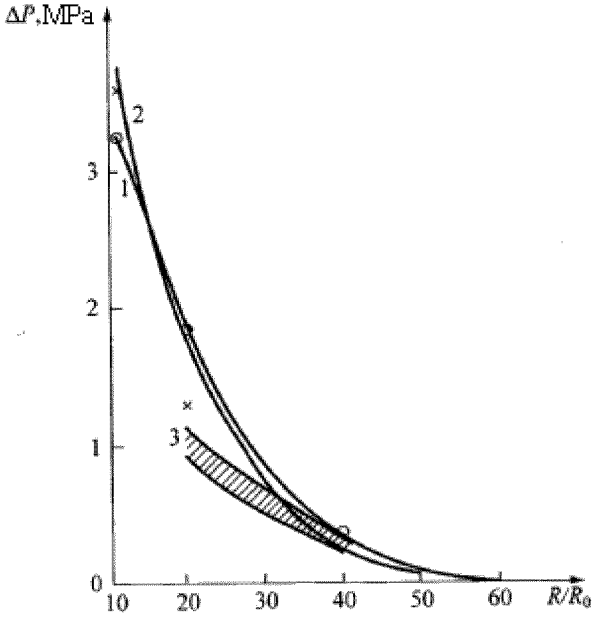

Fig. 6.10. Dependence of overpressure on distance by [6.55]: 1 – in air; 2 – in thin aluminum envelope; 3 – in water + A1 envelope

As the scale for the comparison the radius of a charge R_0 = 4 cm is taken. The line 1 is obtained at HE charges detonation without an envelope in the air. The line 2 corresponds to the calculation of $\Delta P = f(R/R_0)$ at HE charges detonation in a thin aluminum envelope. The differences in the dependences 1 and 2 can be not considered in view of the

measurement errors and accepted assumptions. The band of the values 3 corresponds to the detonation of a charge, immersed into the water. The bottom boundary of the area 3 corresponds to the case $m_w/G = 40$, and the top boundary is responsible for the case $m_w/G = 2$. At the distance $R/R_0 = 40... 50$, i.e. at the distance 160... 200 cm, the distinction of all considered variants is negligible, i.e. the effect of attenuation of loading by the amplitude of a pressure wave is insignificant. Thus, the scheme of a charge placement, shown in the fig. 6.9, does not represent practical interest for the reduction of the blast loadings at HE detonation in the air.

6.4. Attenuation of weak shock waves generated at the detonation of HE charges, placed in gas-contained envelopes

From the ecological safety point of view [6.1,6.3] even the weak quasi-acoustic shock waves are the physical pollution of an environment [6.2,6.5]. In this connection the problem of creation of reliable and effective ways of SW attenuation [6.1, 6.2,6.3, 6.7] is urgent.

As shown in research works of the Institute of Electric Welding IEW (Ukraine), at the welding and the cutting by the explosion in industrial conditions (and also near to inhabited buildings and structures) the methods of protection on the basis of multiphase media [6.4,6.40... 6.42] can be successively applied with the purpose of the ecological safety maintenance. Thus for the solution of a lot of practical tasks it is important to know not only the law of SW attenuation in two-phase mixture, but also the behavior of SW being weakened in the protective screens after their exit into the environment. Of interest is how the protective envelopes made from the gas-filled material decrease the SW overpressure, the impulse and the flow of energy [6.5,6.6,6.17, 6.25, 6.26,6.27,6.29... 6.35].

Let's present the results of experimental studies in IEW, during which the laws of weak SW attenuation were determined at detonation of superimposed HE condensed charges. Also studied are the effects of gas-filled envelopes on the SW parameters. Water-mechanical foam and the snow also were used as protective tools [6.40... 6.42].

The efficiency of SW parameters reduction was determined from the comparison of the parameters of the blast waves generated at detonation of superimposed HE condensed charges and at detonation of HE charges in protective envelopes made from gas-contained materials. The SW parameters were measured with the help of the impulse noise-meters and the pressure gauges having resonant frequency 200 kHz, with the subsequent record on the registration system. Use of the specified methods of measurement has allowed expanding the frequency and the dynamic range of the registered overpressure and to receive the information on SW structure, transmitted through a protective screen [6.4,6.6,6.7,6.25... 6.27].

The experimental dependences from [6.40] for the SW overpressure and the scaled impulse of the compression phase on the scaled distance $R_*=R/G^{0,33}$ are presented in the fig. 6.11 for the detonation of HE charges with the mass from 20 g up to 100 kg, where G is the TNT equivalent of a charge expressed in kg. The relationship between the overpressure at the front of SW and the scaled distance R_* has a form

$$\Delta P=AR_*^m \qquad (6.15)$$

Where A and m are the constants dependent on the properties of a surface, on which there is an explosion; R_* — in m/kg^{0,33}, ΔP — in Pa.

At explosion of the superimposed (on a ground) charges on the sandy ground (A = 5,5·10^5, m = -1,6) the formula (6.15) gives rise to the ΔP values with an error 15... 20 %. For the SW of such intensity at the detonation of the freely suspended HE charges $m \approx$ -1,13 [6.4,6.5]. The effect of the increase of the parameter m at detonation of the superimposed charges is explained in [6.4,6.5] by the energy losses as a result of SW interaction with the surface. Indirect confirmation of this conclusion was obtained in [6.4, 6.5], namely the influence of surface properties on the rate of SW attenuation. So, at rather large distances from the charge (R> 150R_0) the presence of a snow-cover results in the increase of m.

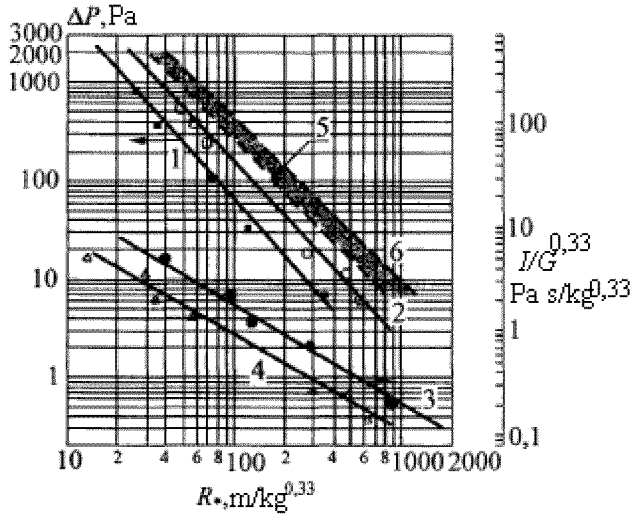

Fig. 6.11. Dependence of the parameters of the quasi-acoustic SW on the distance: 1 — peak pressure in SW after passage of snow-cover; 2 — the same with protection by multifold foam; 3 — impulse of a positive phase without protection; 4 — impulse in case of protective envelope made from multifold foam; 5 — peak pressure in SW at a snow surface; 6 – the same at a rigid ground [6.40]

The performed studies [6.40] have shown, that the SW, generated in the air after the passage through the protective environment, are similar to the waves generated by the detonation of HE charges with smaller energy. The typical records of the quasi-acoustic SW are shown in the fig. 6.12. As it is seen, the pressure waves profiles slightly differ from each other, and the difference between their macroparameters is no more than 10... 15 %. So, the pressure impulse of a positive phase for an open charge is equal 2,8 Pa·s, ΔP = 1 kPa; for the protected charge I = 3,0 Pa·s, ΔP = 1 kPa.

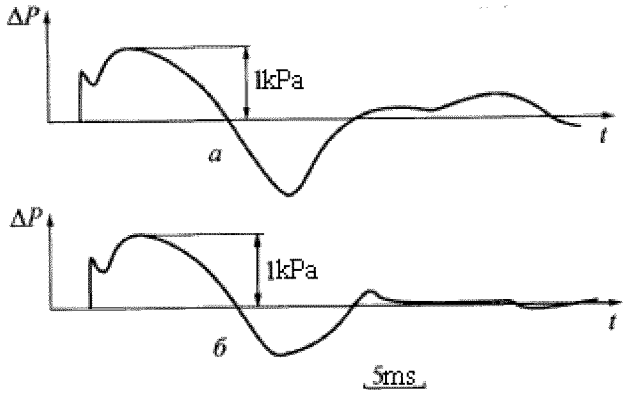

Fig. 6.12. Profiles of pressure for quasi-acoustic shock waves at the distance 30 m from RDX charges with mass 0,15 kg in air (a) and 1 kg - in protection from snow (b) by the data of measurements from [6.40]

Following conclusions of the Institute of Electric Welding [6.40, 6.42], the macroparameters of the SW generated by HE detonation in the gas-filled envelopes can be determined by TNT equivalent G^* of the explosion. The value of G^* is equal to the energy of the unprotected HE charge, at which detonation at the fixed distance from the place of explosion the parameters of SW coincide with the parameters of the blast wave generated by the charge in protective envelope. The efficiency of the protection in this case can be defined by the factor of reduction of the energy of explosion η:

$$G^* = \eta G \tag{6.16}$$

In the case presented in the fig. 6.12 η = 0,15 both for overpressure and impulse. One of the parameters determining the damping properties of gas-contained medium, used for the SW attenuation, is the mass concentration of the condensed phase σ. Changes of the wave duration were not revealed, as well as in [6.17].

At the fixed volume of protective envelope the efficiency of decreasing the SW parameters by multifold foams with σ = 1,5... 2 kg/m^3 has appeared small in comparison with of the snow or the foams with σ = 10... 20 kg/m^3.

For the SW parameter predicting it is necessary to know the relationship between the factor of attenuation and the properties of the medium used for localization of explosion, and geometrical sizes of protection screen. B.I. Palamarchuk analyzed the data [6.3,6.6] and established the criteria of SW attenuation at explosion in gas-contained environment using dimensionless parameter Z

$$Z=(\sigma V_S/G)^{0,33} \tag{6.17}$$

Where σ is the mass concentration of the condensed phase in protective medium, kg/m^3;

V_S is the volume of a protective medium, m^3;

G is the TNT equivalent of the explosion, kg TNT.

The dependence of value ΔL, describing the decrease of the overpressure at the front of SW, on dimensionless value Z is shown in the fig.6.13 for the case of protection based on gas-contained media. The shaded area corresponds to the discrepancy of experimental data for such media as foams and snow. The same area contains the data of experiments on the attenuation of SW, transmitted through protective envelope from the fiber glass, the metal cotton wool, the foams obtained in [6.6]. The dependence presented in fig. 6.13 can be described by the formula:

$$\Delta L = 3Z\text{-}4 = 20\lg(\Delta P_1/\Delta P_2), \tag{6.18}$$

Where ΔL is the difference between the level of sound pressure, dB, at the fixed distance from HE detonating charge without (ΔP_1) and with (ΔP_2) protection.

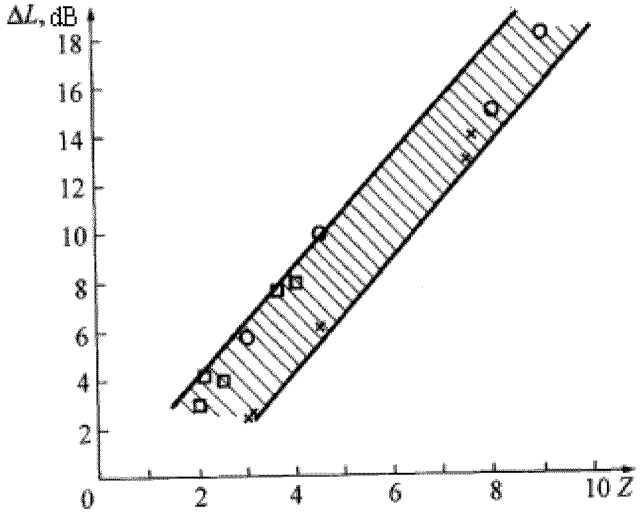

Fig. 6.13. Dependence of SW damping efficiency on the properties of protective envelope at σ, kg/m³: × - water foam (σ = 6... 10); o - snow (σ = 250... 500); □ - sand (σ = 1600)

To determine the factor of explosion energy decrease we rearrange the equations (6.16... 6.18) in the form:

$$\eta = G/G^* = 10^{0,15}\Delta L/m,\ m \approx 1. \qquad (6.19)$$

The presented formulas (6.18 and 6.19) enable to estimate the efficiency of explosion localization by gas-contained media and to optimize the parameters of protection of technological metal processing by the explosion. For the practical applications of interest is to describe the experimental setup in [6.6]. The fig. 6.14 represents the container, in which the detonations of TNT charges were made (the masses of charges were 0,11 kg, 0,57 kg and 2,27 kg).

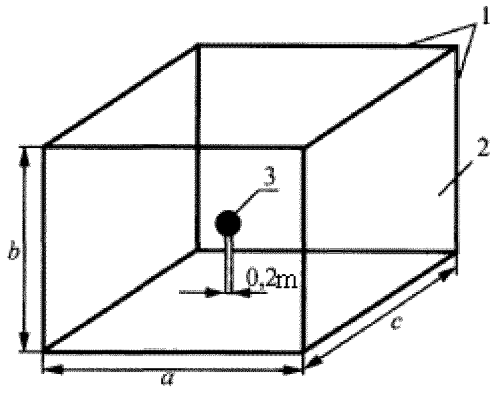

Fig. 6.14. The scheme of experiment for determination of blast waves attenuation efficiency by foam: 1 - wooden frame; 2 - polyethylene film; 3 - HE; $a \approx b \approx c \approx$ (0,9... 1,2) m [6.6]

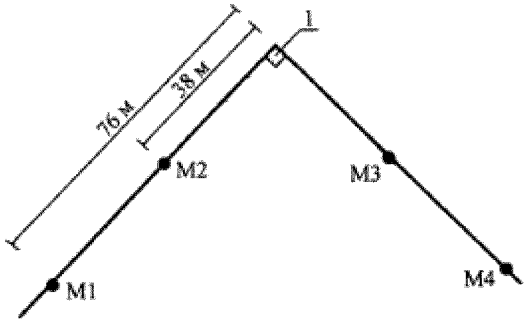

Fig. 6.15. The scheme of microphones positions in experiments [6.6]: 1 - container; M_1, M_2, M_3, M_4, - microphones

The HE charges were placed in the water foam or were buried by porous materials. The multifold of the foam was 30... 250, that corresponds to the concentration of two-phase medium, and equals accordingly σ = 10... 4 kg/m^3. The characteristics of other materials forming the two-phase medium are given in tab. 6.1. Two types of steel fabric, two types of gas balloons, two types of glass-wool, and straw were used. The experiments with the filling of the container by water-mechanical foam were done at the same setup. The measurements were performed by the scheme presented in the fig. 6.15, where the HE charge was in the polyethylene container, and M_1, M_2, M_3, M_4 are the pressure transducers (microphones).

The results of measurements are shown in the fig. 6.16. Here

$l=0,5(abc)^{0,33}=0,5V^{0,33}$,

a, b, and c are the linear sizes of the container, V is the volume of the container. Besides, $\rho_V = \sigma$ is the volumetric density of two-phase filler, so $\rho_V V$ is the mass of the condensed absorber in the container, G is the mass of HE charge.

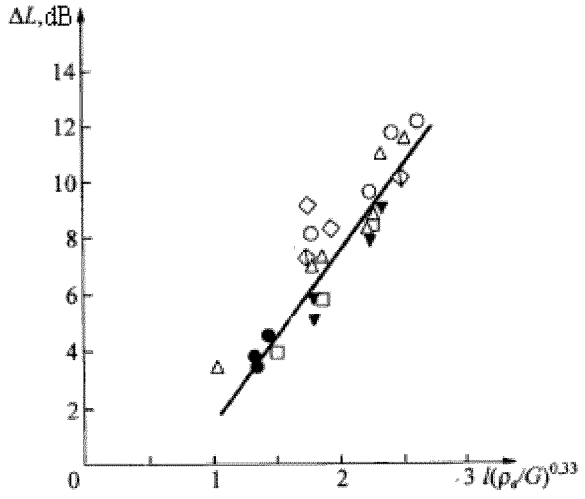

Fig. 6.16. Reduction of the sound pressure level at HE detonation in porous medium. ○ *- steel fabric (thin),* ▼ *- steel fabric (rough),* □ *- gas balloons (small),* ● *- gas balloons (large),* △ *- straw,* ◇ *- glass-wool (thin),* ◁▷ *glass-wool (thick)*

Table 6.1 Parameters of materials for explosion damping

Material	Diameter, μm	Density, kg/m^3	Thermal conductivity, W/m K	Specific heat capacity, J/kg K
Steel fabric, fine	150	7750	60	459
Steel fabric, rough	240	7750	60	459
Air balloons, small	14500	930	0,38	1430
Air balloons, large	29000	930	0,38	1430
Straw	50	43	0,039	1340
Glass-wool, fine	5	2500	0,036	961
Glass-wool, rough	10	2500	0,036	961

The comparison of the shock waves attenuation data at the charges placement in explosion-absorption gas - containing envelopes shows, that the envelopes made from the water-mechanical foam, the snow and other elementary materials have the largest efficiency. The application of the envelopes made from the materials with large structure density does not give rise to appreciable advantages in efficiency, but introduces the serious technical difficulties at realization. Basic difficulty is connected with the inconveniences of formation of a heavy explosion-protective envelope around the explosive object, (as a rule, it is the HE charge with detonator).

6.5. Basic directions of explosion protection

It is possible to distinguish two ways of the explosion protection methods. The first direction is caused by the obvious attempt of HE charge shielding with the help of a firm impenetrable envelope. It is enough to mention a trivial case of placing HE charge in the closed or half-closed container [6.28]. The practice showed the insufficient efficiency of this way of localization. For improvement of operational properties the internal cavity of the container was filled by compressible medium. In [6.58,6.59] the liquid foam was used as filler, in [6.60] — liquid with gas bubbles, in [6.6] — granular or fibrous material. Each of the listed explosion absorbers can be characterized by the effective density σ, differing from the density of the frame material ρ. Thus, for the water foam σ = 10... 30 kg/m^3 at ρ = 1000 kg/m^3, for the water with gas bubbles σ = 900. . 990 kg/m^3 and for the fiber and granular fillers σ > 1000 kg/m^3 at ρ > 2000 kg/m^3.

The second direction of the explosion protection is characterized by principal decision to refuse of application of an impenetrable firm environment around the charge. As limiting here it is possible to examine the variant of the blast wave suppression in the volume of the sprayed liquid (more often water) [6.62, 6.75]. However, the impossibility to obtain the spray with high concentration of a liquid σ> 1... 2 kg/m^3 makes this way of attenuation inapplicable.

To keep the concentration of explosion absorbing material guaranteeing reliable attenuation of the blast waves, the gas-contained covers made from water foam [6.58], polyurethane foam [6.64] were offered. For the water foam σ = 10... 20 kg/m^3, for the polyurethane foam σ = 50... 100 kg/m^3 at ρ = 900 kg/m^3.

The practice of the application of the gas-contained envelopes for localization of the demolition loadings for HE charges up to 3 kg showed, that the basic part of the explosion products energy corresponds to the kinematics acceleration of a mass of protective envelopes [6.66].

Also essential is the transformation of the energy flows at the boundaries: products of explosion — explosion absorption medium — air [6.65]. Quite ineffective were the attempts of explosive loadings regulation by the energy losses due to the processes of evaporation or dispersion of the protective envelope material [6.86... 6.88].

In view of a dominant role of inertial properties of the protective envelopes for the blast waves attenuation, an effective way of explosion suppression is the change of the kinematics characteristics of the medium, which damps the expansion of explosion products. The major characteristic is the compressibility of the medium, surrounding a charge. The reliable suppression of blast loadings is reached, when the protective environment is the liquid guaranteeing (at least at early stages of expansion) against the outflow of explosion products into the protecting atmosphere.

The measure of the compressibility of a liquid is the speed of sound. The regulation of the sound speed in the liquid can be achieved by the introduction of the gas bubbles [6.56,6.63]. The introduction of compressed inclusions in a liquid volume essentially influences the propagation of the blast waves of moderate intensity with the overpressure $P_1/P_0 \leq 1000$. For the waves with larger intensity the presence of compressible elements is not so essential. The immersing of HE charges into compressible two-phase medium repeatedly changes the characteristic temporary scales of all wave processes and expands the opportunities for an effective exchange of energy between explosion products and explosion protective envelope [6.48].

The listed circumstances have allowed offering the new scheme of explosion suppression. Fig. 6.17*a* presents such a scheme for HE charge with the help of a layer of liquid to be dispersed, placed in volume between elastic envelopes [6.61].

The layer of a liquid is separated from HE charge by gaseous gap. The arrangement of the basic elements is different from the traditional scheme [6.66], shown in the fig. 6.17 *b*. The basic role of gaseous gap consists in attenuation of the blast wave amplitude before its incidence with a liquid layer due to distinction of volumes of a charge and internal cavity of an envelope.

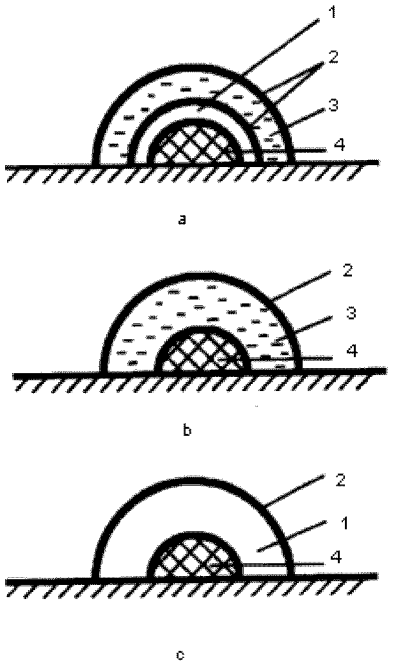

Fig. 6.17. The possible schemes of explosion suppression with the help of liquid elastic containers. 1- gas (gap), 2- envelope (plastic), 3- liquid to be dispersed, 4- HE.

On the basis of the known [6.66] and new experimental data it is possible to compare the efficiency of the air blast waves attenuation using the schemes shown in the fig. 6.17, *a*, *b*. The information on the blast waves attenuation with the help of a water layer around the HE charge, i.e. by the scheme in the fig. 6.17 *b*, was taken from [6.66]. The information on the blast waves attenuation by the scheme in the fig. 6.17 *a* was obtained in a series of experiments, similar to [6.57]. The mass ratio of the water M to the HE charge G was equal to 50, $G = 40$ g in [6.56] and $G = 100$ g in [6.57].

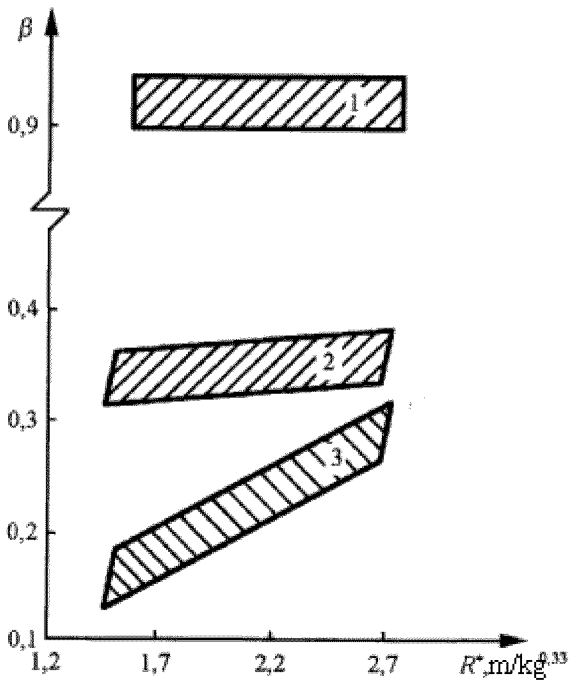

Fig. 6.18. Dependence of the attenuation factor for the blast wave by amplitude on the scaled distance for the various schemes HE detonation

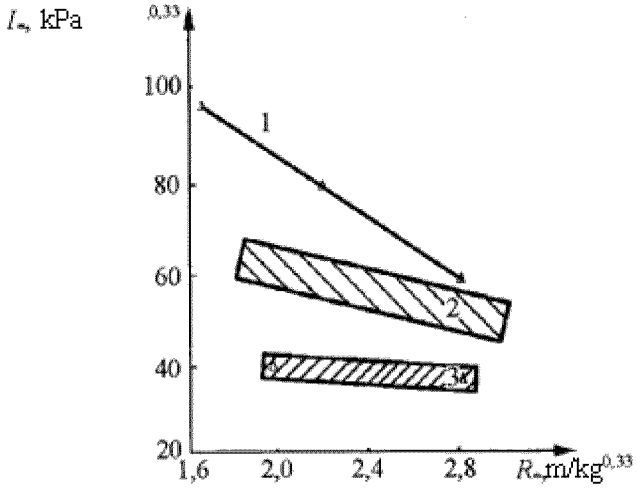

Fig. 6.19. Dependence of the pressure impulse in a phase of compression on the scaled distance for the various schemes of HE detonation

The change of blast wave attenuation factor β by amplitude is shown in the fig. 6.18 depending on the scaled distance $R_*=R/G^{0,33}$. Distance R was counted from the center of explosion up to the place of measurement. Factor of attenuation $\beta = \Delta P(R_*)/\Delta P_0(R_*)$, where $\Delta P(R_*)$ is the amplitude of the air wave at the explosion in the liquid envelope and $\Delta P_0(R_*)$ is the amplitude at the explosion in the gas-filled envelope of the same size by the scheme in the fig. 6.17 *c*. It was made because the value ΔP_0 (shaded strip 1 in the fig. 6.18) is 10... 20 % less, than $\Delta P_1(R_*)$ at a completely open charge.

The strip 2 in the fig. 6.18 is obtained for the explosion by the scheme in the fig. 6.17 *b*, and strip 3 is obtained for the explosion by the scheme in the fig. 6.17 *a*.

Fig. 6.19 demonstrates the change of the impulse I^* in the compression phase with the distance R_* at the detonation of HE charge in the gas-filled air envelope (line 1 by [6.66]). The strip 2 for I^* is obtained for the explosion by the scheme in the fig. 6.17 *b*, and strip 3 is obtained for the explosion by the scheme in the fig. 6.17 *a*.

The diagrams (fig. 6.18 and 6.19) confirm the highest efficiency of the scheme shown in the fig. 6.17 *a* for the reduction of demolition consequences of explosion.

The carried out studies are based on the rational use of the specific features of pressure and rarefaction waves propagation at HE detonation in a medium with elevated compressibility in comparison both with the liquid and the gas.

Essential difference of the suggested scheme of explosion suppression is the preliminary correction of initial conditions of expansion of explosion products with the help of a gas layer between the HE charge surface and the compressible medium.

6.6. Comparative characteristics of two ways of the air shock waves attenuation

Because of various types of blasting operations and the design of the explosion protection structures, there are many works published concerning the problem of decreasing the overpressure and impulse of the air shock waves.

As an example it is possible to list the cited above works on the theoretical and experimental study of the shock waves propagation in channels through the perforated screens, works on the suppression of the air shock waves at the spherical explosion of HE charges when placing the charges in the volume of the water-mechanical foam or in front of the perforated screens. Unfortunately, there are no reliable calculation models, capable to predict in advance the efficiency of particular method of the shock waves attenuation. Therefore when selecting the methods it is necessary to use the experimental data. A choice of the way suppression of air shock waves is difficult, because the developed methods and the approaches are not universal.

Moreover, the transferring of results from one area of parameters on another can result in serious mistakes and obtaining the negative result. Let's present some examples based on the measurement of the shock waves parameters at HE detonation in the water-mechanical foam. As it was already mentioned, the mass of HE charges (TNT) in experiments was varied from 0,01 up to 3 kg. The density of th water-mechanical foam was $\sigma \leq 10$ kg/m^3. The dependence of the factor of shock waves attenuation by pressure $\beta = \Delta P/\Delta P_0$ on the distance R/R_0 is shown in the fig. 6.20. Here ΔP_0 is the shock wave intensity in the air at the distance R, and ΔP_0 is the overpressure in the water-mechanical foam at the same distance, R_0 is the radius of HE charge. It is seen, that at $R/R_0 > 10$ $\Delta P > \Delta P_0$, but at $R/R_0 < 10$ $\Delta P > \Delta P_0$. Thus, the zone of real attenuation of the shock waves is at rather large distance from a charge. The dependence of the factor of attenuation on the overpressure at the SW front is shown in the fig. 6.21. As it is seen, only in the far zone of explosion the limiting attenuation of the shock waves is reached $\beta = 7...10$. The overpressures on the abscissa axis correspond to the detonation of HE charge in the air.

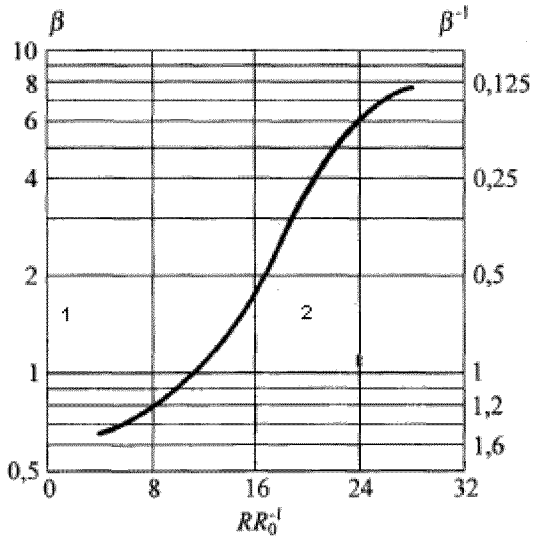

Fig. 6.20. Dependence of the factor of attenuation (amplification) by pressure on the scaled distance to the center of explosion (1- zone of amplification; 2 – zone of attenuation)

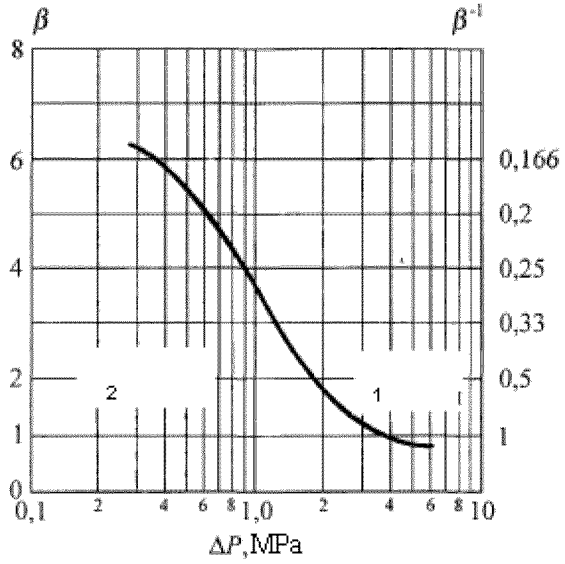

Fig. 6.21. Dependence of the factor of attenuation (amplification) by pressure on the overpressure in the front of a wave (1- zone of amplification; 2 – zone of attenuation)

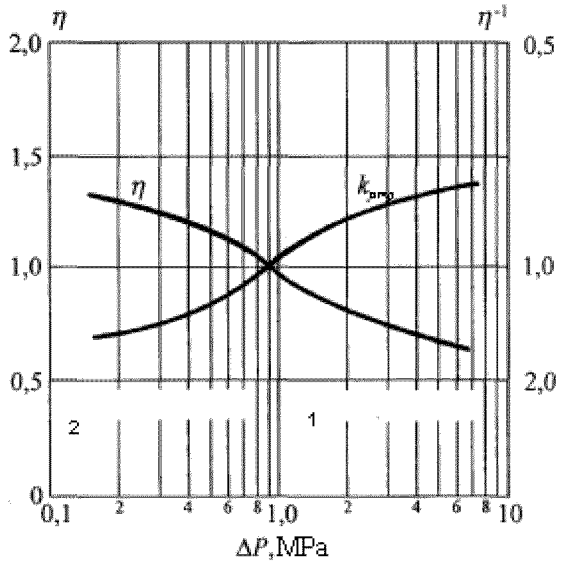

Fig. 6.22. Dependence of the factor of attenuation η (amplification k_{amp}) by impulse on the overpressure in the front of a wave (1- zone of amplification; 2 – zone of attenuation)

Though the information on the impulses of a compression phase in the air wave in porous medium is very limited, nevertheless, on the basis of some measurements it is possible as a first approximation to construct the dependence of the factor of attenuation by impulse η on the intensity of a shock wave. Such dependence is presented in the fig. 6.22. As it is seen, only at $\Delta P < 1$ MPa, i.e. at the distance from the charge $R/R_0 > 20$, the reduction of the impulse becomes appreciable. The reduction of the impulse in a pressure wave when the HE charge is immersed in the foam does not exceed the values η = 1,3... 1,5 at $R/R_0 < 20$, but will be increased with the distance.

According to [6.8,6.43... 6.47,6.52... 6.54] another effective way of the shock waves attenuation is the installation along the waves path of the perforated partitions of various types (which are described in [6.43... 6.47]). The generalization of the investigations on the shock waves propagation through the perforated partitions has allowed obtaining some empirical dependences. According to [6.8] the pressure in an air wave behind a partition is determined by the expression

$$\Delta P = 1{,}41 Z^{-1{,}66} (R^*)^{0{,}27} (\alpha_c)^{0{,}64} \quad \pm 20\ \%. \qquad (6.21)$$

Here $Z = R/G^{0,33}$, $R^* = R/L$, $\Delta P = P_1 - P_0$ in MPa, P_1 is the pressure at the wave front, G is the mass of a charge in kg, R is the distance in m, L is the characteristic size of the partition. The formula (6.21) is valid at $1{,}16 < Z < 8{,}45$ m/kg^{0,33}, $0{,}015 < \Delta P < 1$ MPa, $0{,}69 < R^* < 4{,}55$ and permeability of the partition $0{,}01 < \alpha_c = F_0/F < 0{,}13$. In the expression for α_c there are designations: F_0 - the total area of apertures, F – the area of cross-section of a protective partition. In [6.53] the expression for calculation the intensity of a weak wave, passed through the perforated screen is presented in a form $\Delta P \approx (\alpha_c)^{0,69}$. It is rather close to the conclusions from [6.51]. The change of the compression phase impulse can be determined by the equation for the estimation the impulse behind a barrier

$$I/G^{0,33} = 791 Z^{-0.98} \alpha_c^{0,45} \pm 19\ \%. \qquad (6.22)$$

Here I in Pa·s. According to [6.51] the formula for calculation the impulse is valid at $1{,}16 < Z < 5{,}95$ m/kg^{0,33}, $0{,}03 < \Delta P < 1$ MPa, and $0{,}008 < \alpha_c < 0{,}13$.

The analysis of the presented relationship shows, that for the passing waves the dependence predicts the attenuation by impulse only at $Z^{-0.98} \alpha_c^{0,45} < 0{,}4$. At the reverse ratio the dependence specifies the amplification of the wave transmitted through the screen by impulse. One of the possible reasons of the phenomenon observed is the probability of registration of the impulse from the waves, which have rounded the perforated plate. In this connection the performance of the measurements of impulse in conditions excluding the occurrence of diffracted perturbations is necessary. The estimations of the impulse attenuation to be presented below are made in the area, where the decrease of the wave impulse is marked. In view of these remarks the given dependences allow to determine the factors of attenuation for the shock waves by pressure β and impulse η due to the partitions with different degree of permeability. The dependencies of β on the wave intensity are shown in the fig. 6.23 at $\alpha_c = 0.01$ and 0.1 (the databases in zones I and II accordingly). The shaded zone reflects the distinction of β for the barrier with $R^* = 4{,}5$ (top border of a zone) and with $R^* = 1{,}16$ (bottom border of a zone).

The dependences of factors of attenuation by impulse on the wave intensity are specified in the fig. 6.24 at α_c = 0.01 (line I) and α_c = 0.04 (line II). The lines III in the fig. 6.23 and 6.24 correspond to the immersing of HE charges in the foam. As it is seen, at α_c = 0.01 the perforated partitions are more effective.

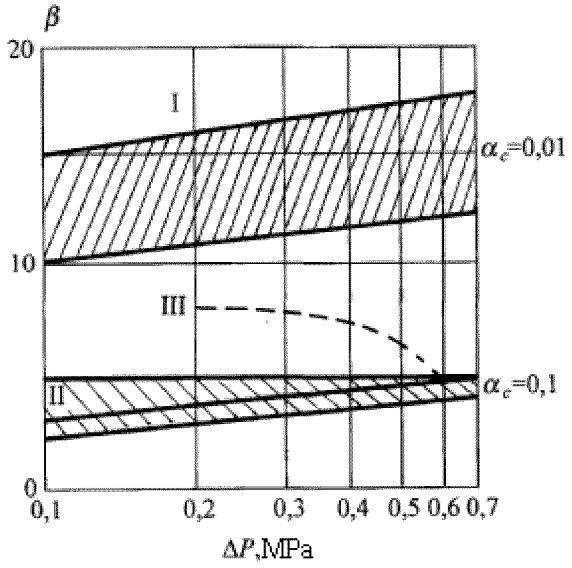

Fig. 6.23. Dependence of the factor of attenuation by pressure on the overpressure in the front of a wave

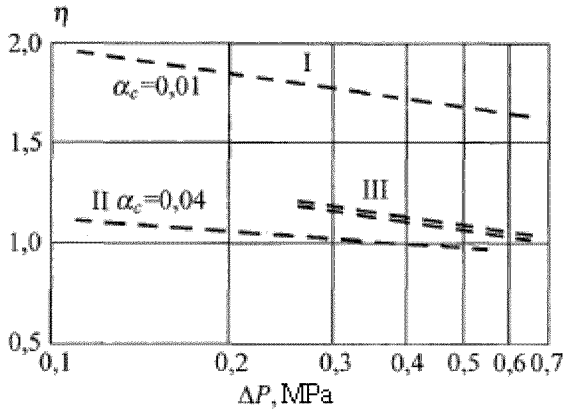

Fig. 6.24. Dependence of the factor of attenuation by the impulse of blast loading on the overpressure in the front of a wave

The Fig. 6.25 allows determining the level of permeability, at which the attenuation of the air shock waves by the partitions is more preferable, than at the HE charges immersing in volume of foam. The dependences I and II show the level of attenuation by pressure at different permeabilities α and the wave intensity ΔP. The zone III corresponds to the shock waves attenuation by the foam at the concentration σ = 10... 15 kg/m^3. At α_c < 0.02…0.03 the partitions are more effective, and at α_c > 0.04 the foam screens are more effective.

As it is seen, the effective attenuation by the perforated partitions is achieved at their small permeability. Taking into account the information presented before, the pressure in the reflected wave at such partition is close the pressure of reflection at continuous wall. It means, that the partition will be subjected to the rather appreciable shock loadings, which are necessary to be parried by the appropriate technical decisions.

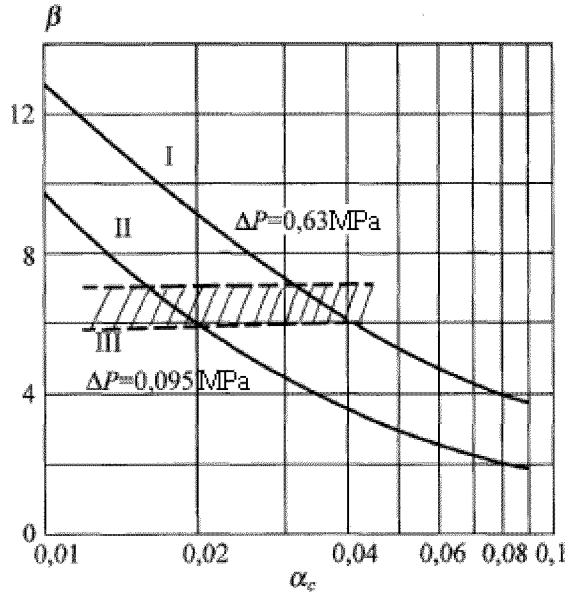

Fig. 6.25. Dependence of the factor of attenuation by pressure on the permeability of a partition

6.7. Efficiency of the combined protection

The reasonable choice of an acceptable combination of the protection methods from fragments and blast loadings can be made on the basis of the experimental data [6.59]. In this work the efficiency of the combined protective surrounding (layers of foam + metal envelope) and the efficiency of the foam layer without a metal envelope were compared. The first configuration is represented in the fig. 6.26, and second one is represented in the fig. 6.14. The basic geometrical sizes of the envelope 3 are the same, as in the fig. 4.1 and 4.2.

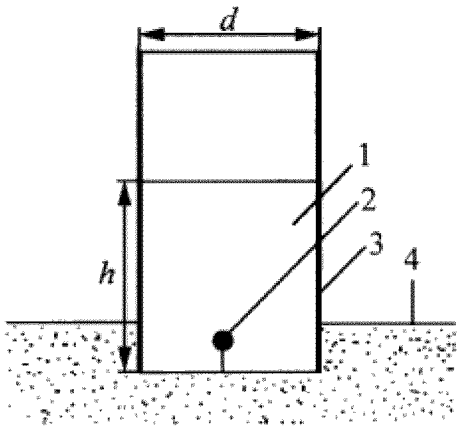

Fig. 6.26. The combined protective configuration: layers of foam + metal envelope: 1 - foam; 2 – HE charge; 3 - metal envelope; 4 - ground

The HE charges 2 (TNT/RDX 9/91 – TNT equivalent is equal to 1,36) were placed at the height of 4 cm above the ground. The envelope was putted 6 cm deeper in the ground for prevention of the shock waves propagation through the gap between the envelope and the ground. All measurements were performed with the foamy layer 1, having the multifold ratio 30, i.e. the density about 33 kg/m^3. Metal envelope 3 is made from a part of the cylindrical pipe with the diameter d and the height h. We shall remind, that the reduction of the sound pressure at the explosion in the empty container (without the foam) does not exceed ΔP = 1 dB.

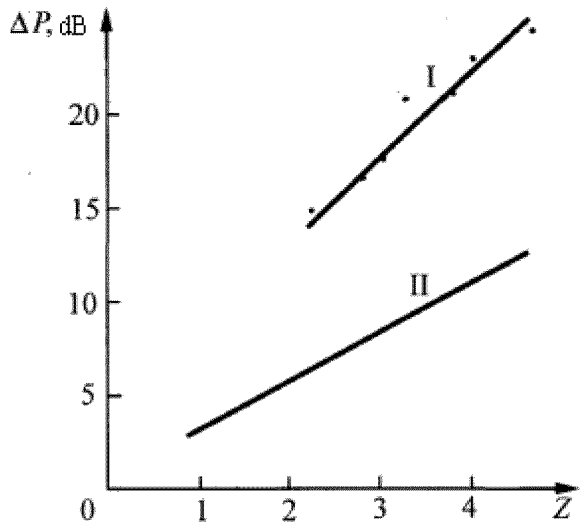

Fig. 6.27 Comparison of efficiency of various protective envelopes by sound pressure $Z=(\sigma V_S/G)^{0,33}$

The comparison of the protective envelopes efficiency by sound pressure is presented in the fig. 6.27, where the line I corresponds to the explosion by the scheme shown in the fig. 6.26, and line II corresponds to the explosion by the scheme shown in the fig. 6.14. Evidently, that the combined protection (fig. 6.26) provides an effective attenuation of the shock waves.

The scheme is simple for the realization and can be recommended for the practical use at the detonation of the charges with mass up to 1... 2 kg TNT. The preferable geometrical sizes of the container: d = 0,92 m; h = 1,22 m and d = 0,86 m; h = 1,16 m, i.e. the volume $V \approx 1$ m^3.

6.8. Attenuation of the air blast waves from HE detonation of charges in a liquid limited elastic envelope

The obtained specific features of the blast attenuation at HE detonations by the gas-contained envelopes give additional opportunities to develop new types of the accident protection devices. It is urgent, as the operative application of the foamy envelopes is

complicated sedimentation of the foam, and the preparation of the protective envelopes with other fillers is connected with a number of technical difficulties.

Let's consider the problem on the increasing the compressibility of a liquid (for example, water) by capsulation in an elastic compressible envelope. The solution of this task is known, and as an example we shall consider the medium water + air bubbles in an impenetrable envelope (for example, in a tube) with flexible walls [6.56,6.63]. The sound speed in such medium can be determined by the relationship:

$$c^2 = \left[\alpha\rho_g + (1-\alpha)\rho_f\right]^{-1}\left[\frac{\alpha}{P} + \frac{1-\alpha}{\rho_f c_f^2} + \frac{2\Theta r}{E\delta}\right]^{-1} \qquad (6.23)$$

Here α is the gas volume fraction in a liquid; ρ_g is the density of a gas; ρ_f is the density of a liquid; P is the pressure; E is the modulus of elasticity of the envelope material (wall of a pipe), Θ is the factor describing the conditions of attaching the envelope (Θ = 1... 0,5μ for a tube fixed at one single end, and $\Theta = 1 - \mu^2$ for a pipe jammed at both ends, μ is the Poisson coefficient), δ is the thickness of the wall of an envelope, r is the radius of an envelope.

Parametrical dependence $c=f(\alpha)$ is shown in the fig. 6.28 for representing the practical interesting case of the medium: water + air bubbles at $P = 10^5$ Pa and the parameter $2\Theta r/\delta = 10$. The line 1 is calculated for the sound speed in the incompressible liquid ($c_f \to \infty$), placed in an incompressible envelope ($E \to \infty$). The line 2 is obtained for the water (c_f = 1450... 1500 m/s) at $E \to \infty$. The line 3 is obtained for the water in a steel pipe at E = 200 GPa. The line 4 is obtained for the water in the envelope made from an elastic material with E = 1 GPa. As it is seen, at $\alpha < 10^{-2}$ the sound speed c is adjusted by the elasticity of the walls of an envelope. At a volume fraction of the gas inclusions in a liquid $\alpha > 10^{-2}$ or, more precisely at $\alpha > \Delta P/\rho_f c_f^2$ the compressibility of the structure: envelope — liquid — gas bubbles does not depend on the properties of the filler and the material of the walls. Here ΔP is the amplitude of the pressure perturbation. The diagram presented in the fig. 6.28 allows to understand the basic features of the suppression of the HE generated blast waves by the envelopes considered in [6.1, 6.3, 6.4, 6.6, 6.17, 6.23,

6.26... 6.30, 6.40... 6.42, 6.48]: 1) at the gas volume fraction in a liquid $\alpha > 10^{-2}$ the effect of the properties of a liquid and the parameters of the envelope material, transmitting a pressure wave, in definition of medium compressibility, is insignificant; 2) high compressibility of transmitting medium can be achieved not only by entering the gas inclusions into water, but also at $\alpha > 10^{-2}$ by the water capsulation into an elastic envelope with $E < 10$ GPa.

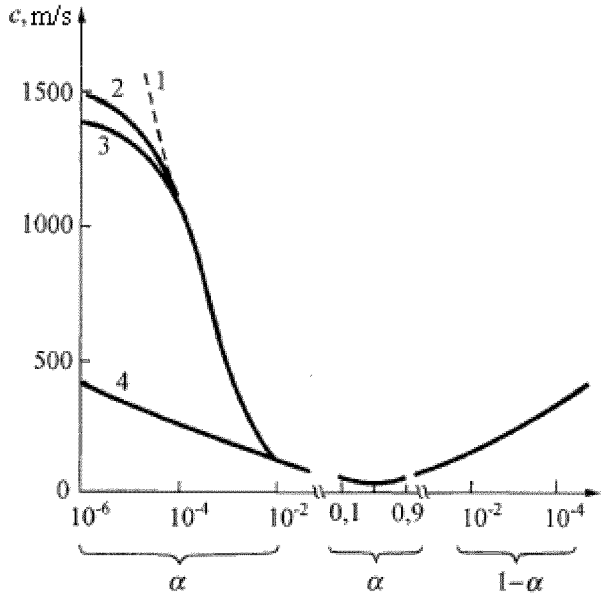

Fig. 6.28. Dependence of the sound speed in the system liquid - air bubbles – envelope on the volume fraction of gas bubbles [6.56,6.57,6.63]

6.9. Checking of the efficiency of the blast loading reduction

Study of the efficiency of the blast effects decreasing by placing the HE charges in a volume of the liquid limited by an elastic envelope, was carried out in a series of polygon tests. The parameters of the air blast waves were measured at the ground explosion of spherical TNT charges with mass 0,1 and 1 kg. To exclude the suppression of the blast waves due to the energy losses by the interaction with ground (formation of a crater, transfer of a part of energy by the wave inside the ground) the HE charges were mounted

on the armour-steel plate with the area 1,2 x 1,2 m^2. The thickness of the plate in the experiments changed from 30 to 60 mm. All explosions were executed in the open district.

The parameters of air blast waves were measured by six piezoelectric pressure gauges located at certain distances from the charge R in two perpendicular directions. In the case of 0,1 kg charges the gauges were established at the height of 0,1 m above the ground. In the case of 1 kg charges the gauges were placed at the height of 1 m to exclude the influence of the reflected waves. The distance of the measurement of the blast waves parameters was in a range 0,8…4,0 m. In the scaled variables of Sadovsky-Hopkinson $R^*=R/(2G)^{0,33}$ for the charges of 0,1 kg at the ground explosion 1,36 m/$kg^{0,33}$<R^*<6,8 m/$kg^{0,33}$ and for the charges of 1 kg 0,63 m/$kg^{0,33}$<R^*<3,2 m/$kg^{0,33}$ accordingly.

The results of the measurements of the pressure waves amplitudes from the open charges have coincided (with accuracy not less than 10 %) with the empirical values calculated by the Sadovsky formulas [2.1], used for the further comparison to the parameters of the waves from the protected charges. The capsulation of charges was achieved by their placing into a double cylindrical elastic envelope filled by the working liquid. The size of internal cylindrical capsule with the volume about 2,6 l: a diameter 0,15 m and height 0,15m. Internal capsule is surrounded by a ring layer with thickness 0,04 m and is limited by the cover with the same thickness from upper side (double envelope with a liquid). Thus, the total volume of liquid filler is about 5,2 l.

The explosion suppressors (envelopes) for HE charges with the mass 0,1 kg TNT were made from sheet polythene with the thickness δ = 2 mm and with limiting axial lengthening ≈ 400%. The mass of an envelope was 0,6 kg. A number of experiments with 1 kg TNT charges was performed in a rubber envelope (the thickness of walls is 1,2 mm) filled by 50 kg of water. Limiting axial lengthening of the rubber was about 400 %. The restriction of the elasticity of the rubber envelope was reached at its covering by hardening polyurethane foam layer outside. The information on the explosion suppressors used is listed in tab. 6.2.

The designations in tab. 6.2 are: c_f – sound speed in the filler; ρ_f - absolute density of liquid filler; $(c\rho)_f$ - acoustic resistance of the filler; M – mass of the filler; $(M/G)^{0,33}$ - parameter of suppressor;

ψ - factor of blast waves attenuation by amplitude

$$\psi = 20 \lg \frac{\Delta P_1}{\Delta P_2};$$

β - factor of blast waves attenuation calculated by (6.18)

$$\beta = \frac{\Delta P}{\Delta P_0}.$$

No special measures on the degasation were undertaken while filling the envelopes by the liquid. The following working liquids are taken: the water, the water solution of calcium chloride, the glycerin. The solution of calcium chloride was used in order to change the density of the liquid [6.85]. Glycerin was taken as a sample of high-viscous liquid [6.88]. A number of experiments were performed with the sand as a filler [6.70].

Table 6.2 Parameters of explosion suppressors

No	Material of envelope	Filler	c_f, m/s	ρ_f, kg/m^3	$(c\rho)_f$, 10^{-6} kg/m^2·s	$(M/G)^{0,33}$	ψ, dB	β	β^1
1	Polyethylene	Solution of calcium chloride	1450	1290	1,87	4,02	8,06±2	2,05…3,25	0,31…0,48
2	Polyethylene	Glycerin	1920	1260	2,42	3,95	7,85±2	1,96…3,1	0,32…0,51
3	Polyethylene	Water	1450	1000	1,45	3,72	7,16±2	1,81…2,87	0,35…0,55
4	Polyethylene	Sand	-	1810	-	4,53	9,59±2	2,27…3,79	0,26…0,42
5	Rubber	Water	1450	1000	1,45	3,68	7,04±2	1,79…2,83	0,35…0,56
6	Rubber + polyurethane foam	Water	1450	1000	1,45	3,68	7,04±2	1,79…2,83	0,35…0,56

6.10. Influence of an elastic envelope on the parameters of air shock wave

The general representation about the change of blast waves parameters at HE charges immersing in gas-filled envelope or in a liquid with an elastic envelope is shown in the fig. 6.29. The line 1 and the experimental points are obtained for the open charges in calculations [2.1] and in experiments [6.80] accordingly. The line 2 was obtained in [6.3,6.48] for TNT detonation in the water-air foam at the concentration of water $\sigma \approx 10$ kg/m^3. The area 3 corresponds to the described experiments with HE charges, shielded by a liquid layer in elastic envelopes [6.94], and data [6.57]. As it is seen, the efficiency of the

shock waves attenuation by the foam or by the liquid in an elastic envelope appears to be comparable.

The effect of various explosion suppressors on the dependence of blast waves amplitude on distance is shown in the fig. 6.30. All liquid suppressors have approximately identical (within the experimental error + 10 %) efficiency. In the experiments with the sand the least degree of blast waves attenuation was obtained. Smaller compressibility of glycerin in comparison with the water (the speed of a sound for glycerin is 1920 m/s and 1450 m/s for the water) compensates the influence of larger density [6.88]. The diagram of dependence of the attenuation factor for blast waves by amplitude on the distance $\beta_e^{-1} = \Delta P_2 / \Delta P_1 = \beta_e^{-1}\left(R^*\right)$ is presented in the fig. 6.31. At HE detonation in the volume of a liquid the value β increases with distance in a range up to $R^* < 2{,}5$ m/kg^{0,33}. The comparison between calculated values (by formula for ψ for gas-filled envelopes) and experimental data of limiting level of attenuation by amplitude β is presented in tab.6.2. It is possible to note the agreement between calculated values of β (taking into account the experimental error) and the values β_e obtained in experiments. The results of measurements of amplitude of waves from explosion of 1 kg HE charge shielded by a water layer in hard (line 3) and not- hard (line 4) rubber envelopes are presented in the fig. 6.32 in comparison with the data for an open charge [6.12]. A conclusion about the influence of envelope elasticity on the air waves formation partially proves to be true. It is useful to add the fig. 6.32 by the calculation results [6.55] for a system: HE charge (mass 0,45 kg) + water bath + thin envelope from an aluminum alloy ($E \approx 70$ GPa) - line 2. No appreciable decrease of the blast waves amplitude was found in calculations [6.55] for the ratio of masses of water and HE charge from 2,1 up to 16 and at $R/R_0 > 30$. It once again reflects the appreciable influence of envelope elasticity at a choice of effective dampers of the blast loadings. The formulas for calculations of the attenuation degree β by amplitude for gas-filled envelopes are inapplicable to the case described in [6.55], when the HE charge was immersed in a liquid and placed in a metal envelope.

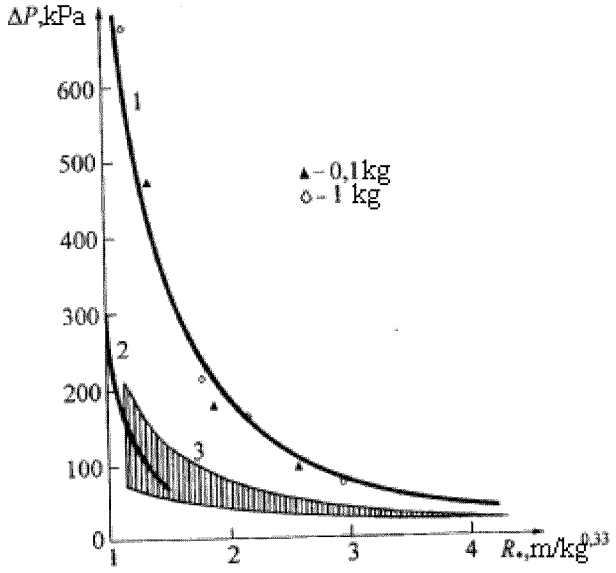

Fig. 6.29. Dependence of air shock wave amplitude on scaled distance. Line 1 - by [2.1]; line 2 - by [6.48]. Points – by the measurements for an open charge [6.57]. The shaded area - for charges in elastic liquid explosion suppressors

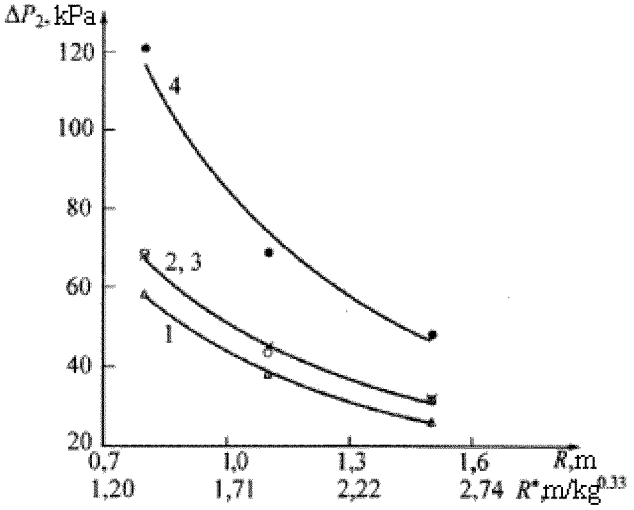

Fig. 6.30. Dependence of air shock wave amplitude on distance for various variants of explosion of 100 g TNT charge. Numbers of curves correspond to numbers of explosion suppressors listed in tab. 6.2

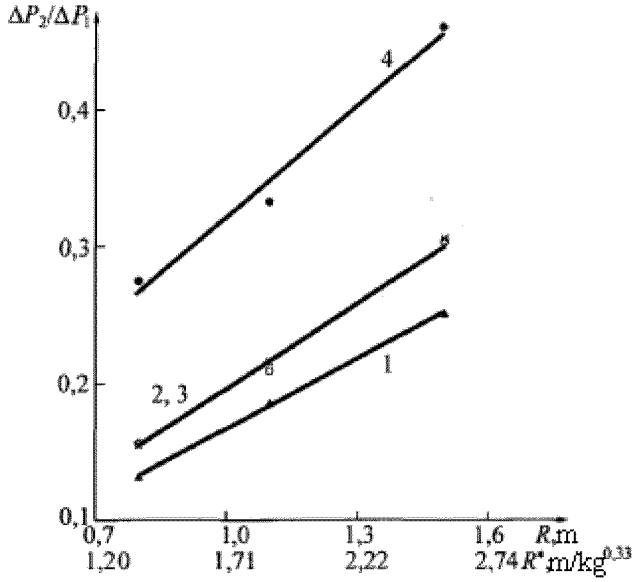

Fig. 6.31. Dependence of air shock wave attenuation factor on distance at ground explosion of 100g TNT charge. Numbers of curves see fig. 6.30

To obtain the complete pattern of the blast waves attenuation from HE detonation, shielded by the protective liquid-elastic container, it is necessary to perform the measurements of the impulse of the static pressure and the duration of the compression phase. The construction of pressure - impulse diagrams, as well as the description of the blast wave profile transformation in coordinates pressure — time at any distance from the charge in comparison with the standard profiles for an open charge, are necessary for the further development of the methods of protection [6.67... 6.70].

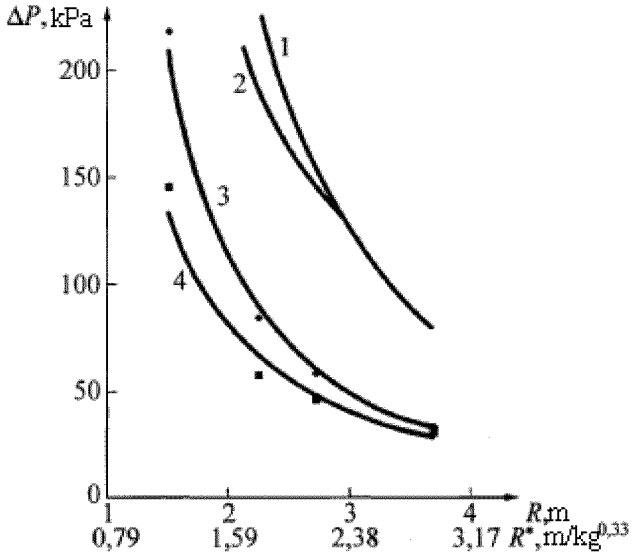

Fig. 6.32. Dependence of air shock wave amplitude on distance at ground explosion of 1 kg TNT charge: 1 - by [2.1]; 2- by [6.55]; 3 - experiments with explosion suppressor No 6 (tab. 6.2); 4 - experiments with explosion suppressor No 5.

The results of the comparison between the pressure at the front of an air SW at free and localized explosions of TNT charge with the mass 0,8 kg are shown in the fig. 6.33. The lines of the pressure levels of 50 and 100 kPa, corresponding to the thresholds of ear damage and lungs damage, show the reduction of radius of the dangerous zone of demolition action in 2…2,5 times as a result of explosion localization. The experimental values of the impulses for free and localized 1 kg TNT are presented in the fig. 6.34.

The obtained dependences of pressure and impulse on the distance and the mass of the open and localized TNT charges (the mass < 1 kg) allow to estimate the blast effect of the explosion, for example, by the construction of the diagrams in ΔP-I coordinates. The example of the diagram is presented in the fig. 6.35.

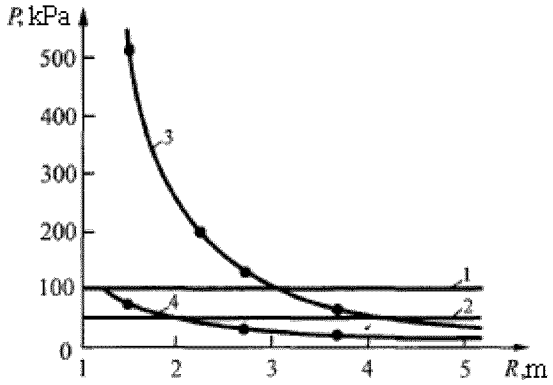

Fig. 6.33. Pressure at the front of air SW depending on the distance at explosion of open and localized 0,8 kg TNT charges: 1 – lethality threshold; 2 –barotraumas threshold; 3 - open charge; 4 - localized charge

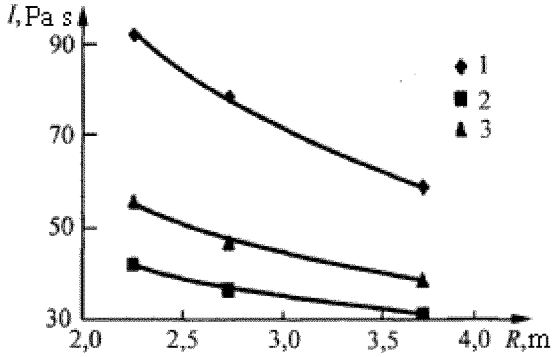

Fig. 6.34. SW impulse depending on distance at 1kg TNT explosion: 1 - open charge, 2 and 3 - charge, localized by the 50 kg samples with various elasticity

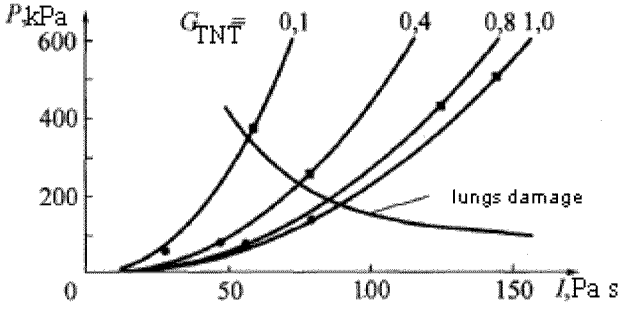

Fig. 6.35. P — I diagrams for the open and localized TNT charges with masses 0,1... 1,0 kg. Experimental points for R = 0,8m (G_{TNT} = 0,1 kg) and R = 1,5m (G_{TNT} = 0,4; 0,8; 1,0m): • - data for the localized charges; ■ - data for the open charges

The presented dependences show, that the blast effect of explosion exceeding a threshold of lungs damage in case of the open charges is reduced down to the safe level with the use of localizators.

6.11. Transformation of the blast waves by the layer of two-phase medium

Experimentally is proved [6.70, 6.71], that at the explosion of the isolated HE charge the blast wave is attenuated at crossing the liquid screen due to the loss of energy on the destruction of localizator and the kinetic energy of the liquid to be dispersed.

The blast wave means the pressure perturbation with a continuously decreasing profile. Due to the energy loss and the transformation of the blast wave in the layered screen the amplitude of an air blast wave nearby localizator is reduced in several times in comparison with the explosion of the non-isolated charge. It seems, that the influence of loalizator is reflected not only in the peak parameters of the blast wave, but also on the frequency - temporary characteristics. The question on the transformation of the blast wave by its peak - frequency parameters under the influence of the gas-liquid screen is not completely resolved till now.

The studies in [6.57,6.70,6.79] have revealed the main role of the compressibility of the liquid working fluid in localizator in the blast wave attenuation and transformation. Efficiency of the blast waves suppression is increased considerably at the replacement of a continuous liquid by the gas-liquid system. Such replacement has ensured the increase of the compressibility of the medium, transmitting the blast energy. Partial, but the not limiting increase of the compressibility of the liquid screen was achieved in [6.57] by the elastic envelope holding a liquid. Additional interest is the specific features of the processes accompanying the blast waves transformation at passage through the layer of a two-phase protective material. The introduction gas bubbles in a liquid changes compressibility of a liquid and drastically changes the speed of sound and shock-wave disturbances [6.73... 6.76]. In two-phase medium a liquid + gas inclusions the speed of a sound depends on the pressure, and it provides the effective blast wave attenuation.

The multifold reduction of the speed of linear and nonlinear pressure disturbances in two-phase medium influences a structure of the pressure in the blast loading due to the stretching of the perturbation in time. The previous studies are limited to the shock waves propagation in gas-liquid media. The known investigations concern either to the very strong waves with the amplitude of several GPa [6.73], or to the rather weak waves with the amplitude up to 1 MPa [6.74, 6.77,6.78]. The duration of the compression phase was those that the statement of a question about the frequency characteristics had not sense. The amplitude of the pressure in the blast waves arising in gas-liquid localozators preventing from a HE charge detonation, typical for the explosive devices, was 0,1... 1,0 MPa.

The propagation of the blast waves in two-phase gas-liquid medium with bubbly structure was analyzed in [6.73,6.79,6.90], where the decrease of the blast waves speed and their effective attenuation by the subsequent rarefaction waves is confirmed. The inclusion of the gas bubbles in liquid localizator results in the increase of the time of destruction and changes all time intervals of interaction. Additional (to a cycle of tests [6.57]) experiments were carried out with the purpose to define the consequences of replacement of a liquid in explosion localizator by the transformation of the blast wave.

6.12. Experimental technique and verification

The TNT charges of mass 75 g equipped by the electrical blasting caps ED-8 were used.

Model samples simulating the dispersed liquid layer in an elastic envelope, were produced in the form of containers made from a goffered cardboard with the thickness of 3 mm and the following sizes: the thickness (the distance between the gauges) δ = 115 mm, the width l = 300 mm, the height H = 340 mm, the height of liquid filling level h = 300 mm. The tensoresistor gauges were pasted inside the opposite walls in the middle part of the container. The hermetical package with liquid to be dispersed was placed into the container tightly to the walls. The two-phase gas-liquid medium of bubbly structure with gas volume fraction 50…60% was used as the working fluid.

The choice of a working body for filling the explosion suppressor is based on a principal property of two-phase gas-liquid media. It is known [6.73], that the equilibrium sound speed in such medium is determined by:

$$c^2 = P_0\left[\rho_1\alpha\left(1-\alpha\right)\right]^{-1}$$

(6.24)

The minimal sound speed is realized at the volume gas fraction in a liquid $\alpha = 0{,}5$, when the product $\alpha(1-\alpha)$ reaches the maximal value 0,25. In a water-air medium at the initial pressure $P_0 = 0{,}1$ MPa we have $c_{min} = 20$ m/s. Thus, the alternation of sound speeds during the blast wave propagation from HE charge proceeds as follows: 340 m/s (air) $\rightarrow$ 20 m/s (two-phase screen) $\rightarrow$ 340 m/s (air).

The tests were carried out in the open district. Samples were placed on a steel plate. The charge was suspended on the rack so, that the center of a charge was on an axis of the gauges and perpendicular to the wall of the container. The distance from the center of a charge to the nearest gauge was $L = 0{,}1$ m, and to a surface of a plate - 0,17 m.

The scheme of tests is presented in the fig. 6.36.

To register the moment of the blast wave arrival the tensoresistor gauges were used. The gauges were made from electrically conducting paper, which resistance is reduced at compression. Registration and subsequent processing of the signals were made using 16-channel computer oscilloscope with the discrete frequency 3 MHz.

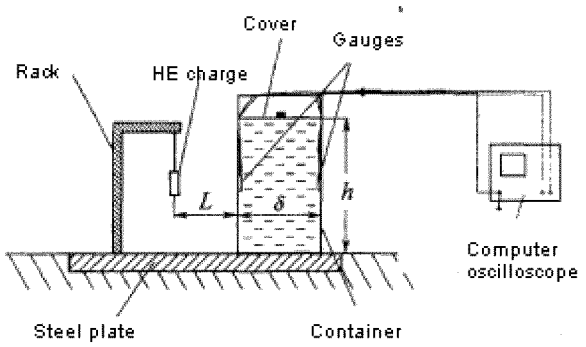

Fig. 6.36. The scheme of tests

The records of the signals from the gauges allowed estimating the time intervals Δt between the impulses at the first and the second gauges (by the start and the amplitude of the pulse). The average by the container thickness speed of the blast wave was determined by the relationship: $D=\delta/\Delta t$.

Experiments with the samples filled by water were carried out for the verification of the proposed measurement technique. The typical example of a record in coordinates output voltage of tensoresistor gauge U – time t is presented in the fig. 6.37. The signals of the channels 1,2 correspond to the windward (nearest to HE charge) and leeward (behind the screen) gauges and are given in a uniform time scale.

The results of reference tests are presented in the first row of tab. 6.3 by the following parameters:

t_{fr1} and t_{fr2} are the durations of the output signal rise at the near and far gauge along to the direction of blast wave propagation.

The listed parameters are given with the indication of the maximal disorder of their values. As it is seen, the average speed of the blast wave is D_u = 1380 ± 30 m/s.

The maximal overpressure ΔP_m in the blast wave at the forward to a charge border air - screen falls in a near zone of explosion [6.80]. At the chosen configuration charge - screen $\Delta P_m \approx 10$ MPa. The reflection of this wave results in transmitting wave into the screen with overpressure $\Delta P_m \approx 10$ MPa.

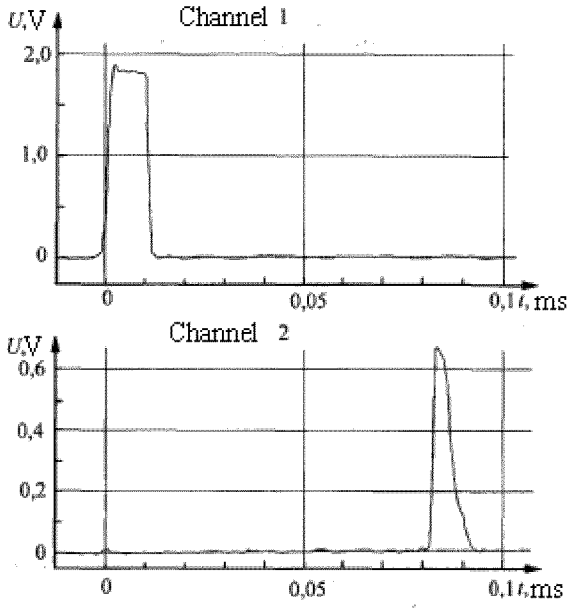

Fig. 6.37. The records of the output signals of tensoresistor gauges in the experiments with liquid to be dispersed without gas inclusions

The wave speed calculated using Tait equation of state [6.73,6.76] in water is D_c = 1580 m/s. The difference between the calculated and the measured values D_c and D_u is 12,3 %, that it is possible to consider satisfactory for the accepted method of the measurement. There are also objective reasons of an expected divergence because of placing the water layer in the container with the flexible walls. Besides, in experiences with the water no special degasation of the layer was performed.

Table 6.3 Results of measurements

Type of working fluid	t_{fr1}, μs	t_{fr2}, μs	D, m/s
Water	2,4 ± 1,3	1,5 ± 0,5	1380 ± 30
Gas - liquid	1,8 ± 0,9	56 ± 14	134 ± 16

6.13. Results of experiments with gas-liquid screens

Consider the experiments on the blast wave transformation by a layer of two-phase gas-liquid working fluid. Typical records of the output signals U - t of tensor-resistance gauges are presented in the fig. 6.38.

The basic parameters are listed in the second row of tab. 6.3.

Comparison of the records of the gauges in a water layer (fig. 6.37) and in gas-liquid screen (fig. 6.38) shows the qualitative distinction of the blast wave transformation process. The duration of the pressure rise at the wave front in the water does not grow. An essential (in ten times) stretching of the blast wave is always marked in gas-liquid screen. The speed of the blast wave in two-phase medium is almost 10 times lower in comparison with the water.

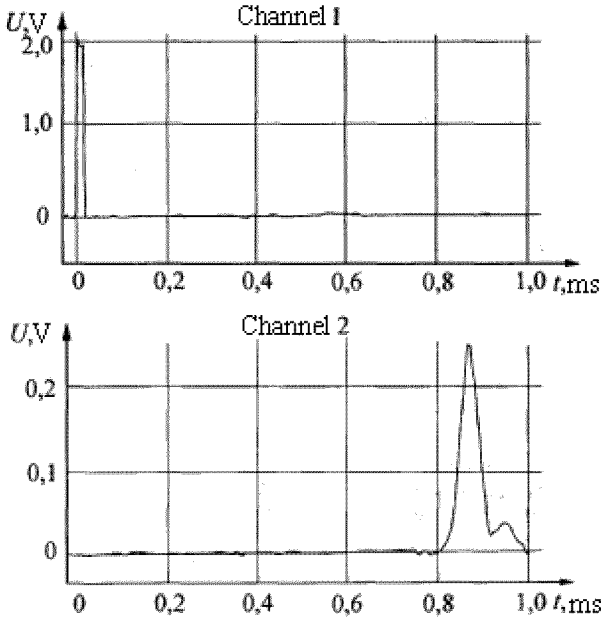

Fig. 6.38. Experimental records for gas-liquid tests.

The output signals from the nearest gauge to a charge (1) and the distant gauge behind the screen for the water (2) and for the gas-liquid medium (3) are combined in the fig. 6.39. In addition, it is possible to note, that the signal amplitude at the distant gauge in water is almost in 3 times higher, than in two-phase medium. It is easy to note quantitative and qualitative distinction of output signals using record, presented in the fig. 6.40.

It means, that the average Mach number of a blast wave in a working body of explosion suppressor between windward and back walls is about $M \geq 6{,}8$. The overpressure in this case is about $P_1/P_0 \approx M^2 \geq 46$. The earlier determined value of pressure in a wave penetrating into two-phase medium, was equal to $P_1^* \approx 800$, that corresponds to the Mach number $M \approx 28{,}2$. Thus, at the distance of $\delta = 115$ mm in two-phase medium with $\alpha \approx 0{,}5$ the blast wave speed decrease almost in 4 times, and the front overpressure - not less than in 16 times.

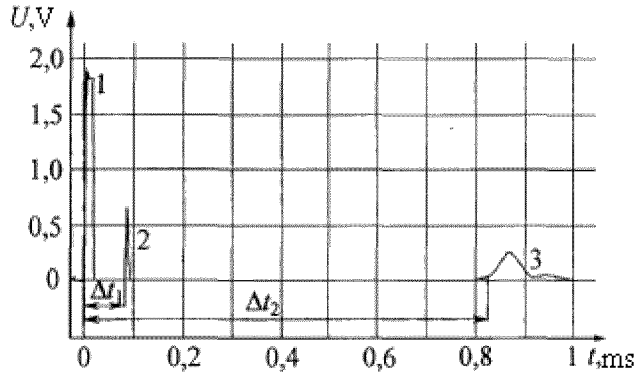

Fig. 6.39. Comparison of output signals U –t at the blast waves transformation in water and gas-liquid layer: Δt_1 is the time of blast wave crosses the water layer, Δt_2 is the time of blast wave crosses the gas-liquid layer

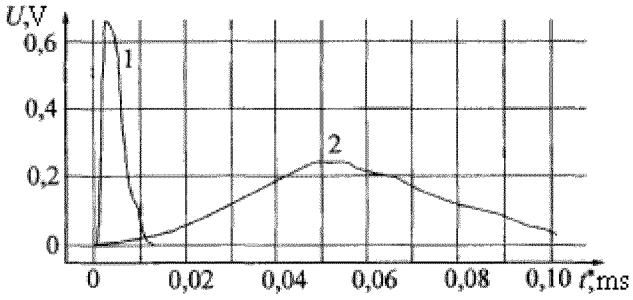

Fig. 6.40. The combined signals from the second gauge for the samples with water (1) and gas-liquid medium (2): t is the time after blast wave crosses protective layer*

As a result, the layer of two-phase medium located on the way of the blast wave, not only reduced the amplitude of the wave past through a layer, but also transformed the form of the blast loading. Instead of the blast wave with abrupt front ahead of the screen we obtained the low-frequency compression wave behind the screen, which is stretched in time.

It is necessary to emphasize the universal character of the marked phenomenon taking into account the data of the experiments in [6.82]. In this work the research of the transformation of underwater blast loadings generated by the TNT charges immersed in the water was performed. The transformation of underwater blast loading was made by the installation of the porous polyurethane plate (the density of the material is 27... 64 kg/m^3) of the thickness δ = 1... 10 cm on the way of the blast wave propagation.

The distance from the porous screen to the charge L = 30... 110 cm. In the experiments performed in [6.82] the sound speed on the way of the blast wave propagation alternated as follows: 1470 m/s (water) $\rightarrow$ 60... 100 m/s (polyurethane foam) $\rightarrow$ 1470 m/s (water).

The results of the experiments on the transformation of consequences of underwater explosion [6.82] are qualitatively and quantitatively close to the described results of the experiments on the transformation of the air blast waves.

The amplitude of the underwater blast wave in [6.82] at the passage of a layer from a material with the lowered speed of a sound is reduced in 30... 50 times. The time of the pressure rise at the front waves has increased almost in 40 times and the blast loading was transformed into the compression wave, stretched in time. The similarity of suppression results for the air and the underwater explosions allows to assume an opportunity of creation of the universal accident protection devices based on the principles of the air blast waves attenuation, formulated in [6.67... 6.71].

The references to chapter 6

6.1. Palamarchuk B.I. Prediction of blast wave effect on bioobjects at blasting operations // Welding, cutting and processing of welded components by explosion. - Kiev: E.O. Paton's Institute of electric welding, 1987, p. 141 - 149. *(In Russian)*.

6.2. Safety regulations at blasting operations.-M.; Nedra, 1968,320 p. *(In Russian)*

6.3. Palamarchuk B.I., Malakhov A.T. The effect of medium properties and energy source characteristics on shock waves attenuation // The use of explosion energy for manufacturing of metal materials with new properties: Proc. VI Int. Symp. Gottwald, Oct. 1985 г. 1985, p. 534 - 544. *(In Russian)*

6.4. Palamarchuk B.I., Vakhnenko V.A., Cherkashin A.V. Air shock waves at welding and cutting by explosion and the methods of their localozation //Automat, welding, 1988. № 2, p. 69 — 72. *(In Russian)*

6.5. Tzeitlin Ya. N., Smolii N.I. On the effect of weak shock-air waves at explosions on excavations. Vzryvnoe delo № 82/39,1980, p. 232 - 247. (*in Russian*).

6.6. Raspet R., Butler P.B. Jahani F. The effect of material properties on reducing intermediate blast noise // Applied Acoustics. 1987. Vol.22, ¹ 3, p. 243 - 259.

6.7. Balashkand M.I., Vekilov E.Kh., Lovlja S.A. et al. New sources of exploration seismology safe for ichthyofauna.-M. Nauka, 1980.78p. *(In Russian)*.

6.8. Baker W.E., Cox P.A., Westine P.S., et.al. Explosion hazards and evaluation, Elsevier, Amsterdam-N.Y.-Oxford, 1983,798 p.

6.9. Protasov V.R., Bogatyrev P.B., Belikov E.Kh. Methods of preserving of ichthyofauna at different types of underwater blasting operations //M.: Leg. and Pisch prom., 1982,88p. *(In Russian)*.

6.10. Held M. Blast waves in free air // Propellants, Explosive, Pyrotechnics. 1983. No.8, p. 158 - 167.

6.11. GOST 12.003-35. Noise, Common safety requirements. Introduced from 01.07.84 till 01.07.89. *(In Russian)*

6.12. Instruction on the determination of the radius of dangerous zone for window glasses in case of air shock waves. M.: Sojuzvzryvprom, 1979, 20p. *(In Russian)*

6.13. Westine P.S., R-W plane Analysis for Vulnerability or Targets to Air Blast // The Shock and Vibration Bulletin. 1972. No. 42, p. 173-183.

6.14. Gurin A.A., Malyi P.S., Savenko S.K. Shock waves in excavations. — M.: Nedra, 1983, 223 p. *(In Russian)*

6.15. Giesbrecht H., Hemmer G., Hess K. et. al. Analysis of Explosion Hazards // Ger. Chem. Eng., 1984, No. 4, p. 315 - 325.

6.16. Palamarchuk B.I. On the energetic similarity of shock waves attenuation // The use of explosion energy in welding technique. - Kiev: E.O. Paton's Institute of electric welding, 1985, p. 157 - 167. *(In Russian)*

6.17. Raspet R., Griffits S. Ê. The reduction of blast noise with aqueous foam // J.Acoust. Soc, Am., 1983, v. 74, No. 6, p. 1757- 1763.

6.18. Thompson S.L., CSQII - An Eulerian finite difference program for two-dimensional material response // Part 1. Material Sections, SAND77-1339, Sandia National Lab., Albuquerque, NM, 1979,28ð.

6.19. Kury J.W., Metal acceleration by chemical explosives // Fourth Symposium (International) on Detonation, U.S. Government Printing Office, Washington, DC, 1965, p. 3 - 13.

6.20. Powers J.M., Krier H., Blast wave attenuation by cylindrical reflecting barriers: A computational study // University of Illinois Report, UILU ENG-84-4014,1984.

6.21. Ficket W., Davis W.C. Detonation. University of California Press, Berkeley, CA, 1979, 289 p.

6.22. Baker W.E. Explosions in Air. University of Texas Press, Austin, TX, 1973,268ð.

6.23. Griiffits S. Aqueous foam blast attenuation // Internal Report, Sandia National Lab., Albuquerque, NM, 1982,32p.

6.24. Shapiro A.H. The Dynamics and Thermodynamics of Compressible Flow, Vol. II, The Ronald Press Company, New York, NY, 1954.

6.25. Bass H.E., Erzell J., Raspet R. Effect of vibrational relaxation on rise times of shock waves in the atmosphere // Acoust. Soc, Amer., 1983, v.74, No. 5, p. 1433 - 1447.

6.26. Panczak T.B., Butler P.B., Krier H. Shock propagation and blast attenuation through aqueous foams // J. Haz. Mater., 1987, v. 14, No. 4, p. 321-336.

6.27. Evans P.L., Jankowski D.F., Hirleman E.D. A preliminary investigation of aqueous foam for blast attenuation- // EBC-R 78050, College of Engineering and Applied Sciences, Arizona State University, Tempe, Arizona, 1979.

6.28. Powers J.M., Krier H. Attenuation of blast waves when detonating explosives inside barriers //J. Haz Mater., 1986, v. 13, No. 1, p. 121-133.

6.29. Dobratz B.M. LLNL Explosives Handbook. University of California, UCRL-52997, 1981, 461 p.

6.30. Panczak T.B., Krier H. Shock Propagation and Blast Attenuation Through Aqueous Foams // UILU ENG 83-4007, University of Illinois, 1983, 38 p.

6.31. Chemical Rubber Company, Handbook of chemistry and physics, 1971,362p.

6.32. Krasinski J.S., Khosla A. Shock attenuation in non-homogeneous and porous media // Report No, 34, University of Calgary, Canada, Dep. Of Mechanical Engineering, March, 1972.

6.33. RameshY., Krasinski J.S. Shock and flame tube laboratory experiments // Report No. 73, University of Calgary, Canada, Dep. of Mechanical Engineering, March 1976.

6.34. Clark A.K., Hubbard P.J., Lee P.R., Woodman H.C. The reduction of noise levels from explosive test facilities using aqueous foams // NSWC/W02TR 77-36. NSWL., July 1977.

6.35. Dadley D.A., Robinson E.Q., PickettY.C. The use of foam muffle blast from explosions // Paper presented, at the IBP-ABCA Meeting, June 1976.

6.36. Taylor G. I. The dynamics of the combustion products behind plane and spherical detonation fronts in explosives // Proc. R. Soc. London, Ser. A, 200 (1950), p. 235.

6.37. Taylor G.I. The air wave surrounding an expanding sphere // Proc. R. Soc. London, Ser. A, 186 (1946), p. 273 - 292.

6.38. Brinkley S.R. And Kirkwood J.G. Theory of the propagation of shock waves // Phys. Rev. 1947, v. 71, No. 9, p. 606 - 611.

6.39. Brode H.L. Blast wave from a spherical charge // Phys, Fluids, 1959, v. 2, No. 2, P. 217-229.

6.40. Palamarchuk B.I. Postnov A.B. Shock waves attenuation at condensed HE detonations placed in gas-contained envelopes // The use of explosion energy in welding technique. - Kiev: E.O. Paton's Institute of electric welding, 1989, p. 39 - 41. *(In Russian)*

6.41. Malakhov A. G. Reflection of the shock waves in gas-contained media // Welding, cutting and processing of welded components by explosion. - Kiev: E.O. Paton's Institute of electric welding, 1987, p. 155 - 161. *(In Russian)*.

6.42. Palamarchuk B.I., Vakhnenko V.A., Cherkashin A.V. Methods of predicting of influence of air shock waves on glass windows at technological explosions // Welding, cutting and processing of welded components by explosion. - Kiev: E.O. Paton's Institute of electric welding, 1987, p. 149 - 155. *(In Russian)*.

6.43. Grodzovsky T.D. Interaction of non-stationary shock waves and perforated walls // Scientific notes of TSAGI, 1975, v. 6, No. 2, p. 7 – 15 *(In Russian)*.

6.44. Ostrovsky E.N.. Absorption of a strong incident shock wave by the perforated barrier. // Scientific notes of TSAGI, v. 6, No. 5, p. 115-118 *(In Russian)*.

6.45. Tong K.O., Night C.J. Interaction of weak shock waves with grids and cellular structures // Rocket engineering and cosmonautics, 1980, v. 18, No. 11, p. 24 — 32. *(In Russian)*.

6.46. Mineev V.N., Klapovsky E.E., Matseevich B.F. et al. Attenuation of air shock wave by perforated barriers // 5th Symp. Explos. Work. Metals, Gottwaldow, 1982, Dum. Techhiky CSVTS Pardubice, 1982, p. 357-361 *(in Russian)*.

6.47. Grin V.T., Kraiko A.N., Miller L.G. On the Riemann problem at perforated partition // ZhPMTF, 1981, No 3, p.95-103 *(in Russian)*.

6.48. Kudinov V.M., Palamarchuk B.I., Gelfand B.E., Gubin S.A. Parameters of shock waves at explosion of HE charge in foam // Doklady. AN USSR, 1974, v. 228, No. 4, p. 555 – 557 *(in Russian)*.

6.49. Vakhnenko V.A., Kudinov V.M., Palamarchuk B.I., On the influence of thermal relaxation on the attenuation of strong shock wave in two-phase medium. Prikladnaya mehanika, 1962, v.18, No. 12, p. 91-97 *(in Russian)*.

6.50. Vakhnenko V.A., Kudinov V.M., Palamarchuk B.I., On attenuation of strong shock waves in relaxation media. FGV, 1981, v. 20, No. 1, p. 105-111 *(in Russian)*.

6.51. Gelfand B.E., Gubanov A.V., Timofeev E.I. Interaction of air shock waves with the porous screen // Izv. AN USSR, MZhG, 1983, No. 4, p.79 - 84. *(in Russian)*.

6.52. Esparaza E.D, Baker W.E., Oldham G.A. Blast pressure inside and outside suppressive structures // EM-CR-76042,1975.

6.53. Klapovsky E.E., Kudinov V.M., Mineev V.N. et.al. Attenuation of an air shock wave by the perforated barrier // FGV, 1983, No. 5, p. 115 - 116. *(in Russian)*.

6.54. Khosla A., Krasinski J.S. Pressure rise inside a vessel communicating with outside through an orifice // Trans. Can. Mech. Eng., 1979, v.5, ¹ 2, p. 95 - 105.

6.55. Fry M.A. Interpretation or shock waves from encapsulated high explosive charges // Proc. 18-th Inter. Symp. On Shock Waves (ed. Takayama K.), 1992, p.901 - 904.

6.56. Mori Y., Hijikata K., Komine. Propagation of pressure waves in two phase flow // Intern. J. Multiphase flow, 1975, v.l, ¹ 1, p. 139-152.

6.57. Gelfand B.E., Silnikov M.V., Mikhailin A.I., Orlov A.V. The attenuation of air-blast waves from the HE explosion in a liquid volume bounded by an elastic envelope // Fizika gorenija i vzryva — 2001. — T. 37. — № 5. — p. 128-133. (*in Russian*)

6.58. Kuroda Å., Yoneda J., YoshimuraK., Sakurai S., Kobayashi N., Imaizumi H., Kunimatsu S., Isei T. B(II)) Proc. Of Symposium on shock waves, Japan-94, CHIDA, 1994, p. 413-416.

6.59. Raspet R., Butler P.B., Yahani F. The reduction of blast overpressures from aqueous foam in rigid confinements // Appl. Acoust. 1987. V.22. No. 1. P. 35 -45.

6.60. Borisov A.A., Gelfand B.E., Timofeev E.I. Shock waves in liquids containing gas bubbles // International J. Multiphase flow. 1983. V.9. No. 5. P.531-543.

6.61. Gelfand B.E., Silnikov M.V. A choice of the optimal scheme of suppression of air shock waves from HE explosion // Doklady RAN. - 2002. - v. 383, № 1. - p. 37 - 39. (*in Russian*)

6.62. Buzukov A.A. Reduction of air shock wave parameters by means of air - water screen // FGV 2000. v. 36. No. 3. p. 120-130. (*in Russian*).

6.63. Aoki T., Takagaki T., Miyazato Y., Matgsuo Y. Weak shock wave propagating through bubbly flow in vertical pipe. Proc. of Symposium on shock waves, Japan-99, Ayoma Gakuin University, Sibuya, 1999, p. 497-500.

6.64. Kleine H., Disconescu K., Lee J.H.S. Blast wave propagation in foam. Proc. 20-th Symp. (International) on shock waves (Ed. By Sturtevant Â., Shepherd J.E., Hornung H.). World Scientific. 1996. V.2. P. 1351 - 1356.

6.65. Voskoboynikov I.M., Gelfand B.E., Gubin S.A., Kogarko S.M., Popov O.E. On the use of a mixture of the liquid with gas bubbles for transmitting the shock wave perturbations// Inzhenerno-fizichesky zhurnal. 1976. v.31. No. 4, p. 674 — 677. (*in Russian*)

6.66. Rinaudo M.A., Smith P.O., RoseT.A. Attenuation of blast resultants using water. CD-ROM Proc. Of 15-th (International) Symposium Military Aspects of Blast and Shock (ed. By D.Bergeron). 1997. ORE, Suffield. P. 225 - 234.

6.67. Silnikov M.V., Kozlov A.V., Orlov A.V., Petrov A.V., Titov A.M. The explosion protection device «Fountain» // Proc. of the 1st All-Russia scientific - practical conference «Urgent problems of protection and safety ». St.Petersburgh, 1998, p. 125. (*in Russian*)

6.68. Silnikov M.V., Mikhailin A.I., Orlov A.V., Serdzev N.I., Nozdrachev A.V. Characteristics of blast effects at localized explosion // Proc. of the 4th All-Russia scientific - practical conference «Urgent problems of protection and safety ». St.Petersburgh. - 2001. - v. 2. - p. 580 (*in Russian*)

6.69. Mikhailin A.I., Orlov A.V., Sadyrin A.I., Silnikov M.V.. Principles of weakening of the dangerous factors of explosion // Proc. of Scientific conference of the Volga regional center RARAN «Modern methods of design and improvement of rocket-artillery arms », 1999 - Sarov: VNIIEF - 2000. - p. 517. (*in Russian*).

6.70. Silnikov M.V., Mikhailin A.I., Orlov A.V. Experimental determination of the effect of the parameters of liquid localizator of explosion on its efficiency // the Collection of lectures of the Third International school - seminar « Nnonsteady combustion and internal ballistics ». — St.-Petersburg, BGTU - 2000. - v. 1.-p. 57-69. (*in Russian*).

6.71. Silnikov M.V., Mikhailin A.I., Khimichev V.A. Energetic model of explosion localization // Works of the First inter-regional scientific - practical conferences « Application of special and operative techniques in activity of MVD ». — St.-Petersburg, March, 2000, St.-Petersburg university MVD Russian Federation. — p. 165. (*in Russian*).

6.72. Sakurau A., Tanaka Ê. Explosion induced stress field in various media-2. Proc. of Symposium on shock wave, Japan-2001, ISAS, Kanagawa, 2001, p.427-430.

6.73. Parkin B.R., Gilmor F.R., Brode G.L Shock waves in water with gas bubbles// Underwater and underground explosions. M. Mir. — 1974. — 152 p. (*in Russian*).

6.74. Gubaidullin A.A., Ivandaev A.I., Nigmatulin R.I. Non-stationary waves in a liquid with gas bubbles// Doklady AN USSR. - 1976. - v. 226. – No. 6. (*in Russian*).

6.75. Kim D., Miyake A., Ogawa Ò., Okada Ê., Yoshida M. Experiments on blast wave propagation through water mist. Proc. Of Symposium on Shockwave, Japan-2001, ISAS, Kanagawa, 2001, p. 395 - 398.

6.76. Lyakhov G.M. Waves in soils and porous multi-component medium. M.: Nauka— 1982. — 288 p. (*in Russian*).

6.77. Nakoryakov V.E., Pokusayev B.G., Shreiber I.R., Kuznetzov V.V., Malykh M.V. An experimental research of shock waves in a liquid with gas bubbles// In « Wave processes in two-phase media », Novosibirsk. - 1975. - p. 54 - 97. (*in Russian*).

6.78. Timofeev E.I., Gelfand B.E., Gumerov A.G., Kofman M.M., Polenov A.N., Khomik S.V., Effect of bubbly screen on shock wave perturbation in liquid // FGV. — v. 21 – No. 3. - 1985. - p. 93 - 102. (*in Russian*).

6.79. Silnikov M.V., Orlov A.V., Sadyrin A.I., Shock wave attenuation in gas-liquid medium// In. « Actual problems of rocket manufacturing ». Rel. 1. BGTU, St-P. — 2001. - p. 74 – 78 (*in Russian*).

6.80. Adushkin V.V. On the formation of a shock wave and the expansion of HE products at explosion in air // PMTF, 1963, № 5, p. 107-114. (*in Russian*)

6.81. Cole R. Underwater explosions. — M.: IL. — 1950. (*in Russian*)

6.82. Bjerne L., Underwater explosion research based on model experiments // In.: Problems of nonlinear acoustics (Ed. Kedrinsky V.K.), 198, part II, Novosibirsk, p. 163 - 177.

6.83. Kleine H., Makris A. Development of blast protection equipment. Proc. Symp. on shock waves, Japan-2000, Tokyo University, 2000, p. 661 - 674.

6.84. Mikhailin A.I., Orlov A.V., Selivanov V.V., Silnikov M.V., An estimation of parameters of a field of condensed HE explosion, weakened by a liquid layer. — Works by First Interregional scientific - practical conference on the application of special and

operative engineering in activity of MVD » St.-Petersburg, March, 2000 - p. 208 – 218 (*in Russian*).

6.85. Orlov A.V, Vasilev N.N., Silnikov M.V Experimental study of the effect of density and viscosity of dispersed liquid on the efficiency of liquid explosion localizator. — Works by First Interregional scientific - practical conferences on the application of special and operative engineering in activity of MVD » St.-Petersburg, March, 2000 - 2000. - p. 179 (*in Russian*).

6.86. Silnikov M.V., Mikhailin A.I., Orlov A.V. An estimation of channels of explosion energy dissipation by liquid localizator // the Collection of lectures of the Third International school - seminar « Nnonsteady combustion and internal ballistics ». — St.-Petersburg, BGTU - 2000. - p. 34. (*in Russian*).

6.87. Silnikov M.V., Mikhailin A.I., Orlov A.V., Sadyrin A.I. The effect of parameters of liquid-capacity elastic container isolating HE charge on the pressure in blast wave. // Proc. of the 2nd All-Russia scientific - practical conference «Urgent problems of protection and safety ». St.Petersburgh. - 1999- v. 2.-p. 189. (*in Russian*)

6.88. Silnikov M.V., Petrov A.V., Mikhailin A.I., Estimation of the effect of dispersed fluid viscosity on shock wave attenuation. — Works Second interregional scientific - practical conference « Development new special technique for MVD ». — St-P University MVD Russian Federation, St.-Petersburg. - 2000. - p. 246. (*in Russian*)

6.89. Silnikov M.V., Orlov A.V., Sadyrin A.I., On the energy consumption by two-phase medium // In. « Actual problems of rocket manufacturing ». Rel. 1. BGTU, St-P. — 2001. - p. 70 (*in Russian*).

6.90. Silnikov M.V., Mikhailin A.I., Orlov A.V., Sadyrin A.I., Nozdrachev A.V. Specific features the shock wave propagation in two-phase gas-liquid medium // Proc. of the 4th All-Russia scientific - practical conference «Urgent problems of protection and safety ». St.Petersburgh. - 2000. - v. 2. - p. 564 (*in Russian*)

6.91. Silnikov M.V., Petrov A.V., Orlov A.V., Sadyrin A.I., Nozdrachev A.V. The change of energy absorption of liquid medium with gaseous phase // Proc. of the 4th All-Russia scientific - practical conference «Urgent problems of protection and safety ». St.Petersburgh. - 2000. - v. 2. - p. 569 (*in Russian*).

6.92. Gelfand B.E., Silnikov M.V., Mikhailin A.I., Orlov A.V. The attenuation of blast overpressures from liquid in an elastic confinement // The 23rd International Symposium on Shock Waves/ Fort Worth, Texas, USA. - July 22-27,2001.

6.93. Gelfand B.E., Silnikov M.V. On the efficiency of explosion localization by multiphase media // Proc. of the 3rd All-Russia scientific - practical conference «Urgent problems of protection and safety ». St.Petersburgh. - 2000. - v. 2. - p. 42 (*in Russian*)

6.94. Gelfand B.E., Silnikov M.V. On the role of medium compressibility in reducing the blast wave amplitude // Proc. of the 3rd All-Russia scientific - practical conference «Urgent problems of protection and safety ». St.Petersburgh. - 2000. - v. 2. - p. 47 (*in Russian*)

6.95. Silnikov M.V., Mikhailin A.I., Orlov A.V. Experimental determination of the parameters of liquid explosion localizator. // Proc. of the 3rd All-Russia scientific - practical conference «Urgent problems of protection and safety ». St.Petersburgh. - 2000. - v. 2. - p. 28 (*in Russian*).